Loughborough University

This item was submitted to Loughborough's Research Repository by the author.
Items in Figshare are protected by copyright, with all rights reserved, unless otherwise indicated.

Synthesis of some organotin monomers and copolymerisation with acrylic monmers

PLEASE CITE THE PUBLISHED VERSION

PUBLISHER

© Saud M. Al-Feir

LICENCE

CC BY-NC-ND 4.0

REPOSITORY RECORD

Al-Feir, Saud M. H.. 2019. “Synthesis of Some Organotin Monomers and Copolymerisation with Acrylic Monmers”. figshare. https://hdl.handle.net/2134/10342.

Loughborough University

This item was submitted to Loughborough University as a PhD thesis by the author and is made available in the Institutional Repository (https://dspace.lboro.ac.uk/) under the following Creative Commons Licence conditions.

creative commons

COMMONS DEED

Attribution-NonCommercial-NoDerivs 2.5

You are free:

- to copy, distribute, display, and perform the work

Under the following conditions:

Attribution. You must attribute the work in the manner specified by the author or licensor.

Noncommercial. You may not use this work for commercial purposes.

No Derivative Works. You may not alter, transform, or build upon this work.

- For any reuse or distribution, you must make clear to others the license terms of this work.
- Any of these conditions can be waived if you get permission from the copyright holder.

Your fair use and other rights are in no way affected by the above.

This is a human-readable summary of the Legal Code (the full license).

Disclaimer

For the full text of this licence, please go to:
http://creativecommons.org/licenses/by-nc-nd/2.5/

Loughborough University

Pilkington Library

Author/Filing Title ..... AL-FEIR, S.M.H.

.....

Accession/Copy No. 0401299074

Vol. No. ..... | Class Mark .....

LOAN COPY

0401299074

Synthesis of Some Organotin Monomers and Copolymerisation with Acrylic Monomers

by

Saud M. Al-Feir

A doctoral thesis
submitted in partial fulfilment of the requirements
for the award of Doctor of philosophy of the
Loughborough University

July 1996

Supervisor Professor John V. Dawkins
B.Sc., Ph.D., D.Sc., C.Chem., F.R.S.C.

Department of Chemistry

by Saud M. Al-Feir 1996.

Loughborough University
Pilkington Library
Date June 97
040129907
9901317

Dedication

To the people whom I owe so much:

My brother Abo Hussam

My wife and children

Acknowledgement

I would like to express my sincere thanks and appreciations to Dean of Science and Professor John V. Dawkins, my supervisor, who has followed the progress of this thesis with constant encouragement, assistance and invaluable advice. I am eternally grateful to him.

I owe my deep sincerest thanks and gratitude to Professor A. F. Shaaban Head of Chemistry Department, Faculty of Science, Zagazig University, Benha-branch Egypt for suggesting the research problem, and also for his encouragement and continuous help.

My deep appreciation and gratitude go to my dear brothers and sisters, and relatives for their continuous support throughout the period of my studies. I wish to thank my wife and children for their patience and support for me.

Words can not express my thanks and appreciations to my dearest brother Abo Hussam, for his limitless social and financial support in performing my education. I must admit that without his help and encouragement I would have never been able to finish my studies.

I am also grateful to my sponsor 'Goverment of Saudi Arabia' for the financial support to pursue my Ph.D studies.

I am particularly grateful to M. O. Taha for all his help.

Last but not least, I would like to thank the members of the Polymer Chemistry group in the Chemistry Department, especially David Wilson, for making my time at Loughborough both enjoyable and beneficial.

ORIGINALITY

This is to certify that I am responsible for the work submitted in this thesis, that the original work is my own except as specified in acknowledgements or in footnotes, and that neither the thesis nor the original work contained therein has been submitted to this or any other institution for a higher degree.

CONTENTS

1	Introduction	1
1.1	Homopolymerisation of Monomers	1
1.1.1	Introduction	1
1.1.2	Effect of Substituents	3
1.1.3	Free Radical Chain Polymerisation	4
1.1.4	Kinetic of Homopolymerisations	7
1.2	Copolymerisation Reaction of Monomers	9
1.2.1	Free radical copolymerisation	9
1.2.1.1	Copolymer composition equation	10
1.2.2	Types of copolymerisation behaviour	12
1.2.3	Methods of calculating monomer reactivity ratios	13
1.2.4	Determination of Q-e Parameters for Monomers	16
1.2.5	Radical and Monomer Reactivities in Free Radical Copolymerisation	17
1.2.5.1	Factors affecting the monomer reactivity	18
1.3	Gel Permeation Chromatography	19
1.4	The Glass Transition	20
1.4.1	Factors which effect the Glass Transition Temperature	23
1.5	Dynamic Mechanical Properties of Polymers	25
1.5.1	Factors Affecting Dynamic Mechanical Behaviour	27
2	Literature review	30
2.1	Acrylamides and methacrylamides	30
2.2	Organotin Polymers	31
2.2.1	Tin atoms in polymer main chain	32
2.2.2	Tin atoms pendant to polymer chain	33
2.3	Aim of the present work	39
3	Experimental	41
3.1	General Experimental	41
3.1.1	List of Chemicals	41
3.1.2	Fourier Transform Infrared Spectroscopy (FTIR)	43
3.1.3	Nuclear Magnetic Resonance Spectroscopy (NMR)	43

3.1.4	Mass Spectroscopy	43
3.1.5	Elemental Analysis	43
3.1.6	Gel Permeation Chromatography (GPC)	43
3.1.7	Dynamic Mechanical Thermal Analysis (DMTA)	45
3.2	Synthesis of Precursor Monomers	45
3.2.1	Synthesis of Acrylamide Derivatives	45
3.2.2	Synthesis of Acryloyloxy Derivatives	47
3.3	Synthesis of Organotin Monomers	48
3.3.1	Synthesis of Acrylamide Derivatives	48
3.3.2	Synthesis of Acryloyloxy Derivatives	49
3.4	Characterisation of Prepared Monomers	50
3.4.1	FTIR Spectral Data for Prepared Mnomers	50
3.4.2	^{1}H NMR Spectral Data	51
3.4.2.1	Precursor Monomers	51
3.4.2.2	Organotin Monomers	52
3.4.3	^{13}C NMR Spectral Data	53
3.4.3.1	Precursor Monomers	53
3.4.3.2	Organotin Monomers	54
3.4.4	Elemental Analysis Data for Prepared Monomers	55
3.4.5	Theoretical Molcular Weights versus Practical Detemined Molecular Ions (Mass Spectra)	56
3.5	Polymerisation Reactions of Organotin Monomers	57
3.6	Copolymerisation Reactions	57
3.7	Determination of Tin Content	58
3.8	Detemination of Monomer Reactivity Ratios	58
4	Results and Discussion	60
4.1	Synthesis of Acrylamide Derivatives	60
4.2	Synthesis of Acryloyloxy Derivatives	61
4.3	Synthesis of Organotin Monomers	62
4.3.1	Synthesis of Acrylylamide Derivatives	62
4.3.2	Synthesis of Acryloyloxy Derivatives	63
4.4	Homopolymerisation of Organotin Monomers	64

4.4.1	Homopolymerisation of Acrylylamide Derivatives	64
4.4.2	Homopolymerisation of Acryloyloxy Derivatives	70
4.5	Copolymerisation of Organotin Monomers	74
4.5.1	Copolymerisation of Acrylylamide Derivatives	74
4.5.2	Copolymerisation of Acryloyloxy Derivatives	76
4.6	Q and e Schemes for Organotin Monomers	78
4.7	Monomer Reactivity	79
4.8	Gel Permeation Chromatography	120
4.8.1	Determination of the Best Elution Conditions	120
4.8.2	Values of M_p for Acrylamide-organotin Polymers	121
4.8.2.1	Values of M_p for Acrylamide-organotin Homopolymers	121
4.8.2.2	Values of M_p for Acryloyloxy-organotin Homopolymers	122
4.8.2.3	Values of M_p for Organotin Copolymers	122
4.9	Dynamic Mechanical Thermal Analysis (DMTA)	127
4.9.1	DMTA Results of Acrylic Homopolymers	127
4.9.1.1	DMTA Results of Organotin Homopolymers	130
4.9.1.2	DMTA Results of Acrylamide Derivatives	130
4.9.2	DMTA Results of Acryloyloxy Derivatives	130
4.9.3	DMTA Results of Copolymers	135
4.9.3.1	DMTA Results for Acrylamide Derivatives	135
	DMTA Results for Organotin Acrylamide Derivatives with MA	135
	DMTA Results for Organotin Acrylamide Derivatives with BA	143
	DMTA Results for Organotin Acrylamide Derivatives with MMA	151
4.9.3.2	DMTA Results for Acryloyloxy Derivatives	161
	DMTA Results for Organotin Acryloyloxy Derivatives with MA	161
	DMTA Results for Organotin Acryloyloxy Derivatives with BA	163
	DMTA Results for Organotin Acryloyloxy Derivatives with MMA	165
5	Conclusions and Recommendations for furthur work	171
5.1	Conclusions	171
5.2	Recommendations for furthur work	172
6	References	173
6.1	References	173

ABSTRACT

The aim of this thesis was to synthesise new organotin monomers based on N-substituted acrylamide and methacrylamide and on acrylic acid and methacrylic acid esters with pendant hydrolysable organotin moieties and to study their copolymerisation with methyl acrylate (MA), butyl acrylate (BA) and methyl methacrylate (MMA). A specific objective was to obtain suitable macromolecular chains, to which the organotin moieties could be attached at some distance from the main backbone. The new organotin monomers which were synthesised are:

m-acrylamidotri-n-butyltin benzoate (*m*-AATBTB), *p*-acrylamidotri-n-butyltin benzoate (*p*-AATBTB), *m*-methacrylamidotri-n-butyltin benzoate (*m*-MAATBTB), *p*-methacrylamidotri-n-butyltin benzoate (*p*-MAATBTB), *o*-acryloyloxytri-n-butyltin benzoate (*o*-AOTBTB) and *o*-methacryloyloxytri-n-butyltin benzoate (*o*-MAOTBTBO). These were prepared by the reaction of bis(tri-n-butyltin) oxide (TBTO) with the corresponding acrylamide or acryloyloxy benzoic acid which were prepared by the reaction of aminobenzoic acid derivatives or salicylic acid with either acryloyl chloride or acrylic anhydride. These organotin monomers were polymerised in dimethylformamide (DMF) solution with azobisisobutyronitrile (AIBN) as initiator. Binary copolymerisation experiments were performed by solution polymerisation in DMF solution with AIBN as initiator. The copolymer composition in each case was determined from tin analysis. Since the properties of these organotin polymers are related to the distribution of monomer units, it is of great interest to determine the actual monomer reactivity ratios which control the sequence length distribution. Monomer reactivity ratios were calculated by the Kelen-Tudos method. All of these organotin polymers and copolymers were characterised by Nuclear magnetic resonance spectroscopy (NMR) and Fourier Transform infrared spectroscopy (FTIR) methods, gel permeation chromatograghy (GPC) and dynamic mechanical thermal analysis (DMTA).

Chapter 1

Introduction

1.1 Homopolymerisation of Monomers

1.1.1 Introduction

Polymers are macromolecules generated by joining together a large number of smaller molecular units (monomers). The overall reaction which combines these monomers is called polymerisation.[1] The classification used in the formative years of polymer science was due to Carothers and is based upon comparison of the molecular formula of a polymer with that of the monomer(s) from which it was formed. Condensation polymers are those which have repeat units with fewer atoms than were present in the monomers from which they were formed. This usually arises from chemical reactions which involve the elimination of a small molecule.[2]

The reaction time in the preparation of condensation polymers generally affects the molecular weights of the generated polymers. The polymer molecular weight rises steadily during the reaction. For example a polyester is formed by typical condensation reactions between bifunctional monomers, with elimination of water as in scheme (1.1).

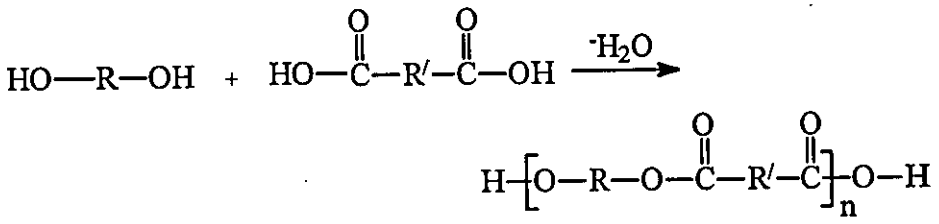

Scheme (1.1)

Addition polymers are those which have repeat units with identical molecular formulae to those of the monomers from which they are formed.[2] Polymers formed from the polymerisation of vinyl monomers are the most common in this class as shown in scheme (1.2).

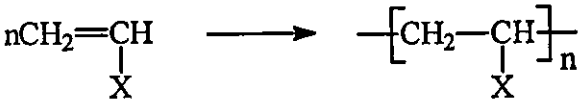

Scheme (1.2)

The reaction time in the preparation of addition polymers affects the number of polymer molecules, while it generally has little or no effect on the molecular weights of the generated polymers. Such polymers can have high average molecular weight at all percentages of conversion. The reaction mixture contains monomer and high molecular weight polymer with the monomer concentration decreasing with reaction time.[1]

The method of classification according to Carothers was found to be unsatisfactory when it was recognised that certain condensation polymers may be produced by methods typically used to prepare addition polymers.[2] A better basis for classification is provided by considering the underlying polymerisation mechanisms, of which there are two general types. Polymerisations in which the polymer chains grow step-wise by reactions that can occur between any two molecular species are known as step-growth polymerisations. Polymerisations in which a polymer chain grows only by reaction of monomer with a reactive end-group on the growing chain are known as chain-growth polymerisations, and usually require an initial reaction between the monomer and an initiator to start the growth of the chain.

Step polymerisation can be defined as follows:
Linear step polymerisation involves reactions of bifunctional monomers. Polycondensation involves reactions in which small molecules are eliminated, with for example the formation of linear polyester as mentioned before. If a trifunctional monomer was included, reaction at each of the three functional groups would lead initially to the formation of a branched polymer.

Chain polymerisation can be classified as follows:
a-Free radical polymerisation.
b-Ionic polymerisation includes cationic and anionic polymerisation.

The research in this thesis is concerned with chain polymerisation, and specifically with propagation of free radicals.

1.1.2 Effect of Substituents

Styrene type monomers can undergo chain type polymerisations using cationic, anionic or free radical initiators as the associated phenyl ring stabilises any positive / negative charge or radical, as indicated in scheme (1.3).[1] By comparison acrylamide- and acryloyloxy- derivatives of benzoic acid can stabilise a free radical on the side chain via conjugation with the aromatic ring, scheme (1.3), which can be accessed by the double bond character of the amidic C-N bond or ester C-O bond.[1,3]

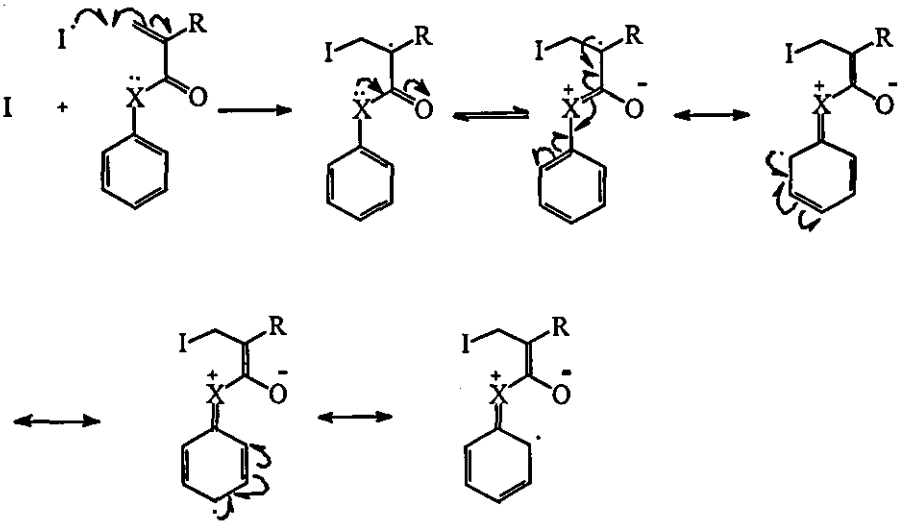

Scheme (1.3)

A tributyltin carboxylate in either the *ortho-* or *para-* position should in a radical initiated polymerisation decrease the reactivity by increasing resonance stabilisation through involvement of the electron withdrawing effect of the carboxylate substituent. On the other hand a similar substitution in the *meta-* position will, though to a lesser degree, stabilise the reactive radical species. This reduced stabilising effect leads to higher monomer reactivity when compared to *para-* and *ortho-* electron withdrawing substituents.

1.1.3 Free Radical Chain Polymerisation

Free radical polymerisation of alkene monomers was first observed in 1839[4,5] without recognising the nature of the reaction. However it was only through the work of Staudinger which began around 1920[6] that polymerisation reactions for producing chain molecules were first postulated.

A free radical is a molecular or an atomic reactive intermediate in which the normal bonding system has been modified such that each of the intermediates possesses an unpaired electron as in scheme (1.4).[7]

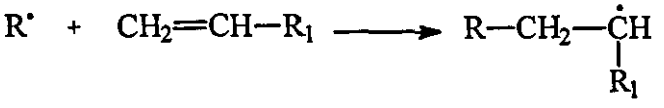

Scheme (1.4)

Polymerisation solvents include tetrahydrofuran, dioxane, toluene, and N,N-dimethylformamide (DMF). In this thesis DMF was used as solvent due to the high solubility of acrylamide- and acryloyloxy- derivatives and the resulting polymers in this solvent. The polymerisation process can be divided into 3 stages:

a-Initiation

Free radicals are generated by a variety of thermal, photochemical and redox methods.[1,6] In order to function as a useful source of radicals, an initiator system should be readily available, stable under ambient or refrigerated conditions and possess a practical rate of radical generation at moderate temperatures (<150°C). The initiator system used in this research was 2,2`-azobisisobutyronitrile (AIBN) which produced free radicals through thermal decomposition. A driving force for this decomposition is the production of stable nitrogen gas.[7]

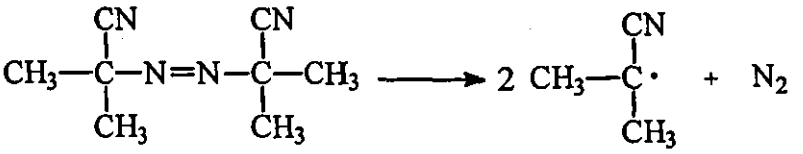

Scheme (1.5)

b-Propagation (Chain Growth)

This reaction involves the addition of a free radical to the double bond of a monomer molecule. The product must itself be a free radical and the process is then repeated.[7] There are three forms of monomer addition, namely: head to tail, head to head or tail to tail, the most likely form being head to tail.

The principal reason for head to tail addition, scheme (1.6), part (A), is the greater thermodynamic stability of a free radical, which can be explained by two factors: (i) a steric effect, as monomers used in addition polymerisation reactions are generally substituted at the head side with bulky groups (X) that hinder addition to another monomeric head as illustrated in scheme (1.6), part (B), (consequently, a steric effect minimises head to head polymerisation) and (ii) a resonance effect, as substituents on a monomeric head are normally efficient radical stabilisers (electron withdrawing groups), and accordingly, a radical should be more stable at the head than at the unsubstituted tail, which also increases the chance of head to tail addition, scheme (1.6), part (A), over tail to tail addition, scheme (1.6), part (C).

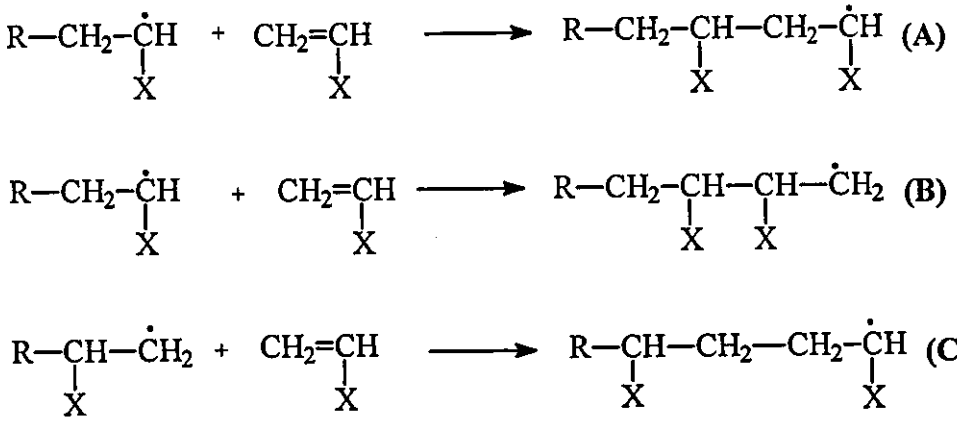

Scheme (1.6)

c-Termination

Free radical chains can be terminated by:

i) Reaction of an active chain end with an initiator radical, such a reaction being defined as primary radical termination.

ii) Interaction with impurities, e.g. oxygen, or inhibitors such as hydroquinone.[5] Such reactions can retard or stop polymerisation.

iii) Termination may occur either by combination, where two radicals can simply combine together to form a long chain or disproportionation, where a hydrogen atom can be transferred from one radical to the other giving two polymer molecules, one saturated and the other possessing an olefinic double bond at one end, as in scheme (1.7). It should be noted that in combination termination a polymer with two initiator fragments (R) per polymer molecule is produced, but disproportionation produces polymer molecules with a single initiator end group. Free radical polymerisations often terminate predominantly by combination rather than disproportionation.[1]

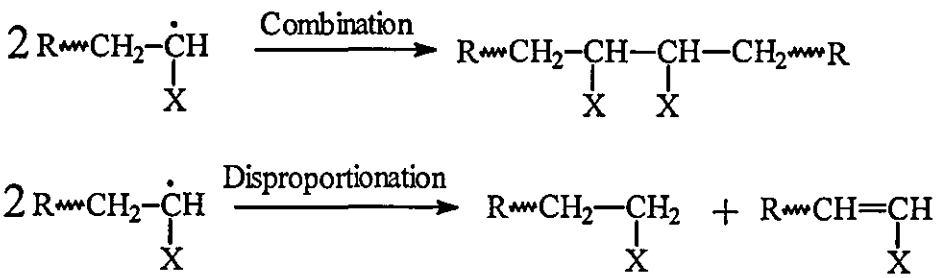

Scheme (1.7)

d-Chain transfer

In an ideal free radical polymerisation, chains become initiated, they propagate, and they are then terminated. The deviation from ideality occurs when a propagating oligomer or polymer radical reacts with another molecule, not by addition, but by abstraction hydrogen or chlorine, for example, from another molecule and thus becomes saturated, and the molecule from which the atom has been abstracted will then become a radical and start a new chain.[7] The chain reaction therefore continues, even though the chain growth of the first macromolecule has stopped. It has transferred the growth reaction to another molecule. This reaction is therefore called a chain transfer reaction, as in scheme (1.8).

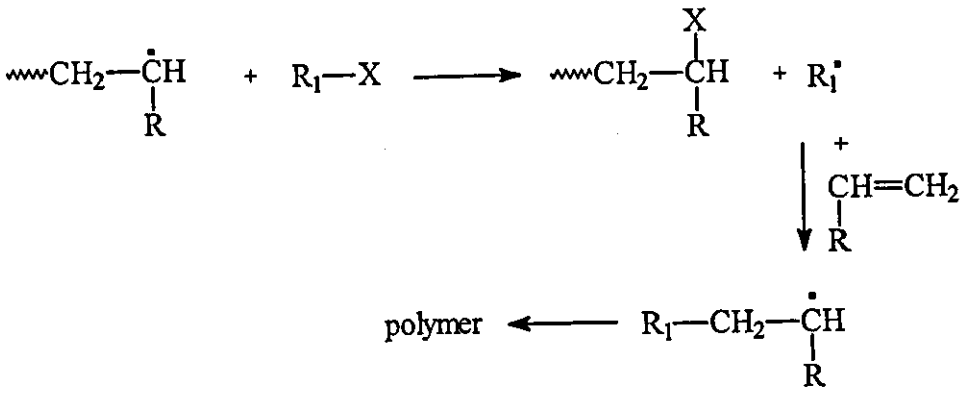

Scheme (1.8)

Chain transfer of this type may occur with initiator, monomer, or solvent. Shorter chain lengths result and hence, lower the number average molecular weight (M_n). Among the common initiators, hydroperoxides have a tendency to transfer reactions, whereas benzoyl peroxide, and especially AIBN, do not take part in transfer reactions.

1.1.4 Kinetics of Homopolymerisations

The three basic steps in the polymerisation process can be analysed to obtain equations that describe the kinetics of free radical polymerisation.

Initiation is a two stage reaction. Decomposition of initiator I

$$I \xrightarrow{k_d} 2\,R^{\bullet}, \quad \text{.....(1.1)}$$

is followed by attack of radical $R^{\bullet}$ on a monomer M to form a chain carrier $RM^{\bullet}$

$$R^{\bullet} + M \xrightarrow{k_i} RM^{\bullet} \quad \text{.....(1.2)}$$

The rate of initiation R_i (thermal initiation) is then the rate of production of chain radicals

$$R_i = \frac{d[RM^{\bullet}]}{dt} = 2\,k_d f\,[I] \quad \text{.....(1.3)}$$

where f represents the efficiency of conversion of these radicals into propagating chains and k_d and k_i are rate constants. Propagation is the addition of monomer to the growing radical

$$RM_n^{\bullet} + M \xrightarrow{k_p} RM_{n+1}^{\bullet} \quad \text{.....(1.4)}$$

where k_p is the rate constant for propagation. The rate of the bimolecular propagation reaction is assumed to be the same for each addition

$$R_p = k_p [M][M^{\bullet}] \quad \text{.....(1.5)}$$

where $[M^{\bullet}]$ represents the concentration of the propagating chains and $[M^{\bullet}]$ is usually low at any particular time. Termination is also a bimolecular process depending on $[M^{\bullet}]$. The rate of termination R_t is given by

$$R_t = 2k_t [M^{\bullet}][M^{\bullet}] \quad \text{.....(1.6)}$$

The rate constant k_t can be obtained from two possible mechanisms, combination or disproportionation. In the polymerisation of many monomers by the thermal decomposition of radical initiators, the mechanism is usually by combination.[5,8] A steady state is reached when the rate of radical formation is exactly counterbalanced by the rate of destruction.

$$R_i = R_t \quad \text{.....(1.7)}$$

For a polymerisation involving the thermal decomposition of a radical initiator, it follows from equations (1.3) and (1.6) that

$$2k_t [M^{\bullet}]^2 = 2k_d f [I] \quad \text{.....(1.8)}$$

Therefore, the radical concentration is given by

$$[M^{\bullet}] = \{ f k_d [I] / k_t \}^{0.5} \quad \text{.....(1.9)}$$

Because the radical concentration is too small to be determined in conventional polymerisation experiments, it is replaced in equation (1.5) by substitution of equation (1.9), giving

$$R_p = k_p \{ f k_d [I] / k_t \}^{0.5} [M] \quad \text{.....(1.10)}$$

Therefore, the rate of polymerisation is proportional to the monomer concentration and to the square root of the initiator concentration, if f is high. For a low efficiency initiator, f becomes a function of $[M]$, and the rate is proportional to $[M]^{1.5}$.

The kinetic chain length $\bar{\nu}$ is a measure of the average number of monomer units reacting with an active centre and is given by

$$\bar{\nu} = \frac{R_p}{R_i} = \frac{R_p}{R_t} = k_p^2[M]^2 / 2k_t R_p \quad \text{.....(1.11)}$$

For termination by combination under steady state conditions, it follows that $\bar{\nu}$ is related to the average degree of polymerisation $\bar{X}_n$ by

$$\bar{X}_n = 2\bar{\nu} \quad \text{.....(1.12)}$$

where $\bar{X}_n$ is given by

$$\bar{X}_n = \bar{M}_n / M_o \quad \text{.....(1.13)}$$

where $\bar{M}_n$ is the number average molecular weight and M_o is the molecular weight of the monomer.

Therefore, the kinetic chain length is inversely proportional to the rate of polymerisation. From an analysis of the temperature dependence of the rate of polymerisation, it follows that the rate of polymerisation will increase and the kinetic chain length will decrease on raising the temperature. The kinetic chain length is also inversely proportional to initiator concentration. Therefore, increasing the initiator concentration will decrease the kinetic chain length (i.e. molecular weight).

1.2 Copolymerisation Reactions of Monomers

1.2.1 Free radical copolymerisation

Free radical copolymerisation may be defined as a process where two or more monomers are integral parts of a high polymer via a radical chain reaction. A copolymer is the product resulting from such a process. The importance of free

radical copolymerisation is as a method for modifying the properties of polymers. Hard polymers, such as PVC, can be made softer by copolymerisation with monomers whose homopolymers are rubber-like, such as a vinyl ether or an acrylic ester. There is a series of monomers, such as maleic anhydride, fumarates, maleates, and vinyl ethers, which by themselves do not polymerise or only polymerise slowly by radical mechanisms, that are often used as components of copolymerisation and which copolymerise by a radical mechanism. Copolymerisation is one of the most important methods of introducing variety into the structure of polymer chains.

1.2.1.1 Copolymer composition equation

The composition of the copolymer molecules which are formed at a given time in a mixture of two monomers depends on the relative rates with which the two kinds of monomer units enter a copolymer molecule. When the rate at which a monomer adds to the polymer chain depends only on the monomer unit at the end of the chain and not on the next to last monomer unit, the composition of the copolymer is determined by the molar composition of the mixture of the monomers and by the rate constants of the following four reactions[1,5]:

$$M_1^{\bullet} + M_1 \xrightarrow{k_{11}} M_1^{\bullet} \quad \text{..... (1-14)}$$

$$M_1^{\bullet} + M_2 \xrightarrow{k_{12}} M_2^{\bullet} \quad \text{.....(1-15)}$$

$$M_2^{\bullet} + M_1 \xrightarrow{k_{21}} M_1^{\bullet} \quad \text{.....(1-16)}$$

$$M_2^{\bullet} + M_2 \xrightarrow{k_{22}} M_2^{\bullet} \quad \text{..... (1-17)}$$

where k_{11} is the rate constant for a propagating chain ending in $M_1^{\bullet}$ when monomer M_1 adds to a radical chain ending in $M_1^{\bullet}$, k_{12} is the rate constant for the reaction in which monomer M_2 adds to a radical chain ending in $M_1^{\bullet}$ etc. The composition of the copolymer that is formed can be related to the concentration of the two monomers in the feed. From the copolymerisation reactions (1-14) to (1-17), monomers M_1 and M_2 are consumed in these reactions as follows:

$$-d[M_1]/dt = k_{11}[M_1^{\bullet}][M_1] + k_{21}[M_2^{\bullet}][M_1] \text{.....(1-18)}$$

$$-d[M_2]/dt = k_{22}[M_1^{\bullet}][M_2] + k_{12}[M_1^{\bullet}][M_2] \quad \text{.....(1-19)}$$

The ratio of the concentrations of the two monomers incorporated into the copolymer in an infinitesimal period of time is given by dividing equation (1-18) by equation (1-19) to obtain:

$$\frac{d[M_1]}{d[M_2]} = \frac{k_{11}[M_1^{\bullet}][M_1] + k_{21}[M_2^{\bullet}][M_1]}{k_{12}[M_1^{\bullet}][M_2] + k_{22}[M_2^{\bullet}][M_2]} \quad \text{.....(1.20)}$$

where $\frac{d[M_1]}{d[M_2]}$ is the ratio of the rates of entry of monomers 1 and 2 into copolymer chains. Assuming a stationary state concentration of $[M_1^{\bullet}]$ and $[M_2^{\bullet}]$, that is, the rates of conversion of $M_1^{\bullet}$ to $M_2^{\bullet}$ and $M_2^{\bullet}$ to $M_1^{\bullet}$ are equal, then:

$$k_{21}[M_2^{\bullet}][M_1] = k_{12}[M_1^{\bullet}][M_2] \quad \text{.....(1-21)}$$

Substituting this result in equation (1-20) gives the copolymer composition equation as:

$$\frac{d[M_1]}{d[M_2]} = \frac{[M_1]}{[M_2]} \times \frac{(r_1[M_1] + [M_2])}{(r_2[M_2] + [M_1])} \quad \text{.....(1-22)}$$

This equation relates the copolymer composition to the comonomer concentration in the feed. The ratios k_{11}/k_{12} and k_{22}/k_{21} are defined by r_1 and r_2 respectively and termed the monomer reactivity ratios which measure the relative affinities of different monomers for the same radical. The copolymerisation equation can also be rearranged in terms of mole fraction instead of concentration as:

$$F_1 = \frac{r_1 f_1^2 + f_1 f_2}{r_1 f_1^2 + 2 f_1 f_2 + r_2 f_2^2} \quad \text{.....(1-23)}$$

where: F_1= mole fraction of monomer unit M_1 in copolymer

f_1= mole fraction of monomer M_1 in feed.

1.2.2 Types of copolymerisation behaviour

From the copolymerisation equations (1.14-1.17) if $k_{11}>k_{12}$ and $k_{22}>k_{21}$ copolymerisation would be insignificant and a mixture of homopolymers and / or block copolymer should be obtained. If $k_{12}>k_{11}$ and $k_{21}>k_{22}$ then copolymers with an alternating sequence will be formed. If $k_{12} = k_{11}$ and $k_{21} = k_{22}$, the frequency with which monomer M_1 or M_2 adds to the chain end is determined by monomer concentration leading to an ideal copolymerisation. These copolymerisations can also be classified by whether the product of the two monomer reactivity ratios r_1r_2 is unity, less than unity, or greater than unity as follows:

a-when $r_1r_2 = 1$. The two types of propagating species $M_1^{\bullet}$ and $M_2^{\bullet}$ show the same preference for adding one or the other of the two monomers, and the monomer units will be incorporated in a random manner influenced by the feed composition. Thus, substituting $r_2=1/r_1$, equations (1-22) and (1-23) simplify to:

$$\frac{d[M_1]}{d[M_2]} = r_1\frac{[M_1]}{[M_2]} \quad \text{.....(1-24)}$$

and

$$F_1 = \frac{r_1 f_1}{r_1 f_1 + f_2} \quad \text{.....(1-25)}$$

b-when $r_1r_2 < 1$. This is the case when r_1r_2 decreases from unity towards zero. Most radical copolymerisations lie between the two extremes of ideal and alternating behaviour. The alternation tendency is measured by the tendency of r_1r_2 product to approach zero. In this case, when r_1 and r_2 are both less than unity, the copolymerisation shows an azeotropic composition at which the copolymer and the feed compositions are the same, and the copolymerisation occurs without change in the feed composition. Solution of equation (1.22) with $d[M_1]/d[M_2]=[M_1]/[M_2]$ gives:

$$\frac{[M_1]}{[M_2]} = \frac{1-r_2}{1-r_1} \quad \text{.....(1-26)}$$

By substitution in equation (1-23) one gets:

$$F_1 = f_1 = \frac{1-r_2}{2-(r_1+r_2)} \quad \text{.....(1-27)}$$

c-when $r_1r_2 > 1$. This is a rare case and if it exists, it leads to the synthesis of blocks in copolymers and / or a mixture of the homopolymers.

1.2.3 Methods of calculating monomer reactivity ratios

All methods for the determinations of monomer reactivity ratios involve the experimental determination of the copolymer composition formed from several different feed compositions. The techniques used for quantitative determination of copolymer composition include elemental analysis, radioisotopic labeling and ultraviolet, infrared and nuclear magnetic spectroscopy methods. All procedures depend on copolymerisations carried out to low degrees of conversion and the experimental data can be analysed in several ways. The more established procedures involving determination of monomer reactivity ratios are:

a-Intersection method

This method, originated by Mayo and Lewis[9], describes the development of a theoretical basis for comparing the behaviour of monomers in copolymerisation for addition (vinyl) polymerisation, and the application of the general concept to the copolymerisation of styrene and methyl methacrylate by a free radical mechanism.

This method depends on the copolymerisation equation(1.22), which can be expressed in terms of molar ratios instead of concentrations as:

$$b = \frac{r_1 a + 1}{r_2 / a + 1} \quad \text{.....(1-28)}$$

where $a = [M_1]/[M_2] = f_1/(1-f_1)$ and $b = d[M_1]/d[M_2] = F_1/(1-F_1)$. Data for the feed and copolymer compositions for each experiment with a given feed are substituted into equation (1.28) and r_2 is plotted as a function of various assumed values of r_1. Each experiment yields a straight line and the intersection of the lines for different feeds gives the best values of r_1 and r_2. Any variations observed in the points of intersection of various lines are a measure of the experimental errors in the composition data and the limitations of the

mathematical treatment. The composition data can also be treated by linear least-squares regression analysis instead of the graphical analysis.

The disadvantages of this method include:

1-The reproducibility of the result and the size of the triangular intersection obtained in an experiment depend on both the procedure for isolating the polymer and the precision of the carbon analysis.

2-Extensive calculations are required, and only a qualitative measure of the precision of the estimates r_1 and r_2 is provided.

3-The observer is required to subjectively weight the data, a task not consistently done even by the same observer.

b-Fineman-Ross method

The method of Fineman and Ross[10] represents a considerable improvement in the direction of straightforward analysis of copolymerisation data. It involves carrying out the copolymerisations to low conversions and using the approximate form of equation (1.23) . The ratios r_1 and r_2 may then be obtained graphically from the initial and final slopes of the usual copolymerisation curve in which the polymer composition is plotted against the monomer composition. By defining $a=[M_1]/[M_2]=f_1/(1-f_1)$ and $b=d[M_1]/d[M_2]=F_1/(1-F_1)$ then equation (1.28) can be rearranged to

$$a-\frac{a}{b}=r_1\frac{a^2}{b}-r_2 \qquad \text{.....(1.29)}$$

Therefore, a plot a -a/b as ordinate and a^2/b as abscissa is a straight line whose slope is r_1 and whose intercept is minus r_2. The disadvantages of this method include:

1-Large uncertainties in the slopes, and consequently in the r_1 and r_2 values, may occur, particulary in those cases where the slopes are steep or where experimental data at very low and very high concentration ratios are unavailable.

2-The reliability of the determined values can be increased by a tedious method of calculating theoretical curves for pairs of values of r_1 and r_2 and fitting them to the experimental curves.

c-Tidwell-Mortimer method

Tidwell and Mortimer[11] pointed out that reactivity ratios should be determined by a non-linear regression technique and that the error associated with the estimates of r_1 and r_2 was a joint error which should be expressed as a joint confidence region. Many reactivity ratios are determined by a set of experiments where the monomer feed ratios are varied. However, Tidwell and Mortimer[12] used a different approach based on the statistical design of experiments using the instantaneous copolymer composition equation and a non-linear least squares estimation. They recommended an experimental design which involved doing a number of experiments at two compositions of monomer only defined by:

$$F_a = \frac{2}{2 + r_1} \quad \text{.....(1.30)}$$

and

$$F_b = \frac{r_2}{2 + r_2} \quad \text{..... (1.31)}$$

where F_a and F_b are the comonomer feed ratios. The r_1 and r_2 values used to define these feed compositions were estimates based on preliminary experiments and chemical intuition. However, this method requires tedious computerised procedures.

d-Kelen-Tudos method

This method proposed by Kelen and Tudos[13] for calculating the monomer reactivity ratios is based on a new graphically linear equation as follows:

$$\eta = \left(r_1 + r_2 / \alpha\right)\xi - \left(r_2 / \alpha\right) \quad \text{.....(1.32)}$$

where

$$\eta = \frac{a(b-1)}{\alpha b + a^2}, \quad \xi = \frac{a^2}{\alpha b + a^2} \quad \text{and} \quad \alpha = \frac{a_{\min} \times a_{\max}}{\left(b_{\min} \times b_{\max}\right)^{\frac{1}{2}}}$$

where $a = [M_1]/[M_2] = f_1/(1-f_1)$ and $b = d[M_1]/d[M_2] = F_1/(1-F_1)$

The variable ξ cannot take any positive value, only those in an interval of $\xi = 0$ to $\xi = 1$. Thus, plotting the η values as a function of $\xi = 0$ to $\xi = 1$ gives $-r_2/\alpha$ and r_1, respectively (both as intercepts).

Advantages

1-An arbitrary positive constant α is introduced to spread the data more evenly so as to give equal weighting to all data points.

2-Re-indexing of the monomers and reactivity ratios does not change the calculated results.

3-The method allows visual estimation of the fact whether the copolymer composition equation (1.22) is adequate for the experimental data in a given system.

4-The linearity of the plot made with equation (1.32) may be used as a test for the assumptions required in the derivation of equation (1.22) for copolymer composition.[14] Examples of curved plots according to equation (1.32) have been identified for cationic copolymerisation systems so that the approximations implicit in the conventional copolymer composition equation do not hold.[15]

1.2.4 Determination of Q-e Parameters for Monomers

Monomer reactivity ratio values, r_1 and r_2 describe the relative tendency of two monomers to add to a particular growing chain. The reactive end of the growing chain is a free radical derived from one of the two monomers, and two types of reactive ends can exist. Because the values obtained experimentally are relative values, they pertain only to one particular pair of monomers. One approach to developing such correlation takes into account the resonance and polar factors inherent in the monomers and is called the Alfrey-Price Q-e relationship.[16] Q is a measure of the resonance stabilisation of monomer and corresponding radical, and *e* describes the polarity interaction of radical and molecule. The relationship between these parameters and actual reactivity ratio was proposed to be:

$$r_1 = \frac{k_{11}}{k_{12}} = \left(\frac{Q_1}{Q_2}\right)\left[\exp -e_1\left(e_1 - e_2\right)\right] \quad \text{.....(1.33)}$$

$$r_2 = \frac{k_{22}}{k_{21}} = \left(\frac{Q_2}{Q_1}\right)\left[\exp -e_2\left(e_2 - e_1\right)\right] \quad \text{.....(1.34)}$$

$$r_1 r_2 = \exp -\left(e_1 - e_2\right)^2 \quad \text{.....(1.35)}$$

$$\ln r_1 r_2 = -\left(e_1 - e_2\right)^2 \quad \text{.....(1.36)}$$

Price chose styrene as the standard monomer with the value Q =1 and e = -0.80. The Q and e values of any monomer that has been copolymerised with styrene can be calculated from r_1 and r_2 values given in the literature. Conversely, knowing the Q and e values for any two monomers the r_1 and r_2 values can be calculated for a monomer pair, whether or not they have ever been copolymerised. While the predicted behaviour is not always exactly the same as the experimental result, the Alfrey-Price scheme nevertheless leads to a good approximation. The major shortcoming of the Q-e scheme is that all radical polymerisations involve not only resonance and polar factors, but also, steric factors. It is certainly conceded that steric factors limit the applicability of the scheme which is an empirical method of correlation.

1.2.5 Radical and Monomer Reactivities in Free Radical Copolymerisation

The monomer reactivity ratios are useful for a study of the relation between structure and reactivity in radical addition reactions. The reactivity of a monomer toward a radical depends on the reactivities of both the monomer and the radical. The relative reactivities of monomers and their corresponding radical can be obtained from an analysis of the monomer reactivity ratios.[17] The reactivity of a monomer can be seen by considering the inverse of the monomer reactivity ratio (1/r). The inverse of the monomer reactivity ratio gives the ratio of the rate of reaction of a radical with another monomer to its rate of reaction with its own monomer[1]

$$\frac{1}{r_1} = \frac{k_{12}}{k_{11}} \quad \text{.....(1.37)}$$

1.2.5.1 Factors affecting the monomer reactivity

a-Resonance Effects

The reactivity of monomers depends on the resonance stabilisation of the radical produced from the monomer. Delocalisation of π-electrons improves resonance stabilisation.[1] The order of substituents in enhancing radical reactivity is opposite to that for monomer reactivity. A substituent which increases monomer reactivity does so because it stabilises and decreases the reactivity of the corresponding radical.

b-Steric Effects

The rates of radical-monomer reactions are also dependent on steric hindrance. For example, compared to vinyl chloride (I), the reactivity of vinylidene chloride (II) increases, whereas the reactivity of 1,2-dichloroethene (III) decreases.[1] The former effect is due to increased stabilisation of the resulting radicals due to two Cl substituents, whereas the latter effect is a result of steric hindrance between the monomer and the radical to which it is adding.

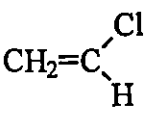

I

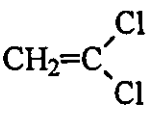

II

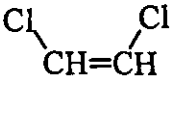

III

A comparison of *cis*- and *trans*-1,2- dichloroethene shows the trans isomer to be the more reactive by a factor of 6.[1] The difference in reactivity has been attributed to the inability of the cis isomer to achieve a completely coplanar conformation in the transition state.

c-Alternation (Polar Effect)

The significant conclusion is that the tendency toward alternation increases as the difference in polarity between the two monomers increases. Monomers with electron donating and electron withdrawing substituents have widely differing polarities and, when copolymerised with each other, can produce highly alternating copolymers.[18] The addition of a Lewis acid, such as

trialkylaluminium, can increase the tendency to form alternating copolymers, even between monomers which do not normally copolymerise in an alternating fashion.[19,20]

d-Solvent Effects

Free radical copolymerisations are generally carried out in solution. Copolymerisations involving non-polar monomers with monomers containing ionisable groups, groups capable of hydrogen bonding interactions or even polar groups may show a marked influence depending on the nature of the solvent.[21] This will give rise to changes in measured reactivity ratios varying with solvent.

Harwood[22] found that, although the reactivity ratios may vary considerably as the reaction solvent is changed, copolymers with identical compositions had the same microstructure. Harwood proposed that the partitioning of monomers between solvent and growing radicals was important. The reactivity ratios determined for polar monomers were products of the true reactivity ratios and the partition coefficients. The reactivity ratios are therefore independent of solvent but the solvent will influence the relative local concentrations of the comonomers to the growing chain end.

1.3 Gel Permeation Chromatography

In gel permeation chromatography[23] molecules are separated on the basis of size alone. The separation takes place in a column packed with beads of a rigid porous gel (usually highly crosslinked polystyrene). The pores in the gel are of similar dimensions to the polymer molecules.

A sample of the polymer in dilute solution is introduced into a solvent stream flowing through the column. As the polymer molecules flow past the porous beads, they can diffuse into the pores of the gel defined as the stationary phase, to an extent that depends on molecular size and the size distribution of the pores. Smaller molecules are able to diffuse into the pores to a greater extent than larger molecules and are therefore retained on the column for longer times.

It follows that larger molecules pass from the column first and have shorter retention times than smaller molecules.

The mobile phase should be chosen carefully. It must completely dissolve the polymer sample, be low enough in viscosity to operate in a normal pressure range, effectively prevent the polymer molecules from interacting energetically with the stationary phase, and permit the polymer to generate an adequate detector response due to a refractive index difference.

The packing material of the stationary phase should not interact chemically with the solute. It should be rendered completely wet by the mobile phase, be stable at the required operating temperature, and have sufficient pore volume and an adequate range of pore sizes to resolve the components of the molecular weight distribution in the sample. Use of excessively large sample volumes can lead to significant peak broadening, resulting in loss of resolution and errors in molecular weight measurement. Sample concentration should be minimised consistent with the sensitivity of the concentration detector employed. The use of high sample concentrations can result in peak shifts to higher retention volumes or band broadening, or even spurious shoulders appearing on the tail of the peak. Another unwanted viscosity effect, that results in higher retention volumes and lower molecular weights, is the shear degradation of high molecular weight polymers at high flow rates. It can be avoided by minimising the flow rate.[24]

1.4 The Glass Transition

When a high molecular weight amorphous polymer in its liquid or rubbery state is cooled, at some temperature, called the glass transition temperature (T_g), the physical and the mechanical behaviour of the polymer will be transformed to that of a rigid glassy material. At this temperature there is a marked change in the temperature dependence of volume (V) and enthalpy (H), as shown in figure (1.1). There is also a discontinuity in the temperature dependence of heat capacity ($C_p = dH/dT$) and expansion coefficient (dV/dT) at the T_g. The position

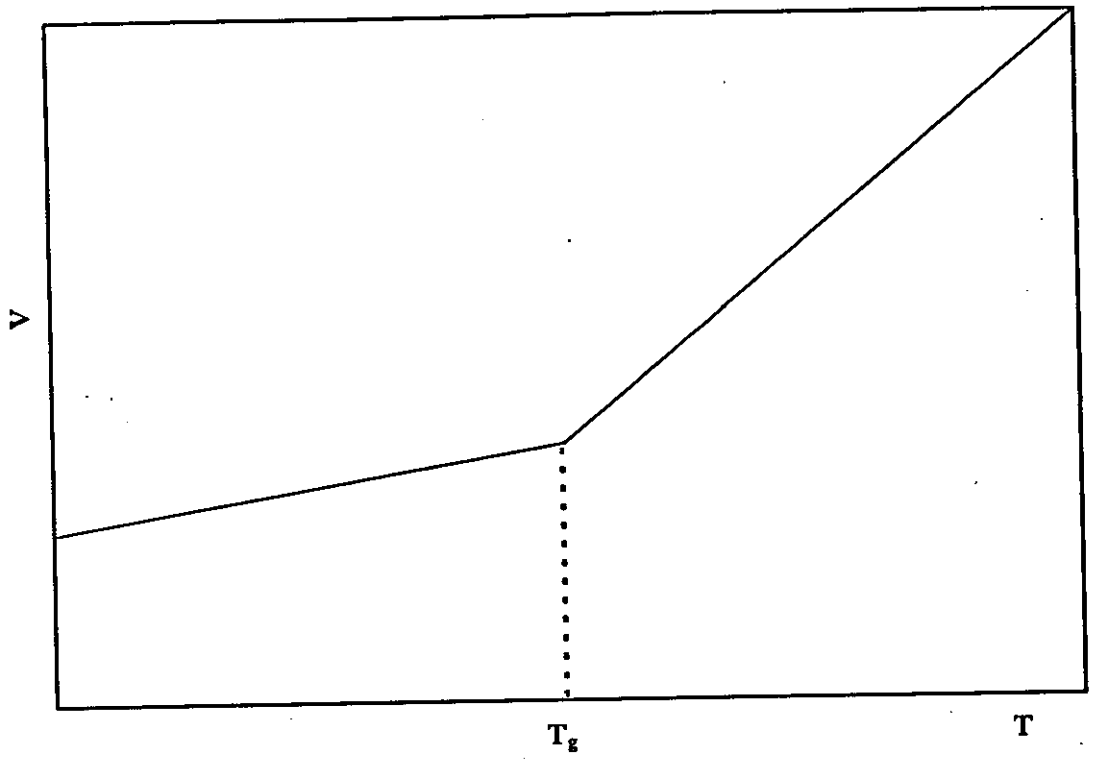

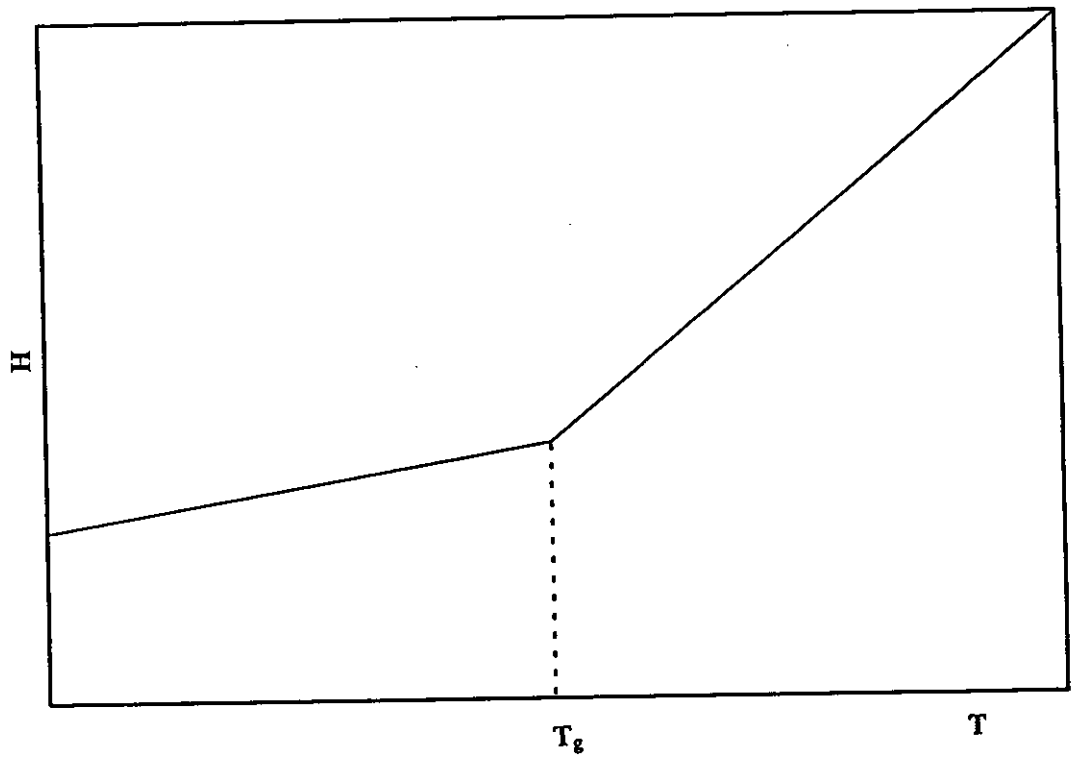

Fig. 1.1 Volume and Enthalpy vs Temperature
Showing Discontinuity at T_g

of the T_g depends on the rate of cooling, with different cooling rates leading to different observed T_g transitions, each reflecting a difference in the nature of the glassy phase formed.

The glass transition temperature can be defined as the temperature at the point of intersection of the extrapolated curves for the melt and glassy phases when quantities such as volume and enthalpy are plotted against temperature. In terms of molecular behaviour T_g is defined as the temperature above which the polymer has acquired sufficient thermal energy for conformational changes due to rotation about bonds in the backbone of the chain. Thus, at and above the glass transition chain segments of polymer molecules begin to participate in general motion. Fox and Flory[25] and Ueberreiter and Kanig[26] suggested that since the free volume increases with rising temperature due to thermal expansion, the glass transition temperature will occur when the fraction of the total volume which is free volume reaches a certain critical value see figure (1.2).

This suggests that the transition temperature and the free volume fraction are intimately connected, and any factor which controls the free volume of a polymer at constant temperature affects the value of T_g. Conformational changes are, therefore, movements of chain segments into free volume. The greater the free volume, the greater the extent of molecular motion possible. The glass transition temperature is the point below which there is insufficient free volume for significant molecular motion to be possible, and so below this temperature the conformational structures of the chains are frozen in.

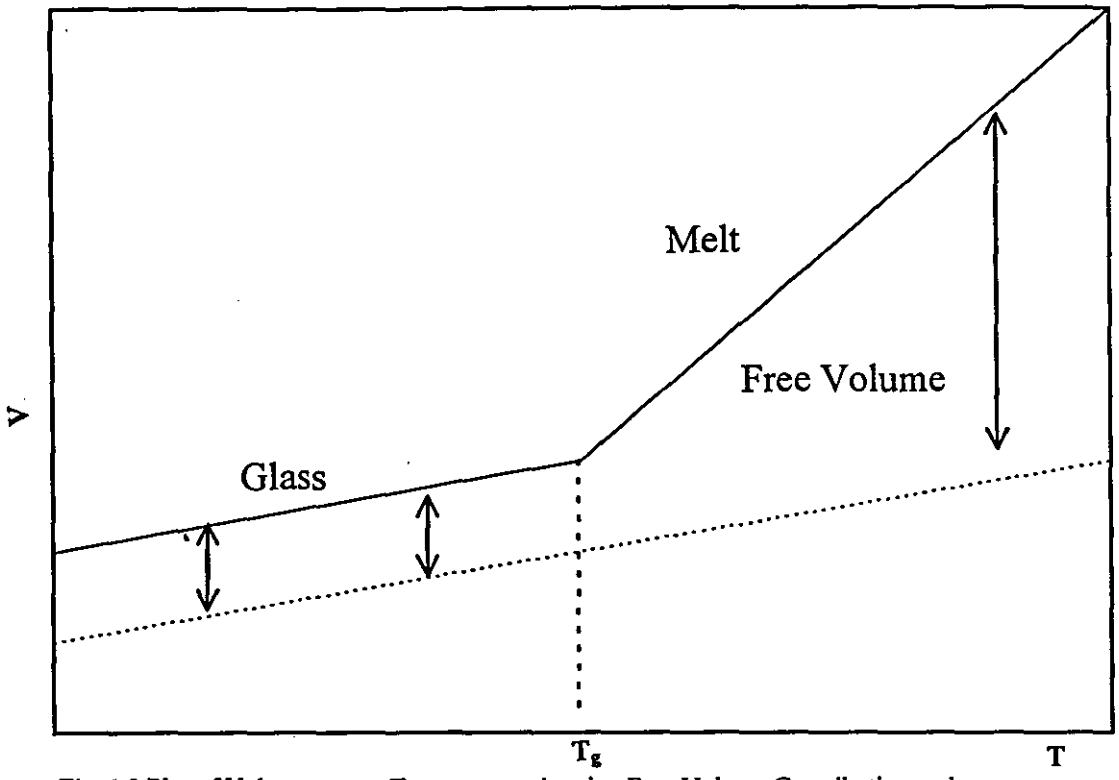

Fig. 1.2 Plot of Volume versus Temperature showing Free Volume Contribution and Location of T_g.

1.4.1 Factors which effect the Glass Transition Temperature

a-Chemical Structure

There are several structural factors which influence the T_g of a polymer, one of the most important being the flexibility of the backbone chain. A polymer having a structure which allows easy rotation around main chain bonds will have a lower T_g than one where such rotations are restricted leading to hindered conformational changes. Side groups also influence the position of the glass transition. For example, poly(methyl acrylate) (poly(MA)) has a T_g of 10°C, whereas poly(methyl methacrylate) (poly(MMA)) has a T_g of 110°C.[27] The methyl group tends to hinder rotation about the main chain leading to a stiffer material and higher T_g. However, in some cases side groups can have the reverse effect. For example, in the following series of poly(acrylates) their respective glass transition temperatures poly(MA) T_g 10°C, poly(ethyl acrylate) (poly(EA)) T_g -24°C, poly(propyl acrylate) (poly(PA)) T_g -37°C and poly(n-butyl acrylate) (poly(BA)) T_g -54°C[27] indicate that as the size of the side groups is increased the

T_g decreases. This is due to an increase in free volume caused by poorer chain packing as the size of the side group increases.

The symmetry of the repeating unit in a polymer chain can also affect the T_g. One example of this type of effect is the variation in T_g between poly(propylene) T_g -8°C and poly(iso-butylene) T_g -50°C.[28] The decrease in T_g caused by the second methyl group can be explained in terms of the energy barriers to rotation between the various conformational isomers. In poly(iso-butylene) the energy barriers between each conformational isomer are approximately equal, because of the symmetry of the carbon atom to which they are attached. This means there is no preferred isomer. This is not true for poly(propylene), where one of the three possible rotational states is of a higher energy than the other two. Therefore, rotation to this conformational isomer is not favourable. This causes a decrease in the tendency to free rotation and this in turn leads to a higher T_g for poly(propylene) than for poly(iso-butylene).

The polarity of substituents also appears to have an effect on the T_g. Polymers having polar groups attached to the chain tend to have higher values of T_g than analogous polymers having no polar groups.

b-Crosslinking

Polymers with strong intermolecular bonds, e.g. chemical crosslinks or hydrogen bonds, exhibit higher values of T_g. Crosslinking reduces free volume and increases T_g.

c-Molecular Weight

For high molecular weight polymers, the T_g is effectively independent of molecular weight. However, the T_g of shorter chain polymers decreases with chain length. For example, the T_g of poly(styrene) with M_n =3000 is 43°C, whereas with M_n =300,000 it is 99°C.[29] This dependence is a result of the contribution of chain end segments to molecular motions, with end groups having somewhat higher free volume. Lower molecular weight polymers have a higher proportion of chain ends and hence free volume. Therefore, the T_g decreases as chain length decreases.

d-Copolymerisation

An amorphous random copolymer generally exhibits a single T_g. For a series of homogeneous copolymers or compatible polymer blends the T_g value is in the range between the values of the parent homopolymers. In many cases a plot of T_g against composition by weight for a series of copolymers lies below the straight line joining the transition temperatures of the two homopolymers.[30,31,32] The relation between glass transition temperature and copolymer composition can be described by the Fox equation.[30]

$$\frac{1}{T_g} = \frac{W_1}{T_{g1}} + \frac{W_2}{T_{g2}} \quad \text{.....(1.38)}$$

where T_{g1} and T_{g2} are the glass transition temperatures in degrees K of the pure homopolymers 1 and 2, respectively, with weight fractions of organotin polymer (W_1) and acrylic polymer (W_2). Equation (1.38) may be interpreted in terms of free volume based on the hypothesis that an amorphous melt on cooling transforms to a glassy solid at a particular fractional free volume (the iso-free volume treatment). For this iso-free volume concept for the glass transition and by assuming that each type of monomer unit retains its characteristic free volume in the copolymer above T_g, then T_g for a copolymer is given by:

$$\frac{1}{T_g} = \frac{1}{(W_1 + BW_2)}\left[\frac{W_1}{T_{g1}} + \frac{BW_2}{T_{g2}}\right] \quad \text{.....(1.39)}$$

In equation (1.39) *B* is a parameter in the theoretical treatment which takes values other than unity. When *B* is exactly unity, then equation (1.39) simplifies to equation (1.38).

1.5 Dynamic Mechanical Properties of Polymers

A material under the effect of an applied strain may be classified as perfectly elastic according to Hooke's Law, the applied strain being proportional to the stress. Perfectly viscous liquids may exhibit Newtonian behaviour, which states that stress is directly proportional to the rate of strain. Both are limiting laws, valid only for small strains or low rates of strain.[33] Polymers may exhibit the

characteristics of both a liquid and a solid when neither of the limiting laws will adequately describe the behaviour. Such materials are termed viscoelastic. One of the most important techniques for studying the viscoelastic behaviour of polymers is dynamic mechanical analysis, which usually entails the application of a sinusoidal load leading to a sinusoidal deformation, as shown in figure (1.3). The resulting strain is neither in phase with the stress (as in perfect elastic materials) nor 90° out of phase (as in perfectly viscous liquids); instead there is a phase lag δ (phase angle). Dynamic mechanical analysis is usually carried out in association with a heating programme as in dynamic mechanical thermal analysis (DMTA). It is possible to carry out the experiment at constant frequency whilst varying the temperature or vice versa. The stress (σ) resulting from the applied strain (γ) is measured and the time dependency of stress and strain can be written:

$$\gamma = \gamma_o \sin \omega t \quad \text{.....(1.39)}$$

$$\sigma = \sigma_o \sin(\omega t + \delta) \text{.....(1.40)}$$

where ω is the cyclic frequency and γ_o and δ_o are the strain and stress amplitudes. Equation (1.40) can be expanded to:

$$\sigma = \sigma_o \sin \omega t \cos\delta + \sigma_o \cos \omega t \sin \delta \text{.....(1.41)}$$

So it can be seen that stress is made up of two components, one which is in phase with strain (of magnitude $\sigma_o \cos \delta$) and one which is out of phase with strain (of magnitude $\sigma_o \sin \delta$).

The stress-strain relationship is therefore as follows:

$$\sigma = \gamma_o E' \sin \omega t + \gamma_o E'' \cos \omega t \text{.....(1.42)}$$

where the storage modulus E' is equal to $(\sigma_o/\gamma_o)\cos \delta$, that is the component of stress in phase with strain divided by the strain amplitude, and where loss modulus E'' is equal to $(\sigma_o / \gamma_o)\sin \delta$, the component of stress out of phase with strain divided by the strain amplitude.

Dividing the loss modulus by the storage modulus leads to the loss tangent:

$$\frac{E'}{E'} = \frac{(\sigma_o / \gamma_o)\sin\delta}{(\sigma_o / \gamma_o)\cos\delta} = \tan\delta \text{.....(1.43)}$$

This effectively means that tan δ is the ratio of energy stored to the energy lost per cycle. A complex modulus can be derived such that:

$$E^* = \sqrt{(E')^2 + (E'')^2} \quad \text{.....(1.44)}$$

This can be represented by an Argand diagram as in figure (1.4). Figure (1.5) shows the variation of E' and tan δ against frequency and temperature for a typical homopolymer in the region of its glass transition. At high frequencies and low temperature the storage modulus $E'g$ is characteristic of a glassy material. On decreasing the frequency or increasing the temperature, the storage modulus becomes characteristic of a rubbery material, the loss modulus in both cases having passed through its peak. The peak in tan δ corresponds to the maximum in the hysteresis or damping and is interpreted as occurring at the glass transition of the polymer.

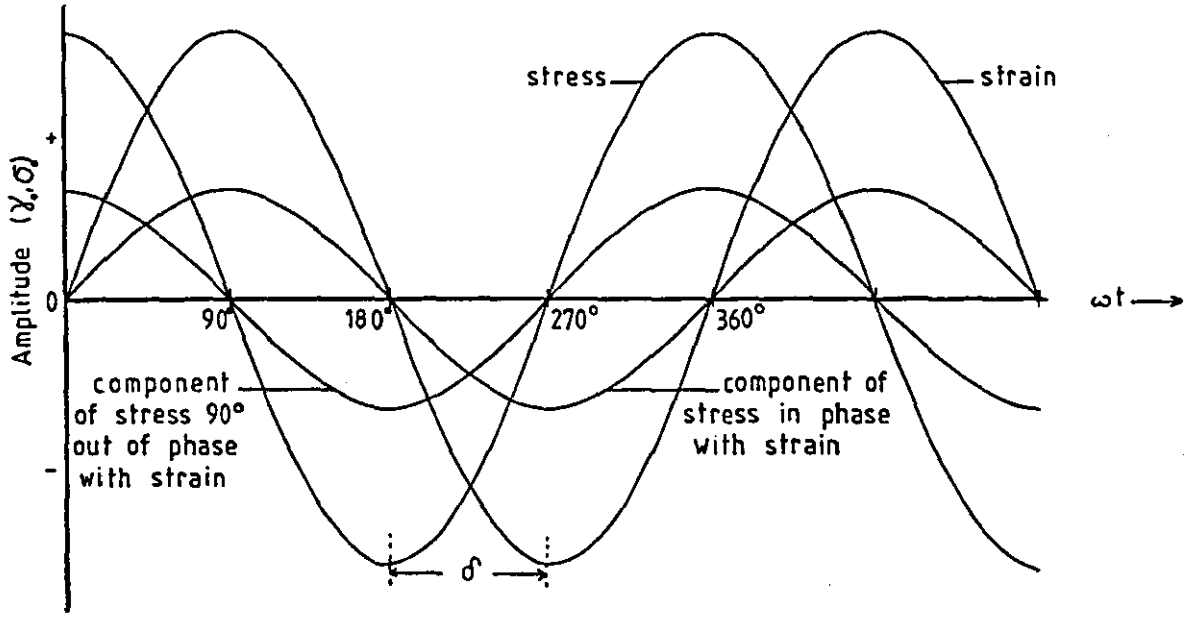

Fig. 1.3 The Relationship Between Stress and Strain in Dynamic Mechanical analysis

1.5.1 Factors Affecting Dynamic Mechanical Behaviour

The glass transition is the phenomenon often studied by this technique and the factors which affect the glass transition will correspondingly affect the dynamic mechanical properties observed. At high molecular weight, the T_g is more or less independent of molecular weight, but at lower chain lengths, decreasing the

molecular weight will cause the observed T_g to decrease. In dynamical mechanical terms, the tan δ peak and fall in loss modulus $E^{/}$ will be shifted to lower temperature at a given frequency for polymer with lower T_g.

Crosslinking tends to cause an increase in T_g, manifested in a shift to high temperature of the tan δ maximum and loss modulus curve. However, with very highly crosslinked networks, the storage modulus tends to be virtually temperature independent and no tan δ peak is observed.

In the region of rubber-like behaviour, at a temperature above T_g, the polymer may experience viscous flow and this results in a gradual decrease in $E^{/}$, due to a greater number of chain entanglements. Random or statistical copolymers are generally characterised by a single T_g and hence, a single tan δ peak at a temperature determined by the composition. A broadening of the peak may be observed if there are long sequences of a given comonomer unit.

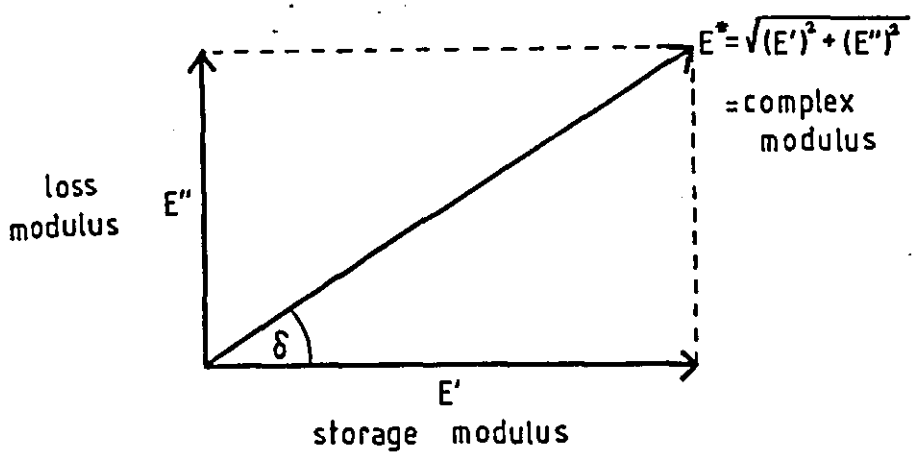

Fig. 1.4 Argand Diagram Relating $E,^{/}$ $E^{//}$ and δ

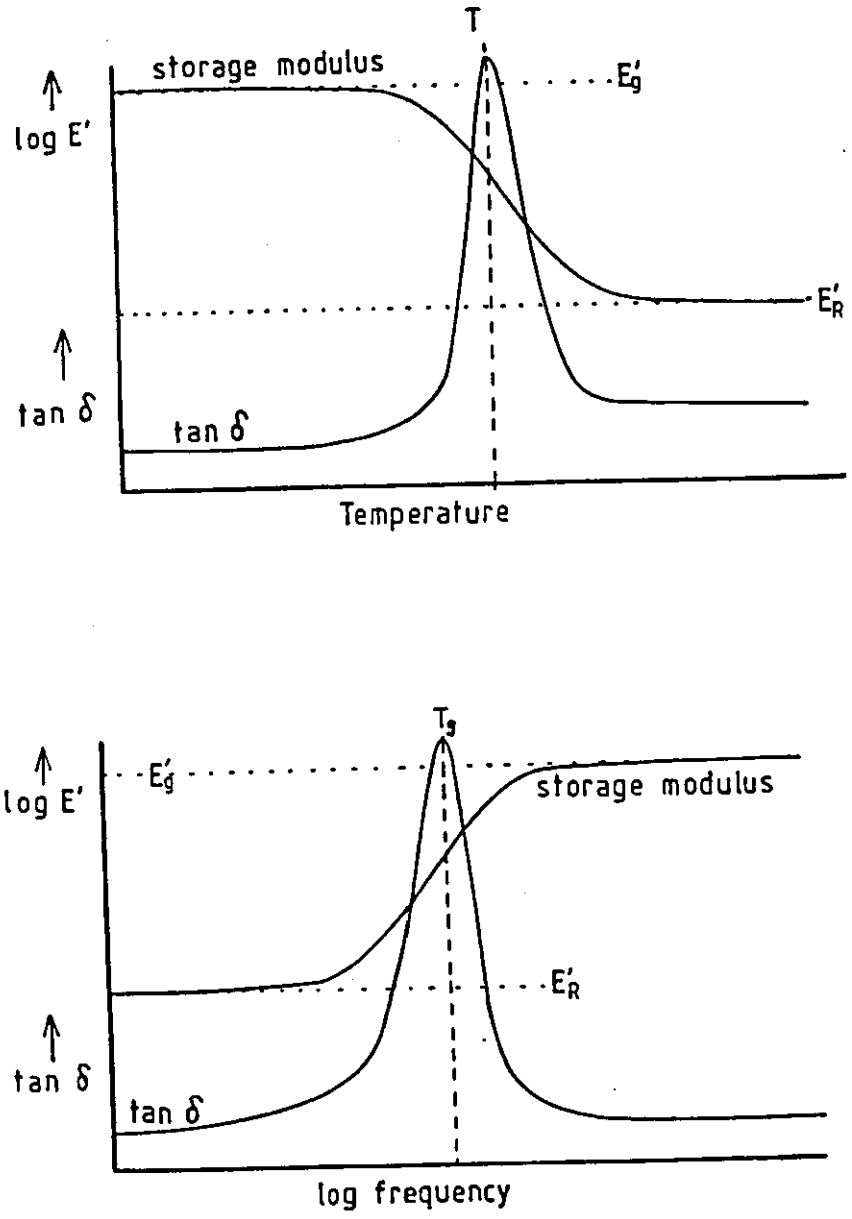

Fig. 1.5 The variation of E′ and tan δ against frequency and temperature

Chapter 2

Literature review

2.1 Acrylamides and methacrylamides

The acrylamide family of monomers is a highly versatile group of chemical intermediates, producing polymers and copolymers having a highly polar functional group attached to the backbone which have major uses. Linear poly(acrylamide) is a hard glassy solid, soluble in water and most aqueous solutions of electrolytes, but insoluble in all but the most polar organic solvents. By replacing one or both of the hydrogen atoms on the nitrogen atom by organic groups, products with increasing solubility in organic solvents and decreasing water solubility are obtained. Numerous copolymers of acrylamide and its derivatives have been prepared. Acrylamide polymers having ionic substituent groups are useful as polyelectrolytes.[34]

Acrylamide monomers contain two functional groups, the double bond and the amide group. The reaction of the double bond is characteristic of an electron deficient bond. Nucleophilic reagents add readily to both acrylamide and methacrylamide. Acrylamide and related monomers have been polymerised by free radical and by ionic initiators. Free radical initiated systems in aqueous media are the most common for acrylamide and methacrylamide. Free radical polymerisations of N-substituted acrylamides proceed at much lower rates than for acrylamide.[34]

The retarding effect of the N-alkyl substituent is primarily steric and has been ascribed to suppression of both the rate constant for propagation k_p and the rate constant for termination k_t by the alkyl group. N,N-disubstituted methacrylamides are so hindered by steric effects and the polar effects of the substituents that they are not susceptible to polymerisation.[35,36] Poly(-N-methylacrylamide) and low molecular weight poly(-N,N-dimethylacrylamide) are soluble in water.

The copolymerisation of acrylamide and methacrylamide occurs readily with acrylates, methacrylates, and most styrene derivatives but acrylamide and methacrylamide do not copolymerise readily with vinyl halides.[34] The amide group is electron withdrawing and activates the double bond. Increasing alkyl

substitution on the nitrogen atom causes the reactivity of the amide radical to decrease and the polarity of the double bond to become less positive. Increasing the size of the alkyl substituent causes a small decrease in reactivity[37,38], but increasing the bulkiness of the group improves reactivity.[39] The effects of an N-alkyl substituent on methacrylamide are similar to those on acrylamide.[40] The non-ionic, anionic, and cationic acrylamide polymers have been used for many industrial applications. However, size exclusion chromatography is not easily carried out for acrylamide polymers because of the high molecular weight (10^6-10^7 g /mole) and the polyelectrolyte characteristics of the charged polymers.[41]

2.2 Organotin polymers

In the past 30-40 years a number of new polymers containing metals as an integral part of the repeating structure unit have been prepared and their properties studied.[42] There is a current trend away from the use of organolead and organomercury compounds due to their high mammalian toxicity and their relatively adverse effects on the environment.

Organotin compounds are eventually degraded in nature to give non-toxic inorganic tin residues.[43,44] Organotin polymers may be classified as substances containing tin atoms, bound to carbon, in the main chain or pendant in side chains.

The actions of organotin compounds towards fungi, bacteria, and insects have been studied. The most important of these is the use of organotin compounds as fungicides in agriculture and applications in antifouling coatings and wood preservation.[45]

Montemarano and Dyckman[46] reported that the incorporation of such biocidal organotin compounds in polymeric side chains, such as polymethacrylates, polystyrenes and polyesters, produced long lived, low-leaching organotin polymers. This chemical conservation of the organotin toxin will provide a long-term biocidal effect, while reducing the pollution hazard attributed to

presently used toxic compounds. These organotin polymers were found to be transparent, non-wettable, film-forming and effective against bacteria, algae and fouling organisms.

2.2.1 Tin atoms in polymer main chain

Generally, the synthesis of polymers containing tin atoms in the polymer backbone is carried out by condensation methods. For example, organotin polyesters were prepared directly by the reaction of organotin dihalides with the sodium salt of diacids as follows:

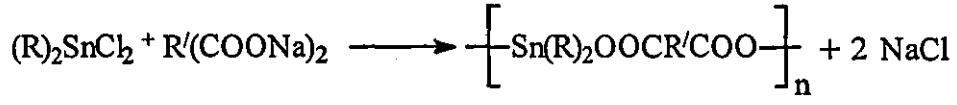

(Scheme 2.1)

Alternatively, dibutyltin diacetates or dibutyltin oxide can be reacted with diacids to form similar products[47], which were characterised by a lower degree of polymerisation due in part to cyclisation reactions. Also, the condensation products of a bisphenol and a mixture of a diorganotin dihalide and acyl halide of a dicarboxylic acid were reported[48] to be linear chains as follows:

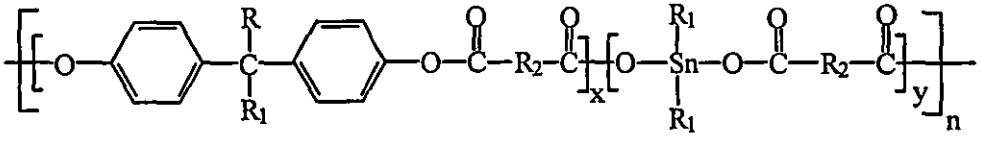

(Scheme 2.2)

The diorganotin compound used in preparing the composition of this mixture may be represented by the formula:

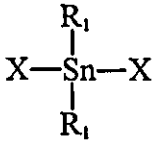

where R_1 represents alkyl and aryl groups, and X represents halogen. A route to the synthesis of a polyurethane having tin in the polymer backbone has been described by Leebrick[49] who prepared polyurethanes containing tin as follows:

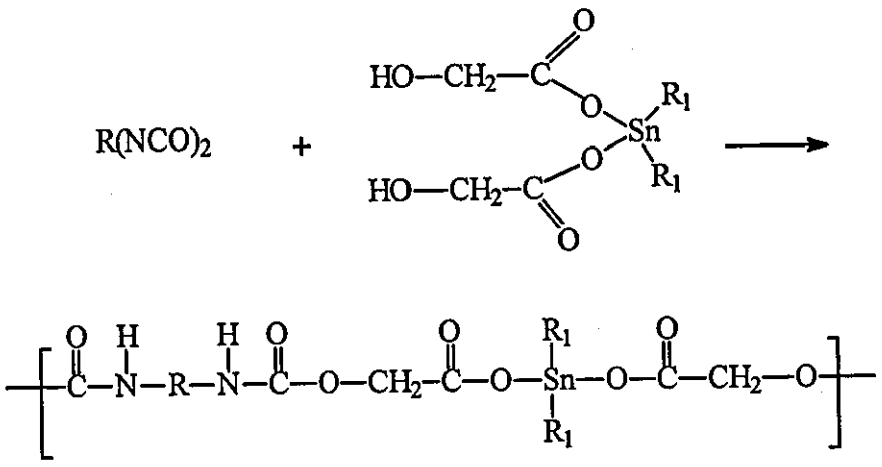

(Scheme 2.3)

Organometallic polymers containing tin and transition metals in the main chain have been synthesised and characterised.[50,51] The polymers, in which tin and transition metals are regularly linked by a conjugated system through M-C bonds are as follows:

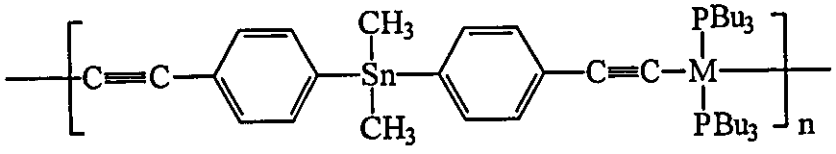

M = Pt or Pd

(Scheme 2.4)

2.2.2 Tin atoms pendant to polymer chain

Polymers containing organotin groups pendant to a carbon backbone are generally obtained by free radical initiated polymerisation of unsaturated organotin ester monomers. Montermoso et al[52] prepared a series of monomers through the reaction of organotin oxides or hydroxides with unsaturated acids as follows:

(Scheme 2.5)

where R, R′, R″ = H, alkyl or aryl. These unsaturated organotin monomers could also be prepared by the reaction of organotin halides or tetra-aryltins with an unsaturated organic acid. Considerable numbers of organotin polyacrylates have been prepared from their respective monomers, which have been polymerised using bulk, solution and emulsion polymerisations; they may find applications as films, and coatings. Leebrick[53] prepared an analogous series of polymers based upon vinyl benzoic acid as illustrated below:

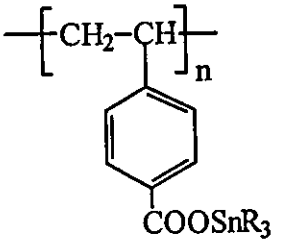

(Scheme 2.6)

Montemarano and Dyckman[46] prepared organotin polymethacrylates based on tri-n-butyltin methacrylate (TBTMA) and tri-n-propyltin methacrylate (TPTMA) with the following structure:

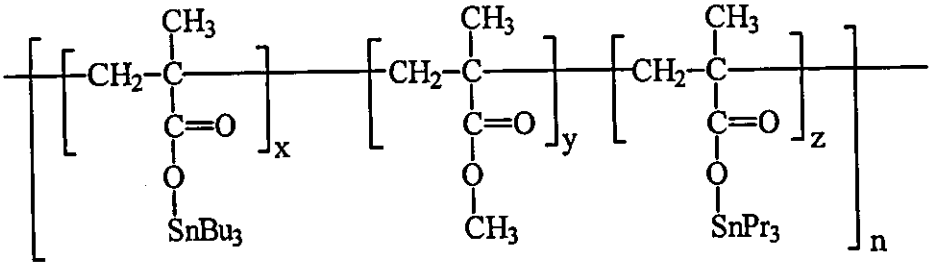

(Scheme 2.7)

They studied the toxin release of such copolymers and reported that a TBTMA-MMA copolymer released 45% less organotin ions than poly(TBTMA), indicating that the degree of leaching from an organometallic polymer may be controlled by chemical modification of its crossliked polymer network. Therefore, the optimal effective material exhibiting a minimal amount of leaching can be obtained by varying the ratio of organometallic monomer to inert comonomer along the copolymer backbone. Evans et al[44] working on the same polymer type reported that the incorporation of two R_3Sn groups such as

tri-n-butyl- and tri-n-propyltins into a polymeric matrix widens the spectrum of effectiveness but otherwise proves too toxic for general use.

Atherton and co-workers[54] examined copolymers prepared from TBTMA with MMA, ST and BA, for the rate of toxin release and film erosion, and concluded that better control of toxin release is possible by the correct choice of the copolymer constituents. Not much work has been reported on studies of the kinetics and copolymerisation parameters of organotin monomers to illustrate the composition and distribution of the organotin moiety within the copolymer chains. However, in a comparison study Koton[55] noted that tri-phenyltin methacrylate (TPHTMA) polymerises more rapidly than MMA. Copolymers of *p*-TPHTST and ST, or vinyl toluene, were prepared and studied kinetically by Sandler et al[56] who reported that the rate of addition of *p*-TPHTST monomer to its own radical is greater than the addition of ST or vinyl toluene monomers suggesting that small blocks of the tin monomer units should be present in the polymer chain of the network.

The monomer reactivity ratios of TBTMA with glycidyl methacrylate were determined by Subramanian et al[57] who reported that the copolymer produced could be self-cured to a crosslinked product by heating. Garg et al[58] studied the copolymerisation reaction of tri-n-butyltin acrylate (TBTA) and TBTMA with vinyl monomers containing either epoxy or hydroxy functional groups.

The monomer reactivity ratios for the copolymerisation reactions of TBTA or TBTMA with each of MMA, n-propyl methacrylate (PMA), EA, n-butyl methacrylate (BMA), allyl methacrylate (AMA), MA, BA, acrylonitrile (AN) and ST were studied.[59,60,61] The values of r_1r_2 obtained indicated that most of the studied copolymer systems should have statistical distributions of the monomer units in the copolymer chain and the tendency towards alternation increases with increasing alkyl chain length of the methacrylate or acrylic acid esters used. Messiha[62] investigated the binary and ternary copolymerisation reactions of TBTA and TBTMA with vinyl acetate (VA)and N-vinyl pyrrolidone (NVP).

The monomer reactivity ratios obtained for the organotin monomers were much greater than the corresponding values of VA and NVP.

Dharia et al[63] studied binary copolymerisation reactions of TBTM with cyclohexyl methacrylate (CHMA), ethoxyethyl methacrylate (EEMA), ethyl methacrylate (EMA), 2-hydroxyethyl methacrylate (HEMA), and 2-hydroxypropyl methacrylate (HPMA). They found that TBTM-HPMA copolymers contained a greater proportion of HPMA than the feed. This phenomenon is more pronounced for TBTM-HEMA copolymers. They concluded that steric effects may influence the reactivities of the different monomers towards the TBTM polymer radical.

Al-Diab et al[64] investigated radical homopolymerisations and copolymerisations of 3-tri-n-butyltin styrene (3-BTST) with ST, EA , MMA, VA and AN. Monomer reactivity ratios and Q-e values were calculated. The T_g and melting temperatures (T_m) of the various polymers were also studied.

The values of r_1 and r_2 were observed to increase in the order, AN< MMA< ST< EA <VA. 3-BTST radicals at the end of the growing chains prefer to add vinyl monomers M_2 because of steric and polar effects from the tri-n-butyltin group. Another contributing factor was the resonance stabilisation of M_2 , which was found to increase in the following order,VA<MMA<ST<EA<AN. However M_2 radicals prefer to add to themselves because of the steric and polar effects of the tri-n-butyltin group in 3-BTST. The e_1 values characterising the polarity of 3-BTST being more negative than those of styrene, makes the copolymer with M_2 more alternating because of the electron-withdrawing group in M_2 and the polarity effect of the organotin group. The Q_1 values characterising the resonance term were less than those of styrene. It follows that the resonance stability contribution in M_1 is decreased by the steric effect. It was found that copoly(3-BTST-MMA) and copoly(3-BTST-EA) had higher values of T_g than poly(MMA) and poly(EA) because of the inter- and intra-molecular co-ordination.

Ham and Ringwald[65] showed that vinyl benzoate polymers and copolymers were invariably crosslinked gels, and they attributed this to the monomer being bifunctional, in that radicals could add to the benzene ring as well as initiate normal polymerisation through the vinyl group. The slow rate of polymerisation of vinyl benzoate was noted although no explanation was presented. The highly branched and crosslinked structure of vinyl benzoate polymers was also shown by Smets and Hertoghe[66] who hydrolysed the polymer and observed a fall in molecular weight which accompanied hydrolysis. This behaviour is consistent with Ham and Ringwald's picture of branching through addition to the aromatic nuclei as such links would be readily hydrolysable. Burnett and Wright[67] showed that the rate of polymerisation was first order with respect to initiator concentration or to the light intensity in the case of photoinitiated polymerisations. The monomer t-butyl-*p*-vinylperbenzoate (TBVP) prepared by Dalton and Tidwell[68] was homo- and copolymerised with ST, methacrylonitrile (MAN), isoprene and phenylmethacrylate. Ready et al[69] studied the free radical copolymerisation of NVP with *o, m, p*-trichlorophenyl acrylate in chloroform, and in the presence of AIBN, at 50°C.

Roman et al[70] prepared *o*-methacryloyloxybenzoic acid by the reaction of salicylic acid with methacryloyl chloride using potassium carbonate as catalyst and acetone as solvent in the presence of a small amount of hydroquinone. Endo et al[71] synthesised a new organotin monomer, N-tri-n-butyltin propyl methacrylamide, and polymerised and copolymerised it with ST. They studied the application of a copolymer as catalyst for reductive dehalogenation of alkyl halides.

Moriya et al[72] synthesised organotin polymers having both organotin and carbonate groups by the reaction of tri-n-butyltin hydride (Bu_3SnH) with monomers such as diallycarbonate and diethylene glycol bis(allyl carbonate) via hydrostannation. Samui et al[73] studied the thermal and tensile behaviour of a copolymer of TBTM and MMA. A thermogravimetric study showed that with

increasing TBTM content in the copolymer the thermal stability decreases. T_g decreases continuously as the TBTM content increases. Shaaban et al[74] synthesised *p*-acryloyloxytri-n-butyltin benzoate (*p*-AOTBTB) which was copolymerised with some acrylic monomers. The values of the monomer reactivity ratio of the organotin monomer (r_1) for all copolymerisation reactions studied were nearly equal to zero, which indicates that, the growing radical ending with an organotin unit prefers an acrylic monomer rather than an organotin monomer in the propagation stage. Azab[75] studied the thermal behaviour of *p*-AOTBTB-AN copolymers. The prepared homopolymer and copolymer were characterised by a variety of spectroscopic and thermal methods.

Joshi and Gupta[76] synthesised α-methyl *p*-acryloyloxytri-n-butyltin benzoate (*p*-MAOTBTB), which was homopolymerised in two solvents Tetrahydrofuran (THF) and DMF. The T_g of the homopolymer was found to be 40°C. Tawfik et al[77] studied the effect of substitution on the reactivity of some *p*-phenylacrylamide derivatives with organotin monomers. They found that the *p*-acrylamido toluene and *p*-acrylamido chlorobenzene polymerise slowly; on the other hand the *p*-acrylamido nitrobenzene did not polymerise. This finding is in agreement with the fact that aromatic nitro compounds inhibit or retard the polymerisation of vinyl compounds. The copolymerisation parameters r_1 and r_2 have values indicating that the copolymer of *p*-acrylamido chlorobenzene with tri-n-butyltin acrylate shows a higher content of *p*-acrylamido chlorobenzene monomer. On the other hand, a *p*-acrylamido toluene-tri-n-butyltin acrylate copolymer shows a lower content of *p*-acrylamido toluene. In contrast, the content of *p*-acrylamido toluene monomer is much higher than that of tri-n-butyltin methacrylate monomer.

El-Hamouly et al[78] studied the binary copolymerisation of N-antipyryl acrylamide (NAA) with MMA, BMA, AN, and VA.

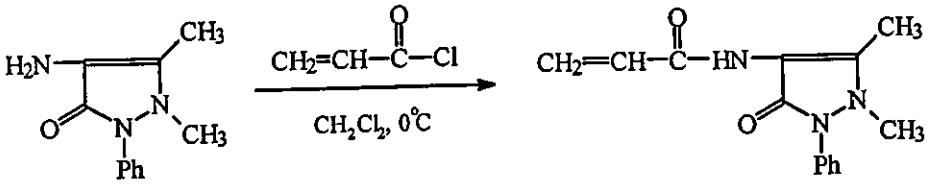

4-Amino antipyrine

N-Antipyryl acrylamide (NAA)

(Scheme 2.8)

Mohmoud et al[79] studied the copolymerisation parameters of *p*-AOTBTB with allyl methacrylate (AMA), NVP and VA. The monomer reactivity ratios indicate that the copolymerisations should give copolymers with a strong tendency to alternation. Associative organotin polymers were prepared, for example tri-alkyltin halide[80,81], as in the solid state organotin halide and pseudohalide have a strong tendency for intermolecular association. Tri-methyltin flouride[82] has been shown by X-ray crystallography to exist as polymeric species having the following structure:

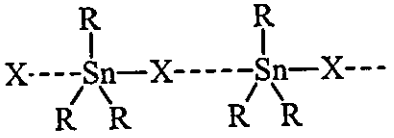

2.3 Aim of the present work

The goal of this project was to prepare homopolymers of *m*- and *p*-acrylamido and methacrylamidotri-n-butyltin benzoate, and also *o*-acryloyloxy and methacryloyloxytri-n-butyltin benzoate, and to copolymerise these monomers with three different acrylic monomers. Such polymeric systems are potentially interesting in terms of properties and have not been thoroughly investigated before, prompting this research.

The tri-n-butyltin carboxylate ester linkage is expected to hydrolyse slowly, releasing tin over a long period of time, hence acting as a potentially useful antifouling agent. Physical and chemical characterisations were conducted on the prepared polymers and copolymers, including nuclear magnetic resonance (NMR) and Fourier transform infrared spectroscopy (FTIR) elemental analysis,

mass spectrometry, gel permeation chromatography (GPC) and dynamic mechanical thermal analysis (DMTA).

Determination of the characteristics of the prepared polymers and copolymers was aimed at providing information that could be useful in the development of this class of polymers in their potential use as antifouling agents.

Chapter 3

Experimental

3.1 General Experimental

3.1.1 List of Chemicals

Commercial chemicals were used without further purification except as specified.

- 2,2- Azobis(isobutyronitrile) (AIBN), was used after recrystallization from methanol.
- Acetone, SLR grade, was supplied by Carless Solvents and distilled before use.
- Acrylic anhydride was used as supplied by Aldrich Chemical Company Ltd.
- Acryloyl chloride 96% was used as supplied by Fluka.
- Anhydrous magnesium sulphate was used as supplied by Fisons PLC.
- Bis(tri-n-butyl tin) oxide (TBTO), 96% was used as supplied by Fluka.
- Butyl acrylate (BA), supplied by Aldrich Chemical Company Ltd, was inhibited with 10 - 55 ppm hydroquinone monoethyl ether and was purified by vacuum distillation.
- Calcium hydride (CaH_2), 95% supplied by Aldrich Chemical Company Ltd was used as a coarse ground powder.
- Diethyl ether, SLR grade, supplied by Carless Solvents was distilled before use.
- Dimethylformamide (DMF), HPLC grade, was used as supplied by Fisons PLC.
- Ethanol, SLR grade, was supplied by Carless Solvents and distilled before use.
- Hexane, SLR grade, supplied by Carless Solvents was distilled before use.
- Hydrochloric acid (HCl), specific gravity 1.38, SLR grade, supplied by Fisons PLC, was diluted with deionised water to the correct molarity.
- Hydroquinone 99% was used as supplied by Aldrich Chemical Company Ltd.
- *m*-Aminobenzoic acid (*m*-ABA), 98% was used as supplied by Aldrich Chemical Company Ltd.
- Methacrylic anhydride was used as supplied by Aldrich Chemical Company Ltd.
- Methacryloyl chloride 98% was used as supplied by Fluka.
- Methanol, SLR grade, supplied by Carless Solvents was distilled before use.

- Methyl methacrylate (MMA), 99% pure inhibited with 10 ppm hydroquinone monomethyl ether, supplied by Aldrich Chemical Company Ltd , was vacuum distilled before use.
- Hydroxybenzoic acid 99% was used as supplied by Aldrich Chemical Company Ltd.
- *p*-Aminobenzoic acid (*p*-ABA), 99% was used as supplied by Aldrich Chemical Company Ltd.
- Petroleum ether 40-60, SLR grade, supplied by Carless Solvents, was distilled before use.
- Methyl acrylate (MA), 99% inhibited with 100 ppm hydroquinone monoethyl ether supplied by Aldrich Chemical Company Ltd, was vacuum distilled before use.
- Nitric acid (HNO_3), SLR grade, were used as supplied by Fisons PLC.
- Potassium carbonate (K_2CO_3), 99% was used as supplied by Aldrich Chemical Company Ltd.
- Pyridine 99% was used as supplied by Aldrich Chemical Company Ltd.
- Sodium hydroxide pellets, SLR grade, were used as supplied by Fisons PLC.
- Sodium 99% supplied by Aldrich Chemical Company Ltd was rinsed in petroleum ether prior to use.
- Sulfuric acid (H_2SO_4), SLR grade, were used as supplied by Fisons PLC.
- Tetrahydrofuran (THF), HPLC grade, was used as supplied by Fisons PLC.
- Toluene, SLR grade, supplied by Carless Solvents, was dried over CaH_2 and distilled before use.
- Triethylamine (TEA), 98% supplied by Fisons PLC was dried over sodium wire.

3.1.2 Fourier Transform Infrared Spectroscopy (FTIR)

A sample was cast from chloroform (or dimethylsulfoxide) onto a plate of sodium chloride, yielding a thin film, which was dried using a hot air blower. A Nicolet 20 DXC Fourier Transform Infrared Spectrometer with OMNIC software was used. A sample was scanned 50 times at a resolution of 1 wavenumber. By taking 50 scans the signal to noise ratio was improved.

3.1.3 Nuclear Magnetic Resonance Spectroscopy (NMR)

All samples were prepared by dissolving approximately 0.05 g of monomer, or homopolymer, or copolymer, in 2-3 ml of deuterated solvent $CDCl_3$ containing 1% tetramethyl silane (TMS) as internal standard except for the precursor acrylamide monomers which were dissolved in deuterated dimethyl sulphoxide (d_6DMSO). A Bruker AC 250 MHz spectrometer was used.

3.1.4 Mass Spectroscopy

Accurate mass measurement was conducted using a Kratos MS 80 Mass Spectrometer, in high resolution mode. A sample was introduced using a direct insertion probe, with ionisation by electron impact. An accurate mass was calculated by using the most abundant isotopes; this was compared with the experimently determined value.

3.1.5 Elemental Analysis

A combustion method to convert the sample elements to simple gases (CO_2, H_2O, and N_2) was used with a Perkin-Elmer 2400 CHN microanalysis instrument. The sample was first oxidized in a pure oxygen environment; the resulting gases were then controlled to exact conditions of pressure, temperature and volume. Finally, the product gases were separated. Then, under steady-state conditions, the gases were measured as a function of thermal conductivity.

3.1.6 Gel Permeation Chromatography (GPC)

A solution of each polymer in unstabilised THF, having a concentration of 0.1% (w/v), was prepared. A solution was filtered through a micro fiber filter paper.Then, 2 drops of toluene were incorporated in to the solution to act as internal reference. Each solution was loaded into a 6-port injection valve having a100µl loop. The

polymer was eluted with unstabilised THF using a Knauer high performance liquid chromatography pump 64 at a flow rate of 1.0 ml per minute through a PL mixed gel B (10 micron) with column dimensions 300 x 7.8 mm and a Knauer refractive index detector which was connected to a PL data capture unit (DCU). The column was calibrated with polystyrene standards supplied by Polymer Labratories Ltd figure (3.1). Values of molecular weights of samples were obtained using PL Caliber computer software.

Fig 3.1 GPC calibration curve for polystyrene standards in THF for the mixed gel B column

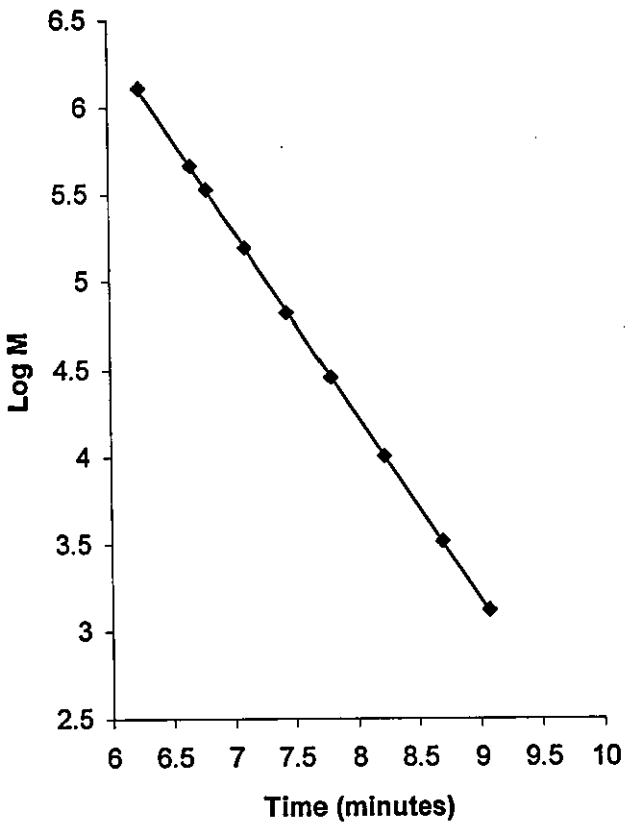

3.1.7 Dynamic Mechanical Thermal Analysis (DMTA)

Polymers and copolymers were studied using a Polymer Laboratories Dynamic Mechanical Thermal Analysis (DMTA) instrument. The cantilever bending mode was used to study the samples. This involves clamping a rectangular sample onto a fixed frame. The sample is then oscillated at its centre via a clamp attached to a drive shaft linked to a mechanical oscillator. The amplitude (strain) and frequency of oscillation are set on the instrument, along with the temperature range to be studied and the heating rate. The resistance to the applied sinusoidal displacement was recorded as a function of the phase and magnitude of this displacement. The instrument converts these signals to yield the dynamic storage modulus. The glass transition of the polymer is characterised by a damping effect, resulting in a peak in the tan δ curve and corresponding to a drop in modulus, which is due to the softening of the polymer at this point. A polymer was impregnated into a filter paper. Samples were prepared on a heated press, at a temperature 10-20°C above the T_g of the component having the highest T_g. A sandwich of polymer and filter paper, between two pieces of mould-release film was pressed for a few seconds at a pressure of 300 p.s.i. Samples were securely clamped onto the clamping frame, and were cooled to at least 40°C below the T_g of the component having the lowest T_g, by passing liquid nitrogen through the cooling coils of the furnace arrangement of the DMTA measuring head. All samples were heated at 2°C / minute, at a frequency of 1 Hz and a strain of x 4.

3.2 Synthesis of Precursor Monomers

3.2.1 Synthesis of Acrylamide Derivatives

A Non-methylated derivatives

These include *m*-acrylamidobenzoic acid (*m*-AABA) and *p*-acrylamidobenzoic acid (*p*-AABA).

These two monomers were prepared by two methods.

(i) The reaction of *m*-aminobenzoic acid (*m*-ABA) or *p*-aminobenzoic acid (*p*-ABA) with acryloyl chloride was performed in alkaline media.[83] To a solution of *m*-ABA or *p*-ABA (13.7 g, 0.1 mol) in distilled water (200 ml), sodium hydroxide (16 g, 0.4 mol) was added and the solution was cooled to 0-5°C. Acryloyl chloride (9.1 g, 0.1 mol) was then added dropwise with stirring for 1/2 hr and then left at room temperature for 1 hr, After acidification with cooled diluted hydrochloric acid the precipitate was collected by filtration and recrystallisation from ethanol yielded *m*-AABA (14.9 g, 78%) as colourless needles (m.p. 238-240°C) and *p*-AABA (15.9 g, 81%) as colourless needles (m.p. 232-234°C) .

(ii) The reaction of *m*-ABA or *p*-ABA with acrylic anhydride was performed by treating a solution of the selected aromatic amino acid (13.7 g, 0.1 mol) in dry acetone (100 ml) and cooling to 0-5°C. Then acrylic anhydride (12.6 g, 0.1 mol) was added dropwise for 1/2 hr. By further stirring at room temperature for 1 hr, the solvents were evaporated and the crude products were purified by crystallisation from ethanol to give the same products as in **(i)**.

B Methylated derivatives

These include *m*-methacrylamidobenzoic acid (*m*-MAABA) and *p*-methacrylamidobenzoic acid (*p*-MAABA).

These two derivatives were prepared by the following two methods.

(i) In a typical experiment a suspension of aminobenzoic acids (*m*- or *p*- , 0.1 mol), pyridine (0.02 mol) and hydroquinone (0.005 mol) in dry toluene (200ml) was placed in a three necked flask provided with a stirrer, thermometer and dropping funnel.[84] The apparatus was cooled to 0°C and a solution of methacryloyl chloride (0.1 mol) in dry toluene (100 ml) was added dropwise over a period of 1/2 hr. The reaction mixture was refluxed for 5 hrs, upon cooling the crude product was collected and washed with cold dilute hydrochloric acid. The crude products were crystallised from ethanol to yield *m*-MAABA in (16.2 g, 79%) as reddish colour needles (m.p. 215-217°C) and *p*-MAABA (15.2 g, 74%) as colourless needles (m.p. 210-212°C).

(ii) The reaction of *m*-ABA or *p*-ABA with methacrylic anhydride was performed by treating a solution of the selected aminobenzoic acid (13.7 g, 0.1 mol) in dry acetone (100 ml) and then cooling to 0-5°C. Methacrylic anhydride (15.4 g, 0.1 mol) was added dropwise for 1/2 h followed by further stirring at room temperature for 1 hr. The solvents were evaporated and the crude products were purified by crystallisation from ethanol to give the same products as in **(i)**.

3.2.2 Synthesis of Acryloyloxy Derivatives

A Non-methylated derivative, i.e. *o*- acryloyloxybenzoic acid (*o*-AOBA)

This monomer was prepared by reacting acryloyl chloride and salicylic acid in the presence of triethylamine.[85] In a three necked flask equipped with a stirrer, dropping funnel, thermometer, salicylic acid (13.8 g, 0.1 mol) dissolved in 200 ml dry diethyl ether and 2 mol of triethylamine were added over 1 hr. The solution was then cooled with an ice-water bath and acryloyl chloride (0.12 mol), in diethyl ether (100 ml) was added dropwise over 1/2 hr. The mixture was allowed to stand overnight and solvent was removed under reduced pressure using a Rotavapor. The solid product was dissolved in water, hydroquinone (0.12g) was added and the solution was acidified with cooled hydrochloric acid. After cooling, the solid was filtered off and dried. The crude product was crystallised from toluene yielding colourless needles (65%) (m.p.135-137 °C).

B Methylated derivative, i.e. *o*- methacryloyloxybenzoic acid (*o*-MAOBA)

This monomer was prepared by reacting methacryloyl chloride and salicylic acid in the presence of TEA[86] in a three necked flask equipped with a stirrer, dropping funnel, and thermometer. Salicylic acid (13.8 g, 0.1 mol) dissolved in toluene 100 ml and triethylamine (1 mol) were introduced. Methacryloyl chloride (1.5 mol) was placed in a dropping funnel. The flask was cooled down to 0°C, and then methacryloyl chloride was added dropwise with continuous stirring. When all the methacryloyl chloride was added, the bath was removed and stirring was continued for about 4 hrs, and left overnight. The hydrochloride salt of TEA was filtered off and washed with toluene. The solution was shaken three times with water and the

separated organic layer was dried with anhydrous magnesium sulfate. After filtering the solution from the drying agent, toluene was partially distilled off under vacuum and the residue was precipitated in petroleum ether. The product was purified by repeated crystallisation in hexane yielding colourless needles (60%)(m.p. 80-81°C).

3.3 Synthesis Of Organotin Monomers

3.3.1 Synthesis of Acrylamide Derivatives

A Non-methylated derivatives

These include *m*-acrylamidotri-n-butyltin benzoate (*m*-AATBTB) and *p*-acrylamidotri-n-butyltin benzoate (*p*-AATBTB).

To a well stirred solution of TBTO (59.6g, 0.1mol) in dry acetone (200 ml) *m*-AABA or *p*-AABA (38.2g 0.2 mol) was added and stirred for 2 hrs at room temperature. Then calcium chloride (~30g) was added to remove generated water. Finally, the reaction mixture was filtered from the dehydrating agent and the solvent was removed under reduced pressure. The residue (*m*-AATBTB) solidified within a few hours and was recrystallised from petroleum ether yielding colourless needles(80.15 g, 83%) m.p. (70-72°C). The residue (*p*-AATBTB) was recrystallised from toluene giving colourless needles (82.3g, 85%) (m.p. 151-153°C).

B Methylated derivatives

These include *m*-methacrylamidotri-n-butyltin benzoate (*m*-MAATBTB) and *p*-methacrylamidotri-n-butyltin benzoate (*p* -MAATBTB).

To a well stirred solution of TBTO (59.6g, 0.1mol) in acetone (200 ml) *m*-MAABA or *p*-MAABA (41g, 0.2 mol) was added and stirred for 2 hrs at room temperature. Then calcium chloride (~30g) was added to remove generated water. Finally the reaction mixture was filtered from the dehydrating agent and the solvent was removed under reduced pressure. The residue (*m*-MAATBTB) was obtained as a liquid. The ^{1}H NMR and ^{13}C NMR spectra indicate a product of sufficient purity for characterisation and further polymerisation. The solid residue (*p*-MAATBTB) was recrystallised from toluene giving colourless needles(79.6 g, 80.6%) (m.p.117-119°C).

3.3.2 Synthesis of Acryloyloxy Derivatives

A Non-methylated derivative, i.e. *o*-acryloyloxytri-n-butyltin benzoate (*o*-AOTBTB)

To a well stirred solution of TBTO (59.6 g, 0.1mol) in dry acetone (200 ml) *o*-AOBA (38.4 g, 0.2 mol) was added and stirred for 2 hours at room temperature. Calcium chloride was added and filtered off followed by solvent removal under reduced pressure as in previous procedures. The residue (*o*-AOTBTB) was a liquid, The ^{1}H NMR and ^{13}C NMR spectra indicate a product of sufficient purity for structure characterisation and further polymerisation.

B Methylated derivative, i.e. *o*-methacryloyloxytri-n-butyltin benzoate (*o*-MAOTBTB)

To a well stirred solution of TBTO (59.6g, 0.1mol) in dry acetone (200 ml) *o*-MAOBA (41.2 g, 0.2 mol) was added and stirred for 2 hours at room temperature. Calcium chloride was added and filtered off, followed by solvent removal under reduced pressure as in previous procedures. The residue (*o*-MAOTBTB) was a liquid. The ^{1}H NMR and ^{13}C NMR spectra indicate a product of sufficient purity for structure characterisation and further polymerisation.

3.4 Characterisation Data for Prepared Monomers

Table 3.4.1 FTIR Spectral Data for Prepared Monomers

	Corresponding Wavenumber (λ , cm^{-1})			
monomers	**C=O**	**C=C**	**OH**	**NH**
m-AABA	1685, 1660	1630	2500 - 3200	3375
p-AABA	1680, 1660	1620	2600 - 3180	3353
m-MAABA	1704, 1650	1623	2850 - 2970	3286
p-MAABA	1677, 1665	1626	2854 - 2980	3310
o-AOBA	1740, 1680	1630	2500 - 3150	----------
o-MAOBA	1700, 1735	1609	2749 -3434	----------
m-AATBTB	1680, 1580	1620	----------	3375
p-AATBTB	1685, 1595	1610	----------	3340
m-MATBTB	1666, 1545	1643	----------	3315
p-MATBTB	1670, 1528	1620	----------	3307
o-AOTBTB	1735, 1695	1630	----------	----------
o-MAOTBTB	1740, 1656	1635	---------	----------

Table 3.4.2 ^{1}H NMR Spectral Data

3.4.2.1 Precursor Monomers

Monomers	Structure	Assignment	Chemical shift (ppm)
m-AABA	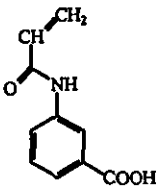	CH_2= CH- , (3H) C_6H_4 - , *meta* , (4H) - NH , (1H) -COOH , (1H)	5.73 - 6.48 (2m) 7.43 - 8.29 (m) 10.31 (s) 11.90 (brs)
p-AABA	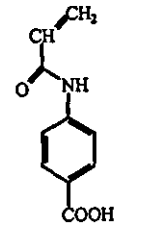	CH_2= CH- , (3H) C_6H_4 - , *para* , (4H) - NH , (1H) -COOH , (1H)	5.75 - 6.51 (2m) 7.76 - 7.93 (2 d) 10.44 (s) 12.68 (brs)
m-MAABA	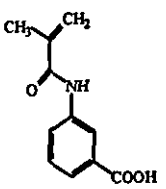	CH_3 - , (3H) CH_2 = , (2H) C_6H_4 - , *meta* , (4H) - NH , (1H) -COOH , (1H)	1.94 (s) 5.51 (s) , 5.83 (s) 7.38 - 8.32 (m) 9.93 (s) 12.83 (brs)
p-MAABA	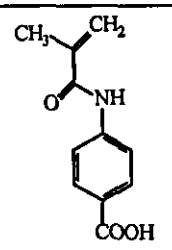	CH_3 - , (3H) CH_2 = , (2H) C_6H_4 - , *para* , (4H) - NH , (1H) -COOH , (1H)	1.94 (s) 5.54 (s) , 5.83 (s) 7.79 - 7.91 (2d) 10.06 (s) 11.5 (br.s)
o-AOBA	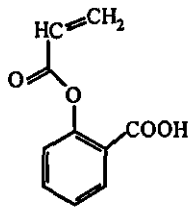	CH_2=CH-, (3H) C_6H_4 - , *ortho*, (4H) -COOH , (1H)	6.01-6.67 (3m) 7.16-8.14 (m) 10.75 (br.s)
o-MAOBA	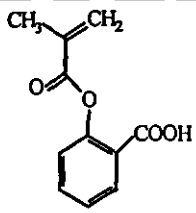	CH_3 - , (3H) CH_2 = , (2H) C_6H_4 - , *ortho*, (4H) -COOH (1H)	2.08 (s) 5.75,6.37 (s) 7.16-8.15 (m) 11.05 (br.s)

3.4.2.2 Organotin Monomers

Monomers	Structure	Assignment	Chemical shift (ppm)
m-AATBTB	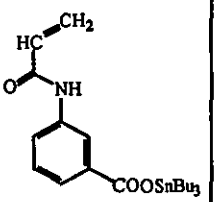	3{$CH_3(CH_2)_3$}, (27H) CH_2=CH-, (3H) C_6H_4- , *meta*, (4 H) -NH, (1H)	0.87-1.68 (m) 5.71-6.39 (2m) 7.36-7.97 (m) 10.32 (br.s)
p-AATBTB	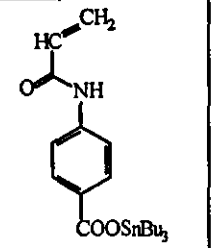	3{$CH_3(CH_2)_3$}, (27H) CH_2=CH-, (3H) C_6H_4- *para* (4 H) -NH , (1H)	0.87-1.69 (m) 5.73-6.48 (2m) 7.36(d), 8.06(d) 10.50 (br.s)
m-MAATBTB	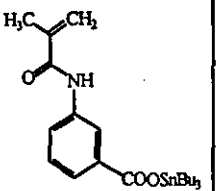	3{$CH_3(CH_2)_3$}, (27H) CH_3- , (3H) CH_2= , (2H) C_6H_4- *meta* (4H) -NH , (1H)	0.84-1.68 (m) 1.99 (s) 5.09 (s), 5.86 (s) 7.02-7.98 (m) 11.0 (br.s)
p-MAATBTB	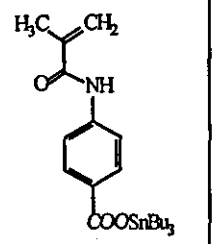	3{$CH_3(CH_2)_3$}, (27H) CH_3- , (3H) CH_2= , (2H) C_6H_4-, *para*, (4H) -NH , (1H)	0.86-1.68 (m) 2.02 (s) 5.43 ,5.78 (s) 7.61(d), 8.01(d) 11.5 (br.s)
o-AOTBTB	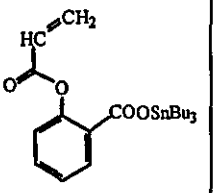	3{$CH_3(CH_2)_3$}, (27H) CH_2=CH-, (3H) C_6H_4- ,*ortho*, (4H)	0.85-1.72 (m) 5.91-6.58 (m) 7.02-8.005 (m)
o-MAOTBTB	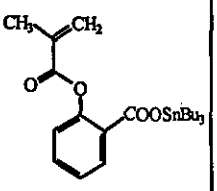	3{$CH_3(CH_2)_3$}, (27H) CH_3- , (3H) CH_2= , (2H) C_6H_4- , *ortho*, (4H)	0.905 - 1.60 (m) 2.08 (s) 5.73 (s), 6.36(s) 7.08 - 8.02 (m)

Table 3.4.3 ^{13}C NMR Spectral Data

3.4.3.1 Precursor Monomers

Monomers	Structure	Assignment	Chemical shift (ppm)
m-AABA	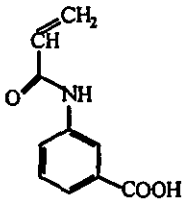	5 x (CH) 1 x (CH_2) 2 x (C) 2 x (C=O)	125.31, 128.57, 129.45, 134.07, 136.78 132.78 136.46, 144.34 168.52, 172.31
p-AABA	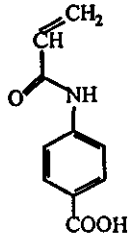	5 x (CH) 1 x (CH_2) 2 x (C) 2 x (C=O)	2 x (123.80), 2 x (135.54), 136.69 132.79 130.50, 148.17 168.66, 172.05
m-MAABA	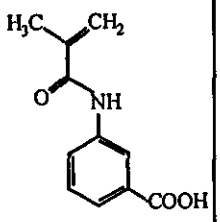	1 x (CH_3) 4 x (CH) 3 x (C) 1 x (CH_2) 2 x (C=O)	23.78 126.12, 129.37, 133.87 136.26, 144.40, 145.29 125.43 172.04, 172.34
p-MAABA	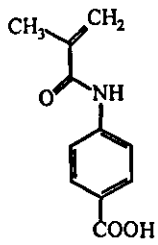	1 x (CH_3) 4 x (CH) 1 x (CH_2) 3 x (C) 2 x (C=O)	18.70 2 x (119.33), 2 x (130.21) 120.63 125.33, 140.21, 143.23 167.02, 167.23
o-AOBA	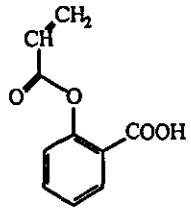	5 x (CH) 2 x (C) 1 x (CH_2) 2 x (C=O)	123.91, 128.13, 127.61, 132.41, 134.74 122.36, 150.93 132.72 165.51, 170.05
o-MAOBA	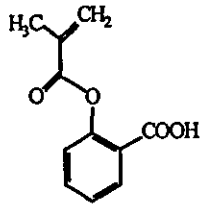	1 x (CH_3) 4 x (CH) 3 x (C) 1 x (CH_2) 2 x (C=O)	16.26 124.01, 125.96, 132.44, 134.72 135.65, 151.41, 122.15 127.34 166.12, 170.12

3.4.3.2 Organotin Monomers

Monomers	Structure	Assignment	Chemical shift (ppm)
m-AATBTB	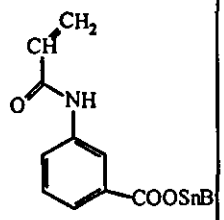	3 x (CH_3) 10 x (CH_2) 5 x (CH) 2 x (C) 2 x (C=O)	13.50 16.57, 27.54, 27.70, 127.41 121.81, 124.05, 125.90, 128.59, 131.20 132.75, 138.09 164.25, 172.25
p-AATBTB	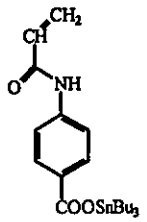	3 x (CH_3) 10 x (CH_2) 5 x (CH) 2 x (C) 2 x (C=O)	13.56 16.52, 26.93, 27.60, 128.24 2 x (118.85), 2 x (131.25), 130.90 141.19, 127.12 163.57, 171.91
m-MAATBTB	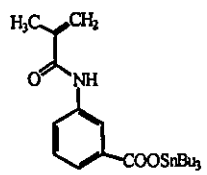	4 x (CH_3) 10 x (CH_2) 4 x (CH) 3 x (C) 2 x (C=O)	13.55, 18.61 16.55, 26.93, 27.58, 119.97 121.43, 123.77, 125.95, 128.82 133.21, 137.11, 142.51 167.21, 171.52
p-MAATBTB	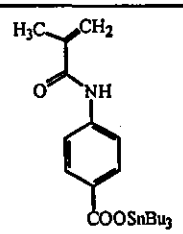	4 x (CH_3) 10 x (CH_2) 4 x (CH) 3 x (C) 2 x (C=O)	13.56, 18.63 16.57, 26.93, 27.44, 120.08 2 x (118.78), 2 x (131.27) 113.64, 127.82, 141.07 166.45, 170.11
o-AOTBTB	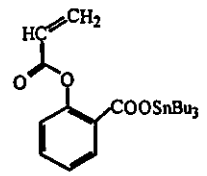	3 x (CH_3) 10 x (CH_2) 5 x (CH) 2 x (C) 2 x (C=O)	13.53 16.59 , 27.54 , 27.70 , 131.88 123.05 , 125.73 , 128.16 , 132.22 , 132.55 150 , 137.2 165.2 , 170.1
o-MAOTBTB	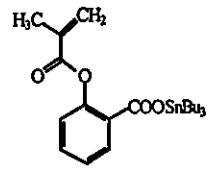	4 x (CH_3) 10 x (CH_2) 4 x (CH) 3 x (C) 2 x (C=O)	13.89, 31.15 16.94, 27.38, 27.70, 127.16 123.56, 125.96, 131.51, 132.61 150.70, 136.43, 126.30 166.05, 170.34

Table 3.4.4 Elemental Analysis Data for Prepared Monomers

Monomers	Carbon %		Hydrogen %		Nitrogen %		Tin %		
	calc.	Found	calc.	Found	calc.	Found	calc.	Found	% Error in Found
m-AABA $C_{10}H_9NO_3$	62.83	62.36	4.71	4.65	7.33	7.20	------	------	------
p-AABA $C_{10}H_9NO_3$	62.83	62.23	4.71	4.55	7.33	7.00	------	------	------
m-MAABA $C_{11}H_{11}NO_3$	64.39	63.94	5.36	5.00	6.83	7.09	------	------	------
p-MAABA $C_{11}H_{11}NO_3$	64.39	64.62	5.36	5.23	6.83	7.10	------	------	------
o-AOBA $C_{10}H_8O_4$	62.50	62.71	4.17	3.85	-----	-------	------	------	------
o-MAOBA $C_{11}H_{10}O_4$	64.08	63.68	4.85	4.60	-----	-------	------	------	------
m-AATBTB $C_{22}H_{35}NO_3Sn$	55.00	55.42	7.29	7.12	2.92	2.63	24.79	25.14	0.48
p-AATBTB $C_{22}H_{35}NO_3Sn$	55.00	55.08	7.29	7.08	2.92	2.88	24.79	24.43	0.32
m-MAATBTB $C_{23}H_{37}NO_3Sn$	55.87	56.14	7.49	7.50	2.83	3.09	24.08	24.75	0.54
p-MAATBTB $C_{23}H_{37}NO_3Sn$	55.87	56.21	7.49	7.39	2.83	3.22	24.08	23.83	0.42
o-AOTBTB $C_{22}H_{34}O_4Sn$	54.88	53.90	7.07	7.27	-----	-------	24.74	25.16	0.65
o-MAOTBTB $C_{23}H_{36}O_4Sn$	55.76	55.31	7.27	7.22	-----	-------	24.04	23.72	0.64

Table 3.4.5 Theoretical Molecular Weights versus Practically Determined Molecular Ions (Mass Spectra)

Monomers	Calculated Mol. Wt *	Found M^+ **	% Intensity ***
m-AABA $C_{10}H_9NO_3$	191.0582	191.0571	33.1
p-AABA $C_{10}H_9NO_3$	191.0582	191.0556	19.9
m-MAABA $C_{11}H_{11}NO_3$	205.0739	205.0743	12.6
p-MAABA $C_{11}H_{11}NO_3$	205.0739	205.0746	12.6
o-AOBA $C_{10}H_8O_4$	192.0423	192.0423	3.5
o-MAOBA $C_{11}H_{10}O_4$	206.0579	206.0499	2.1
m-AATBTB $C_{22}H_{35}NO_3Sn$	481.1639	481.1644	> 0.1
p-AATBTB $C_{22}H_{35}NO_3Sn$	480.1651	480.1654	0.5
m-MAATBTB $C_{23}H_{37}NO_3Sn$	494.1807	494.1810	0.7
p-MAATBTB $C_{23}H_{37}NO_3Sn$	494.1807	494.1797	0.2
o-AOTBTB $C_{22}H_{34}O_4Sn$	482.1479	482.1454	0.2
o-MAOTBTB $C_{23}H_{36}O_4Sn$	496.1635	496.1733	0.1

* Mol. Wt : Molecular Weight.
** M^+ : Found Molecular Ion.
*** % Intensity : Percent intensity of the molecular ion peak compared to the base peak.

3.5 Polymerisation Reactions of Organotin Monomers

Polymerisations of organotin monomers were carried out by a solution process. To a solution of the prepared organotin monomer (5g, 0.01mol) in DMF (7ml) AIBN (0.016g, 0.001 mol) was added. After purging with deoxygenated nitrogen the solutions were allowed to stand at 65-70°C for 3-6 hrs. Isolation of the polymers from the resulting viscous mixtures was achieved by precipitation from 80% methanol. The homopolymer was purified by repeated dissolution and precipitation. Finally the polymer was dried at 80°C in vacuum to constant weight.

3.6 Copolymerisation Reactions

Binary copolymers were obtained by a solution polymerisation process. Pre-determined amounts of comonomers were placed in a three-necked round bottom flask, and diluted with DMF, so that the total concentration of monomers was 3 mol / l. The polymerisation was commenced by adding AIBN (1 mol / 100 mol total monomers). A flask was flushed with oxygen-free nitrogen for 10 minutes, capped and thermostated at 65-70°C for 20-60 minutes depending on the comonomer pair and composition. The copolymers were purified by repeated dissolution and precipitation. Finally the copolymer was dried at 80°C in vacuum to constant weight. The conversion was limited to less than 10% in every case. The percent conversion of each sample was evaluated as the weight of the copolymer produced with respect to the total weight of comonomer.

3.7 Determination of Tin Content

The tin content of the prepared monomers, homopolymers and copolymers was determined gravimetrically through oxidation of the sample to tin oxide according to the method of Gilman and Rosenberg.[87] Typically, 0.2 g of the tin containing sample was placed in a 30 ml crucible. To this was added, 1 ml of concentrated sulfuric acid and 5 drops of concentrated nitric acid. The crucible was heated slowly over a hot plate until the sample turned black, and then continuous heating was maintained until the excess acid was removed. Subsequently, the carbonaceous material formed by the action of the acid was completely ignited 6 hrs over high heat (700°C) leaving the tin oxide as an ample yellow solid residue. From the weight of this residue, the tin content of the sample was calculated as follows:

$$Sn\% = \frac{\text{weight of tin oxide} \times 119 \times 100}{\text{weight of sample} \times 151} \quad \text{.....(3.1)}$$

The error in this procedure for monomers, was calculated to be in the range 0.32-0.65% as illustrated in table (3.4.4), while for homopolymers it was in the range 0.38-0.61%. On the other hand the error in this procedure for copolymers having 40% acrylate composition was found to be in the range 0.56-0.78%, having 60% acrylate composition in the range 0.73-1.1%, and having 90% acrylate composition in the range 2.25-2.72%.

3.8 Determination of Monomer Reactivity Ratios

The monomer reactivity ratios (r_1 and r_2) of the binary copolymerisation systems involving organotin monomers were determined on the basis of the comonomer-copolymer composition relationship. The copolymer composition of each sample was calculated through its tin content as follows:

$$b = \frac{\text{Sn\% of copolymer} \times \text{Mol. wt. of } M_2}{\left(\text{Sn\% of } M_1 \times \text{Mol. wt. of } M_1 - \text{Sn\% of copolymer} \times \text{Mol. wt. of } M_1\right)} \quad \text{.....(3.2)}$$

where M_1 is an organotin monomer and $b=(m_1 / m_2)$ is the molar ratio of monomer units in a copolymer. The mol fraction of M_1 monomer (F_1) in the copolymer could be calculated as $F_1 = b/1+b$ The monomer reactivity ratios of each system were calculated according to the method proposed by Kelen and Tudos.[13]

Chapter 4

Results and Discussions

4.1 Synthesis of Acrylamide Derivatives

A Non-methylated derivatives

The compounds *m*-AABA and *p*-AABA have been prepared according to the following scheme (4.1):

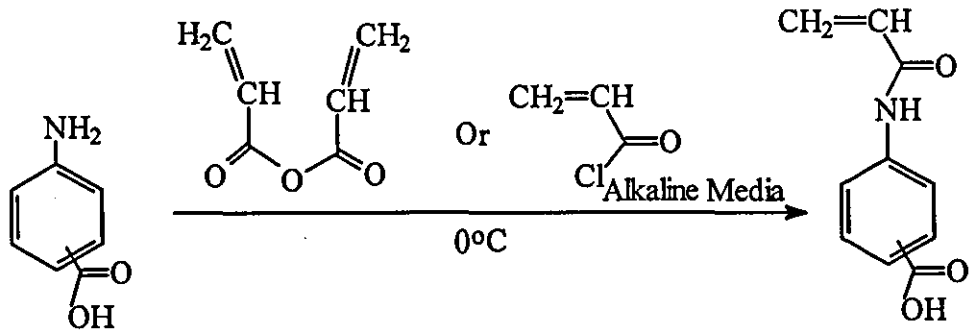

Scheme (4.1)

B Methylated derivatives

The compounds *m*-MAABA and *p*-MAABA have been prepared according to the following scheme (4.2):

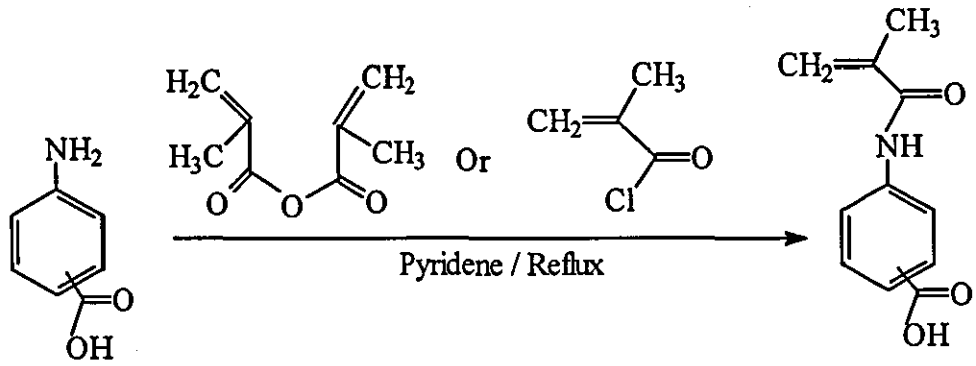

Scheme (4.2)

It was reported that the non-methylated acrylamide derivatives can be prepared by refluxing acryloyl chloride with an aminobenzoic acid in benzene, using pyridine as the catalyst.[84] However, upon repeating this procedure in toluene, the reaction failed to generate the target non-methylated acrylamide monomer, possibly due to polymerisation of acryloyl chloride (suggested from ^{1}H NMR). This method (with reflux in toluene) efficiently generated the methylated derivatives from methacryloyl chloride.

4.2 Synthesis of Acryloyloxy Derivatives

A Non-methylated derivative

The compound *o*-AOBA was prepared using a modified procedure scheme (4.3) from the one described in the literature.[85]

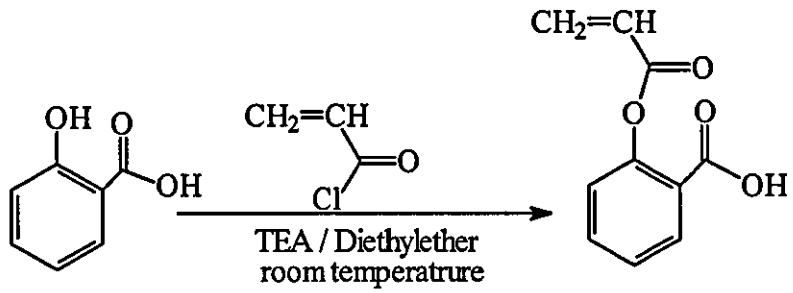

Scheme (4.3)

B Methylated derivative

The compound *o*-MAOBA was prepared according to the following scheme (4.4). A similar procedure for the generation of this monomer has been reported in the literature.[86]

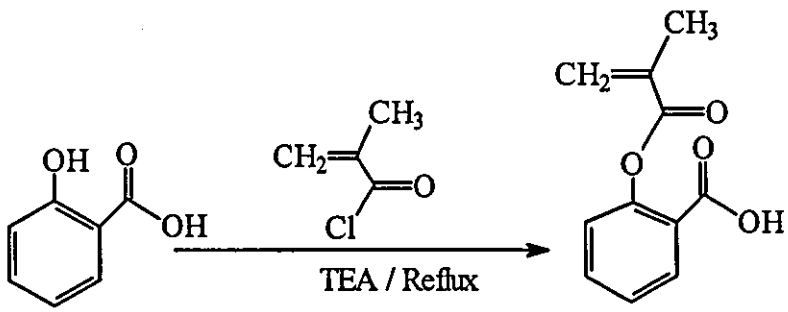

Scheme (4.4)

Upon repeating the procedure followed in the preparation of the non-methylated derivative (*A*) for the preparation of the methylated monomer (*B*), i.e. triethylamine in ether at room tempreture, the reaction produced a sticky material which did not precipitate by acid treatment. Recovery of the product was facilitated by performing this reaction under reflux conditions.

4.3 Synthesis of Organotin Monomers

4.3.1 Synthesis of Acrylamide Derivatives

All monomers including methylated and non-methylated derivatives were prepared by the esterification of *m*-AABA, *p*-AABA, *m*-MAABA and *p*-MAABA with TBTO according to the method described by Cummins and Dunn[88] scheme (4.5).

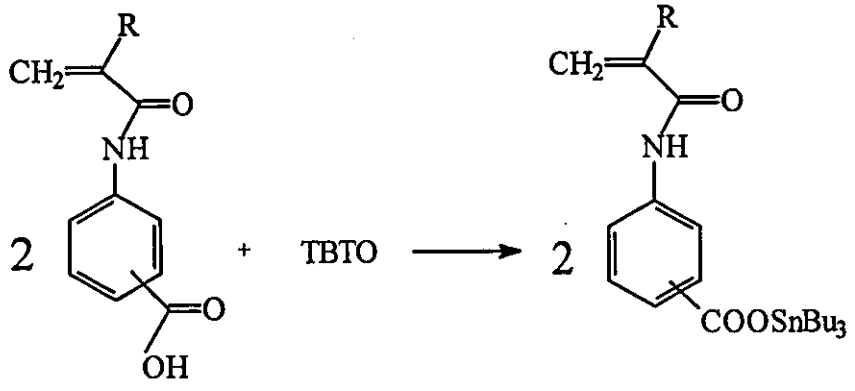

R= H for non-methylated derivatives

R= CH_3 for methylated derivatives

Scheme (4.5)

Joshi and Gupta[89] synthesised *p*-AATBTB by two steps:

i) esterification of *p*-aminobenzoic acid (*p*-ABA) with TBTO (70%) followed by ii) amidification with acryloyl chloride (63%). In this thesis organotin monomers were prepared by amidification with acryloyl (or methacryloyl) chloride followed by esterification with TBTO. This sequence of reactions has the advantages of higher yields (65%, 74%) and improved purity of monomers by crystallisation in both steps.

4.3.2 Synthesis of Acryloyloxy Derivatives

An approach similar to that used to generate benzoic acid derivatives of acrylamide was followed to prepare the organotin esters scheme (4.6).

R= H for non-methylated derivatives

R= CH_3 for methylated derivatives

Scheme (4.6)

N,N-dicyclohexylcarbodiimide (DCCI) in dichloromethane was used previously as a dehydrating agent for the esterification of *p*-hydroxy tri-n-butyltin benzoate (HBTB) with methacrylic acid, to prepare tri-n-butyltin methacryloyloxy benzoate.[74,76] However, all attempts to couple acrylic (or methacrylic) acid with *m*- or *p*-amino- and *o*-hydroxy- tri-n-butyltin benzoate in the presence or absence of this dehydrating agent failed. Instead, a transesterifcation reaction took place, in which the tri-butyltin moiety was transferred from the benzoic acid to the acrylic (or methacrylic) acid, according to the following scheme:

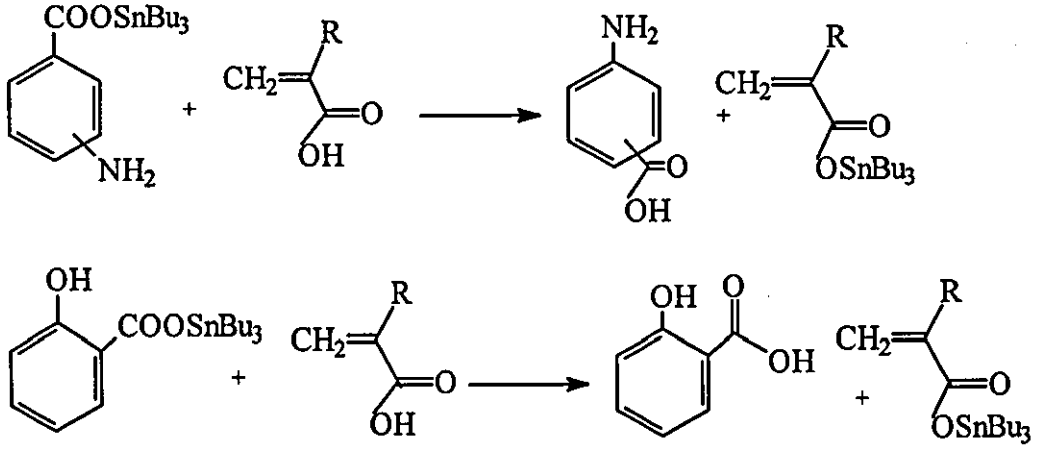

R= H for acrylic acid

R= CH_3 for methacrylic acid

Scheme (4.7)

Since transesterfications are acid or base catalysed equilibrium reactions, the driving force behind the above mentioned reactions was thought to be the fast precipitation of the tri-n-butyltin acrylate (or methacrylate) upon the introduction of acrylic (or methacrylic) acid in to the reaction mixture.

4.4 Homopolymerisation of Organotin Monomers

4.4.1 Homopolymerisation of Acrylamide Derivatives

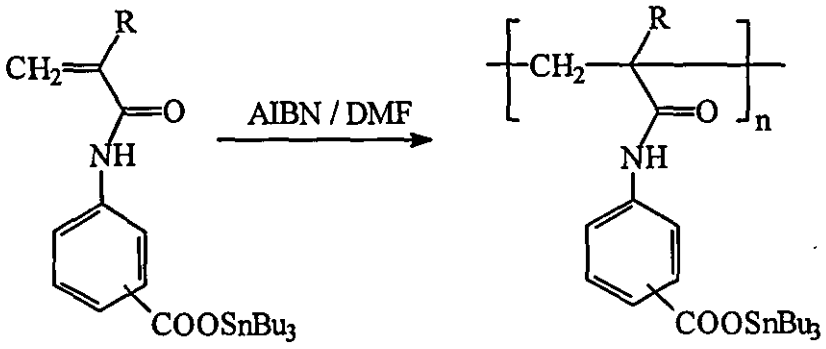

R = H for non-methylated derivatives

R= CH_3 for methylated derivatives

Scheme (4.8)

The polymerisation was conducted in DMF using AIBN as initiator at 65°C scheme (4.8). By comparing the weights of formed polymers, generated after constant reaction time and under similar reaction conditions, i.e. the same monomer and initiator concentrations, it was indicated that the polymerisation rates of the methylated monomers were faster than the non-methylated ones. Presuming that all reaction conditions are held constant, then it is clear from equation (1.10) that polymerisation rates will depend on $k_p/k_t^{0.5}$ The reactivities of monomers and radicals will determine the ratios of the rate constants. The types of factors which might determine faster polymerisation rates for methylated monomers are:

(i) methyl group bulkiness in the monomer twists the double bond from planarity (to escape the eclipsed geometry with the aromatic amide group) leading to reduced π overlap (electronic strain), and minimising double bond

conjugation with the carbonyl group, consequently increasing double bond reactivity (reducing its stability) towards incoming alkyl radicals.[90]

(ii) the methylated radical should have improved stability compared to the non-methylated, due to the combined electron-donating effect of the methyl group through σ bond (mesomeric effect) and the hyperconjugation forms produced by the methyl hydrogen atoms as in scheme (4.9)[3] together with the steric hindrance imposed by the methyl group on approaching monomer units.

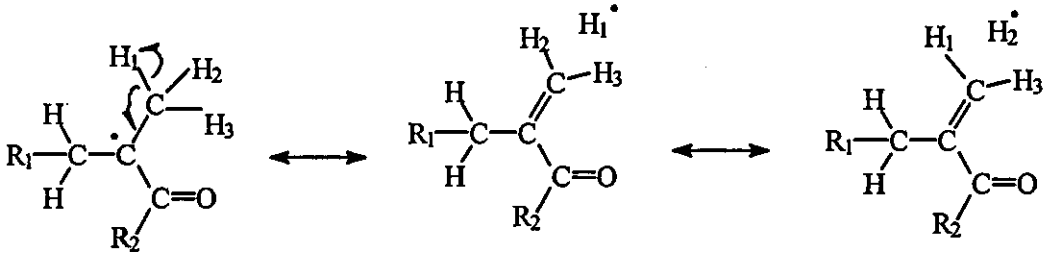

Scheme (4.9)

Joshi and Gupta[89] found that *p*-AATBTB polymerises slowly in the presence of AIBN as radical initiator in dioxane at 100°C .

The composition of the polymers was investigated by tin analysis which was found to be 24.6% for poly(*m*-AATBTB) and 24.5% for poly(*p*-AATBTB), against the calculated values of 24.79% for non-methylated derivatives with monomer unit $C_{22}H_{35}NO_3Sn$, 23.7%, for poly(*m*-MAATBTB) and 23.6% for poly(*p*-MAATBTB) against the calculated values of 24.08% for methylated derivatives with monomer unit $C_{23}H_{37}NO_3Sn$.

Acrylamide-organotin monomers, homopolymers and copolymers are characterised by the following IR bands: 3300 - 3400 cm^{-1} due to amidic N-H stretching vibrations, and 2960 cm^{-1} corresponding to C-H stretching. The amidic carbonyl (C=O) stretching corresponded to approximately 1666 cm^{-1} and 1545 cm^{-1} in the monomer figure (4.1) and table(3.4.1), while in the homopolymers and copolymers the same group absorbed at approximately 1687 cm^{-1} and 1532 cm^{-1}. This difference could be attributed to the fact that in the

monomer the amide was α, β unsaturated while it was saturated in the polymers and copolymers.[91] Two characteristic bands appeared at about 1650 cm^{-1} and 1590 cm^{-1} in the homopolymers and copolymers corresponding to the (COO-Sn) stretching band. In the monomers the first band appeared at 1630 cm^{-1} while the second band remained at 1590 cm^{-1}. In the FTIR of the copolymer there was an extra band at approximately 1740 cm^{-1} corresponding to an ester carbonyl.

The case of *m*-MAATBTB is taken as a typical example for discussion. The presence of a sharp narrow absorption peak at 3451 cm^{-1} which resulted from the free amidic N-H stretching, and a wide band at 3350 cm^{-1} for the hydrogen bonded N-H. Both bands were nearly equivalent in intensity figure (4.2).

Similarly, *m*-MAATBTB-MA and *m*-MAATBTB-MMA copolymers figure (4.3) and figure (4.4) each had a shoulder at 3451 cm^{-1} and a broad band at 3363 cm^{-1} and 3377 cm^{-1} respectively. However, the ratio between the intensities of the broad hydrogen bonded bands and the free N-H shoulders was higher than the respective ratio in the homopolymer case which indicated a higher level of hydrogen bonding in the copolymers.[91]

Furthermore, by examining the position of the amidic (C=O) stretching vibrations for the homopolymer and the copolymers it was evident that the wavenumber for both amidic bands was nearly the same, i.e. at 1687 cm^{-1} and 1532 cm^{-1}, which indicates that the increase in the number of formed hydrogen bonds noticed in the copolymers was through the involvement of the newly introduced comonomer ester carbonyl (C=O) groups rather than the increased involvement of the monomer amidic group (C=O) as the hydrogen bond acceptor. The ester carbonyl (C=O) band appeared at 1740 cm^{-1} and 1735 cm^{-1} for *m*-MAATBTB-MA and *m*-MAATBTB-MMA copolymers respectively, which was at the lower range limit for the usual ester carbonyl groups, indicating involvment with H-bonding.[92]

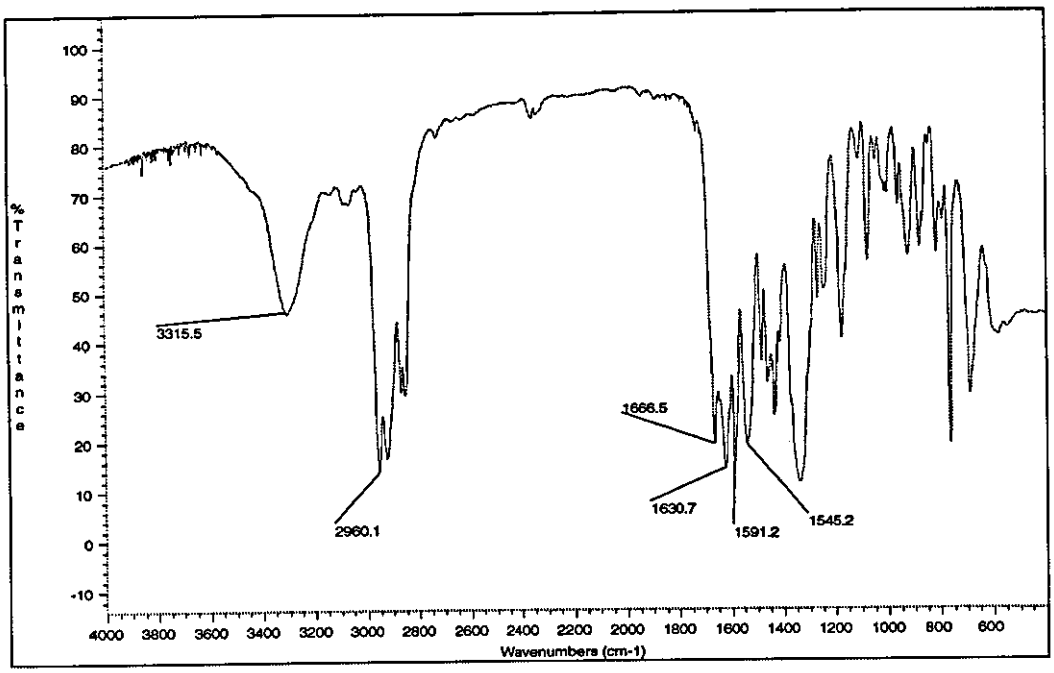

Fig. 4.1 FTIR spectrum for *m*-MAATBTB monomer

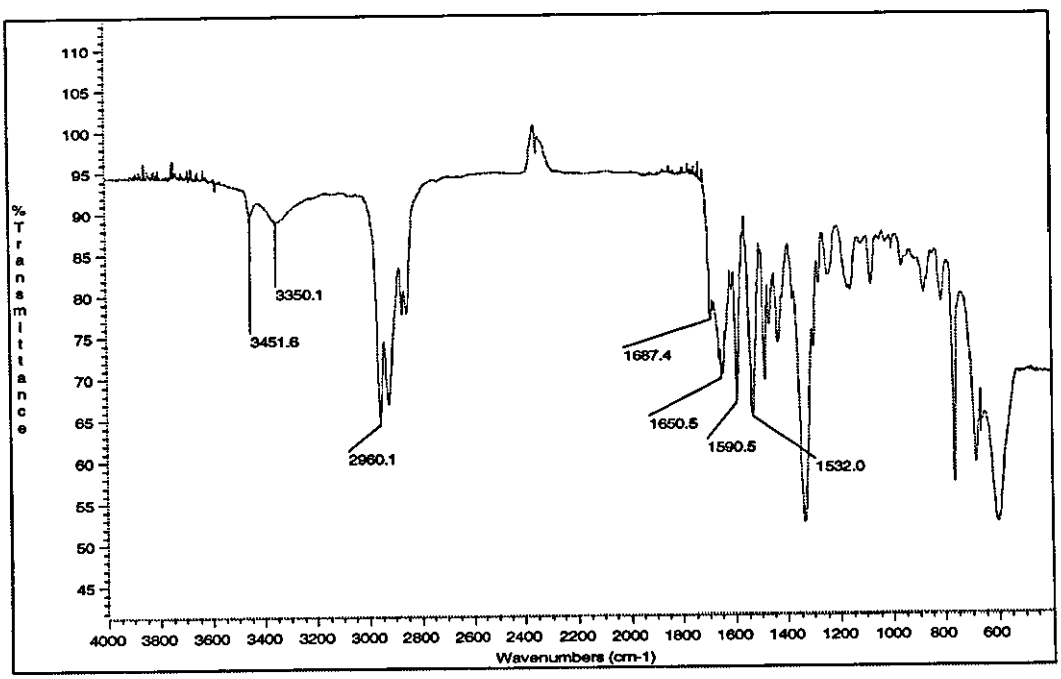

Fig. 4.2 FTIR spectrum for poly(*m*-MAATBTB)

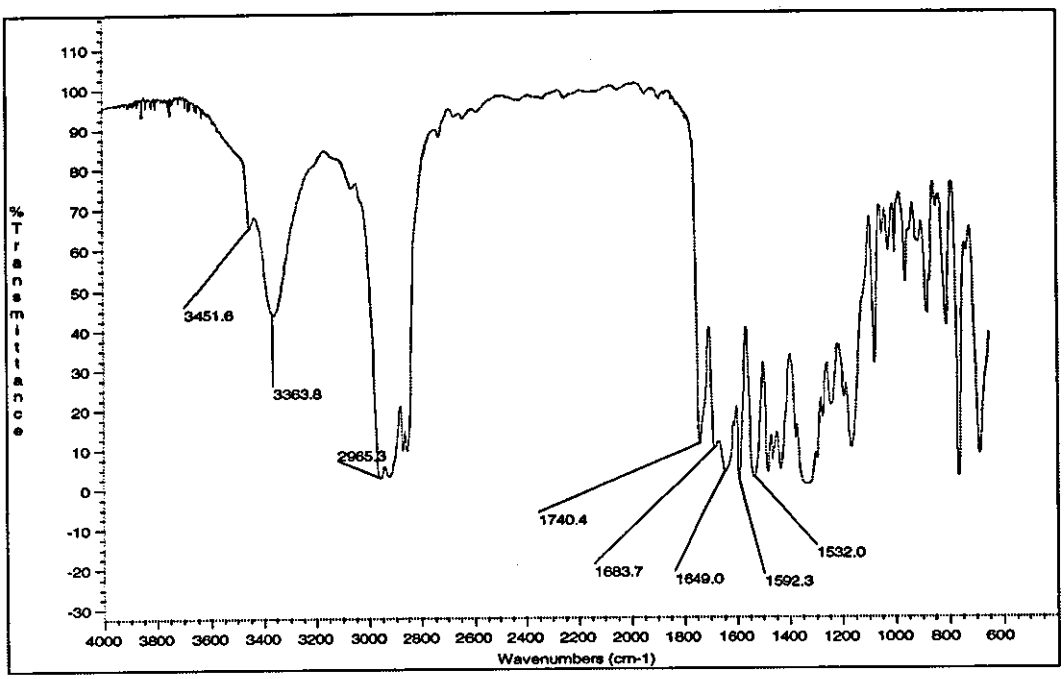

Fig. 4.3 FTIR spectrum for *m*-MAATBTB-MA copolymer

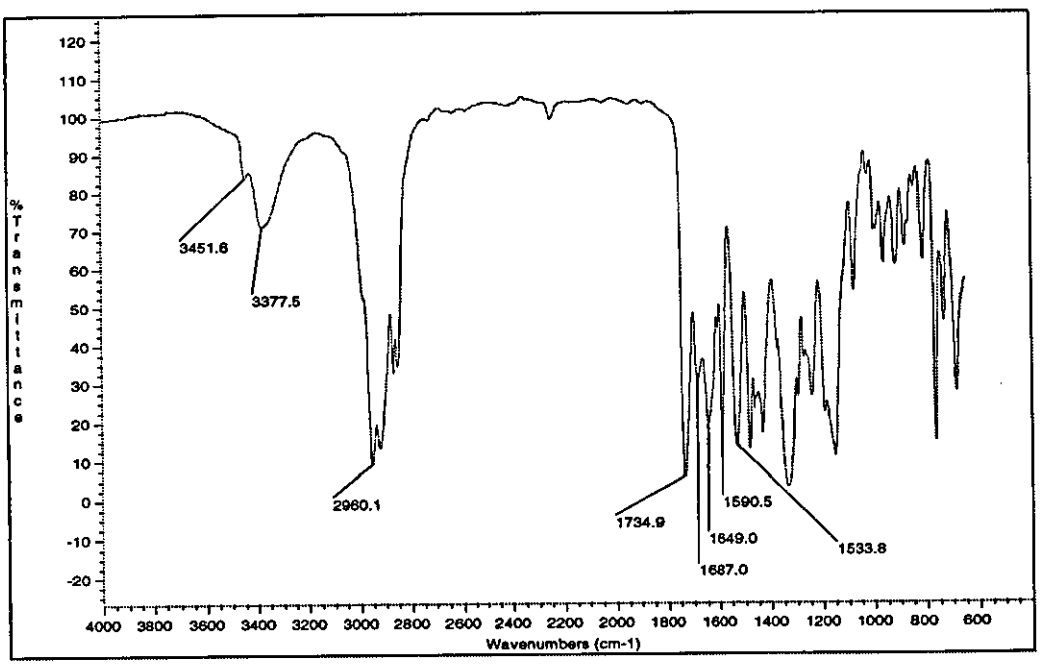

Fig. 4.4 FTIR spectrum for *m*-MAATBTB-MMA copolymer

The ^1H NMR spectrum of the organotin polymer, based on *m*-AATBTB, is shown figure (4.5). Resonances observed at δ 7.02–7.61 ppm are due to protons of the phenyl ring and those at δ 0.83–2.86 ppm are due to protons of the $-CH_2-$ and $-CH_3$ groups in the three n- butyl groups. In figure (4.5) for the homopolymer there are no peaks at signal at δ 5.71-6.39 ppm due to the vinyl group of the monomer.

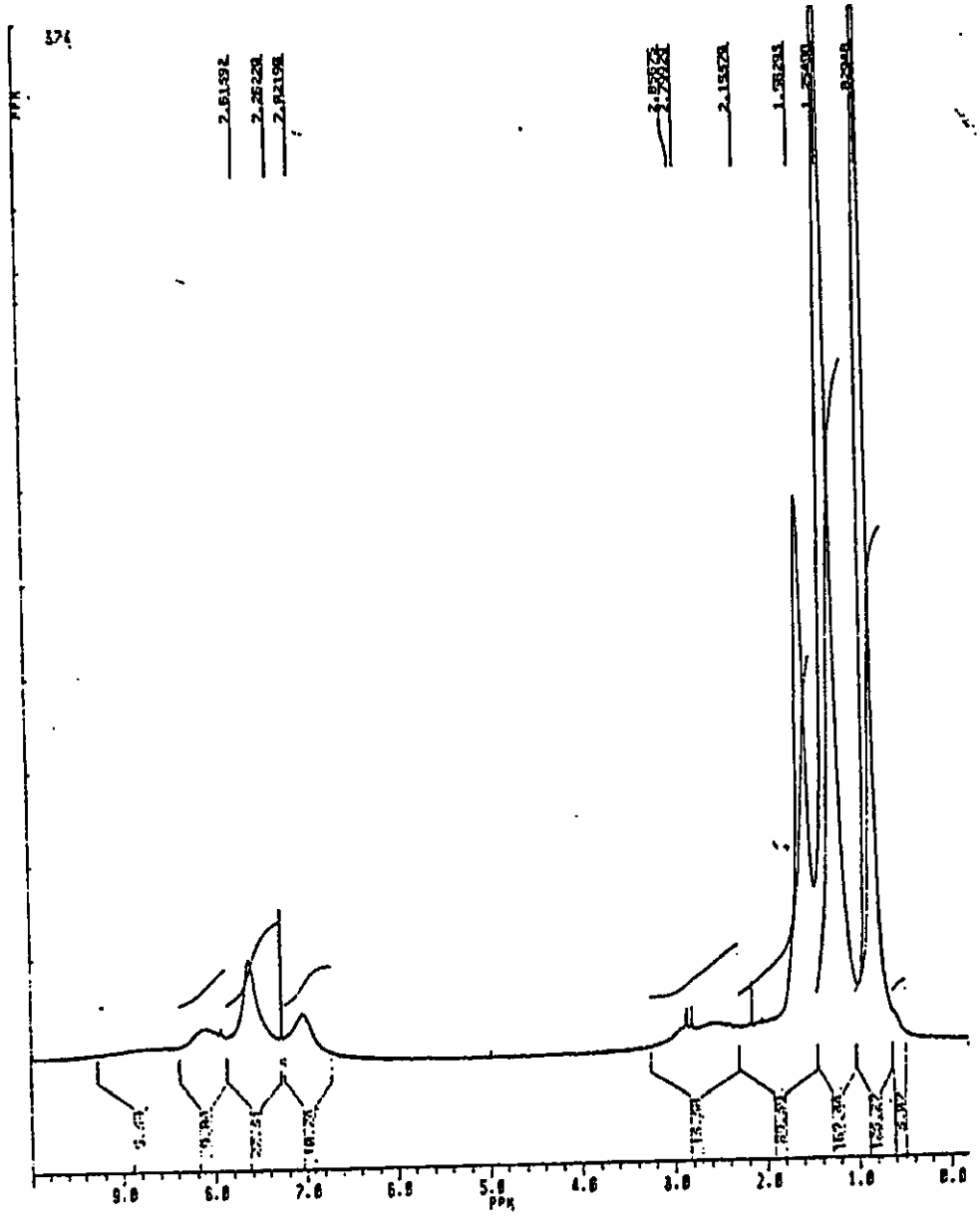

Fig. 4.5 ^1H NMR spectrum of organotin polymer poly(*m*-AATBTB)

4.4.2 Homopolymerisation of Acryloyloxy Derivatives

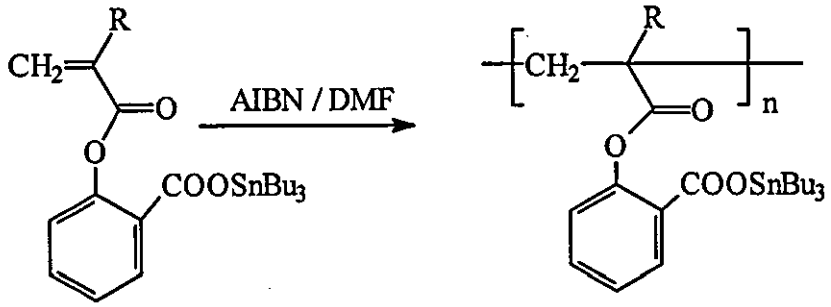

R= H for non-methylated derivatives

R= CH_3 for methylated derivatives

Scheme (4.10)

The polymerisation of *o*-AOTBTB and *o*-MAOTBTB was conducted in DMF using AIBN as initiator at 75°C scheme (4.10). As with the acrylamide derivatives, the rate of polymerisation of the methylated derivatives was faster than for the non-methylated monomers for the same reasons mentioned in section 4.4.1. The composition of the polymers was investigated by tin analysis which was found to be 24.3%, against the calculated value of 24.74% for non-methylated derivatives with monomer unit $C_{22}H_{34}O_4Sn$, and 23.7%, against the calculated value of 24.04% for methylated derivatives with monomer unit $C_{23}H_{36}O_4Sn$. The acryloyloxy organotin monomer, homopolymers and copolymers were characterised by the following IR bands: 2960 cm^{-1} corresponding to C-H stretching, an ester carbonyl (C=O) stretching corresponding to approximately 1740 cm^{-1} and 1656 cm^{-1} in the monomer table (3.4.1), while in the homopolymers and copolymers the same group absorbed at approximately 1755 cm^{-1}.

This difference could be attributed to the fact that in the monomer the ester is α, β unsaturated while it is saturated in the polymers and copolymers. Two characteristic bands appeared at about 1650 cm^{-1} and 1610 cm^{-1} in the homopolymers and copolymers corresponding to the (COO-Sn) stretching band. In the monomers the first band appeared at 1636 cm^{-1} while the second band appeared at 1605 cm^{-1} figures (4.6-4.9) illustrate the FTIR spectra for *o*-

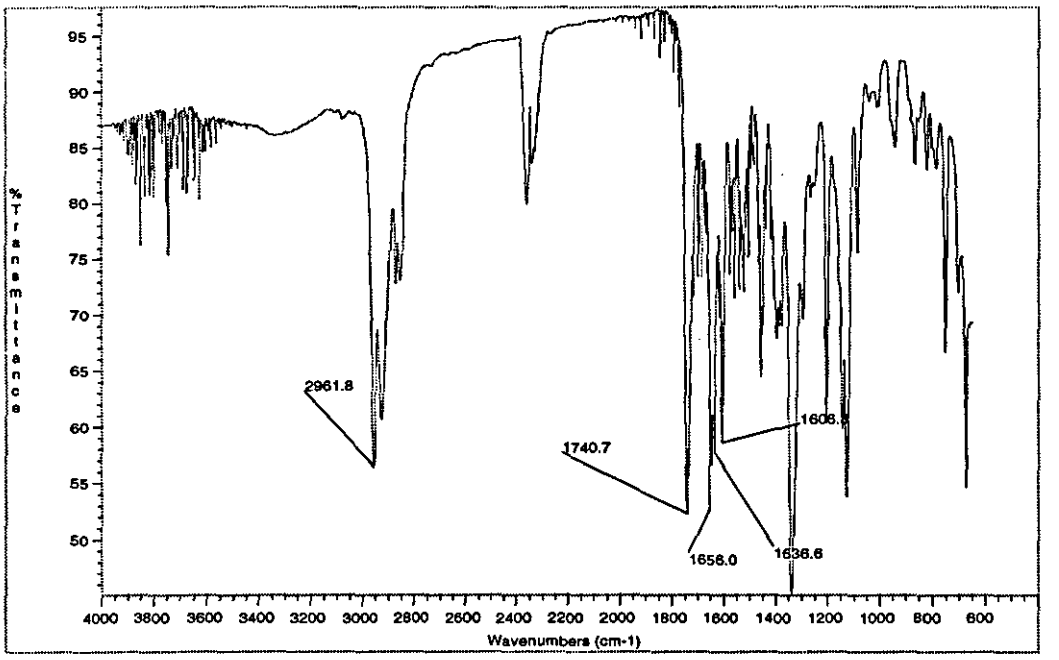

Fig. 4.6 FTIR spectrum for *o*-MAOTBTB monomer

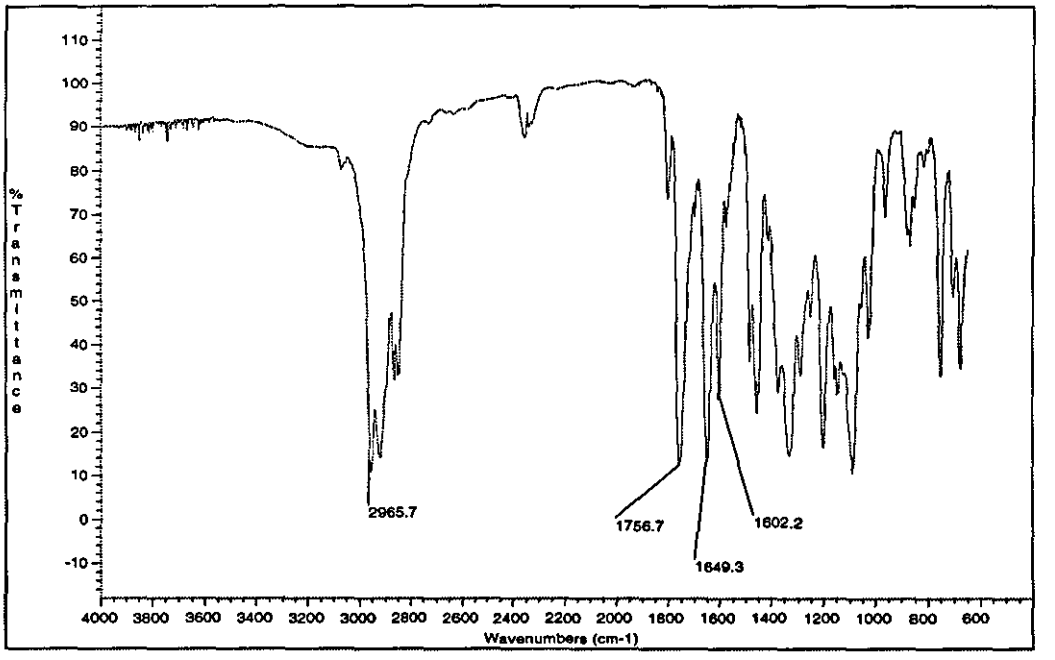

Fig. 4.7 FTIR spectrum for poly(*o*-MAOTBTB)

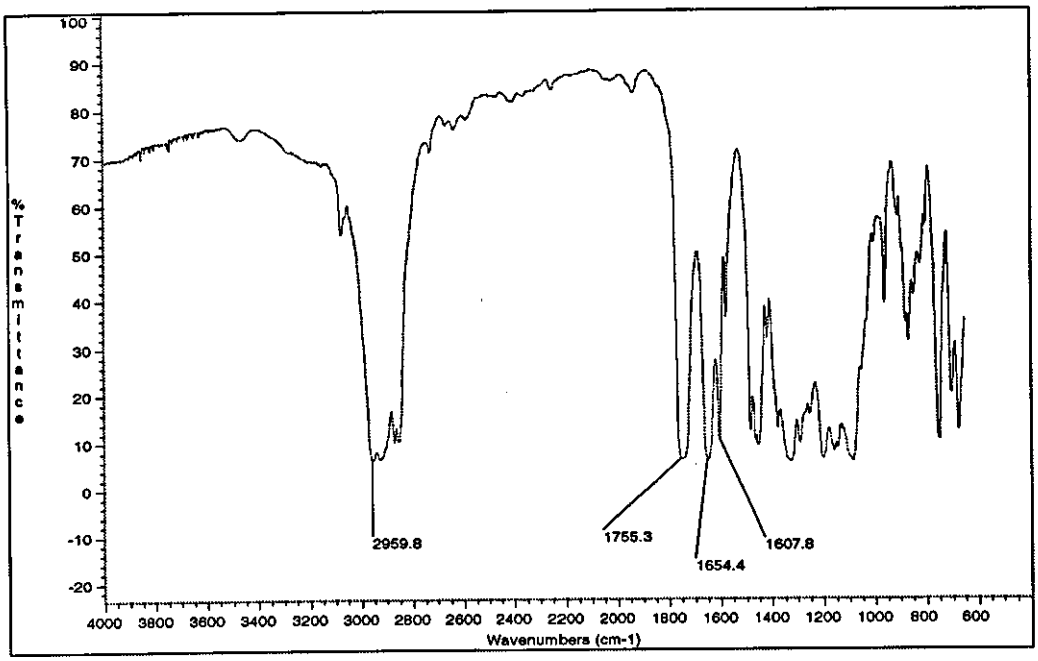

Fig. 4.8 FTIR spectrum for *o*-MAOTBTB-MA copolymer

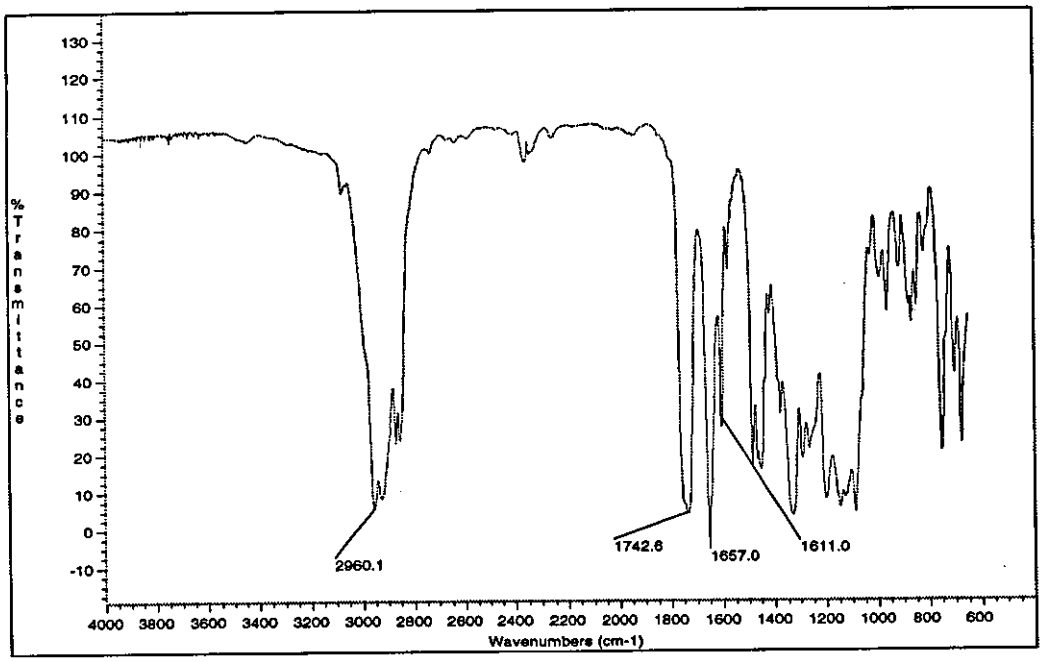

Fig. 4.9 FTIR spectrum for *o*-MAOTBTB-MMA copolymer

MAOTBTB monomer, poly(*o*-MAOTBTB) and *o*-MAOTBTB-MA and *o*-MAOTBTB-MMA copolymers. The ^{1}H NMR spectrum of the organotin polymer, based on *o*-MAOTBTB is shown as an example for discussion in figure (4.10). Resonances observed at δ 7.09–7.26 ppm were due to protons of the phenyl ring and those at δ 0.76–2.65 ppm were due to protons of the -CH_2- and -CH_3 groups in the three n-butyl groups. In figure (4.10) for the polymer, there were no peaks at signal at δ 5.71-6.36 ppm due to the vinyl group of the monomer .

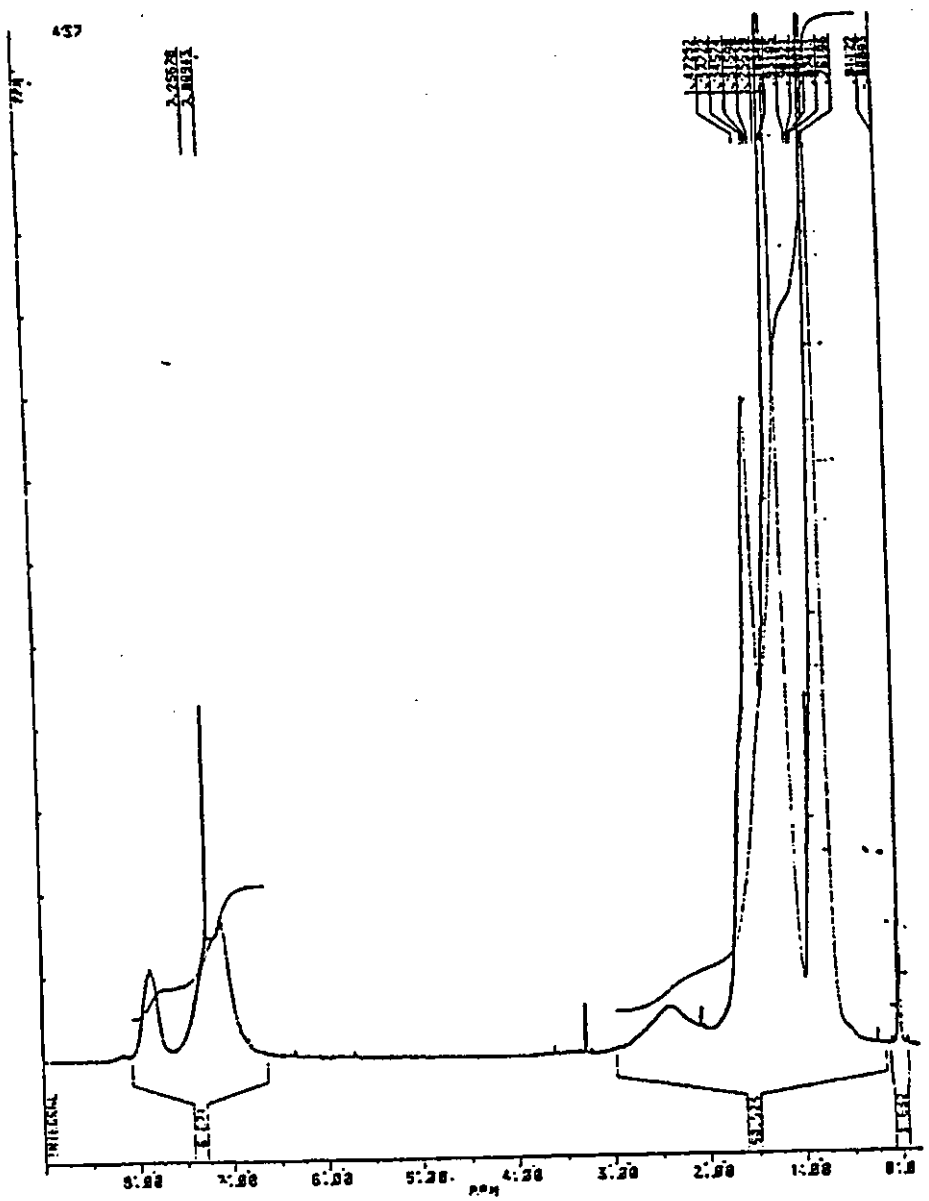

Fig. 4.10 ^{1}H NMR spectrum of organotin polymer poly(*o*-MAOTBTB)

In contrast to *meta-* and *para-* acrylamide monomers the polymerisation of *o-*AOTBTB and *o*-MAOTBTB monomers proceeded at higher temperatures and required longer periods of time. Such lower reactivity might be attributed to the presence of the bulky tri-n-butyl tin group in the *ortho-* position, which was thought to lead to a higher degree of steric hindrance than substituents at *meta-* or *para-* positions.

4. 5 Copolymerisation of Organotin Monomers

4. 5.1 Copolymerisation of Acrylamide Derivatives

The organotin monomers *m*-AATBTB, *p*-AATBTB, *m-* MAATBTB and *p*-MAATBTB have been copolymerised with MA, BA and MMA. The reactions can be represented as in scheme (4.11):

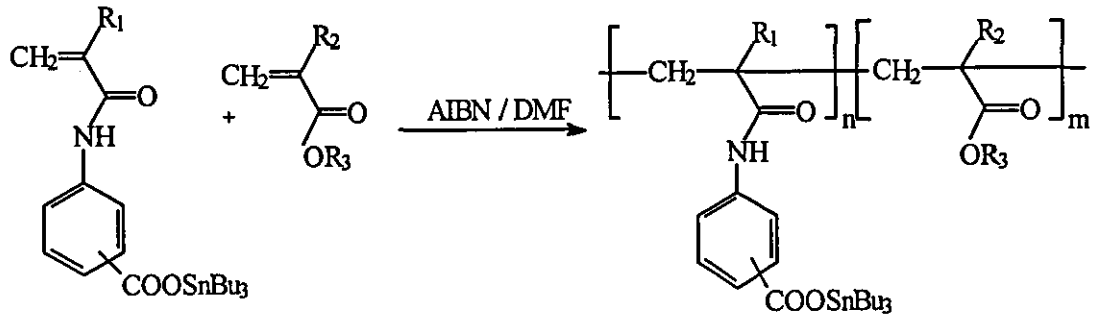

R_1 Non-methylated H

Methylated CH_3

where oganotin monomer is M_1

and acrylic monomer is M_2

	R_2	R_3
MA	H	CH_3
BA	H	C_4H_9
MMA	CH_3	CH_3

Scheme (4.11)

The experimental conditions and the results of the copolymerisations are illustrated in tables (4.1-4.12). From the experimental data of the twelve systems studied the monomer reactivity ratios (r_1 and r_2) for each system were calculated by the Kelen-Tudos method and the standard deviations of the results were calculated by regression analysis. Figures (4.11a-4.22a) illustrate the Kelen-Tudos plots of the twelve systems which give r_1 and $-r_2/\alpha$, both as intercepts. It is observed that good linearity remained by equation (1.32), and accurate slopes are shown. The method to find (r_1 and r_2) requires identification of intercepts

which generally are easily formed except in figures (4.11a and 4.17a) where the first and last data points in each figure have a pronounced effect. The results are summarised in table (4.14).

From table (4.14) it is clear that value of reactivity ratios (r_1 and r_2) for the copolymerisation reactions of organotin monomers *m*-AATBTB and *p*-MAATBTB with MA and BA are both less than unity and that the copolymerisation reactions of these systems should have an azeotropic composition at which a homogeneous copolymer is formed at various degrees of conversion. Figures (4.11b, and 4.12b) show that the copolymer composition curve has $f_1=F_1$ at mol fractions 0.30 and 0.41 for copolymerisations of *m*-AATBTB with MA and BA respectively. Figures (4.20b, and 4.21b) show that the copolymer composition curve has $f_1=F_1$ at mol fractions 0.85 and 0.55 for copolymerisations of *p*-MAATBTB with MA and BA respectively. The (r_1 r_2) values for copolymerisations of *m*-AATBTB-MA, *m*-AATBTB-BA, *m*-AATBTB-MMA, *p*-AATBTB-MA, *m*-MATBTB-BA, *p*-MATBTB-MA, *p*-MATBTB-BA,and *p*-MATBTB-MMA are 0.33, 0.18, 0.31, 0.76, 0.73, 0.81, 0.48, 0.77 respectively indicating that the copolymer should have a statistical distribution of monomer units. A tendency towards alternation increases with increasing length of the alkyl chain of the acrylic acid ester, while for the *p*-AATBTB-MMA, *m*-MATBTB-MA, *m*-MATBTB-MMA systems the (r_1r_2) values of 1.55, 1.2, 2.47 illustrate a low tendency of the monomer units to alternate and the copolymer should be composed mainly of short sequences of monomeric units of the same type. On the other hand the copolymer of *p*-AATBTB-BA shows almost ideal behaviour (r_1 r_2) = 1.04.

The monomer reactivity ratios of AATBTB-MA were determined on the basis of calculating the copolymer composition of each sample by ^{1}H NMR spectroscopy. The distribution of protons is an important factor to distinguish the units in the copolymer chain.[93] Figure (4.23) shows a typical ^{1}H NMR spectrum of a *p*-AATBTB-MA copolymer sample as follows:

i- two peaks at δ 7.4 ppm and 7.8 ppm due to phenyl protons C_6H_4- of a *p*-AATBTB unit.

ii- One peak at δ 3.42 ppm due to the methoxy group of a MA unit.

iii- All the aliphatic protons CH_3-, -CH_2- and -CH- of *p*-TAABTB and MA units are overlaping and appear at δ 0.70, 1.50, and 2.7 ppm, respectively. The copolymer composition (**b**) was determined by the following equation:

$$\int C_6H_4 / \int OCH_3 = (4/3)\ \mathbf{b} \quad \text{.....(4.1)}$$

where $\int C_6H_4$ and $\int CH_3$ are the integrated traces of C_6H_4 and CH_3- protons, respectively. Table (4.13) illustrates analytical data for the copolymerisation reactions in the case of the *p*-AATBTB-MA copolymer system. Table (4.14) illustrates the monomer reactivity ratios(r_1 and r_2) for the *p*-AATBTB-MA copolymer system based on the ^1H NMR spectra data. The values of r_1 and r_2 calculated from ^1H NMR spectroscopy are almost identical to those obtained from tin analysis. Figure (4.24) shows the Kelen-Tudos plot for the *p*-AATBTB-MA copolymer system based on ^1H NMR spectra data.

4.5.2 Copolymerisation of Acryloyloxy Derivatives

The organotin monomers *o*-AOTBTB and *o*-MAOTBTB have been copolymerised with MA, BA and MMA. These reactions can be represented as:

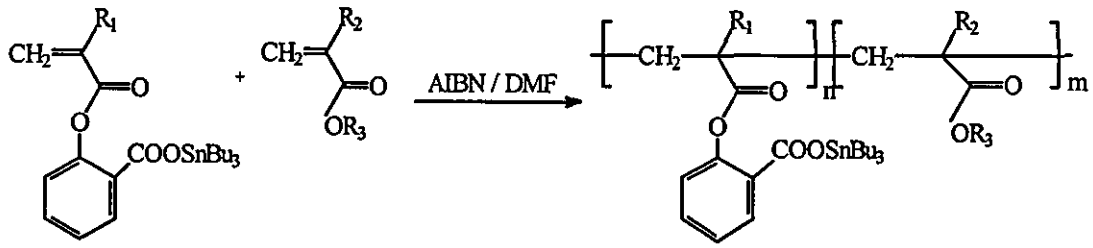

R_1 Non-methylated H

Methylated CH_3

	R_2	**R_3**
MA	H	CH_3
BA	H	C_4H_9
MMA	CH_3	CH_3

Scheme (4.12)

The experimental conditions and results of the copolymerisation reactions are illustrated in tables (4.15-4.20). From the experimental data of the six systems studied the monomer reactivity ratios for each system were calculated by the Kelen-Tudos method and the standard deviations of the results were calculated by regression analysis. Figures (4.25a-4.30a) show Kelen-Tudos plots for copolymerisation reactions of *o*-AOTBTB-MA, *o*-AOTBTB-BA, *o*-AOTBTB-MMA, *o*-MAOTBTB-MA, *o*-MAOTBTB-BA, and *o*-MAOTBTB-MMA which give r_1 and $-r_2/\alpha$, both as intercepts. These plots exhibit good linearity according to equation (1.32) and monomer reactivity ratios are easily formed except for figure (4.29a) where some scatter of the data points is observed. The results are summarised in table (4.21). From table (4.21) it clear that values of monomer reactivity ratios(r_1 and r_2) for the copolymerisation reactions of organotin monomers *o*-AOTBTB with MMA and *o*-MAOTBTB with MA and BA are less than unity and that the copolymerisation reactions of these systems should have an azeotropic composition. Figure (4.27b) shows that the copolymer composition curve has $f_1=F_1$ at mole fraction 0.48 for the copolymerisation of *o*-AOTBTB with MMA. Figures (4.28b and 4.29b) show that the copolymer composition curves have $f_1=F_1$ at mole fractions 0.52 and 0.22 for copolymerisations of *o*-MAOTBTB with MA and BA respectively. The values of (r_1 r_2) for *o*-AOTBTB-MMA, *o*-MAOTBTB-MA, *o*-MAOTBTB-BA and *o*-MAOTBTB-MMA were 0.48, 0.38, 0.11, 0.58 respectively, indicating that these copolymers should have a statistical distribution of monomer units. For the *o*-AOTBTB-MA and *o*-AOTBTB-BA systems the (r_1 r_2) values 1.17 and 1.06 show almost ideal behaviour.

Manesh et al[85] studied the copolymerisation reactions of methacryloyloxy benzoic acid with ST and with NVP and determined reactivity ratios and molecular weights. They found a strong tendency for alternation for the first system, with an azeotropic composition at about 50 mole percent for methacryloyloxy benzoic acid, whereas the azeotropic composition for the second system occurred at about 70 mole percent for methacryloyloxy benzoic acid.

4.6 Q and e Schemes for Organotin Monomers

From table (4.14), the Q_1 values[94] for *p*-AATBTB were less than those of *p*-acrylamido toluene and *p*-acrylamido chlorobenzene (1.45 and 0.99 respectively) reported by Tawfik *et al.*[77] It follows that such a decrease in the Q_1 values is caused by steric hindrance induced by the tri-n-butyl chains, rather than a reduction in the resonance stabilising effect of the *p*-carboxyphenyl substituent. In contrast, the *meta-* carboxy substutituent in *m*-tri-n-butlytincarboxyphenyl-acrylamides has a reduced resonance stabilising effect, which is reflected in a slight decrease in the Q_1 values as illustrated in table (4.14).

Positive *e* values[94] table (4.14) for the *para*-substitiuted monomer correlate well with the fact that the *para-* carboxyl substituent reduces the electron density on an acrylamide double bond through resonance structures, while they are negative for the *meta-* derivatives reflecting high electron density at the polymerisable acrylamide double bond, resulting from the limited electron withdrawing action by the *meta-* carboxyl group. It follows that *m*-acrylamidotri-n-butlytin benzoate are more nearly alternating than the *para*-derivative in their copolymers (with MA, BA, and MMA). The presence of a methyl group on the polymerisable double bond, generally decreased the *e* value, due to its electron donating effect. For example it is noticed clearly when *p*-MAATBTB is compared with *p*-AATBTB.

Regarding *o*-acryloyloxy and methacryloyloxytri-n-butyltin benzoates, as expected, negative *e* values table (4.21) increased due to the presence of the electron donating methyl group. This can be demonstrated by examining *o*-AOTBTB and *o*-MAOTBTB. The Q_1 values for both acryloyloxy and methacryloyloxy derivatives are comparable with those of the acrylamide and methacrylamide series table (4.14).

4.7 Monomer Reactivity

From table (4.14), two factors influence the reactivity of the acryalmide monomers. These are:

1- Position of the tri-n-butyltin carboxylate substituents on the aromatic ring.

2- Effect of methyl group substitution on the polymerisable double bond.

By comparing *m*-AATBTB and *p*-AATBTB table (4.14), the monomer reactivities ($1/r_1$) of the acrylates MA, MMA, and BA with the *meta*-acrylamide radical are higher than that with the *para*- radical (for each acrylic monomer). This can be attributed to the position of the carboxyl group on the aromatic ring as the *meta* substituent contributes to a lesser degree in radical stabilisation. The free radical generated on the acrylic double bond during polymerisation is stabilised according to the radical resonance structures for *para* and *ortho* positions see scheme (1.3) and refer to introduction section (1.1.2). However, upon comparing the acrylate monomers (MA, BA, and MMA) reactivity ratios with *m*-MAATBTB and *p*-MAATBTB radicals, it is apparent that both radicals have similar reactivities towards the mentioned monomers within experimental error. Both are lower than that of *m*-AATBTB and equivalent to that of *p*-AATBTB. This can be interpreted by the steric effect exerted by the methyl group which leads to a marked influence on the radical reactivity of the reactive *m*-AATBTB while minimum or no effect on the poorly reactive *para*-derivative.

Table 4.1: Copolymerisation of *m*-acrylamidotri-n-butyltin benzoate with methyl acrylate.

Initial composition		Conv.%	Sn %	Copolymer composition		Kelen-Tudos parameters	
a^*	f_1^0			b^*	F_1^0	η	ξ
1.50	0.60	8.98	20.73	0.93	0.48	-0.04	0.83
1.00	0.50	7.24	20.15	0.79	0.44	-0.15	0.72
0.67	0.39	6.53	18.57	0.71	0.42	-0.24	0.56
0.43	0.30	8.29	17.64	0.45	0.31	-0.58	0.45
0.25	0.20	7.15	15.05	0.28	0.22	-0.88	0.30
0.11	0.10	4.25	9.88	0.12	0.11	-1.35	0.17

* molar ratio
° mole fraction

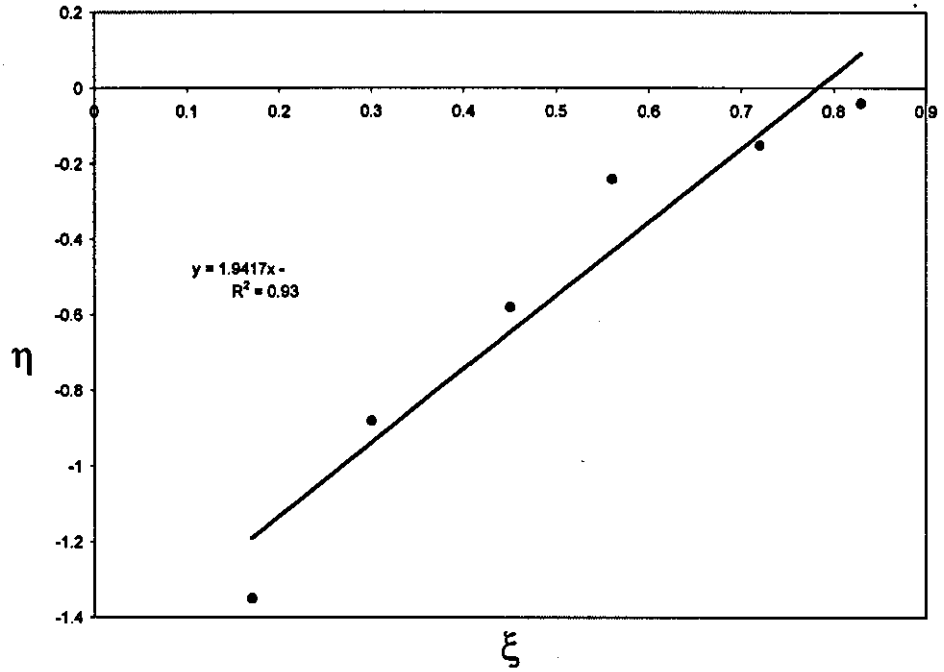

Fig. 4.11a, Kelen-Tudos plot for copolymerisation of *m*-AATBTB-MA.

$$\xi = \frac{a^2}{\alpha\ b + a^2} \quad \text{and} \quad \eta = \frac{a(b-1)}{\alpha\ b + a^2}$$

where a and b are the molar ratios of the comonomer in the feed and copolymer, respectively, and

$$\alpha = \frac{a_{min} \times a_{max}}{(b_{min} \times b_{max})^{1/2}}$$

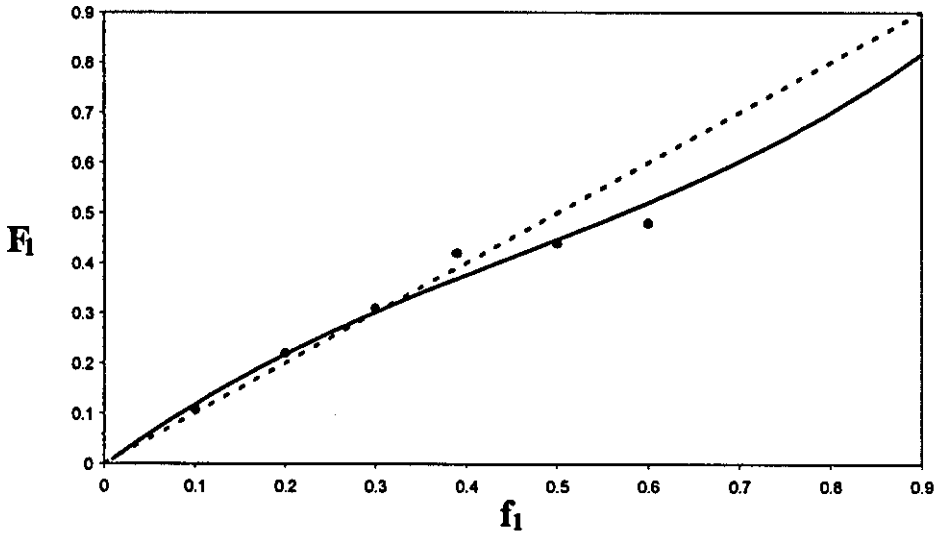

Fig. 4.11b, Composition curve for copolymerisation of *m*-AATBTB-MA, Curve represents calculated values and ● represents experimental values , where f_1 = mole fraction of M_1 in feed F_1 = mole fraction of M_1 in copolymer

Table 4.2: Copolymerisation of *m*-acrylamidotri-n-butyltin benzoate with butyl acrylate.

Initial composition		Conv.%	Sn %	Copolymer composition		Kelen-Tudos parameters	
a^*	f_1^0			b^*	F_1^0	η	ξ
1.50	0.60	8.31	20.03	1.12	0.53	0.07	0.84
1.00	0.50	8.51	19.15	0.91	0.48	-0.07	0.75
0.66	0.39	9.53	17.68	0.66	0.39	-0.33	0.64
0.43	0.30	7.81	16.02	0.49	0.33	-0.61	0.51
0.25	0.20	5.38	13.47	0.32	0.24	-0.96	0.35
0.11	0.10	6.26	10.27	0.19	0.17	-1.11	0.15

* molar ratio
° mole fraction

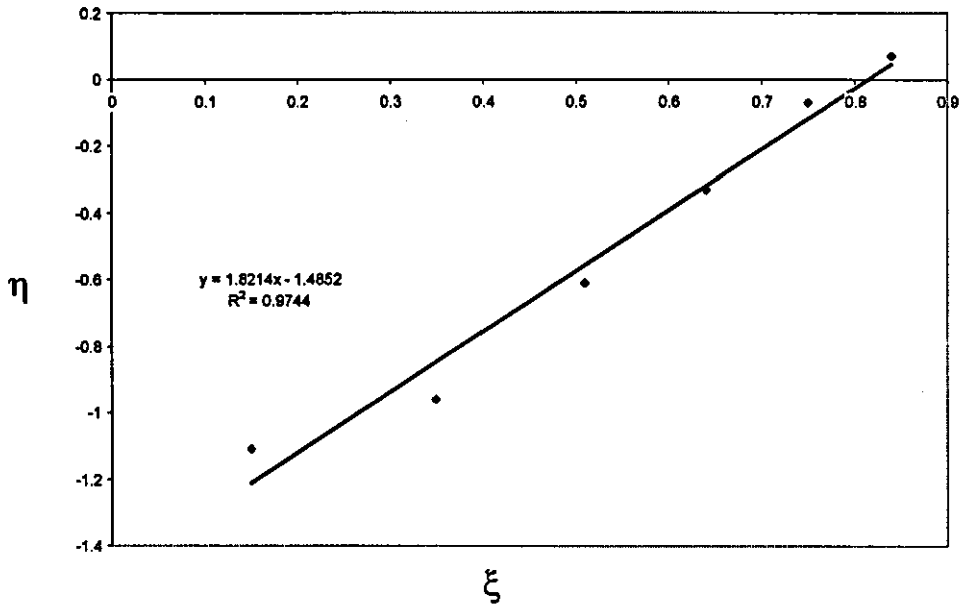

Fig. 4.12a, Kelen-Tudos plot for copolymerisation of *m*-AATBTB-BA.

$$\xi = \frac{a^2}{\alpha\, b + a^2} \quad \text{and} \quad \eta = \frac{a(b-1)}{\alpha\, b + a^2}$$

where a and b are the molar ratios of the comonomer in the feed and copolymer, respectively, and

$$\alpha = \frac{a_{min} \times a_{max}}{(b_{min} \times b_{max})^{1/2}}$$

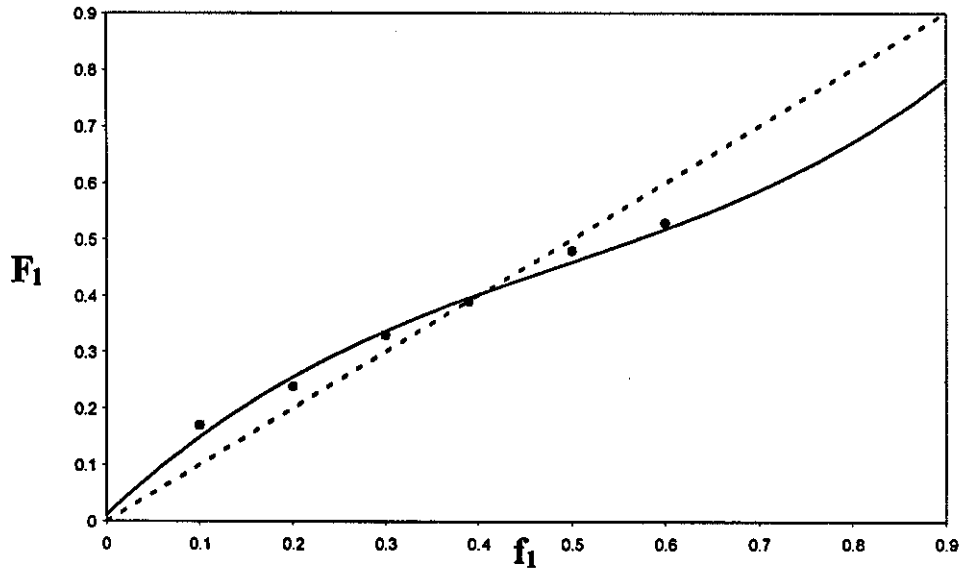

Fig. 4.12b, Composition curve for copolymerisation of *m*-AATBTB-BA, Curve represents calculated values and ● represents experimental values , where f_1 = mole fraction of M_1 in feed F_1 = mole fraction of M_1 in copolymer

Table 4.3: Copolymerisation of *m*-acrylamidotri-n-butyltin benzoate with methyl methacrylate

Initial composition		Conv.%	Sn %	Copolymer composition		Kelen-Tudos parameters	
a^*	f_1^o	%		b^*	F_1^o	η	ξ
4.00	0.80	5.91	21.38	1.30	0.57	0.06	0.87
1.85	0.65	6.07	20.13	0.90	0.47	-0.04	0.68
1.22	0.55	9.78	18.63	0.63	0.38	-0.17	0.57
0.82	0.45	8.13	16.52	0.42	0.29	-0.34	0.48
0.54	0.35	9.25	14.09	0.27	0.22	-0.50	0.37
0.18	0.13	6.53	9.15	0.12	0.11	-0.63	0.13

* molar ratio
° mole fraction

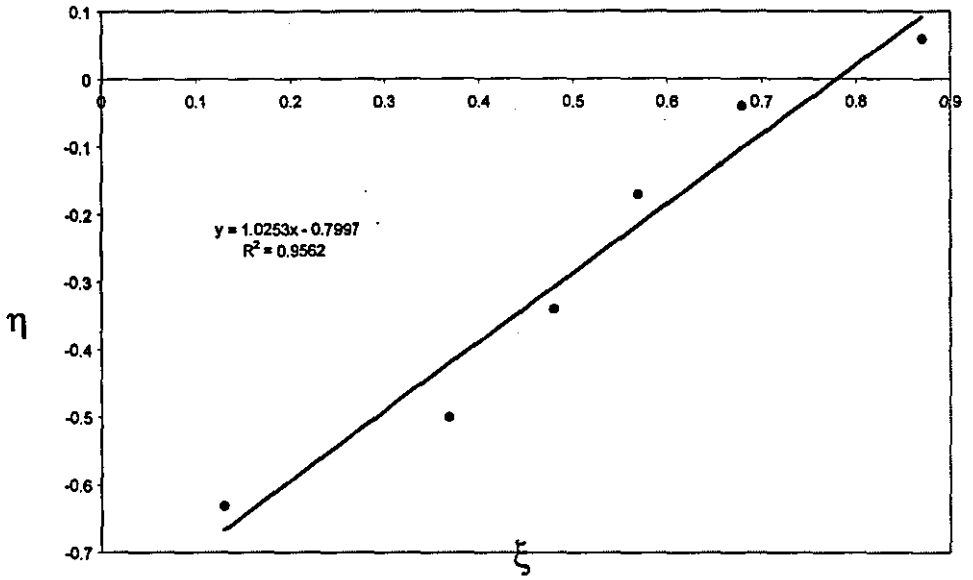

Fig. 4.13a, Kelen-Tudos plot for copolymerisation of *m*-AATBTB-MMA.

$$\xi = \frac{a^2}{\alpha\ b + a^2} \quad \text{and} \quad \eta = \frac{a(b-1)}{\alpha\ b + a^2}$$

where a and b are the molar ratios of the comonomer in the feed and copolymer, respectively, and

$$\alpha = \frac{a_{min} \times a_{max}}{(b_{min} \times b_{max})^{1/2}}$$

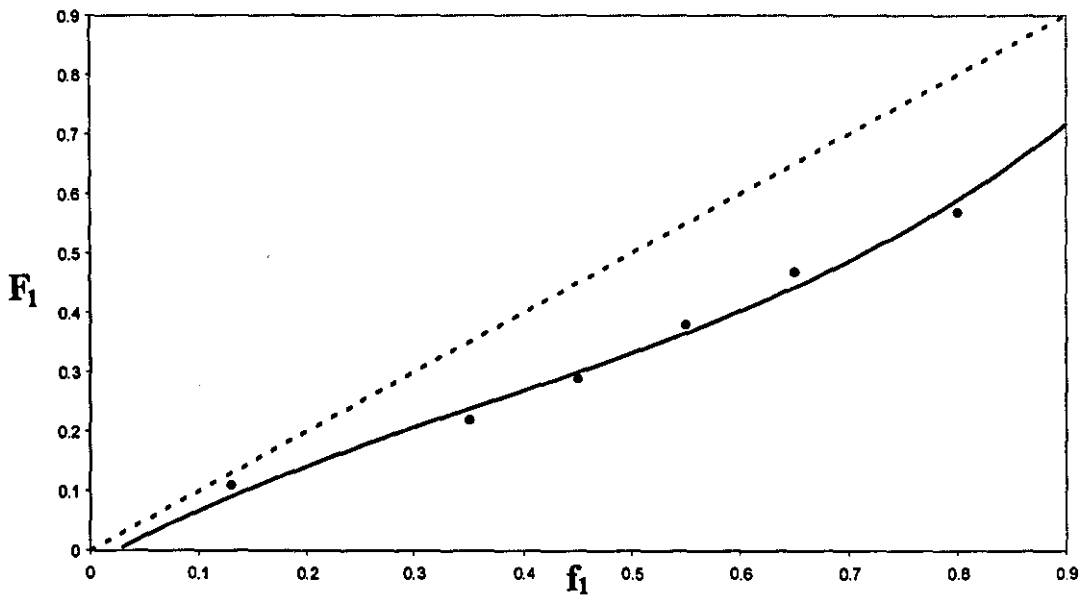

Fig. 4.13b, Composition curve for copolymerisation of *m*-AATBTB-MMA, Curve represents calculated values and ● represents experimental values , where f_1 = mole fraction of M_1 in feed F_1 =mole fraction of M_1 in copolymer

Table 4.4: Copolymerisation of *p*-acrylamidotri-n-butyltin benzoate with methyl acrylate

Initial composition		Conv.%	Sn %	Copolymer composition		Kelen-Tudos parameters	
a^*	f_1^0	%		b^*	F_1^0	η	ξ
1.69	0.63	7.97	22.61	1.86	0.48	0.41	0.81
0.98	0.49	8.29	21.37	1.13	0.44	0.09	0.69
0.65	0.39	6.38	20.59	0.88	0.42	-0.10	0.57
0.44	0.30	6.37	18.91	0.58	0.31	-0.46	0.47
0.26	0.20	7.88	16.13	0.33	0.22	-0.91	0.35
0.12	0.10	9.18	11.25	0.12	0.15	-1.44	0.19

* molar ratio
^{0} mole fraction

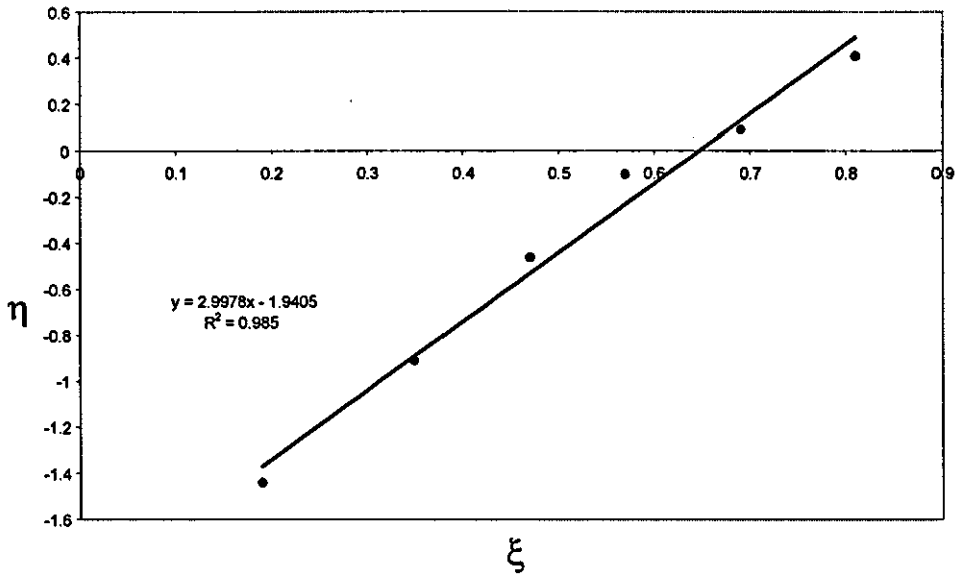

Fig. 4.14a, Kelen-Tudos plot for copolymerisation of *p*-AATBTB-MA.

$$\xi = \frac{a^2}{\alpha\ b + a^2} \text{ and } \eta = \frac{a(b-1)}{\alpha\ b + a^2}$$

where a and b are the molar ratios of the comonomer in the feed and copolymer, respectively, and

$$\alpha = \frac{a_{min} \times a_{max}}{(b_{min} \times b_{max})^{1/2}}$$

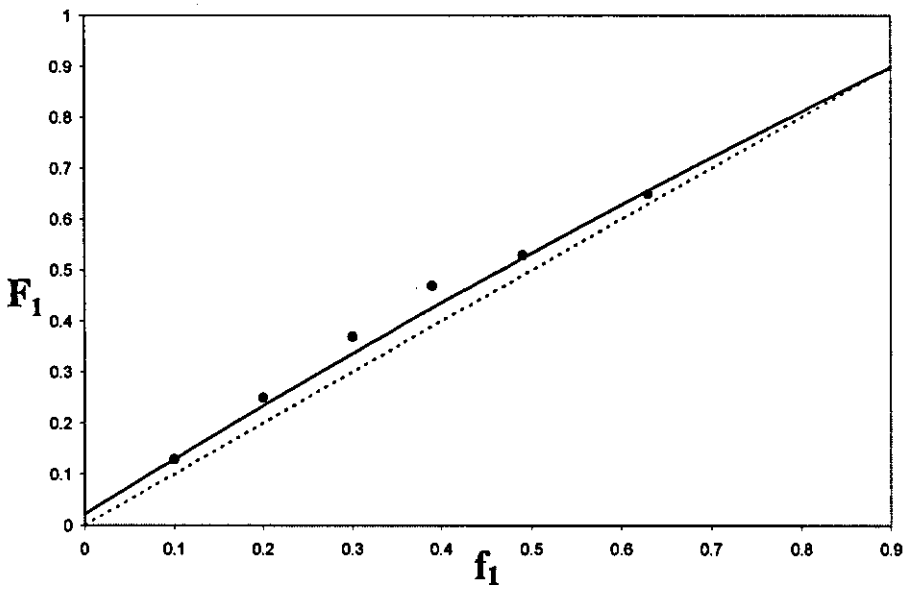

Fig. 4.14b, Composition curve for copolymerisation of *p*-AATBTB-MA, Curve represents calculated values and ● represents experimental values , where f_1 = mole fraction of M_1 in feed F_1 = mole fraction of M_1 in copolymer

Table 4.5: Copolymerisation of *p*-acrylamidotri-n-butyltin benzoate with butyl acrylate.

Initial composition		Conv.%	Sn %	Copolymer composition		Kelen-Tudos parameters	
a^*	f_1^0	%		b^*	F_1^0	η	ξ
1.38	0.58	7.68	21.12	1.53	0.61	0.30	0.77
0.93	0.48	8.32	19.72	1.03	0.51	0.02	0.69
0.62	0.38	6.33	18.54	0.78	0.44	-0.19	0.57
0.39	0.28	7.42	15.94	0.48	0.32	-0.62	0.47
0.26	0.21	6.73	12.72	0.28	0.22	-1.11	0.40
0.12	0.11	8.67	8.20	0.13	0.12	-1.66	0.23

* molar ratio
^{0} mole fraction

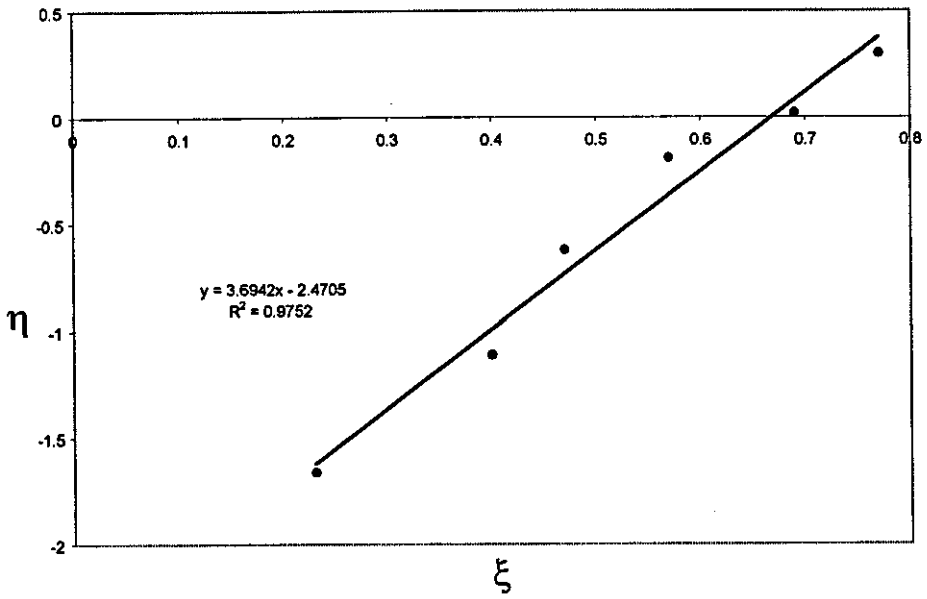

Fig. 4.15a, Kelen-Tudos plot for copolymerisation of *p*-AATBTB-BA.

$$\xi = \frac{a^2}{\alpha\, b + a^2} \quad \text{and} \quad \eta = \frac{a(b-1)}{\alpha\, b + a^2}$$

where a and b are the molar ratios of the comonomer in the feed and copolymer, respectively, and

$$\alpha = \frac{a_{min} \times a_{max}}{(b_{min} \times b_{max})^{1/2}}$$

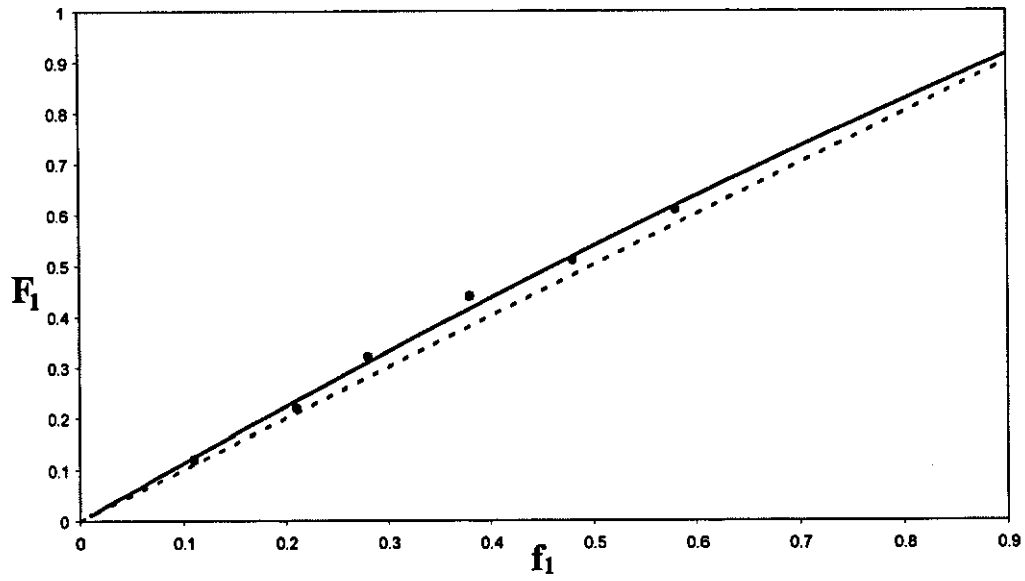

Fig. 4.15b, Composition curve for copolymerisation of *p*-AATBTB-BA, Curve represents calculated values and ● represents experimental values , where f_1 = mole fraction of M_1 in feed F_1 = mole fraction of M_1 n copolymer

Table 4.6: Copolymerisation of *p*-acrylamidotri-n-butyltin benzoate with methyl methacrylate.

Initial composition		Conv.%	Sn %	Copolymer composition		Kelen-Tudos parameters	
a^*	f_1^0	%		b^*	F_1^0	η	ξ
1.55	0.61	7.67	21.68	1.45	0.59	0.22	0.77
0.91	0.48	8.97	19.94	0.85	0.46	-0.10	0.66
0.67	0.40	6.53	17.94	0.55	0.35	-0.42	0.62
0.41	0.29	7.32	14.96	0.32	0.24	-0.85	0.51
0.25	0.20	8.33	12.13	0.19	0.17	-1.23	0.39
0.12	0.10	9.53	7.37	0.09	0.08	-1.83	0.23

* molar ratio
^{0} mole fraction

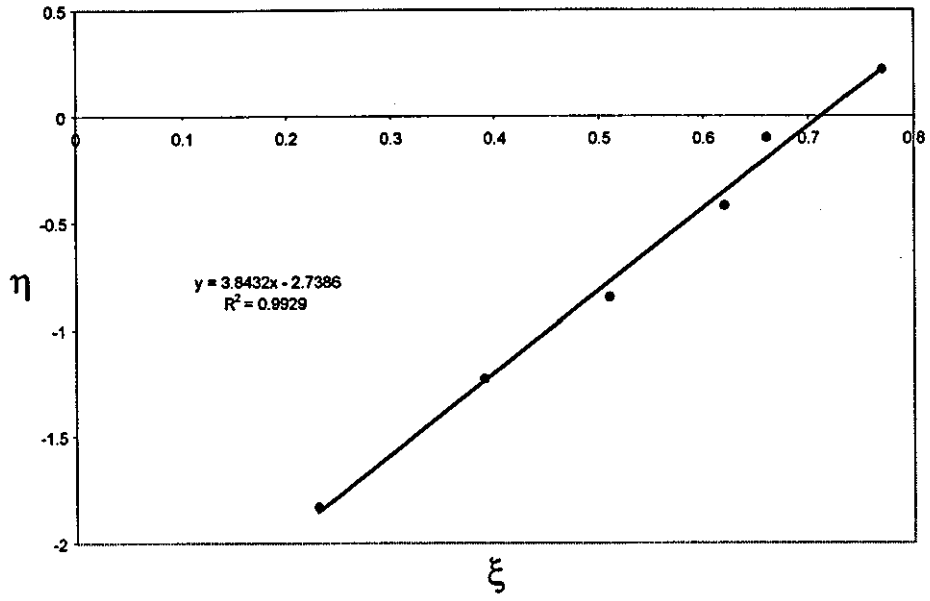

Fig. 4.16a, Kelen-Tudos plot for copolymerisation of *p*-AATBTB-MMA.

$$\xi = \frac{a^2}{\alpha\ b + a^2} \quad \text{and} \quad \eta = \frac{a(b-1)}{\alpha\ b + a^2}$$

where a and b are the molar ratios of the comonomer in the feed and copolymer, respectively, and

$$\alpha = \frac{a_{min} \times a_{max}}{(b_{min} \times b_{max})^{1/2}}$$

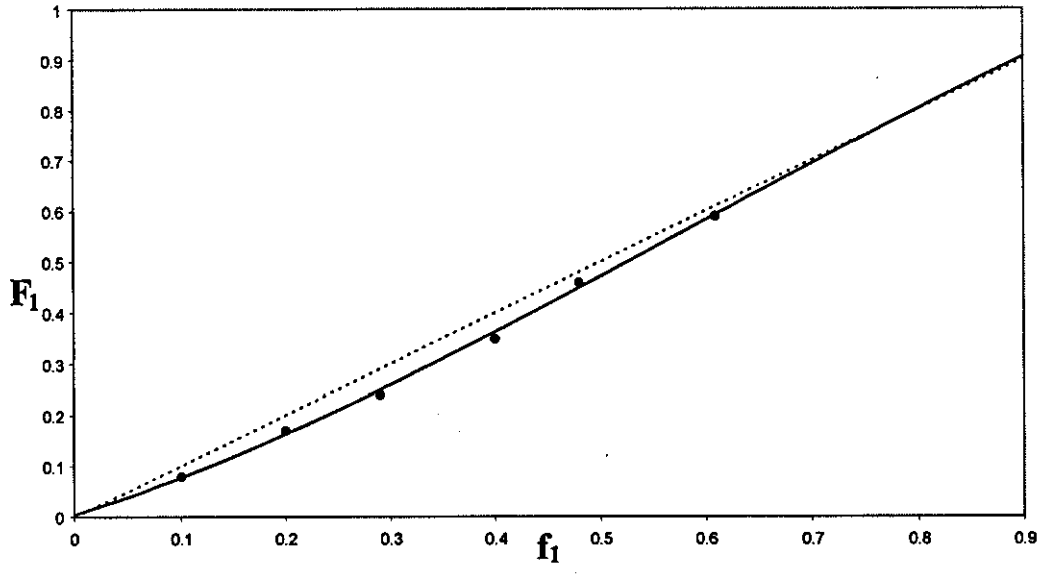

Fig. 4.16b, Composition curve for copolymerisation of *p*-AATBTB-MMA, Curve represents calculated values and ● represents experimental values , where
f_1 = mole fraction of M_1 in feed F_1 = mole fraction of M_1 in copolymer

Table 4.7: Copolymerisation of *m*-methacrylamidotri-n-butyltin benzoate with methyl acrylate.

Initial composition		Conv.%	Sn %	Copolymer composition		Kelen-Tudos parameters	
a^*	f_1^0	%		b^*	F_1^0	η	ξ
1.55	0.61	8.97	22.11	1.94	0.66	0.47	0.78
0.96	0.49	7.51	20.39	0.96	0.49	-0.03	0.73
0.57	0.36	8.97	17.65	0.48	0.32	-0.54	0.63
0.42	0.30	9.22	16.76	0.39	0.28	-0.79	0.56
0.23	0.18	6.54	12.37	0.18	0.16	-1.48	0.42
0.10	0.09	8.75	9.09	0.11	0.10	-1.9	0.22

* molar ratio
^{0} mole fraction

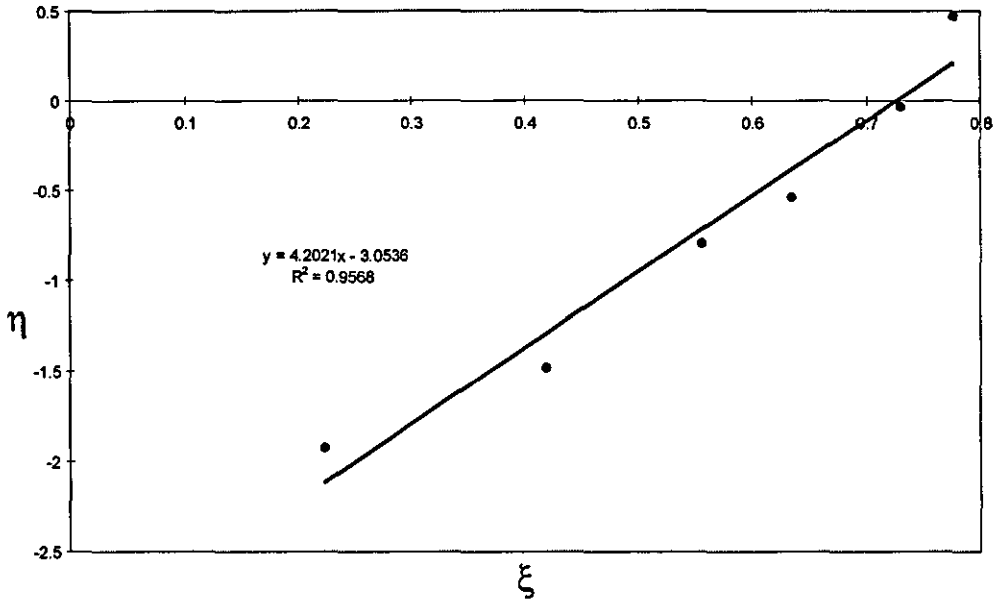

Fig. 4.17a, Kelen-Tudos plot for copolymerisation of *m*-MAATBTB-MA.

$$\xi = \frac{a^2}{\alpha\ b + a^2} \quad \text{and} \quad \eta = \frac{a(b-1)}{\alpha\ b + a^2}$$

where a and b are the molar ratios of the comonomer in the feed and copolymer, respectively, and

$$\alpha = \frac{a_{min} \times a_{max}}{(b_{min} \times b_{max})^{1/2}}$$

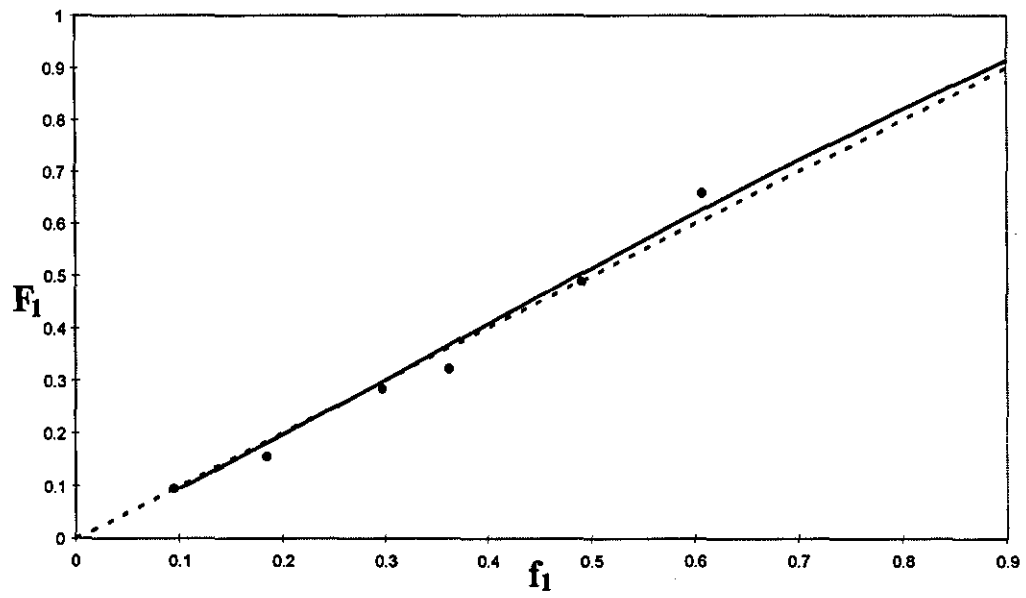

Fig. 4.17b, composition curve for copolymerisation of *m*-MAATBTB-MA, Curve represents calculated values and ● represents experimental values , where f_1 = mole fraction of M_1 in feed F_1 = mole fraction of M_1 in copolymer

Table 4.8: Copolymerisation of *m*-methacrylamidotri-n-butyltin benzoate with butyl acrylate.

Initial composition		Conv.%	Sn %	Copolymer composition		Kelen-Tudos parameters	
a^*	f_1^0			b^*	F_1^0	η	ξ
1.35	0.57	8.76	19.12	1.01	0.50	0.00	0.79
0.93	0.48	7.53	17.75	0.73	0.42	-0.21	0.72
0.59	0.37	9.51	15.10	0.43	0.30	-0.60	0.63
0.42	0.30	8.24	13.84	0.35	0.26	-0.80	0.52
0.24	0.19	7.52	10.08	0.19	0.16	-1.34	0.39
0.11	0.10	9.63	6.26	0.09	0.08	-1.78	0.21

* molar ratio
° mole fraction

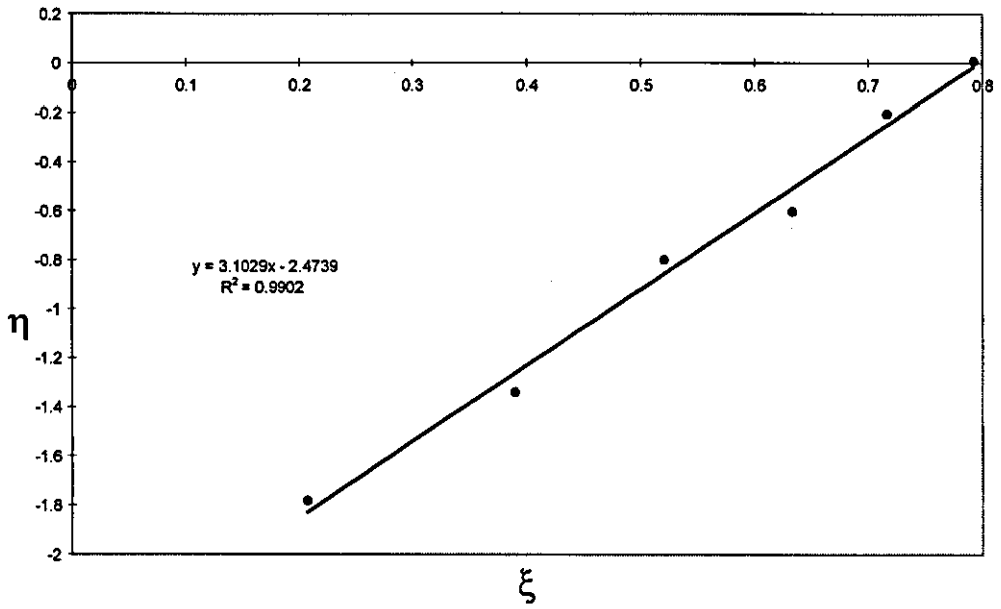

Fig. 4.18a, Kelen-Tudos plot for copolymerisation of *m*-MAATBTB-BA.

$$\xi = \frac{a^2}{\alpha\ b + a^2} \quad \text{and} \quad \eta = \frac{a(b-1)}{\alpha\ b + a^2}$$

where a and b are the molar ratios of the comonomer in the feed and copolymer, respectively, and

$$\alpha = \frac{a_{min} \times a_{max}}{(b_{min} \times b_{max})^{1/2}}$$

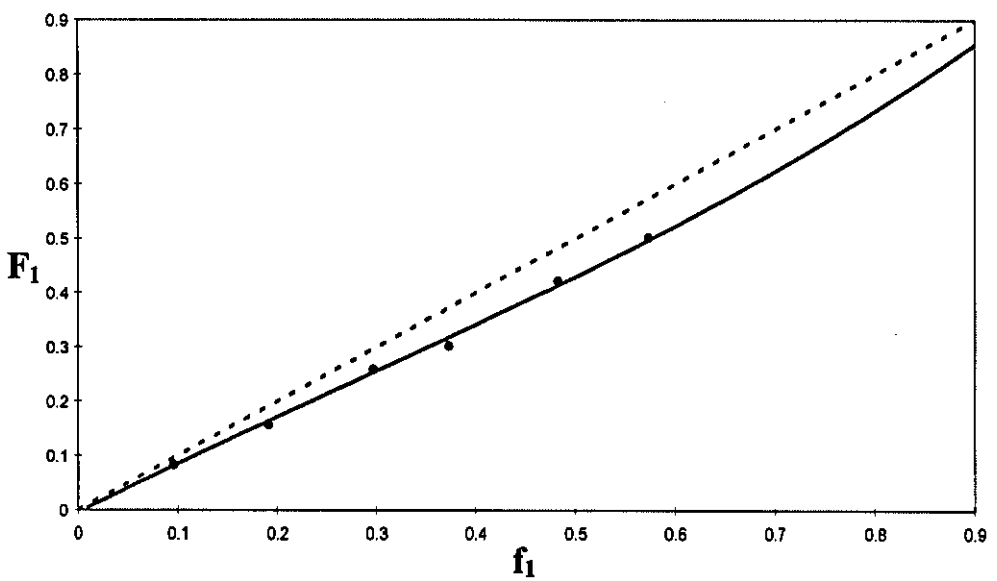

Fig. 4.18b, Composition curve for copolymerisation of *m*-MAATBTB-BA, Curve represents calculated values and ● represents experimental values , where f_1 = mole fraction of M_1 in feed F_1 = mole fraction of M_1 in copolymer

Table 4.9: Copolymerisation of *m*-methacrylamidotri-n-butyltin benzoate with methyl methacrylate.

Initial composition		**Conv.%**	**Sn %**	**Copolymer composition**		**Kelen-Tudos parameters**	
a^*	f_1^0			b^*	F_1^0	η	ξ
1.25	0.55	7.52	18.04	0.60	0.38	-0.24	0.75
0.68	0.41	8.20	14.22	0.29	0.23	-0.67	0.65
0.40	0.28	9.63	10.96	0.17	0.14	-1.09	0.52
0.24	0.19	8.64	7.54	0.09	0.08	-1.59	0.43
0.10	0.09	9.65	3.56	0.04	0.03	-2.40	0.24

* molar ratio
° mole fraction

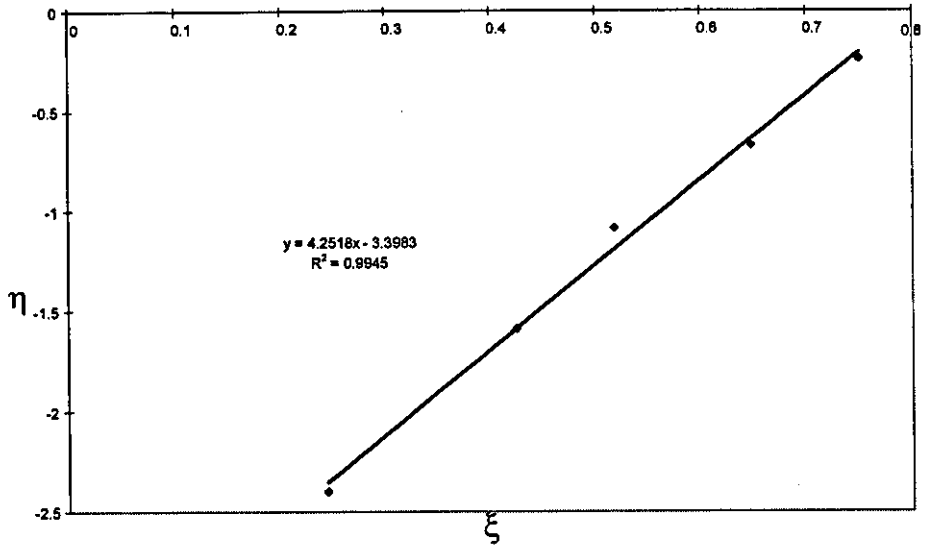

Fig. 4.19a, Kelen-Tudos plot for copolymerisation of *m*-MAATBTB-MMA.

$$\xi = \frac{a^2}{\alpha\ b + a^2} \quad \text{and} \quad \eta = \frac{a(b-1)}{\alpha\ b + a^2}$$

where a and b are the molar ratios of the comonomer in the feed and copolymer, respectively, and

$$\alpha = \frac{a_{min} \times a_{max}}{(b_{min} \times b_{max})^{1/2}}$$

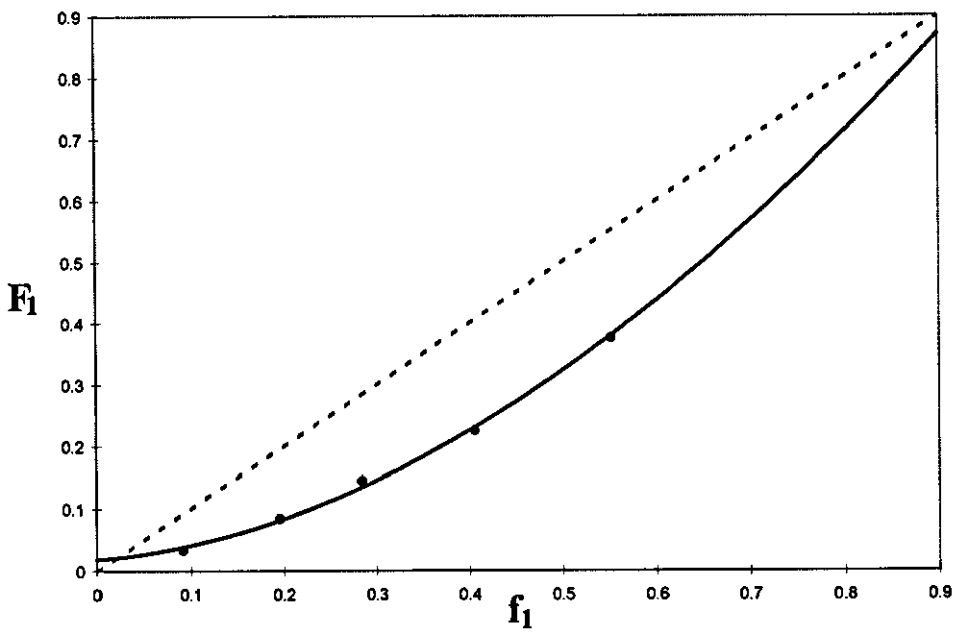

Fig. 4.19b, Composition curve for copolymerisation of *m*-MAATBTB-MMA, Curve represents calculated values and ● represents experimental values , where f_1 = mole fraction of M_1 in feed F_1 = mole fraction of M_1 in copolymer

Table 4.10: Copolymerisation of *p*-methacrylamidotri-n-butyltin benzoate with methyl acrylate.

Initial composition		**Conv.%**	**Sn %**	**Copolymer composition**		**Kelen-Tudos parameters**	
a^*	f_1^0			b^*	F_1^0	η	ξ
1.49	0.60	8.56	21.59	1.51	0.60	0.27	0.80
0.99	0.50	7.65	20.77	1.09	0.52	0.06	0.71
0.62	0.38	9.54	19.37	0.71	0.42	-0.27	0.60
0.42	0.29	9.52	17.66	0.47	0.32	-0.63	0.49
0.24	0.19	7.56	14.38	0.26	0.21	-1.19	0.38
0.11	0.09	8.23	10.19	0.13	0.11	-1.61	0.19

* molar ratio
^{0} mole fraction

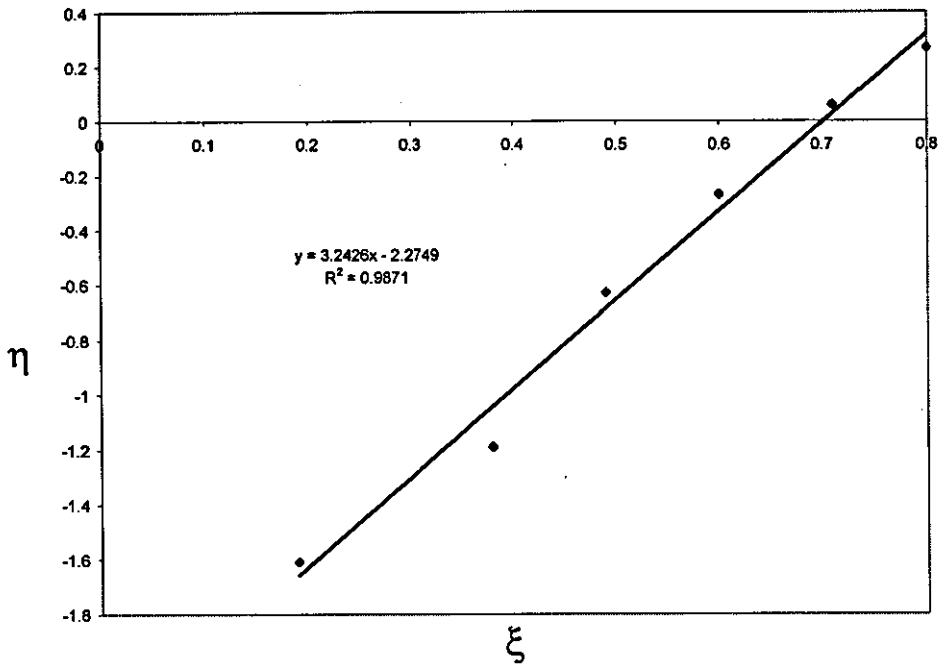

Fig. 4.20a, Kelen-Tudos plot for copolymerisation of *p*-MAATBTB-MA.

$$\xi = \frac{a^2}{\alpha\ b + a^2} \quad \text{and} \quad \eta = \frac{a(b-1)}{\alpha\ b + a^2}$$

where a and b are the molar ratios of the comonomer in the feed and copolymer, respectively, and

$$\alpha = \frac{a_{min} \times a_{max}}{(b_{min} \times b_{max})^{1/2}}$$

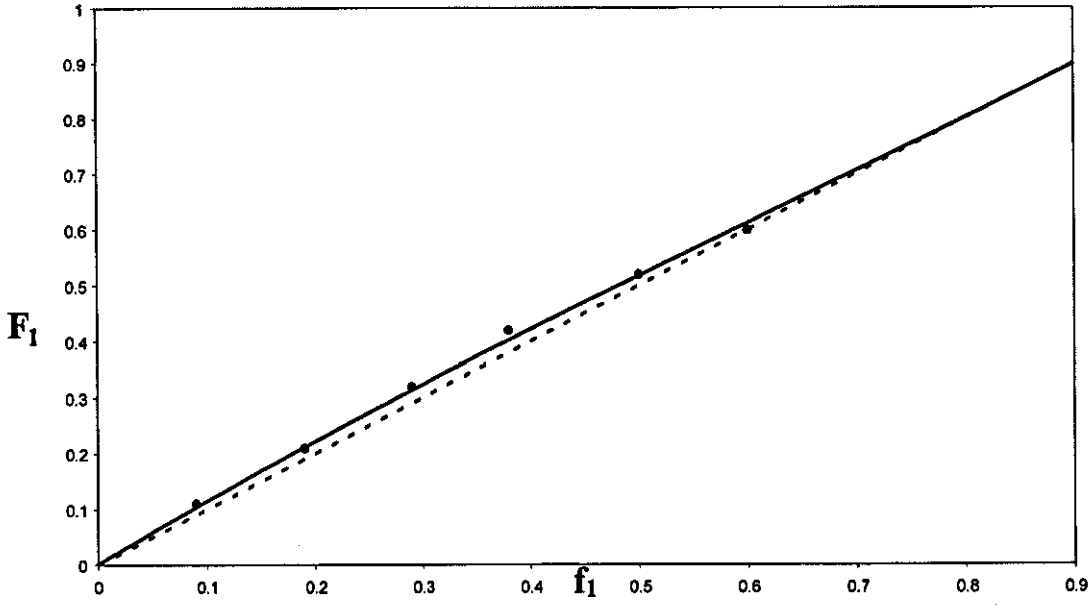

Fig. 4.20b, Composition curve for copolymerisation of *p*-MAATBTB-MA, Curve represents calculated values and ● represents experimental values , where f_1 = mole fraction of M_1 in feed F_1 = mole fraction of M_1 in copolymer

Table 4.11: Copolymerisation of *p*-methacrylamidotri-n-butyltin benzoate with butyl acrylate.

Initial composition		Conv.%	Sn %	Copolymer composition		Kelen-Tudos parameters	
a^*	f_1^0			b^*	F_1^0	η	ξ
1.35	0.57	7.25	19.97	1.25	0.56	0.16	0.82
0.63	0.38	9.58	17.63	0.71	0.42	-0.29	0.64
0.41	0.29	7.45	16.19	0.53	0.35	-0.57	0.49
0.233	0.19	6.89	13.15	0.31	0.24	-1.05	0.35
0.09	0.09	8.58	7.99	0.12	0.11	-1.66	0.18

* molar ratio
° mole fraction

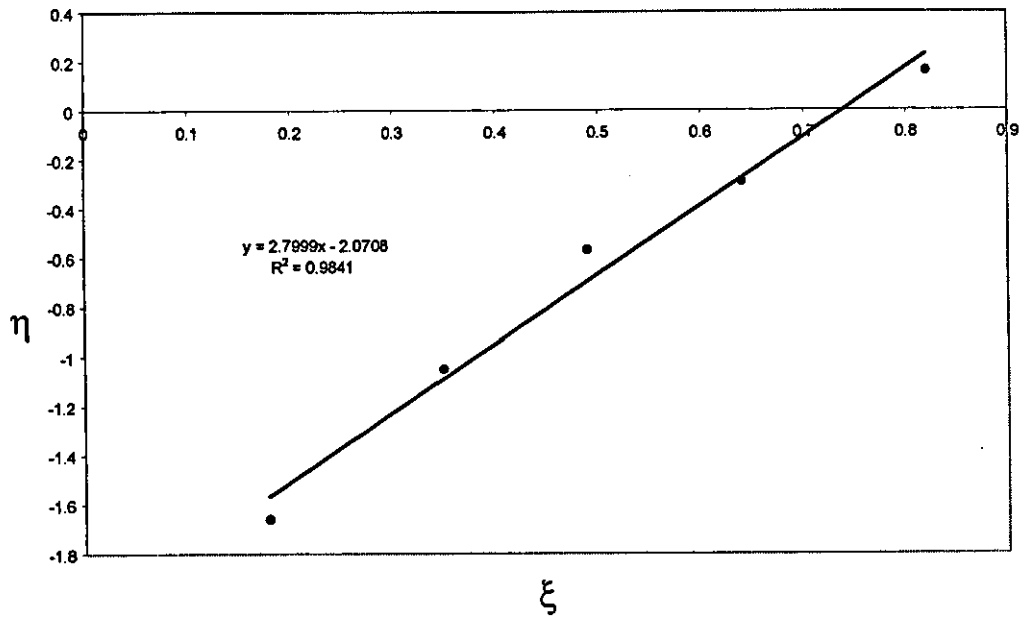

Fig. 4.21a, Kelen-Tudos plot for copolymerisation of *p*-MAATBTB-BA.

$$\xi = \frac{a^2}{\alpha\ b + a^2} \quad \text{and} \quad \eta = \frac{a(b-1)}{\alpha\ b + a^2}$$

where a and b are the molar ratios of the comonomer in the feed and copolymer, respectively, and

$$\alpha = \frac{a_{min} \times a_{max}}{(b_{min} \times b_{max})^{1/2}}$$

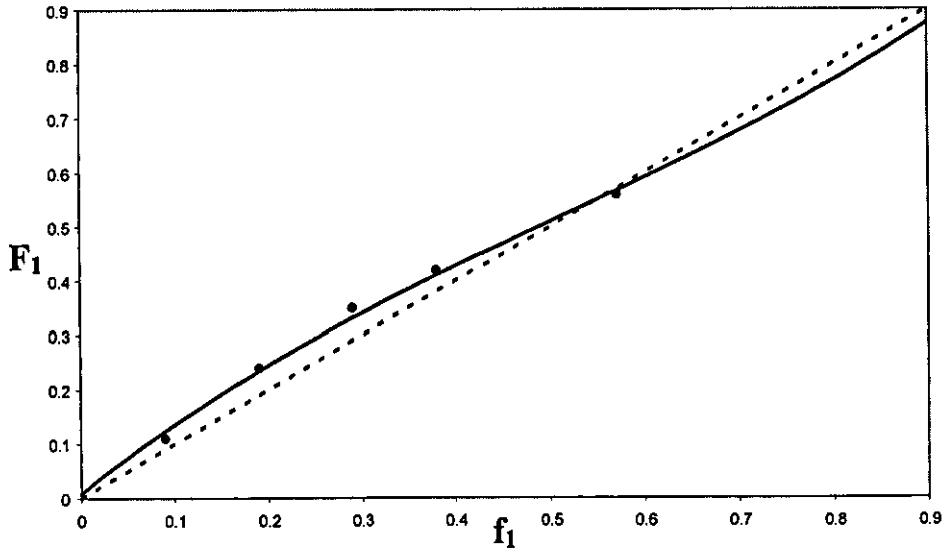

Fig. 4.21b, Composition curve for copolymerisation of *p*-MAATBTB-BA, Curve represents calculated values and ● represents experimental values , where f_1 = mole fraction of M_1 in feed F_1 = mole fraction of M_1 in copolymer

Table 4.12: Copolymerisation of *p*-methacrylamidotri-n-butyltin benzoate with methyl methacrylate.

Initial composition		Conv.%	Sn %	Copolymer composition		Kelen-Tudos parameters	
a^*	f_1^0			b^*	F_1^0	η	ξ
1.57	0.61	8.25	20.36	1.10	0.52	0.05	0.79
1.05	0.51	9.54	18.84	0.73	0.42	-0.19	0.73
0.65	0.39	7.25	16.66	0.45	0.31	-0.52	0.62
0.43	0.30	6.54	15.04	0.34	0.25	-0.76	0.49
0.24	0.19	7.25	11.76	0.19	0.16	-1.17	0.35
0.11	0.09	8.45	6.82	0.08	0.07	-1.74	0.20

* molar ratio
^{0} mole fraction

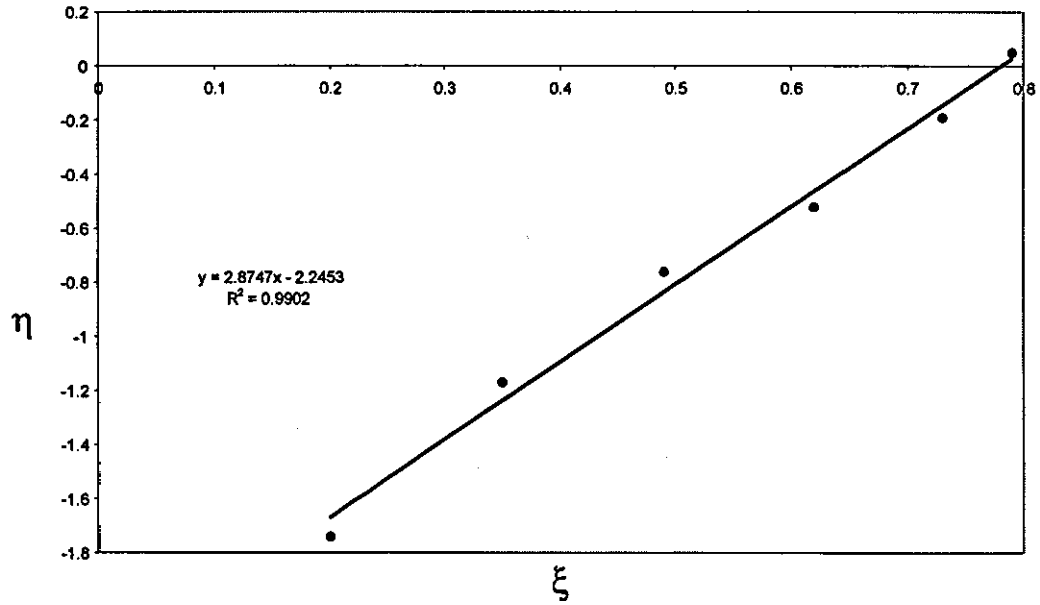

Fig. 4.22a, Kelen-Tudos plot for copolymerisation of *p*-MAATBTB-MMA.

$$\xi = \frac{a^2}{\alpha\ b + a^2} \quad \text{and} \quad \eta = \frac{a(b-1)}{\alpha\ b + a^2}$$

where a and b are the molar ratios of the comonomer in the feed and copolymer, respectively, and

$$\alpha = \frac{a_{min} \times a_{max}}{(b_{min} \times b_{max})^{1/2}}$$

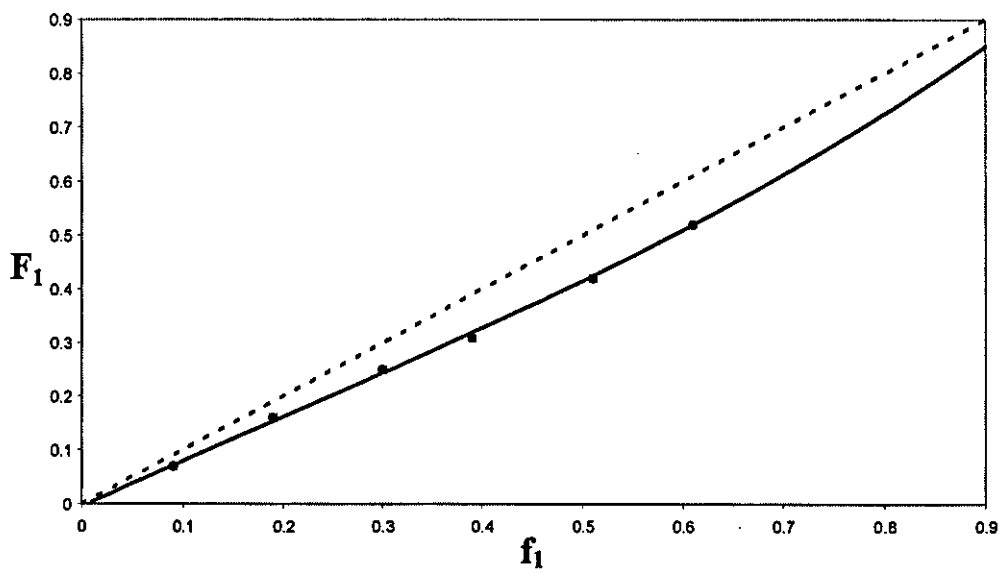

Fig. 4.22b, Composition curve for copolymerisation of *p*-MAATBTB-MMA, Curve represents calculated values and ● represents experimental values , where f_1 = mole fraction of M_1 in feed F_1 = mole fraction of M_1 in copolymer

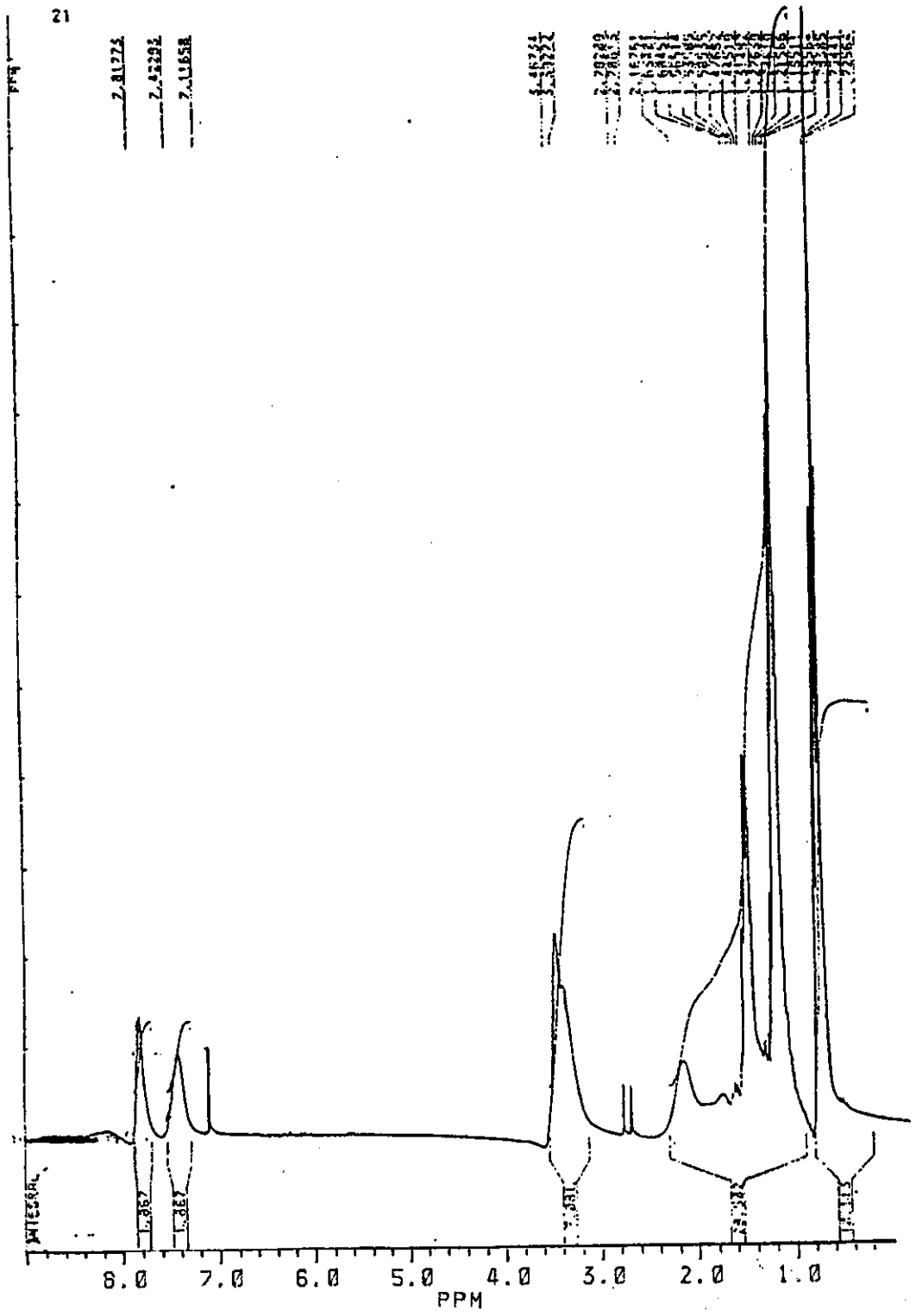

Fig. 4.23 ^{1}H NMR spectrum of (*p*-AATBTB-MA)copolymer

Table 4.13: Copolymerisation of *p*-acrylamidotri-n-butyltin benzoate with methyl acrylate.[+]

Initial composition		Conv.%	Copolymer composition		Kelen-Tudos parameters	
a^*	f_1^0	%	b^*	F_1^0	η	ξ
1.69	0.63	7.97	1.75	0.64	0.36	0.81
0.98	0.50	8.29	1.12	0.53	0.09	0.79
0.65	0.39	6.38	0.83	0.46	-0.15	0.57
0.44	0.30	6.37	0.54	0.35	-0.51	0.48
0.26	0.20	7.88	0.31	0.24	-0.95	0.35
0.12	0.10	9.18	0.14	0.13	-1.43	0.19

* molar ratio
^{0} mole fraction
+ Estimated by ^{1}H NMR Spectroscopy

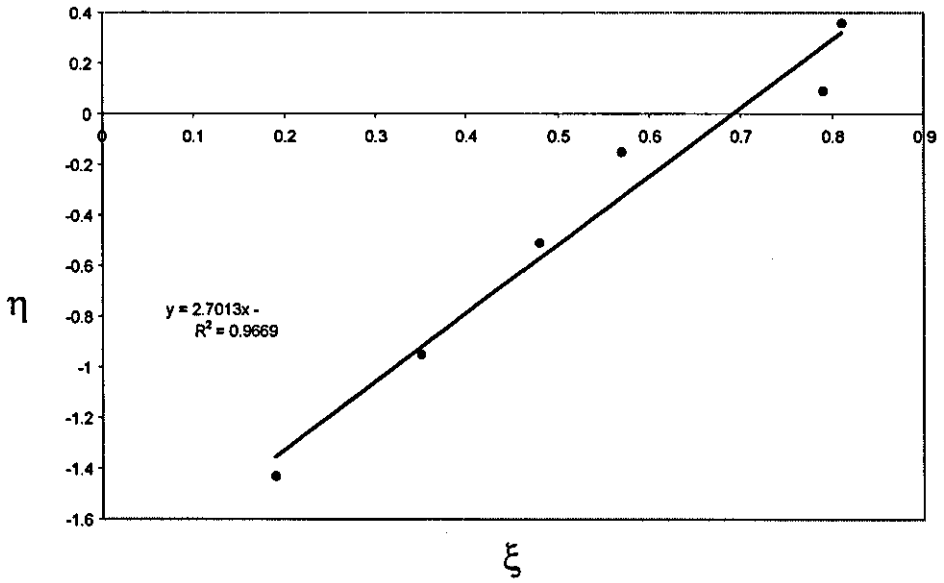

Fig. 4.24 Kelen- Tudos plot for copolymerisation of *p*-AATBTB-MA (estimated by ^{1}H NMR spectroscopy)

Table 4.14: Monomer reactivity ratios for copolymerisation of organotin acrylamide derivatives as monomers with MA,BA and MMA

M_1 - M_2	r_1	r_2	$1/r_1$	r_1 r_2	Q_1	e_1	α
m-AATBTB-MA	0.43±0.06	0.76±0.07	2.33	0.33	0.30	-0.42	0.494
m-AATBTB-BA	0.33±0.02	0.54±0.03	3.03	0.18	0.23	-0.46	0.357
m-AATBTB-MMA	0.22±0.03	1.41±0.02	4.54	0.31	0.36	-0.68	1.823
p-AATBTB-MA	1.06±0.07	0.72±0.04	0.94	0.76	0.43	0.13	0.429
p-AATBTB-MA*	1.01±0.05	0.76±0.03	0.99	0.76	0.43	0.13	0.409
p-AATBTB-BA	1.18±0.08	0.88±0.03	0.85	1.04	------	-------	0.371
p-AATBTB-MMA	1.12±0.05	1.38±0.05	0.89	1.55	------	-------	0.515
m-MAATBTB-MA	1.15±0.1	1.08±0.02	0.87	1.24	------	-------	0.336
m-MAATBTB-BA	0.63±0.03	1.16±0.04	1.59	0.73	0.20	0.29	0.492
m-MAATBTB-MMA	0.85±0.03	2.90±0.05	1.17	2.49	------	-------	0.806
p-MAATBTB-MA	0.97±0.05	0.84±0.03	1.03	0.81	0.40	0.19	0.369
p-MAATBTB-BA	0.72±0.05	0.66±0.03	1.39	0.48	0.28	-0.01	0.314
p-MAATBTB-MMA	0.61±0.03	1.26±0.04	1.64	0.77	0.50	-0.11	0.582

* estimated by ^{1}H NMR spectroscopy

NB: The empty spaces for e_1 values are imaginary numbers generated from the square root of negative values, by substituting the variables in equation (4.2), which was derived from equation (1.35).

$$e_1 = e_2 \pm \sqrt{(-\ln r_1 r_2)} \quad \text{.....(4.2)}$$

Similarly, Q_1 values were imaginary when their corresponding e_1 values were also imaginary, since Q_1 is calculated from e_1, as in equation (4.3), which was derived from equation (1.33).

$$Q_1 = \left(Q_2 / r_2\right)\exp\left[-e_2\left(e_2 - e_1\right)\right] \text{.....(4.3)}$$

When e_1 values were calculated according to equation (4.2), two numerical values were found for each, the lower values were quoted, since the higher ones were higher than the reported e values for known acrylate monomers such as methyl acrylate (e = 0.64) and butyl acrylate (e = 0.85), which is inconsistent, since methylated aromatic amides, such as the oragnotin monomer synthesised in this thesis (e.g. *p*-MAATBTB), should have higher electron density, and hence lower e values.

Table 4.15: Copolymerisation of *o*-acryloyloxytri-n-butyltin benzoate with methyl acrylate.

Initial composition		Conv.%	Sn %	Copolymer composition		Kelen-Tudos parameters	
a^*	f_1^0			b^*	F_1^0	η	ξ
1.51	0.60	6.54	21.35	1.35	0.57	0.18	0.78
0.99	0.50	9.56	21.12	0.96	0.49	-0.03	0.69
0.65	0.39	7.54	19.08	0.60	0.37	-0.37	0.61
0.42	0.30	8.65	16.20	0.34	0.25	-0.84	0.53
0.24	0.19	9.23	13.40	0.21	0.17	-1.22	0.37
0.11	0.10	8.21	8.31	0.09	0.08	-1.83	0.22

* molar ratio
^{0} mole fraction

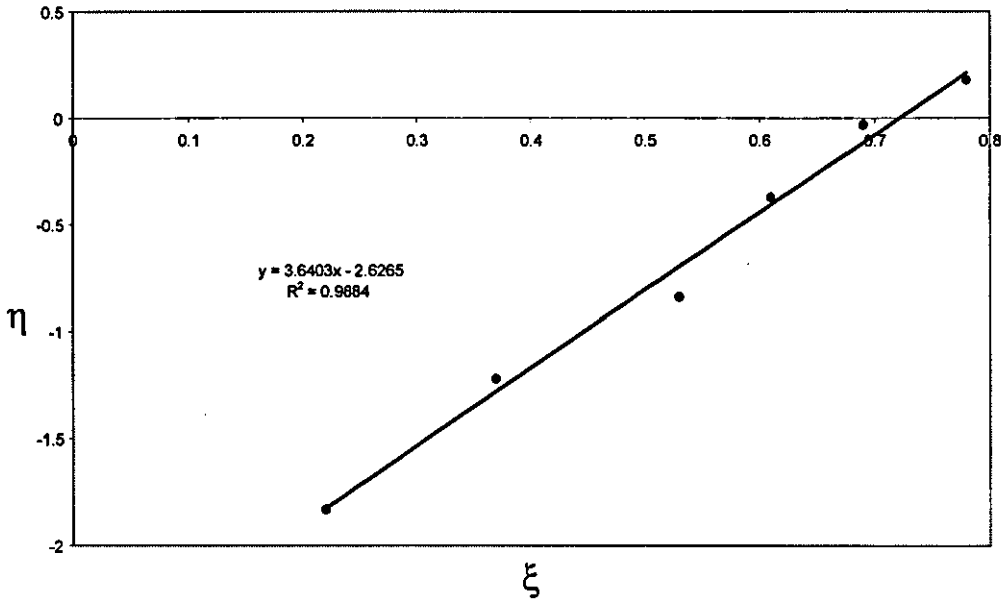

Fig. 4.25a, Kelen-Tudos plot for copolymerisation of *o*-AOTBTB-MA.

$$\xi = \frac{a^2}{\alpha\ b + a^2} \quad \text{and} \quad \eta = \frac{a(b-1)}{\alpha\ b + a^2}$$

where a and b are the molar ratios of the comonomer in the feed and copolymer, respectively, and

$$\alpha = \frac{a_{min} \times a_{max}}{(b_{min} \times b_{max})^{1/2}}$$

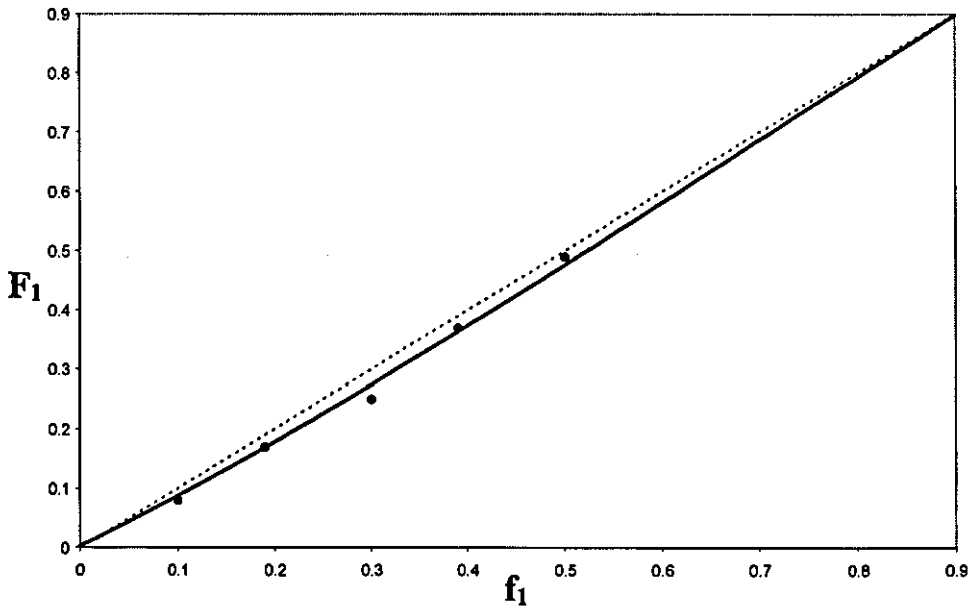

Fig. 4.25b, Composition curve for copolymerisation of *o*-AOTBTB-MA, Curve represents calculated values and ● represents experimental values , where f_1 = mole fraction of M_1 in feed F_1 = mole fraction of M_1 in copolymer

Table 4.16: Copolymerisation of *o*-acryloyloxytri-n-butyltin benzoate with butyl acrylate.

Initial composition		Conv.%	Sn %	Copolymer composition		Kelen-Tudos parameters	
a^*	f_1^0			b^*	F_1^0	η	ξ
1.59	0.61	7.21	20.43	1.26	0.59	0.13	0.80
1.01	0.50	8.92	19.26	0.93	0.48	-0.04	0.69
0.62	0.38	8.32	17.18	0.60	0.37	-0.36	0.56
0.41	0.29	9.24	14.52	0.38	0.27	-0.72	0.47
0.23	0.19	7.25	10.46	0.19	0.16	-1.25	0.36
0.10	0.09	8.10	6.08	0.08	0.08	-1.76	0.19

* molar ratio
^{0} mole fraction

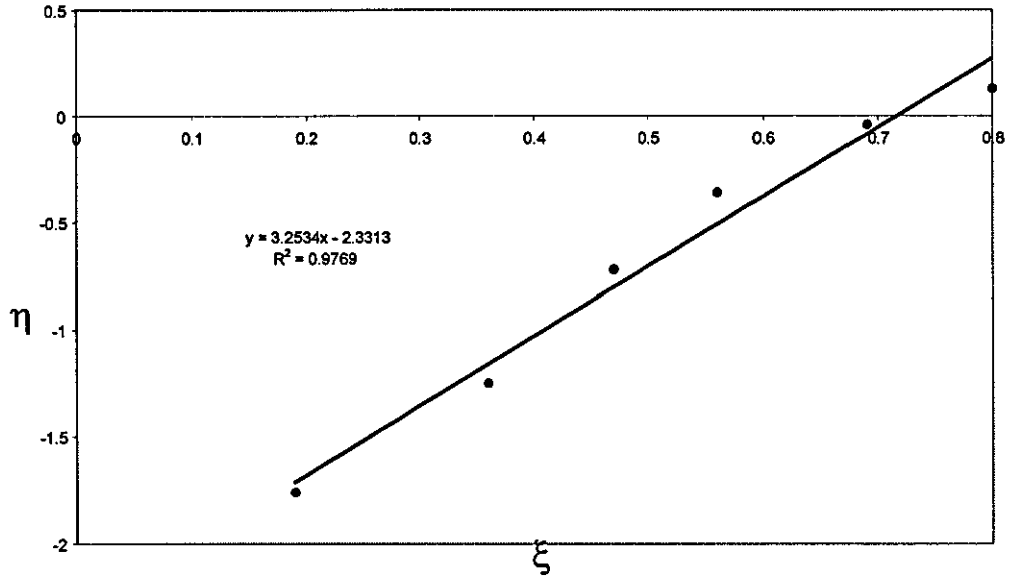

Fig. 4.26a, Kelen-Tudos plot for copolymerisation of *o*-AOTBTB-BA.

$$\xi = \frac{a^2}{\alpha\ b + a^2} \quad \text{and} \quad \eta = \frac{a(b-1)}{\alpha\ b + a^2}$$

where a and b are the molar ratios of the comonomer in the feed and copolymer, respectively, and

$$\alpha = \frac{a_{min} \times a_{max}}{(b_{min} \times b_{max})^{1/2}}$$

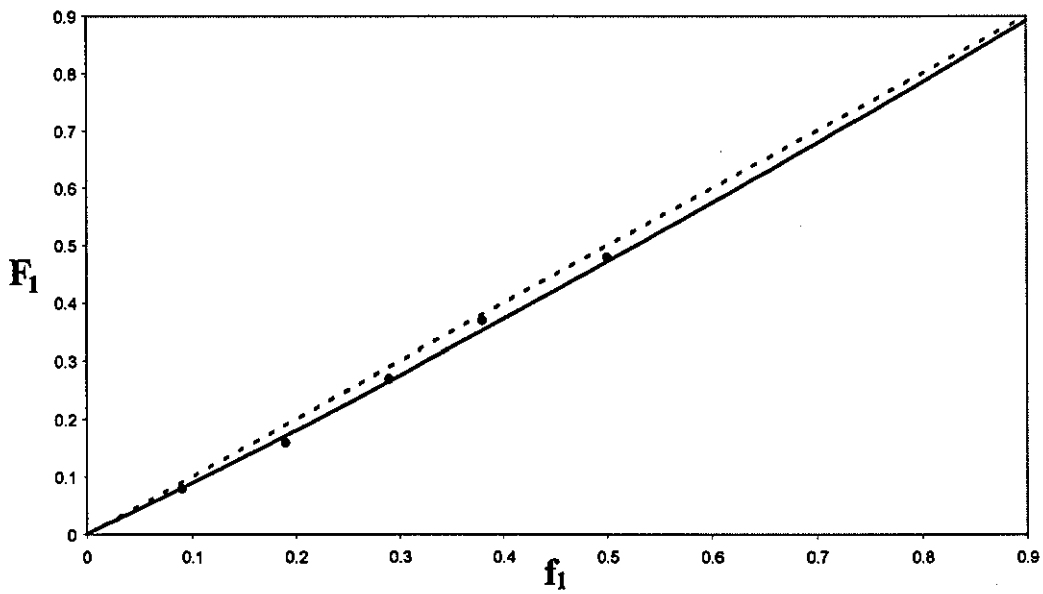

Fig. 4.26b, Composition curve for copolymerisation of *o*-AOTBTB-BA Curve represents calculated values and ● represents experimental values , where f_1 = mole fraction of M_1 in feed F_1 = mole fraction of M_1 in copolymer

Table 4.17: Copolymerisation of *o*-acryloyloxytri-n-butyltin benzoate with methyl methacrylate.

Initial composition		Conv.%	Sn %	Copolymer composition		Kelen-Tudos parameters	
a^*	f_1^0			b^*	F_1^0	η	ξ
1.44	0.59	8.54	21.31	1.29	0.56	0.16	0.81
0.98	0.49	9.21	20.37	0.97	0.49	-0.02	0.72
0.64	0.39	7.24	19.13	0.70	0.41	-0.27	0.60
0.40	0.28	8.25	17.00	0.46	0.31	-0.64	0.47
0.25	0.20	7.25	14.41	0.29	0.22	-1.02	0.35
0.12	0.09	8.56	10.71	0.16	0.14	-1.35	0.19

* molar ratio
° mole fraction

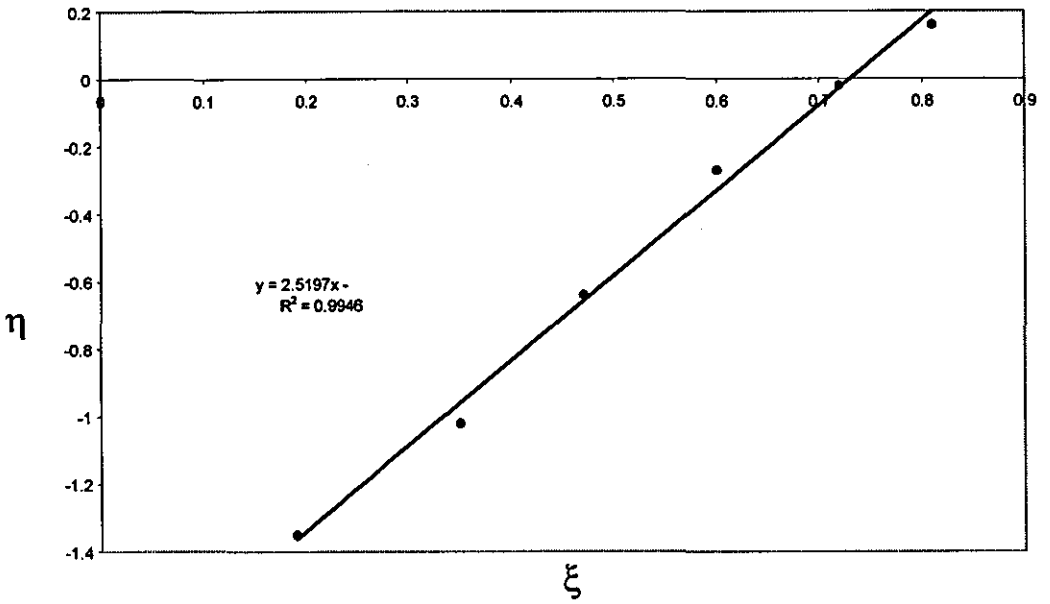

Fig. 4.27a, Kelen-Tudos plot for copolymerisation of *o*-AOTBTB-MMA.

$$\xi = \frac{a^2}{\alpha\ b + a^2} \quad \text{and} \quad \eta = \frac{a(b-1)}{\alpha\ b + a^2}$$

where a and b are the molar ratios of the comonomer in the feed and copolymer, respectively, and

$$\alpha = \frac{a_{min} \times a_{max}}{(b_{min} \times b_{max})^{1/2}}$$

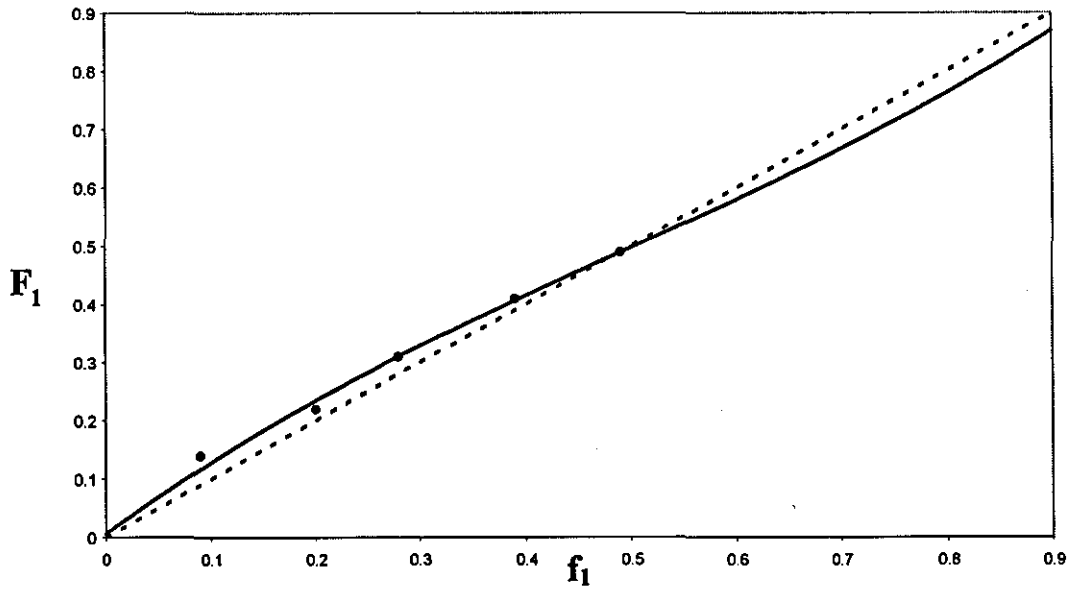

Fig. 4.27b, Composition curve for copolymerisation of *o*-AOTBTB-MMA, Curve represents calculated values and ● represents experimental values , where f_1 = mole fraction of M_1 in feed F_1 = mole fraction of M_1 in copolymer

Table 4.18: Copolymerisation of *o*-methacryloyloxytri-n-butyltin benzoate with methyl acrylate.

Initial composition		Conv.%	Sn %	Copolymer composition		Kelen-Tudos parameters	
a^*	f_1^0			b^*	F_1^0	η	ξ
1.49	0.60	8.56	21.35	1.38	0.58	0.21	0.82
1.00	0.5	7.33	20.65	1.06	0.51	0.04	0.73
0.66	0.40	9.24	19.94	0.85	0.46	-0.14	0.60
0.44	0.30	8.25	17.92	0.57	0.36	-0.49	0.50
0.25	0.20	9.33	16.42	0.37	0.27	-0.83	0.34
0.11	0.10	7.59	11.99	0.17	0.15	-1.30	0.18

* molar ratio
^{0} mole fraction

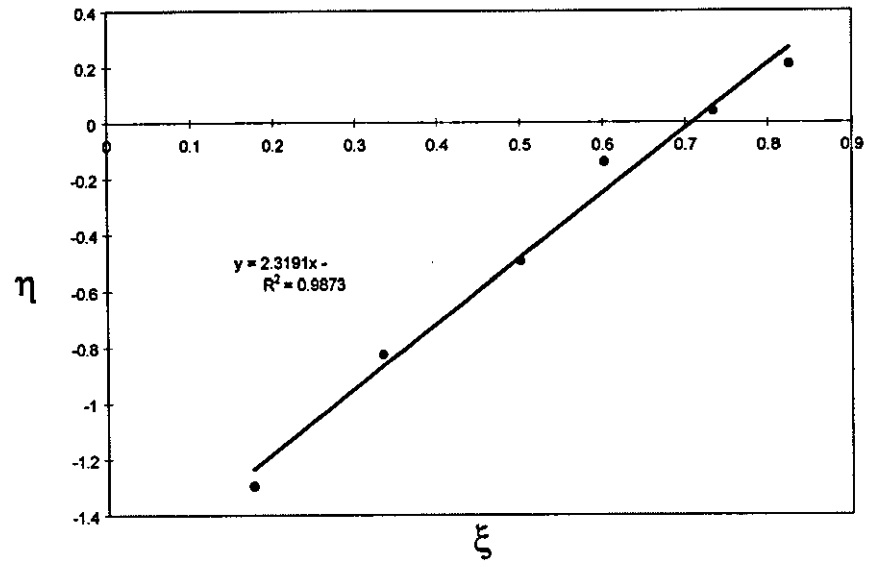

Fig. 4.28a, Kelen-Tudos plot for copolymerisation of *o*-MAOTBTB-MA.

$$\xi = \frac{a^2}{\alpha\ b + a^2} \quad \text{and} \quad \eta = \frac{a(b-1)}{\alpha\ b + a^2}$$

where a and b are the molar ratios of the comonomer in the feed and copolymer, respectively, and

$$\alpha = \frac{a_{min} \times a_{max}}{(b_{min} \times b_{max})^{1/2}}$$

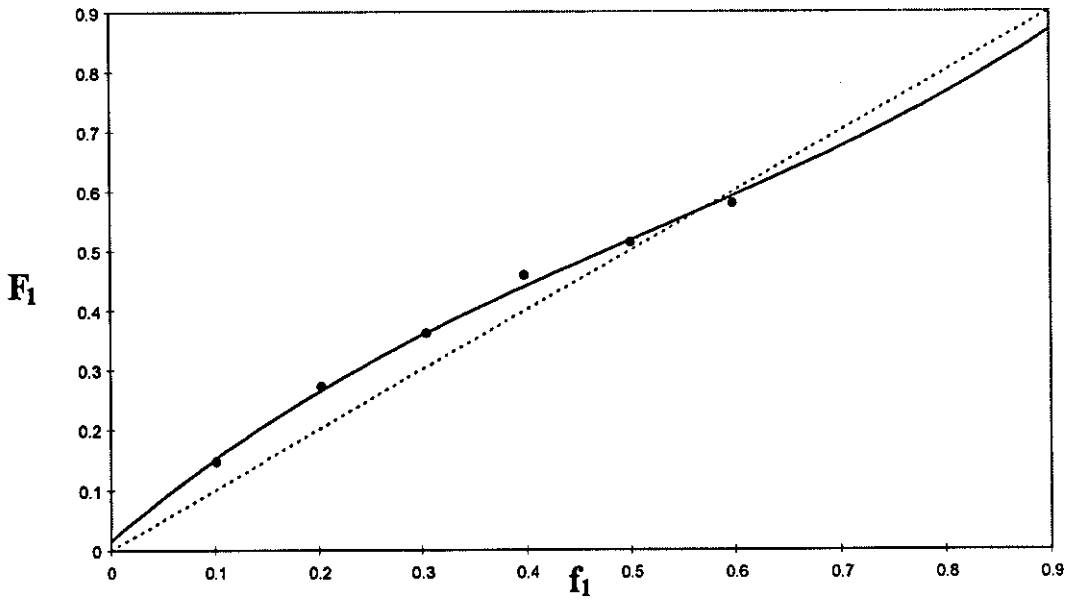

Fig. 4.28b, Composition curve for copolymerisation of *o*-MAOTBTB-MA, Curve represents calculated values and ● represents experimental values , where f_1 = mole fraction of M_1 in feed F_1 = mole fraction of M_1 in copolymer

Table 4.19: Copolymerisation of *o*-methacryloyloxytri-n-butyltin benzoate with butyl acrylate.

Initial composition		**Conv.%**	**Sn %**	**Copolymer composition**		**Kelen-Tudos parameters**	
a^*	f_1^0			b^*	F_1^0	η	ξ
1.55	0.61	8.20	18.91	0.95	0.49	-0.03	0.83
1.01	0.50	9.12	17.92	0.76	0.43	-0.18	0.73
0.71	0.42	7.35	15.61	0.48	0.32	-0.50	0.68
0.48	0.32	8.32	14.10	0.37	0.27	-0.73	0.55
0.24	0.19	9.20	12.15	0.26	0.21	-0.93	0.30
0.12	0.11	8.21	8.39	0.14	0.12	-1.22	0.17

* molar ratio
° mole fraction

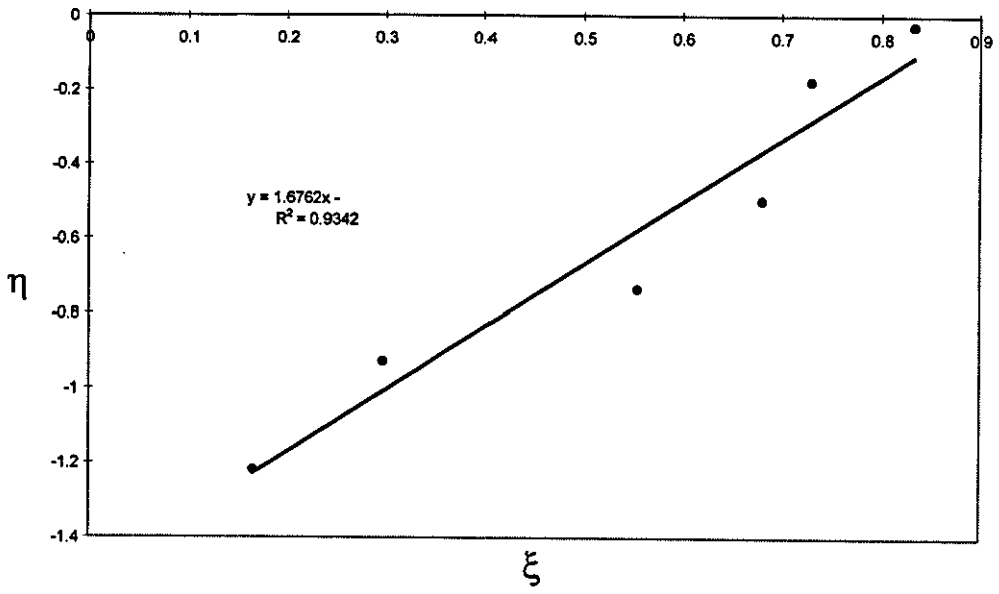

Fig. 4.29a, Kelen-Tudos plot for copolymerisation of *o*-MAOTBTB-BA.

$$\xi = \frac{a^2}{\alpha\ b + a^2} \quad \text{and} \quad \eta = \frac{a(b-1)}{\alpha\ b + a^2}$$

where a and b are the molar ratios of the comonomer in the feed and copolymer, respectively, and

$$\alpha = \frac{a_{min} \times a_{max}}{(b_{min} \times b_{max})^{1/2}}$$

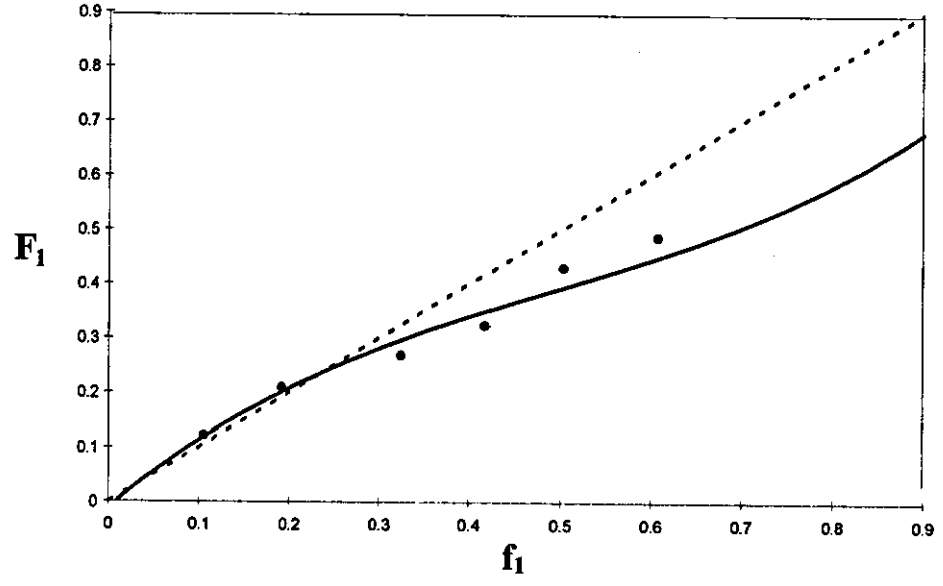

Fig. 4.29b, Composition curve for copolymerisation of *o*-MAOTBTB-BA, Curve represents calculated values and ● represents experimental values , where f_1 = mole fraction of M_1 in feed F_1 = mole fraction of M_1 in copolymer

Table 4.20 Copolymerisation of *o*-methacryloyloxytri-n-butyltin benzoate with methyl methacrylate.

Initial composition		Conv.%	Sn %	Copolymer composition		Kelen-Tudos parameters	
a^*	f_1^0			b^*	F_1^0	η	ξ
1.51	0.60	8.11	19.96	0.99	0.50	-0.00	0.81
1.04	0.51	9.79	19.70	0.91	0.48	-0.06	0.69
0.66	0.40	7.62	16.72	0.46	0.32	-0.52	0.65
0.43	0.30	8.52	15.64	0.38	0.27	-0.70	0.49
0.26	0.20	9.62	12.40	0.22	0.18	-1.13	0.37
0.11	0.09	8.52	7.71	0.10	0.09	-1.57	0.19

* molar ratio
° mole fraction

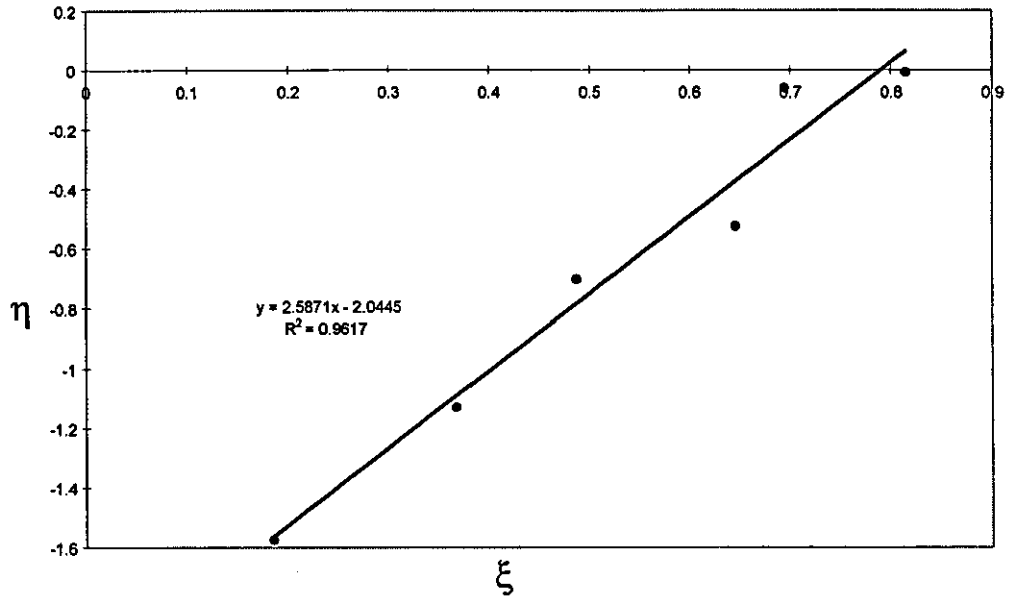

Fig. 4.30a, Kelen-Tudos plot for copolymerisation of *o*-MAOTBTB-MMA.

$$\xi = \frac{a^2}{\alpha\ b + a^2} \quad \text{and} \quad \eta = \frac{a(b-1)}{\alpha\ b + a^2}$$

where a and b are the molar ratios of the comonomer in the feed and copolymer, respectively, and

$$\alpha = \frac{a_{min} \times a_{max}}{(b_{min} \times b_{max})^{1/2}}$$

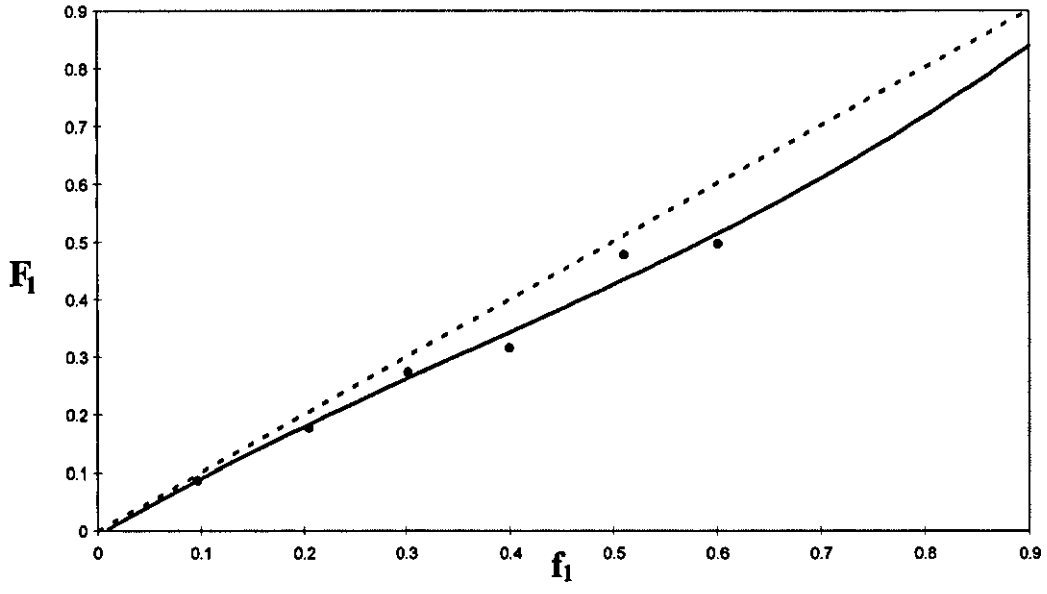

Fig. 4.30b, Composition curve for copolymerisation of *o*-MAOTBTB-MMA, Curve represents calculated values and ● represents experimental values , where f_1 = mole fraction of M_1 in feed F_1 = mole fraction of M_1 in copolymer

Table 4.21: Monomer reactivity ratios for copolymerisations of organotin acryloyloxy derivatives as monomers with MA,BA and MMA

M_1 - M_2	r_1	r_2	$1/r_1$	r_1r_2	Q_1	e_1	α
o-AOTBTB-MA	0.99±0.05	1.19±0.05	1.01	1.17	-------	-------	0.476
o-AOTBTB-BA	0.92±0.07	1.16±0.06	1.09	1.06	------	-------	0.500
o-AOTBTB-MMA	0.69±0.02	0.71±0.02	1.45	0.48	0.50	-0.11	0. 380
o-MAOTBTB-MA	0.68±0.04	0.56±0.03	1.47	0.38	0.43	-0.34	0.338
o-MAOTBTB-BA	0.15±0.02	0.76±0.08	6.67	0.11	0.14	-0.62	0.510
o-MAOTBTB-MMA	0.54±0.05	1.07±0.01	1.85	0.58	0.54	-0.34	0.528

NB: The empty spaces for Q_1 and e_1 values are explained for acrylamide derivatives table (4.14).

4.8 Gel Permeation Chromatography

4.8.1 Determination of the Best Elution Conditions

A mixed PL Gel (10 μm MIXED-B column) was selected as a stationary phase due to its wide pore size distribution for separation of a wide range of molecular sizes. The mobile phase selection was somewhat more complex due to the poor solubility of some of the prepared polymers and copolymers in DMF. In the first elution trials, pure DMF was utilised as mobile phase. However, two main problems were evident:

(i) Early polymer elution from the column, leading to an extremely high molecular weight result.

(ii) The elution profiles appeared to be slightly odd in that whilst the leading edge of the peak was resolved the trailing edge of the peak was truncated. This may suggest that whilst DMF is a reasonable solvent for samples and permits their elution in the chromatographic system, it is possible that some non- size exclusion behaviour exists, e.g. a type of ion-exclusion which has been suggested for elutions of non-ionic polar polymers with DMF.[95,96] For example, elutions of copolymers of *o*-AOBA with NVP from GPC studies with DMF[85] have suggested high polydispersities, and it is possible that copolymers containing amide groups are not separated by a simple size exclusion mechanism.

When lithium bromide was introduced in the mobile phase, to prevent any possible ion-based fractionation, the polymers were not soluble at all in the new solution (suggesting a salting out effect). However, when the samples were dissolved in pure DMF and eluted with DMF/LiBr solution it was not possible to recover the samples from the GPC column. Such an effect is also thought to be due to salting out effects, by which LiBr competes with the large bulky polymers for solvent molecules, leading to less solvation of the polymers and their eventual separation from the solution and precipitation on the column packing. THF gave satisfactory results regarding peak shape and retention time, and was subsequently used in GPC analyses of the formed polymers and copolymers.

4.8.2 Values of M_p for Acrylamide-organotin Polymers.

The choice of M_p values for discussing molecular weight differences among various organotin polymers (both homopolymers and copolymers) in contrast to M_w and/or M_n values (weight average molecular weight, and number average molecular weight)[97] was based on the following factors:

1) M_w and M_n are highly influenced by the tails of the molecular weight distribution. The M_p (peak average molecular weight) is simply the molecular weight of the most frequent polymer chains in the overall polymer sample and is less influenced by the high and low molecular weight polymer tails in the distribution. The GPC system used to analyse polymers in this thesis indicated the presence of tailing possibly arising from non-exclusion mechanisms. Other separation mechanisms, such as ion exchange, ion exclusion and adsorption, can interfere with size exclusion, leading to tailing, which influences M_w and M_n values while having a smaller effect on the values of M_p.[98,99]

2) Absolute values of M_w and M_n cannot be computed without calibration standards having similar chain microstructures to tin containing polymers. Erroneous molar mass values may be obtained because polymer and calibrants have somewhat different structures though based on the same polymerisable unit due to different size behaviour in solution. In this thesis, polystyrenes were utilised as calibration standards, and so relative molecular weights are obtained for the polymers investigated.

4.8.2.1 Values of M_p for Acrylamide- organotin Homopolymers.

From tables (4.22-4.24) it is evident that the M_p values of the various organotin homopolymers are arranged in the following order:

$$p\text{-MAATBTB} \approx m\text{-MAATBTB} > p\text{-AATBTB} \approx m\text{-AATBTB}$$

From this order it is understood that the major factor influencing the molecular weight of the generated homopolymers is the presence of the methyl group at the polymerisable double bond. In order to compare reactivities of monomers, it may be assumed that polymerisations are performed such that the concentrations of monomer and initiator are held fixed at the same constant values respectively. Inspection of equation (1.10) and (1.11) then indicates that the dependence of kinetic chain length on rate constants may be written:

$$\bar{v} = A(k_p / k_t^{0.5}) \quad \text{.....(4.3)}$$

Assuming that termination is by radical-radical combination, then it follows from equations (1.12) and (1.13) that equation (4.3) can be written:

$$\bar{M}_n = A(2M_o)\left(k_p / k_t^{0.5}\right) \quad \text{.....(4.4)}$$

A = constant

Equation (4.4) indicates that the polymer molecular weight is directly proportional to the rate constant for propagation and inversely proportional to the square root of the rate constant for termination, presuming that all other conditions in polymerisations of monomers are held constant. The types of reactivity factors for monomers and radicals with methyl group substitution at a polymerisable double bond were considered in relation to $k_p/k_t^{0.5}$ in section (4.4.1).

4.8.2.2 Values of M_p for Acryloyloxy- organotin Homopolymers

Tables (4.25-4.27) show that the methylated acryloyloxy homopolymer has a higher M_p value than the non-methylated one, which is thought to be due to the presence of the methyl group at the polymerisable double bond, as mentioned in the previous section. The relatively low molecular weight for this group is in contrast to the acrylamide group, suggesting steric hindrance imposed on the polymerisable double bond by the nearby bulky *ortho* tri-n-butyltin carboxylate might be a factor influencing monomer addition. This effect will be more pronounced when this group is in the *ortho* position rather than in the *meta* or *para* positions.

4.8.2.3 Values of M_p for Organotin Copolymers

Six copolymer samples of each organotin acrylamide or acryloyloxy derivatives with MA, BA and MMA were obtained for each copolymer system to illustrate the effect of monomeric percentage on the copolymer.

Through comparing copolymers generated from *meta* and *para* acrylamide derivatives (from methylated and non-methylated organotin monomers with MA, BA or MMA), it is evident that their differences in M_p values are small.

From tables (4.22- 4.24) the following observations can be noted :

In the acrylamide-organotin homopolymers, the methylated homopolymers have higher average M_p values than the non-methylated samples (due to factors discussed in the section 4.8.2.1). However, upon the incorporation of the acrylate monomers (MA, BA, and MMA), the copolymers corresponding to the non-methylated *para* acrylamide-oragontin monomers generally showed higher M_p values than the methylated ones. However, the *meta* series showed variable results with each individiual acrylate monomer. With MMA, a similar trend to the *para* organotin- acrylate copolymers was observed in table (4.24), while with MA, both methylated and non-methylated *meta* copolymers exhibit comparable M_p values table (4.22). On the other hand with BA, the methylated *meta* copolymers show higher M_p values than the non-methylated series.

From tables (4.25-4.27) the following observations can be noted:

In the acryloyloxy-organotin copolymers (with MA, BA, and MMA) the M_p values for polymers generated from methylated organotin monomers are comparable to but often higher than those for the non-methylated derivatives due to factors discussed in section (4.8.2.1). In the corresponding copolymers for both the methylated and non-methylated monomers with MA, the results exhibit fluctuations with changing acrylate weight percentage table (4.25).

Table 4.22: Values of M_p for methyl acrylate / acryalmide organotin copolymer.

	AATBTB		MAATBTB	
WC(%)	*meta*	*para*	*meta*	*para*
0	66000	67000	100000	126000
40	82000	93000	93000	62000
50	85000	60000	80000	38000
60	85000	-------	66000	68000
70	83000	--------	71000	92000
80	97000	58000	93000	125000
90	116000	119000	96000	-------
100	69000	69000	69000	69000

WC: Methyl acrylate percentage weight composition.
AATBTB: Acrylamidotri-n-butyltin benzoate.
MAATBTB: Methacrylamidotri-n-butyltin benzoate.

Table 4.23: Values of M_p for butyl acrylate / acryalmide organotin copolymer.

	AATBTB		MAATBTB	
WC(%)	*meta*	*para*	*meta*	*para*
0	66000	67000	100000	126000
40	72000	--------	82000	160000
50	70000	121000	79000	-------
60	54000	184000	99000	105000
70	69000	156000	97000	110000
80	------	192000	97000	134000
90	------	217000	92000	-------
100	69000	69000	69000	69000

WC: Butyl acrylate percentage weight composition.
AATBTB: Acrylamidotri-n-butyltin benzoate.
MAATBTB: Methacrylamidotri-n-butyltin benzoate.

Table 4.24: Values of M_p for methyl methacrylate / acryalmide organotin copolymer.

	AATBTB		MAATBTB	
WC(%)	*meta*	*para*	*meta*	*para*
0	66000	67000	100000	126000
40	189000	-------	68000	113000
50	165000	111000	88000	108000
60	141000	171000	110000	122000
70	124000	131000	90000	112000
80	108000	133000	69000	87000
90	------	99000	68000	72000
100	50000	50000	50000	50000

WC: Methyl methacrylate percentage weight composition.
AATBTB: Acrylamidotri-n-butyltin benzoate.
MAATBTB: Methacrylamidotri-n-butyltin benzoate.

Table 4.25: Values of M_p for methyl acrylate / acryloyloxy organotin copolymer.

WC(%)	*o*-AOTBTB	*o*-MAOTBTB
0	2400	6000
40	--------	39000
50	37000	109000
60	51000	82000
70	69000	111000
80	108000	76000
90	78000	71000
100	69000	69000

WC: Methyl acrylate percentage weight composition.
AOTBTB: Acryloyloxytri-n-butyltin benzoate.
MAOTBTB: Methacryloyloxy tri-n-butyltin benzoate.

Table 4.26: Values of M_p for butyl acrylate / acryloyloxy organotin copolymer.

WC(%)	*o*-AOTBTB	*o*-MAOTBTB
0	2400	6000
40	23000	60000
50	43000	72000
60	73000	93000
70	71000	91000
80	85000	71000
90	74000	70000
100	69000	69000

WC: Butyl acrylate percentage weight composition.
AOTBTB: Acryloyloxytri-n-butyltin benzoate.
MAOTBTB: Methacryloyloxy tri-n-butyltin benzoate.

Table 4.27: Values of M_p for methyl methacrylate / acryloyloxy organotin copolymer.

WC(%)	*o*-AOTBTB	*o*-MAOTBTB
0	2400	6000
40	56000	56000
50	55000	57000
60	63000	61000
70	-----	67000
80	66000	82000
90	64000	79000
100	50000	50000

WC: Methyl methacrylate percentage weight composition.
AOTBTB: Acryloyloxytri-n-butyltin benzoate.
MAOTBTB: Methacryloyloxy tri-n-butyltin benzoate.

4.9 Dynamic Mechanical Thermal Analysis (DMTA)

Methods to determine the T_g of polymeric materials may be classified under static and dynamic techniques. Differential thermal analysis (DTA), and differential scanning calorimetry (DSC) are often regarded as static methods although the measured value of T_g is influenced by the rate of heating. In DTA the temperature difference between the material under study and an inert standard is measured. In DSC analyses the sample is kept at the same temperature as the reference and the heat flow necessary to maintain this temperature is measured. This is achieved by placing separate heating elements in the sample and reference chambers; the rate of heating by these elements can be controlled and measured as desired, representing the amount of electrical energy supplied to the system. In dynamic methods the polymeric material is subjected to a sinusoidal stress during the heating process. In dynamic mechanical thermal analysis the application of a sinusoidal load leading to a sinusoidal deformation, see section (1.5), permits the determination of modulus E', and loss tangent tan δ, for a polymeric material as a function of temperature. The location of T_g is identified by a significant fall in modulus or by the peak maximum in tan δ. Whilst both temperature profiles are presented here, it is the tan δ curve which has been used.

The purpose of this section is to study the thermal behaviour of the homopolymers and copolymers of the organotin monomers by measuring the transition temperature T_g using DMTA . However, the values of T_g obtained by this technique are found to occur approximately 20° C higher than those stated in the literature as obtained by static methods. This was confirmed by DMTA studies of the acrylic homopolymers of MA, BA and MMA, which were found to have values of T_g at 30° C , -30° C and 133° C respectively, while the values studied by static methods are at 10° C, -54° C and 110° C respectively.[27]

4.9.1 DMTA Results of Acrylic Homopolymers

DMTA traces of poly(MA), poly(BA) and poly(MMA) are presented in figures (4.31a,b and c) respectively showing single tan δ peaks at 30 °C, -30 °C and 133 °C for MA, BA and MMA homopolymers respectively. From these results, it can

be seen that two factors influence the values of T_g in the mentioned homopolymer systems: (i) the presence or absence of a methyl group attached to the polymerisable double bond, as the methyl group tends to hinder rotation about the backbone polymer chain leading to a stiffer material and higher T_g (MA compared to MMA) (ii) the size of the side chain (BA compared to MA), showing that as the length of the side chain increases the values of T_g decrease, and such behaviour has been described in the literature.[33] Hoff et al[100] studied the effect of an ester side chain from methyl to n-butyl on the softening process of several polymers, and concluded that upon increasing the length of an ester side chain the main softening process moved to a lower temperature due to a reduction of interchain cohesive forces.

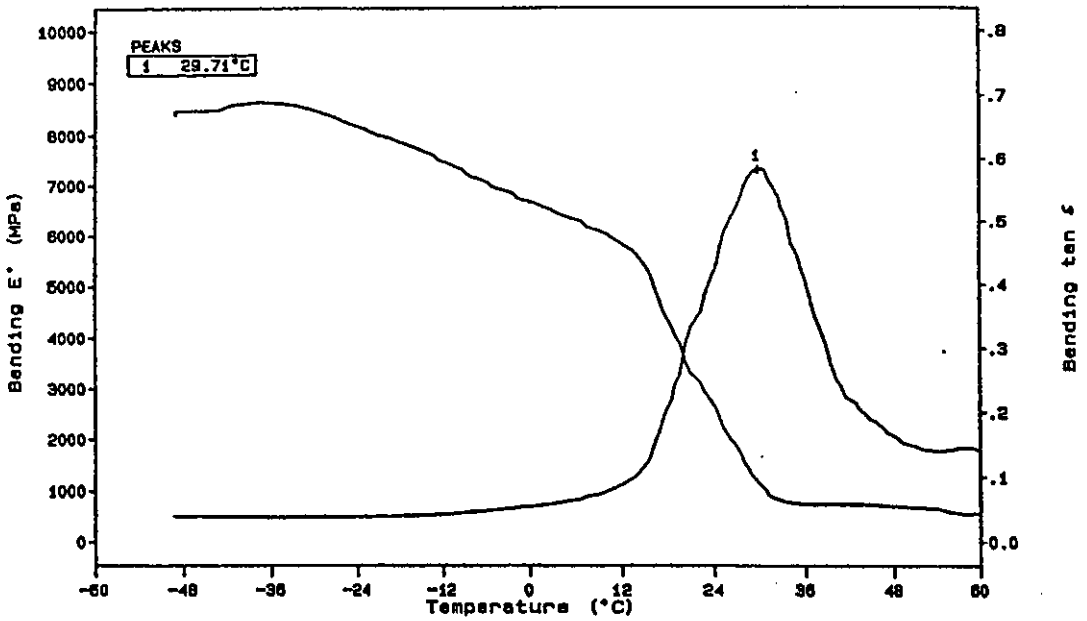

Fig. 4.31a DMTA traces of poly(MA)

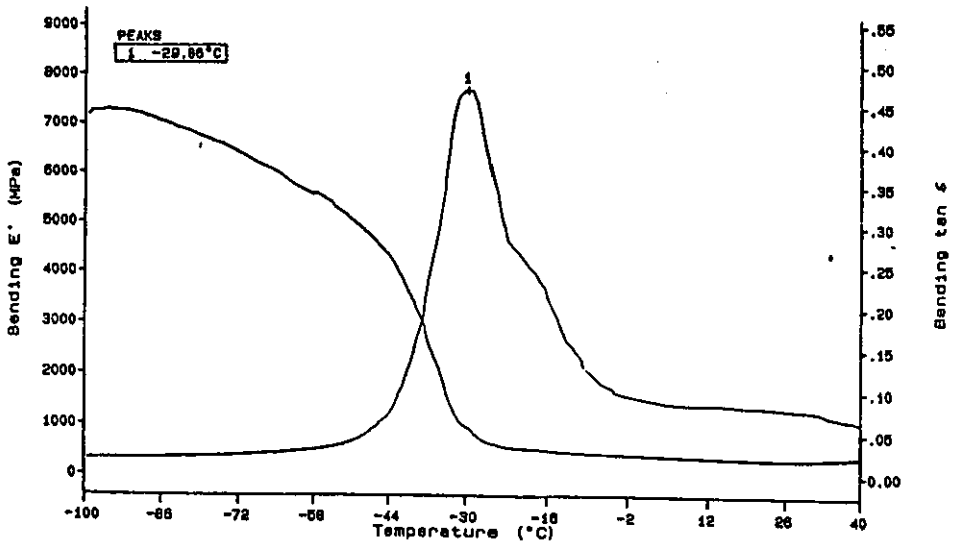

Fig. 4.31b DMTA traces of poly(BA)

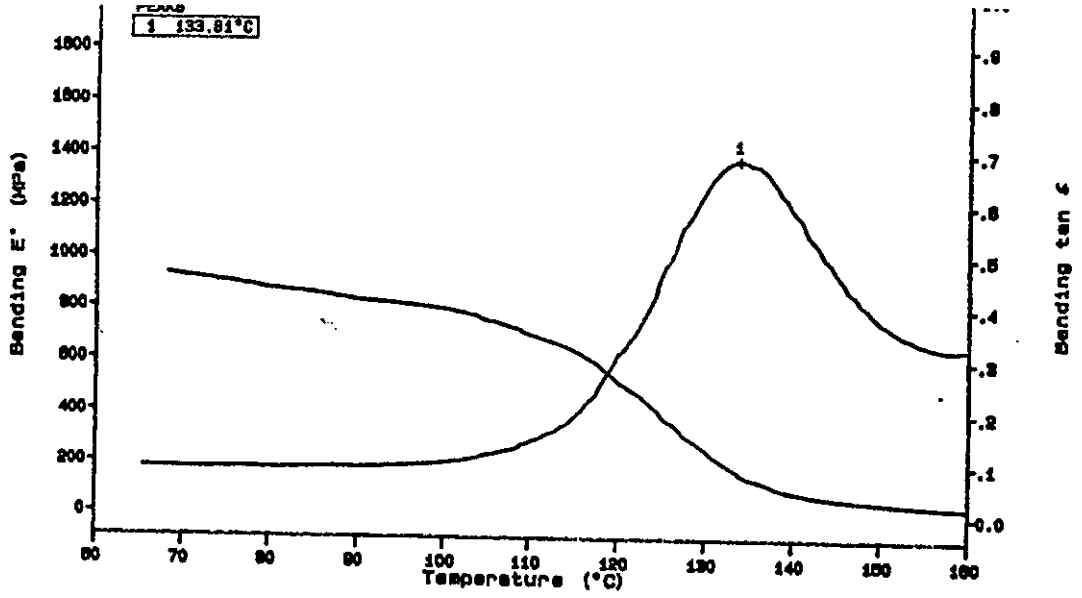

Fig. 4.31c DMTA traces of poly(MMA)

Eighteen copolymer systems were prepared from the previously described organotin monomers (acrylamide and acryloxyderivatives) and acrylic monomers (MA, BA and MMA). The dynamic mechanical behaviour of each of the copolymer systems was studied as a function of copolymer composition. It was reasonable first to study the DMTA behaviour of organotin homopolymers, and then assess the effects of the introduced acrylic monomers on the values of T_g of the generated copolymers. The results of this study will illustrate the DMTA behaviour of the copolymers in each system.

4.9.2 DMTA Results of Organotin Homopolymers

4.9.2.1 DMTA Results of Acrylamide Derivatives

DMTA results for the polymers poly(*m*-AATBTB), poly(*p*-AATBTB), poly(*m*-MAATBTB) and poly(*p*-MAATBTB)are presented in figures (4.32a,b,c and d) respectively. Poly (*m*-AATBTB), poly(*m*-MAATBTB), and poly(*p*-AATBTB) showed single tan δ peaks at 121°C, 144°C, and 168°C respectively, but poly (*p*-MAATBTB) exhibited a poorly defined tan δ peak and an assigned value of T_g at 184°C can only be regarded as approximate. It would appear that this polymer, and to a lesser extent poly(*p*-AATBTB), have decreased thermal stability above 180°C, so that both physical and chemical changes contribute to thermal behaviour. It can be seen that two factors influence the values of T_g in these homopolymer systems, namely (i) the presence or absence of a methyl group attached to the polymerisable double bond, as mentioned in the previous section (4.9.1), (ii) the position of the tri-n-butyltin carboxylate on the aromatic ring, substitution at the *para* position leading to increased values of T_g in comparison with the meta derivatives. Such differences can be attributed to steric factors.[100]

4.9.1.2 DMTA Results of Acryloyloxy Derivatives.

DMTA traces of poly(*o*-AOTBTB) and poly(*o*-MAOTBTB), are shown in figures (4.33a and 4.33b) respectively. Single tan δ peaks at 59 °C and 73 °C for *o*-AOTBTB and *o*-MAOTBTB homopolymers respectively are observed. The difference between the two polymers is attributed to the methyl group, as

mentioned in the previous section. The acryloyloxy homopolymers are characterised by lower values of T_g, compared to the acrylamide-based homopolymers. Such a difference is attributed to (i) the hydrogen bonding associated with amidic hydrogens (refer to sections 4.4.1 and 1.4.1), (ii) the acryloyloxy derivatives have low molecular weight compared to the acrylamide derivatives, see sections (1.4.1) and (4.8.2.2).

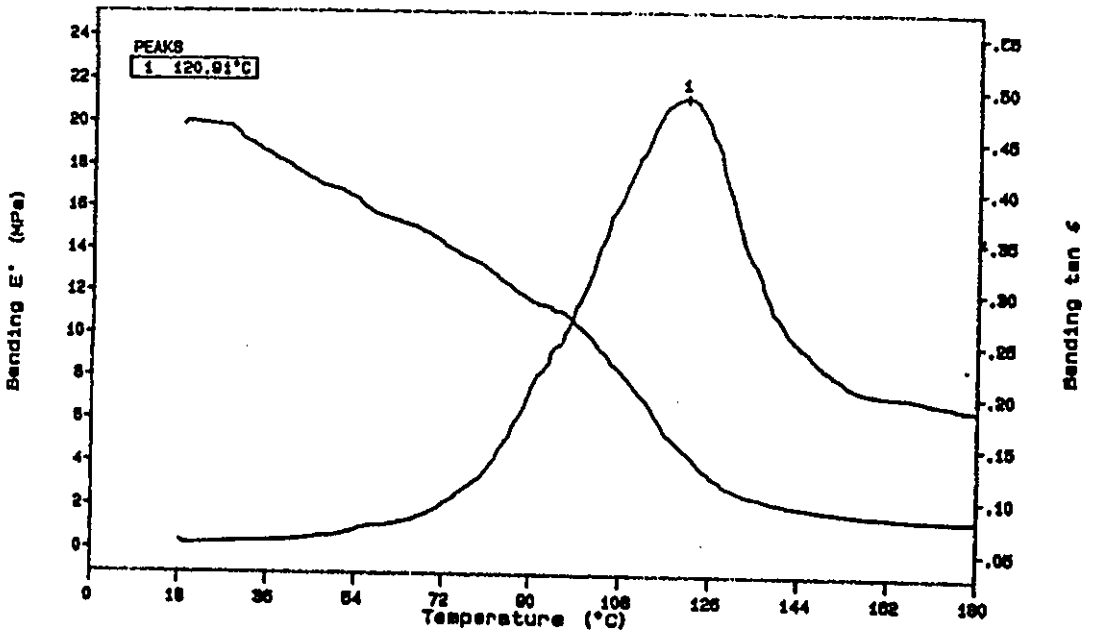

Fig. 4.32a DMTA traces of poly(*m*-AATBTB)

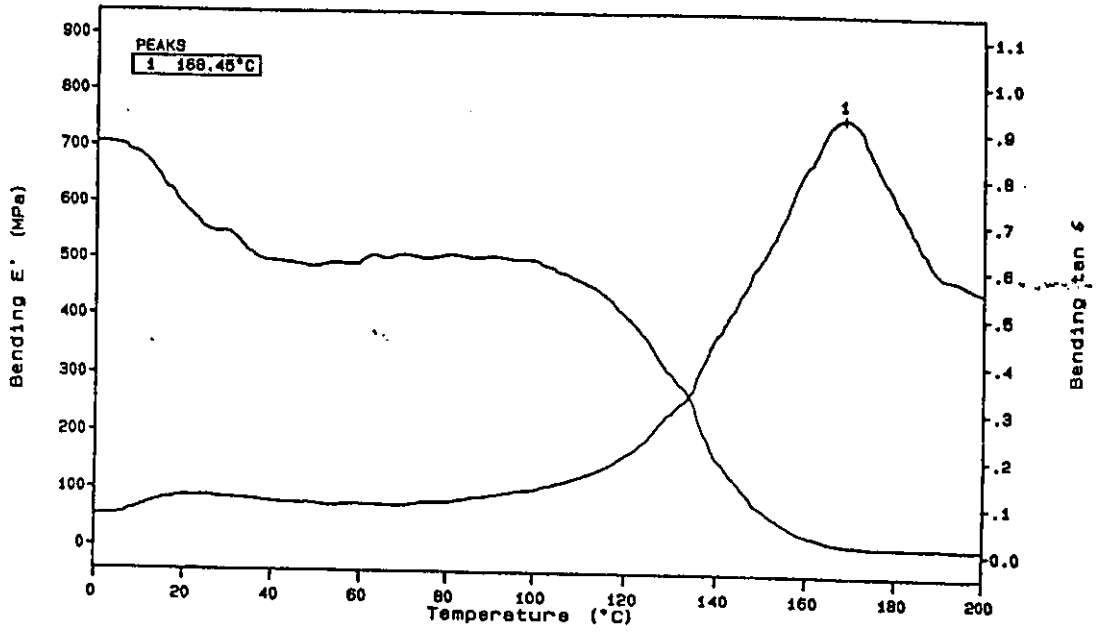

Fig. 4.32b DMTA traces of poly(*p*-AATBTB)

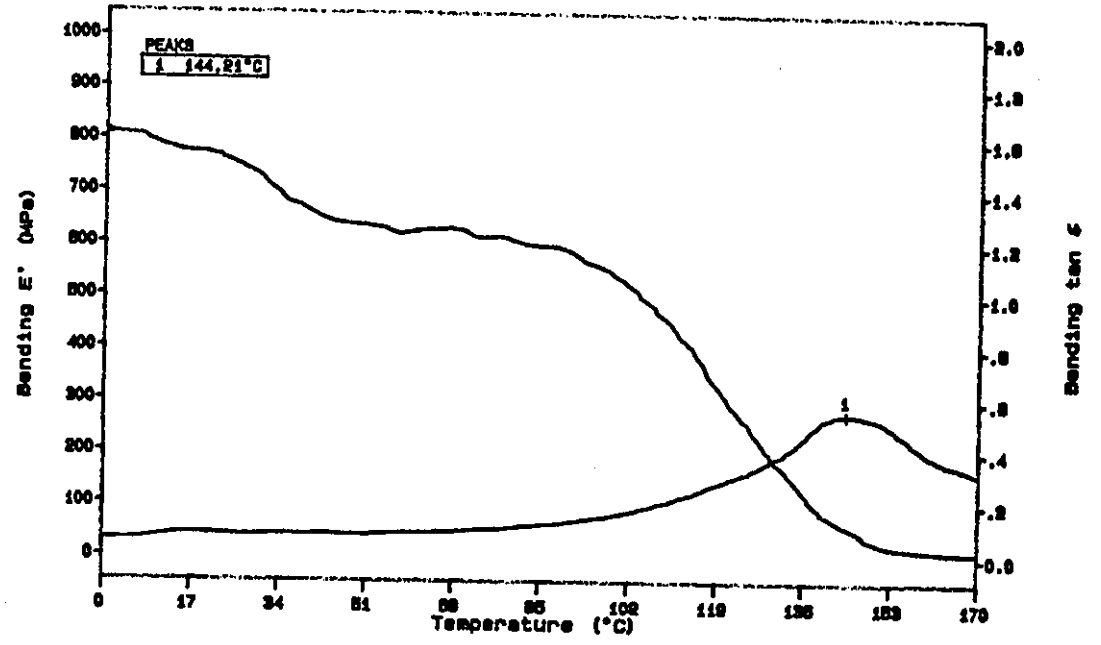

Fig. 4.32c DMTA traces of poly(*m*-MAATBTB)

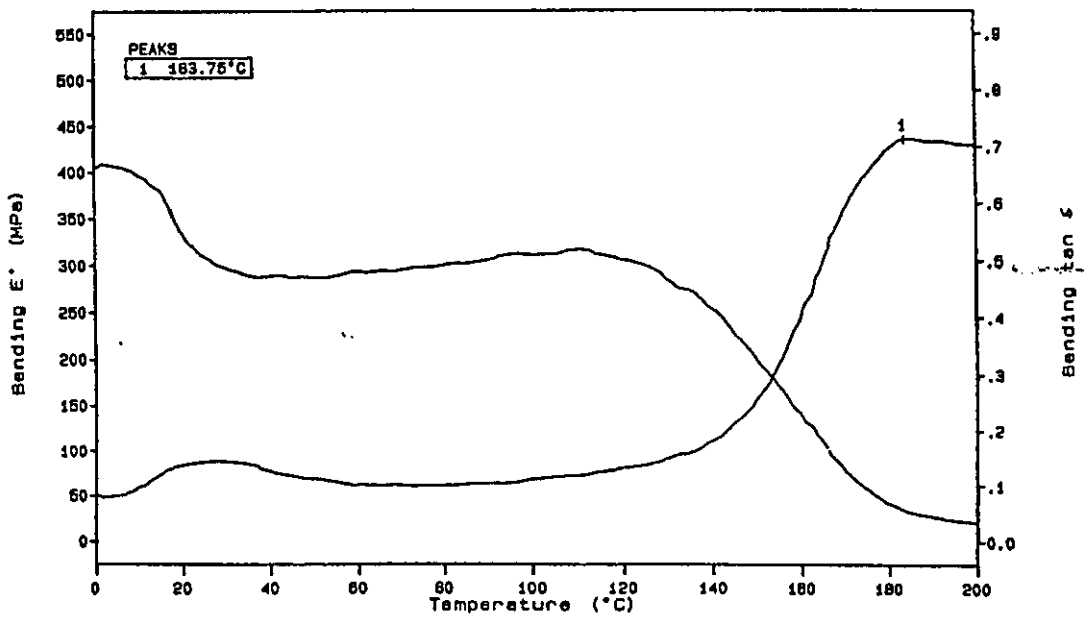

Fig. 4.32d DMTA traces of poly(*p*-MAATBTB)

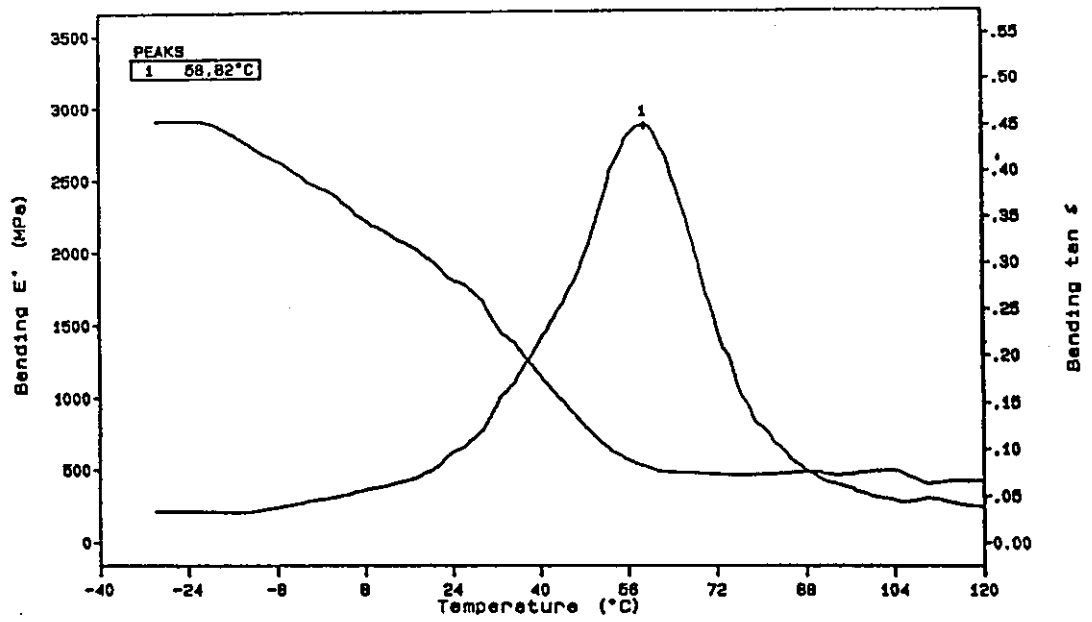

Fig. 4.33a DMTA traces of poly(*o*-AOTBTB)

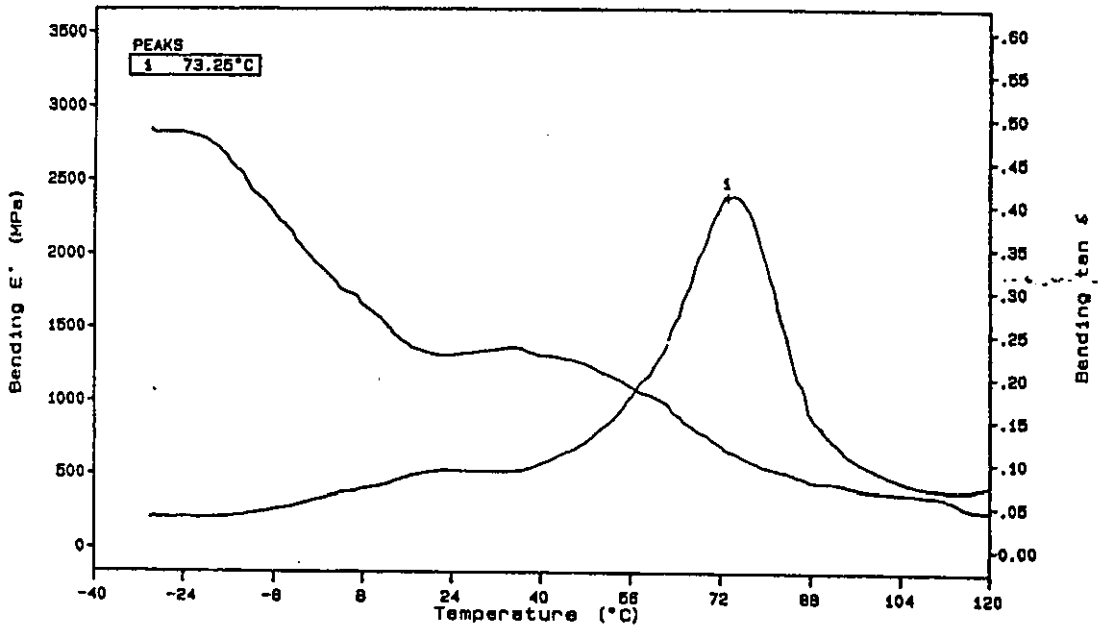

Fig. 4.33b DMTA traces of poly(*o*-MAOTBTB)

4.9.3 DMTA Results of Copolymers

It is generally expected that the value of T_g for a statistical copolymer will be between the values for the corresponding homopolymers,[33] with the location of T_g dependent on the relative percentages of each monomer in the total copolymer. All the generated organotin acrylamide- or acryloyloxy-acrylic copolymers appeared to have a single phase nature as indicated by the single tan δ peak from the DMTA experiments, but some peaks are broad.

4.9.3.1 DMTA Results for Acrylamide Derivatives

Three samples were selected for each copolymer system (40%, 60%, and 90% percentage weight composition of MA, BA and MMA) to illustrate the effect of monomeric percentage on the values of T_g for copolymers.

DMTA Results for Organotin Acrylamide Derivatives with MA.

The DMTA traces of the copolymer system *m*-AATBTB/MA figures (4.34a, b and c) show the values of T_g as 97°C, 60°C and 64°C for MA weight compositions 40%, 60% and 90% respectively. Thus as the MA composition increases in the copolymer so the values of T_g decrease. This can be explained since poly(methyl acrylate) has a low value of T_g 30°C compared to the higher value for poly *m*-AATBTB homopolymer 121°C. Similar trends appear for copolymers of *p*-AATBTB, *m*-MAATBTB and *p*-MAATBTB with MA figures (4.35a, b, c, 4.36a, b, c, 4.37a, b, c, and table 4.28). The overall effect of increasing MA percentage on the values of T_g of organotin acrylamide copolymers is illustrated in figure (4.38).

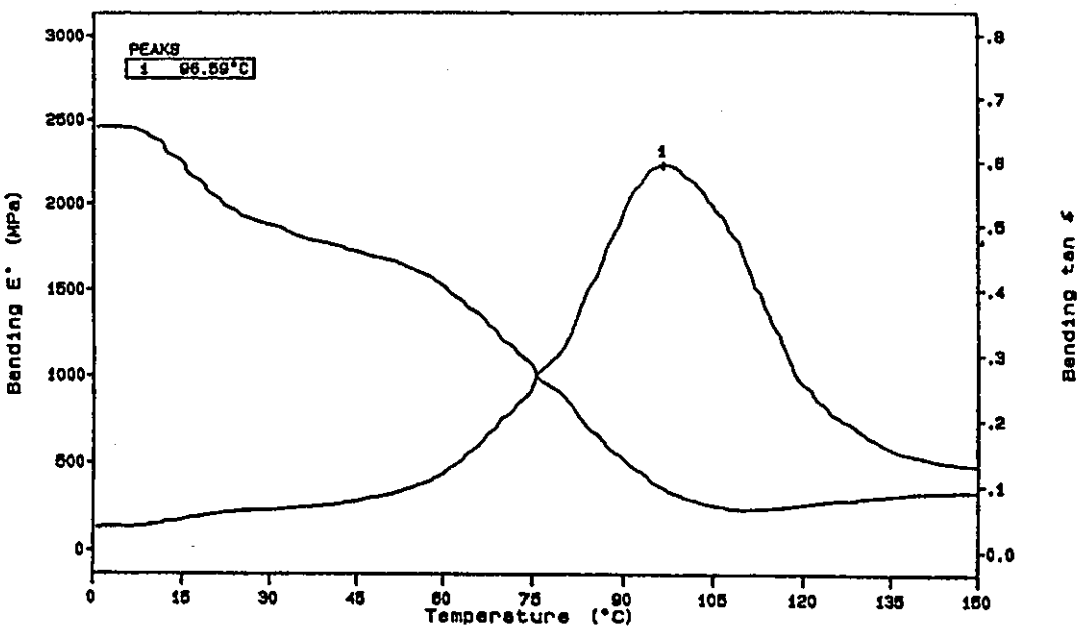

Fig. 4.34a DMTA traces of *m*-AATBTB with MA
40% MA Composition

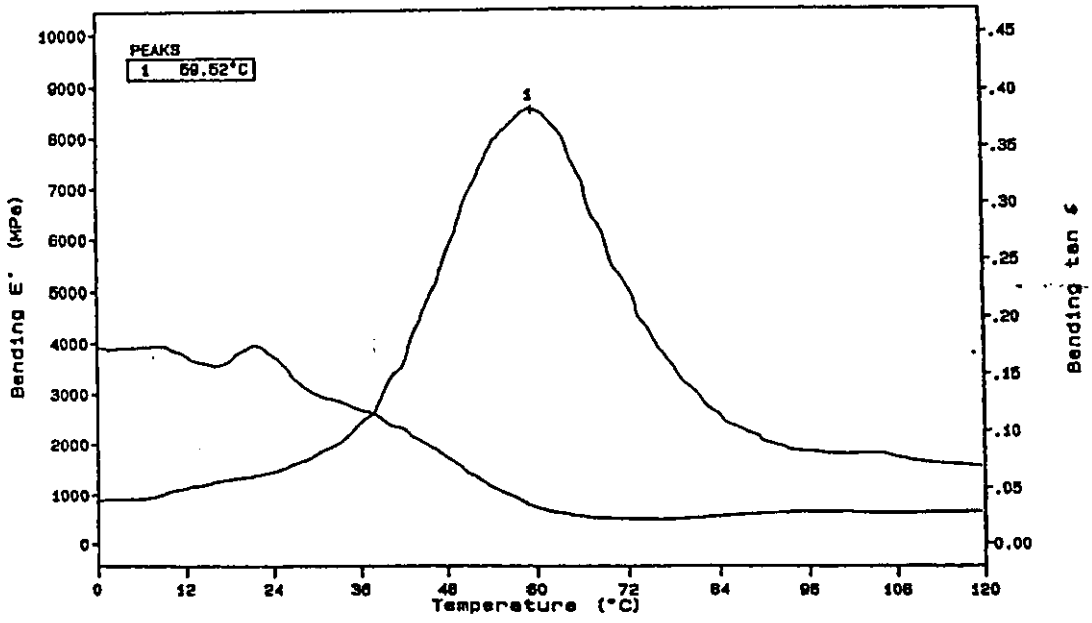

Fig. 4.34b DMTA traces of *m*-AATBTB with MA
60% MA Composition

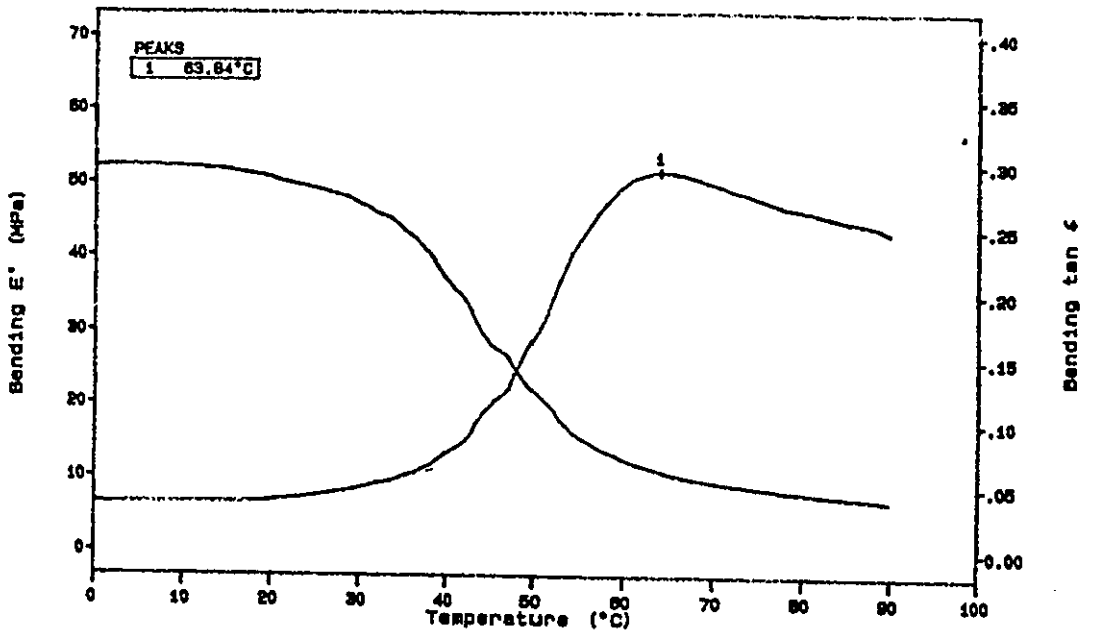

Fig. 4.34c DMTA traces of *m*-AATBTB with MA
90% MA Composition

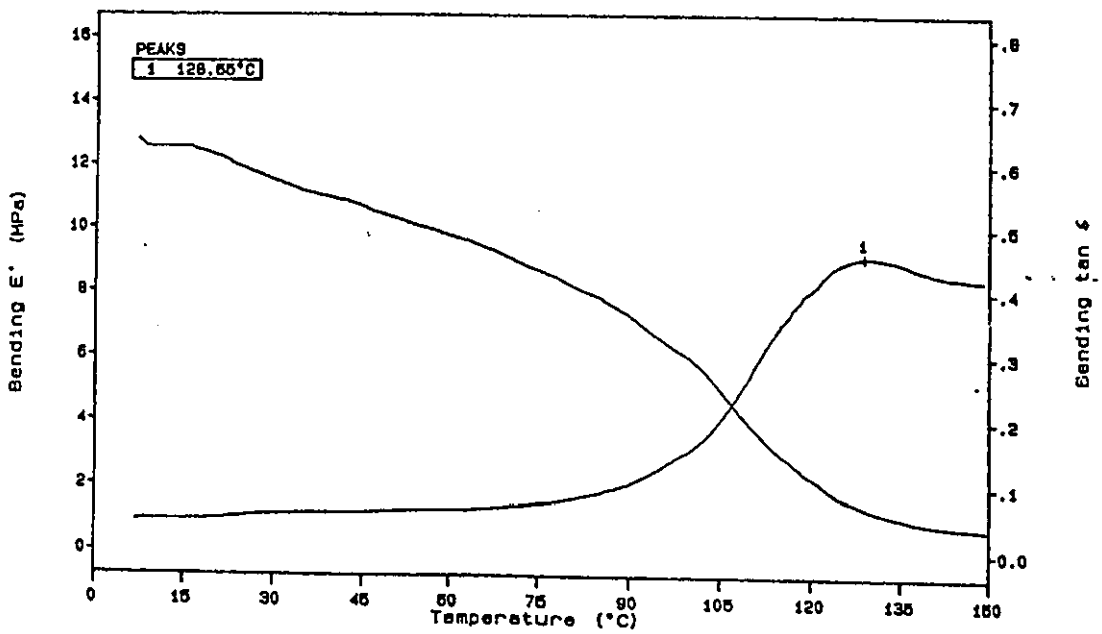

Fig. 4.35a DMTA traces of *p*-AATBTB with MA
40% MA Composition

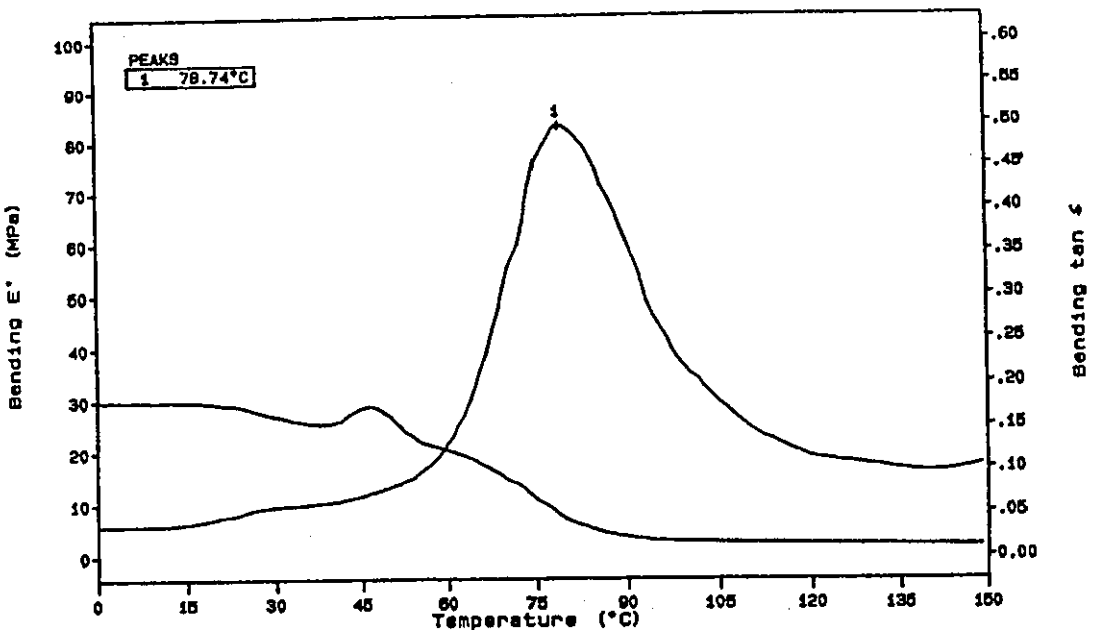

Fig. 4.35b DMTA traces of *p*-AATBTB with MA
60% MA Composition

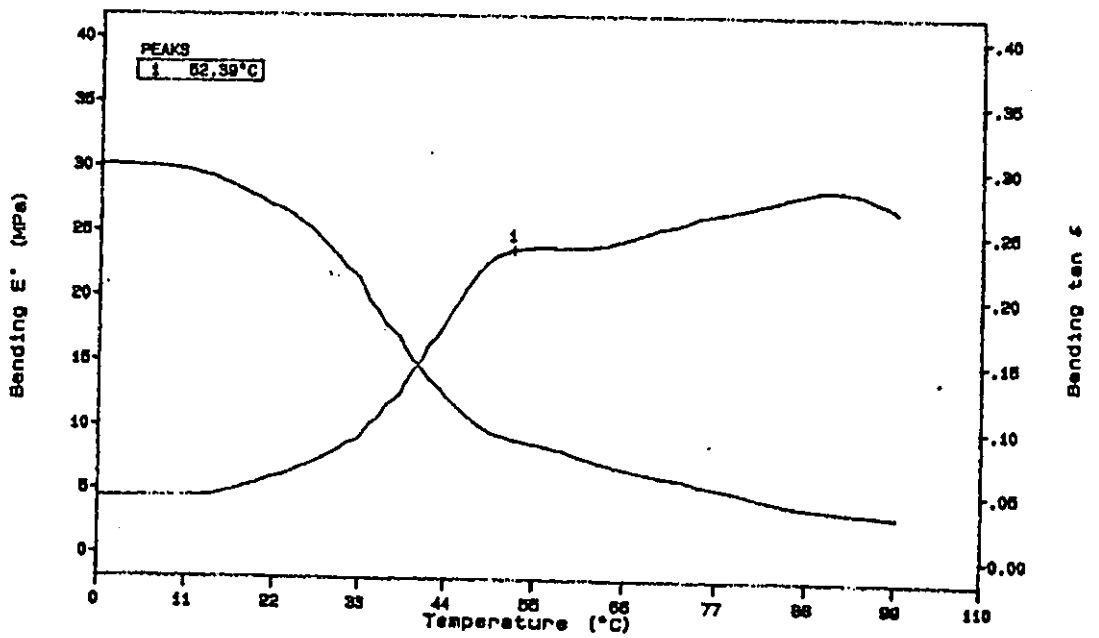

Fig. 4.35c DMTA traces of *p*-AATBTB with MA
90% MA Composition

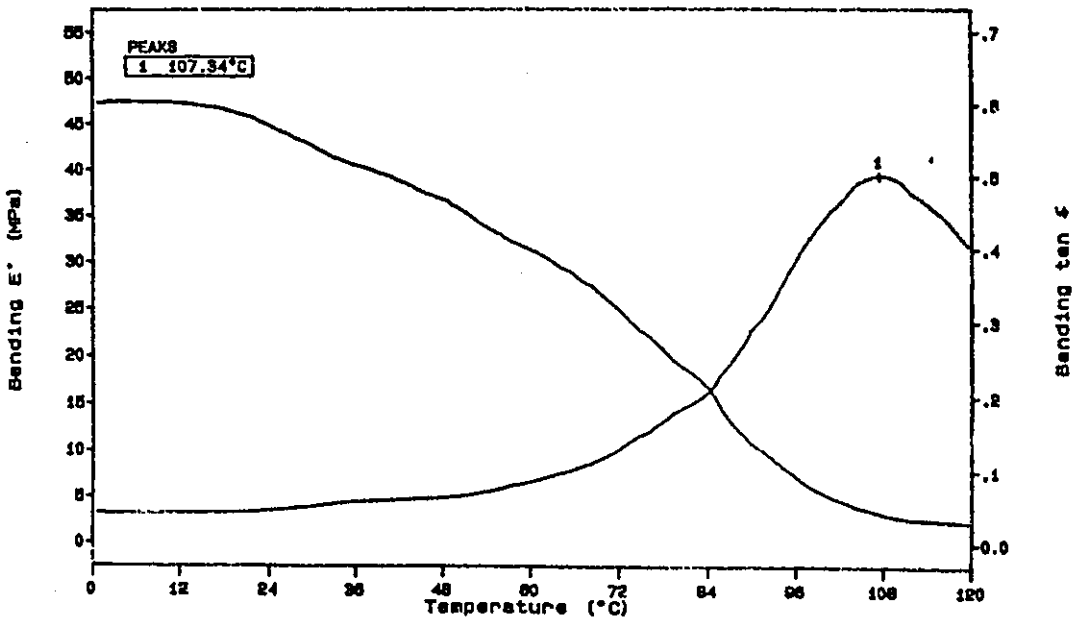

Fig. 4.36a DMTA traces of *m*-MAATBTB with MA
40% MA Composition

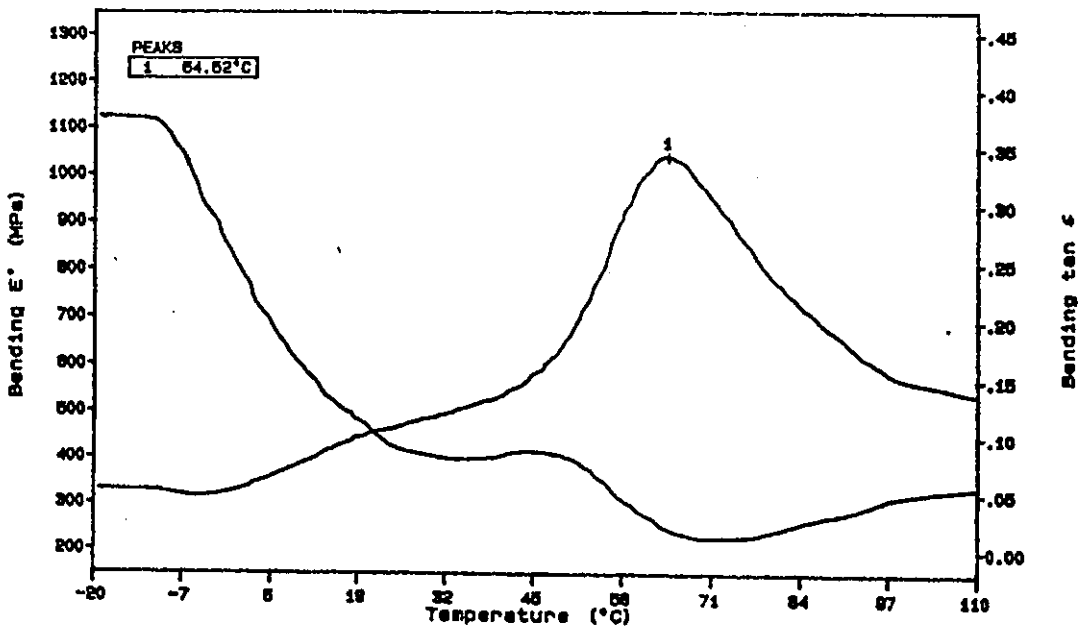

Fig. 4.36b DMTA traces of *m*-MAATBTB with MA
60% MA Composition

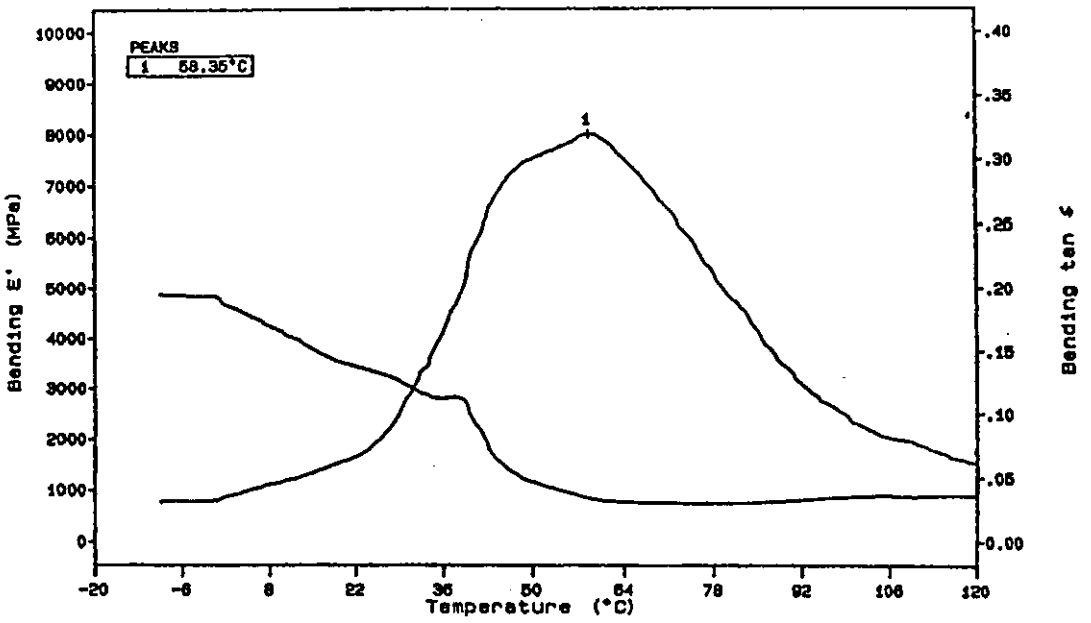

Fig. 4.36c DMTA traces of *m*-MAATBTB with MA
90% MA Composition

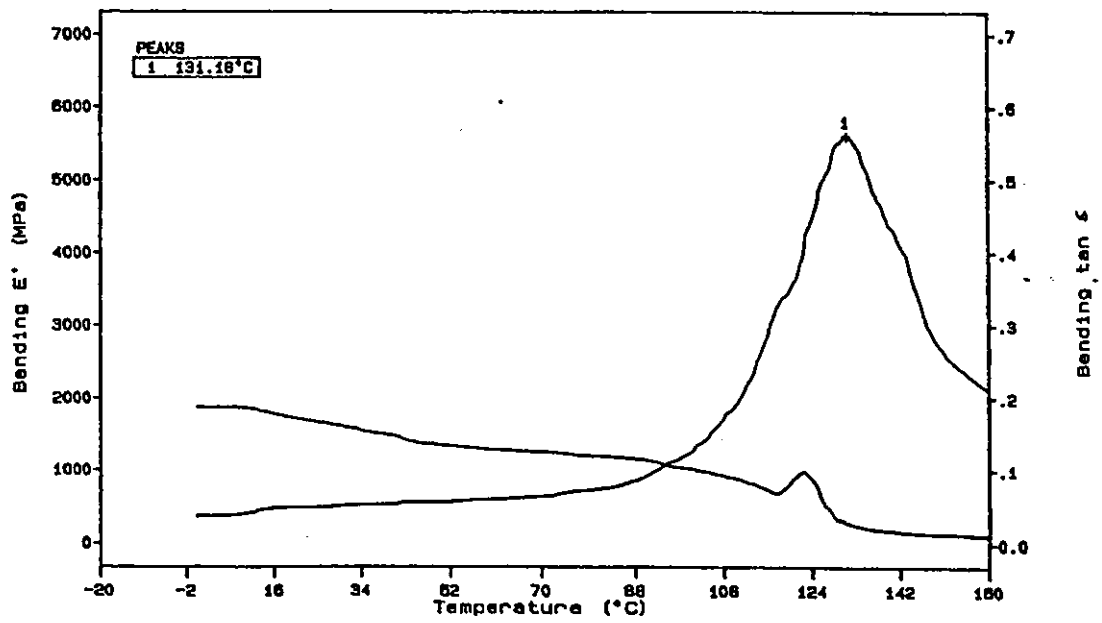

Fig. 4.37a DMTA traces of *p*-MAATBTB with MA
40% MA Composition

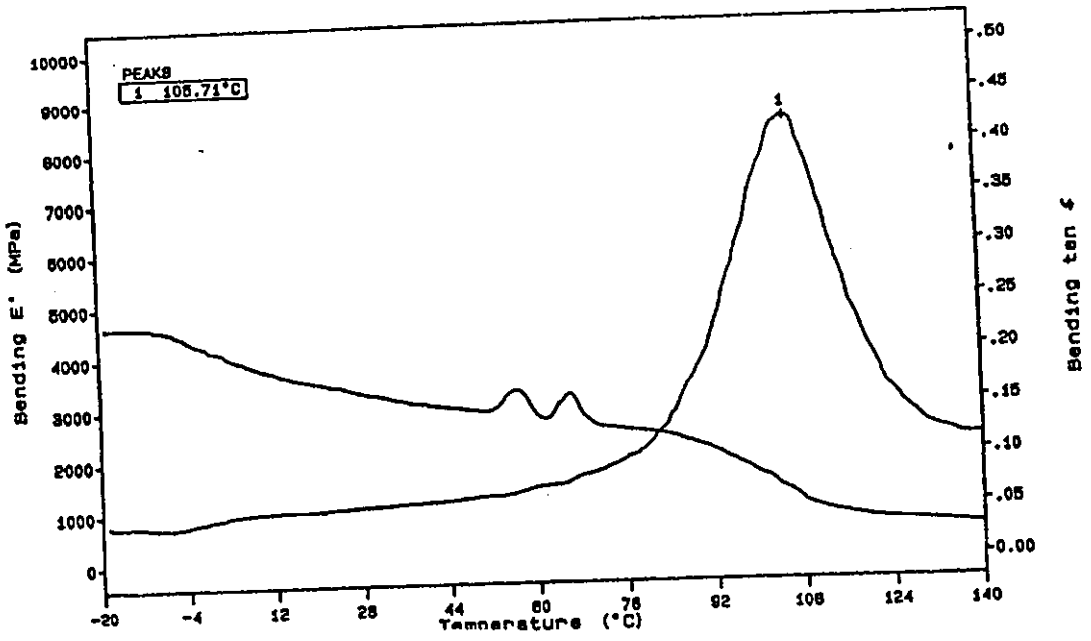

Fig. 4.37b DMTA traces of *p*-MAATBTB with MA
60% MA Composition

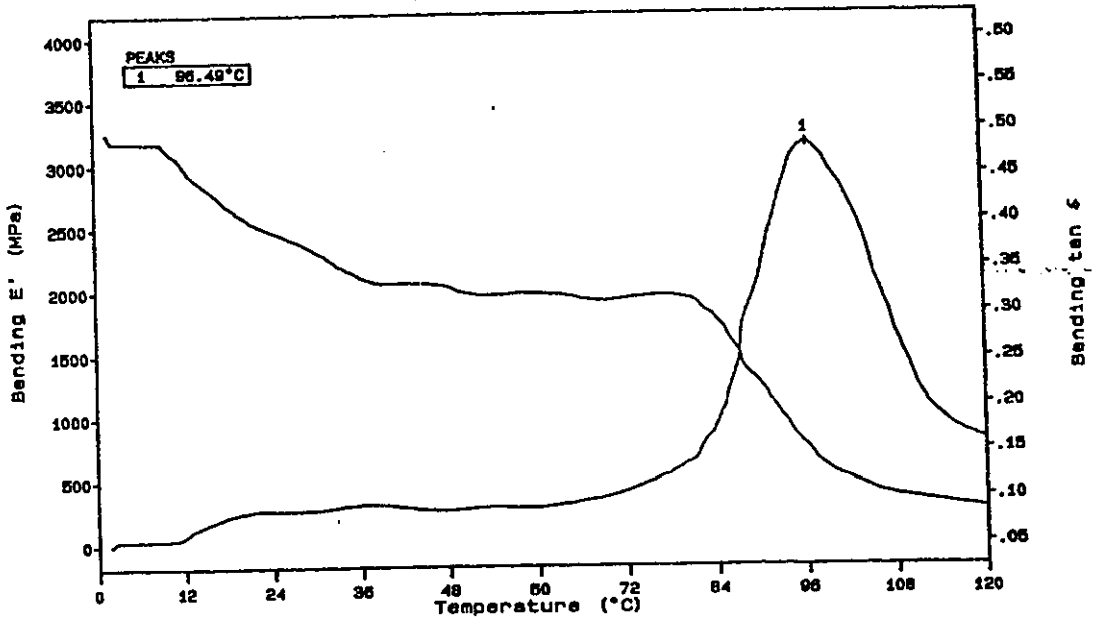

Fig. 4.37c DMTA traces of *p*-MAATBTB with MA
90% MA Composition

Table 4.28: Values of T_g for methyl acrylate / acryalmido organotin copolymer.

	AATBTB		MAATBTB	
WC(%)	*meta*	*para*	*meta*	*para*
0	121	168	144	183*
40	97	129*	107*	131
60	60	79	65	106
90	64*	52*	58	96
100	30	30	30	30

WC: Methyl acrylate percentage weight composition.
AATBTB: Acrylamide tri-n-butyltin benzoate.
MAATBTB: Methacrylamide tri-n-butyltin benzoate.
* Poorly defined tan δ peak.

Fig. (4.38): Values of Tg for acrylamido organotin polymers with methyl acrylate (MA)

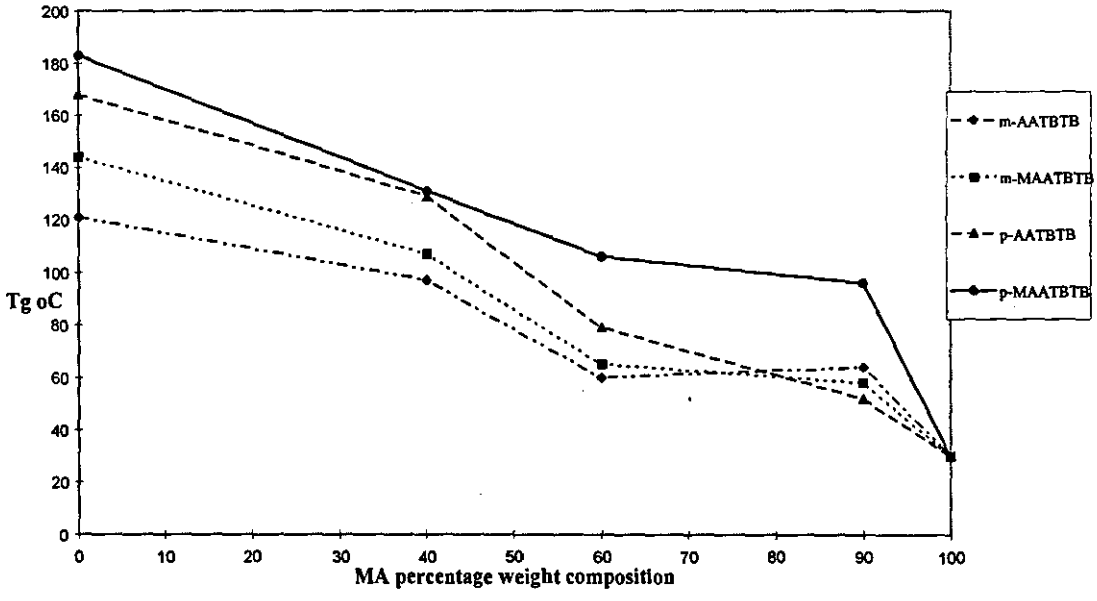

Table (4.28) and figure (4.38) indicate that the values of T_g for organotin acrylamide-MA copolymers are in the following general order:

p-MAATBTB > *p*-AATBTB > *m*-MAATBTB > *m*-AATBTB

The order of values of T_g corresponds to the order of decreased copolymer flexibility which is influenced by two factors; the position of the tri-n-butyltin carboxylate on the phenyl ring and the presence of the methyl group on the polymerisable double bond (see section 4.9.2.1). The *para - meta* difference has a greater influence on the values of T_g than the presence or absence of the methyl group, as indicated in table 4.28 and figure (4.38). This might be due to the greater steric size of the tri-n-butyltin group compared to the methyl group.

DMTA Results for Organotin Acrylamide Derivatives with BA

DMTA traces of the copolymer system *m*-AATBTB-BA figures (4.39a, b and c) show the values of T_g as 58°C, 56°C and 5°C respectively for BA percentage weight compositions 40%, 70% and 90% respectively. Thus, as the BA composition increases in the copolymer values of T_g decrease. This can be explained by the following. As the size of the side group increases chain packing becomes poorer which in turn increases the free volume and intermolecular distances consequently reducing interchain cohesive forces and reducing values of Tg.[100] Similar trends appear in copolymers of *p*-AATBTB, *m*-MAATBTB and *p*-MAATBTB with BA figures (4.40a, b, c, 4.41a, b, c, 4.42a, b, c and table 4.29). The overall effect of increasing BA composition on the values of T_g of organotin acrylamide copolymers is illustrated in figure (4.43).

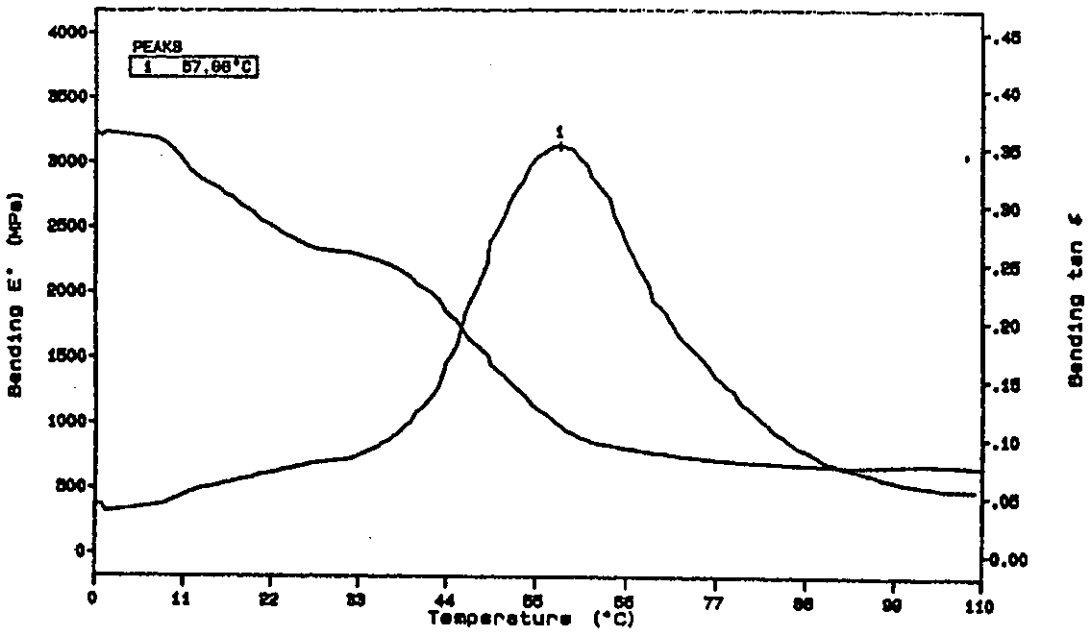

Fig. 4.39a DMTA traces of *m*-AATBTB with BA
40% BA Composition

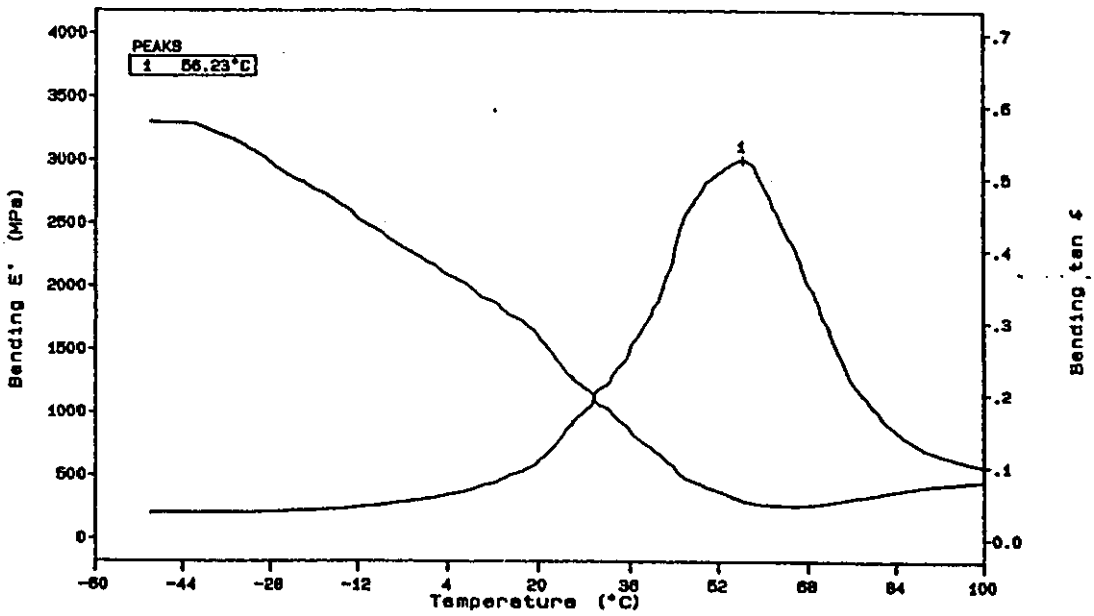

Fig. 4.39b DMTA traces of *m*-AATBTB with BA
70% BA Composition

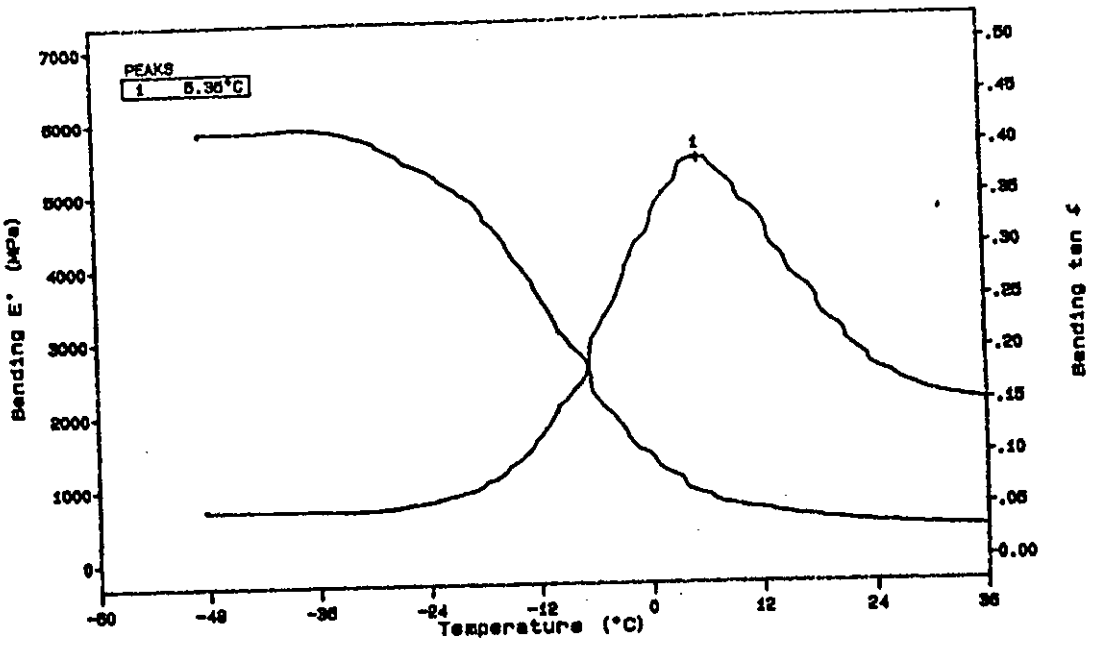

Fig. 4.39c DMTA traces of *m*-AATBTB with BA
90% BA Composition

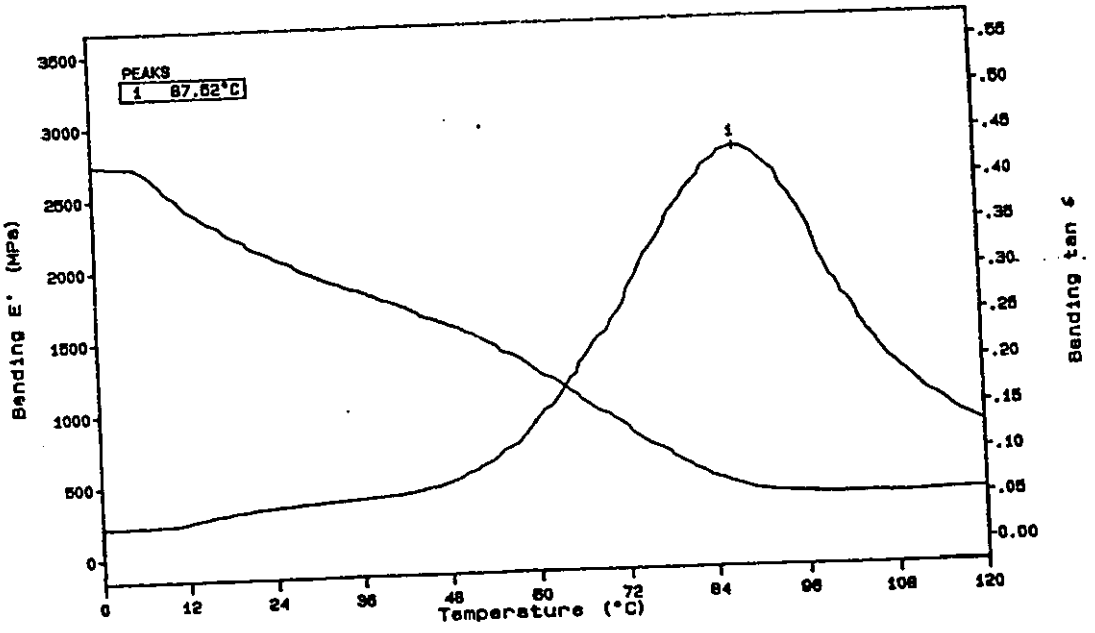

Fig. 4.40a DMTA traces of *p*-AATBTB with BA
40% BA Composition

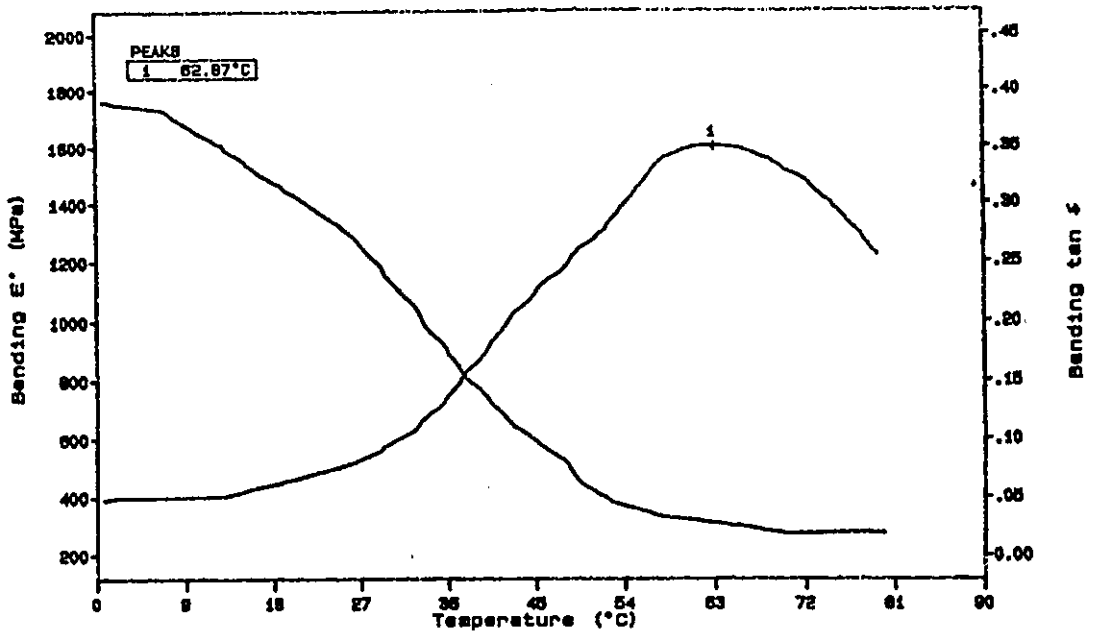

Fig. 4.40b DMTA traces of *p*-AATBTB with BA
60% BA Composition

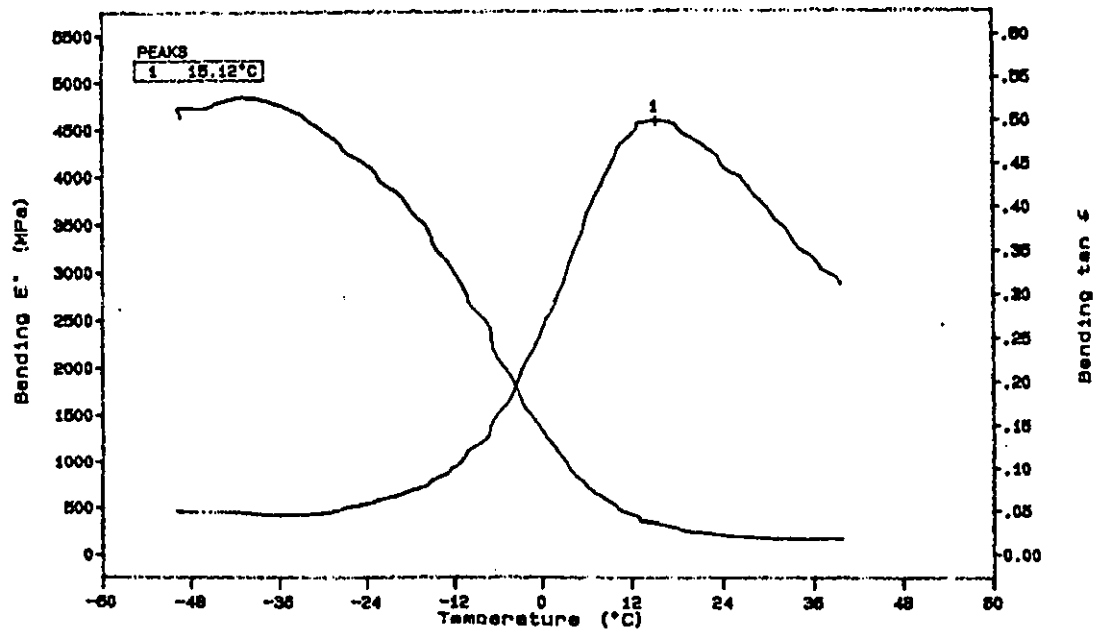

Fig. 4.40c DMTA traces of *p*-AATBTB with BA
90% BA Composition

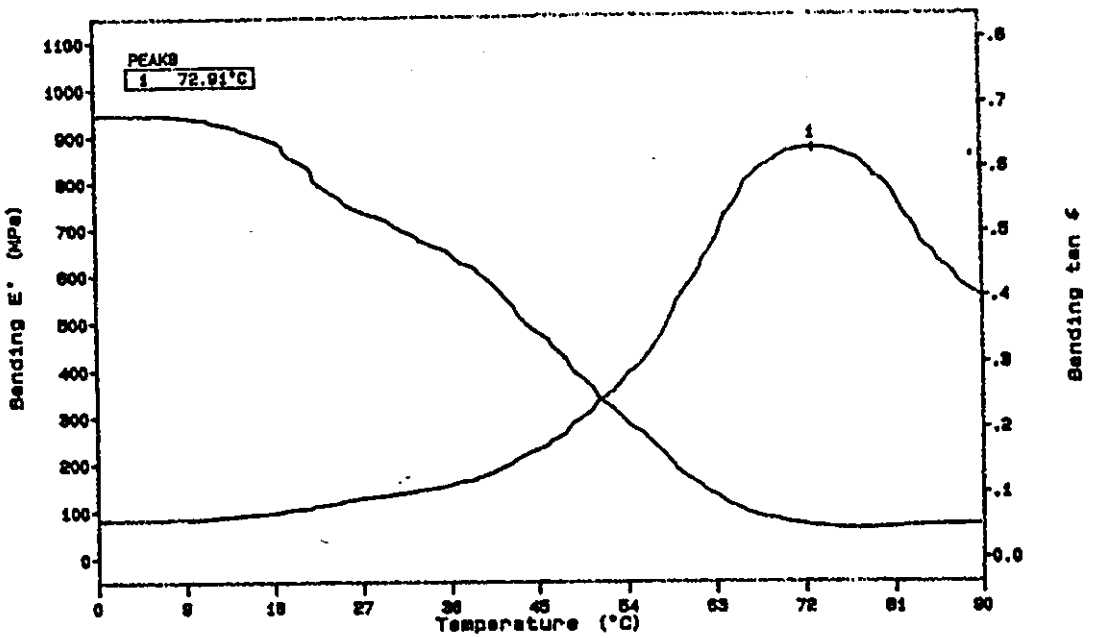

Fig. 4.41a DMTA traces of *m*-MAATBTB with BA
40% BA Composition

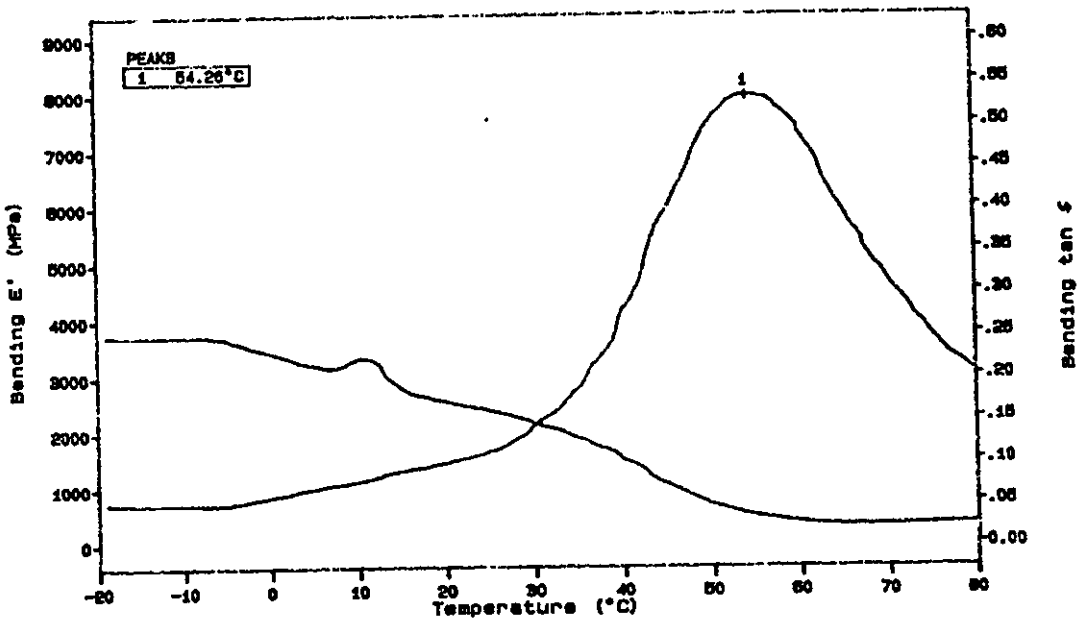

Fig. 4.41b DMTA traces of *m*-MAATBTB with BA
60% BA Composition

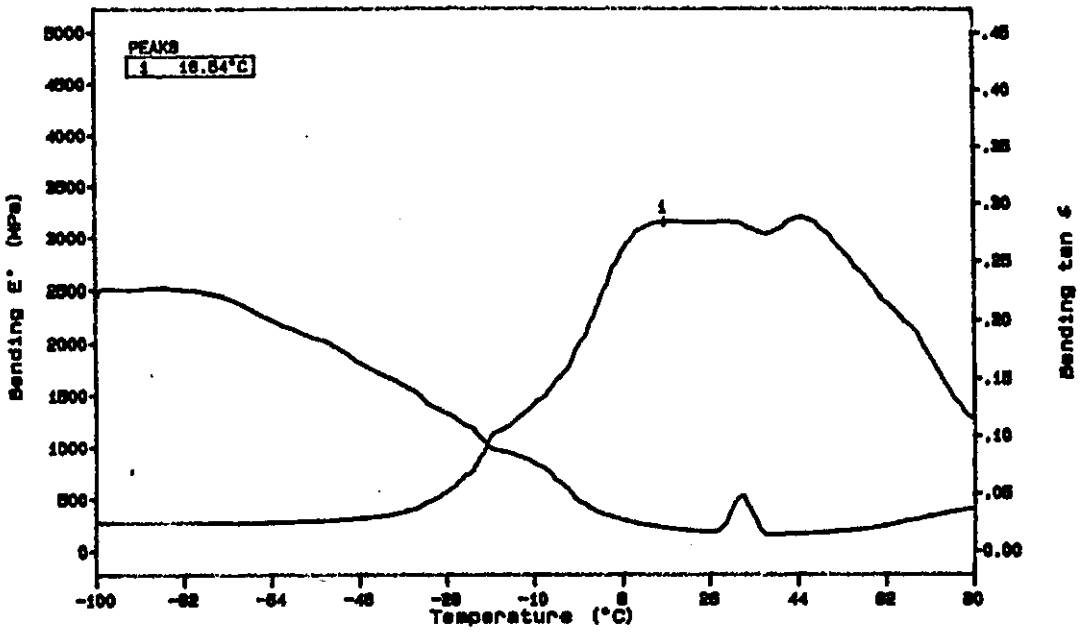

Fig. 4.41c DMTA traces of *m*-MAATBTB with BA
90% BA Composition

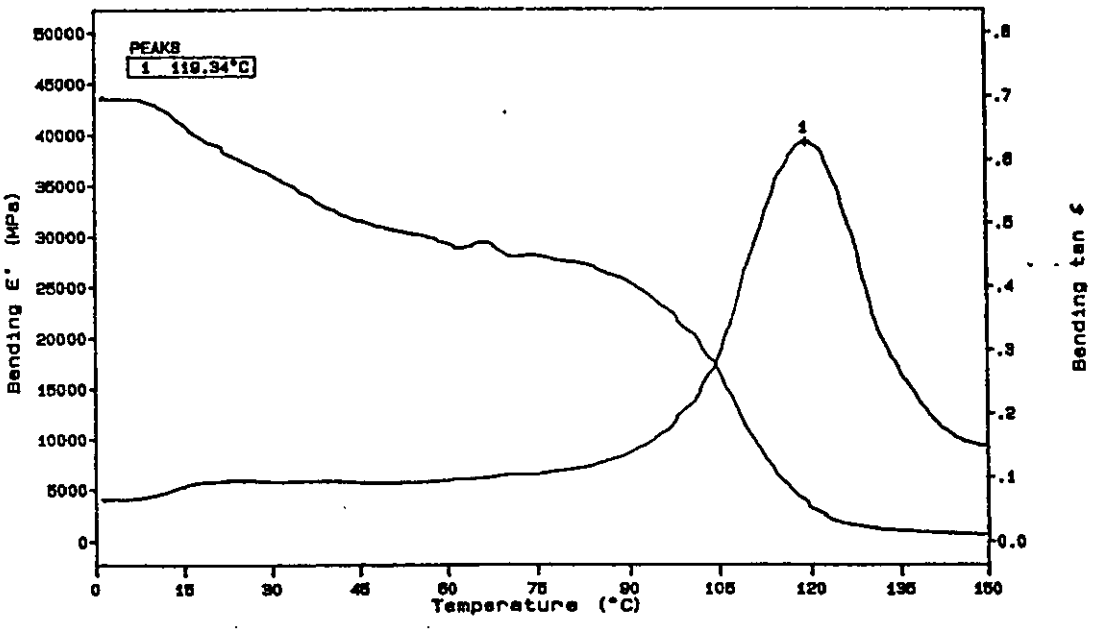

Fig. 4.42a DMTA traces of *p*-MAATBTB with BA
40% BA Composition

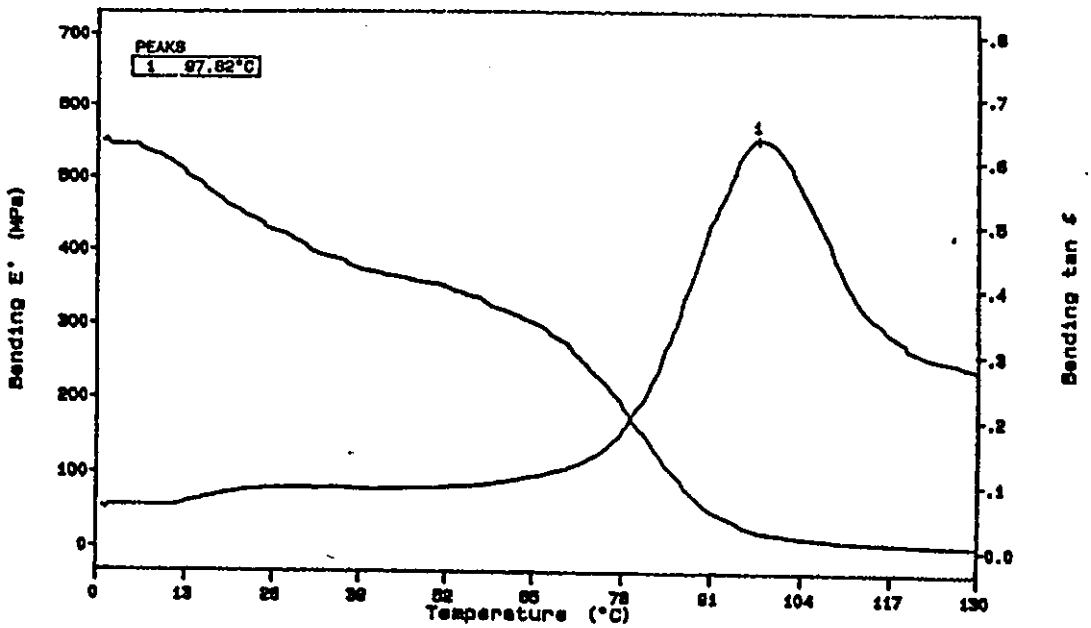

Fig. 4.42b DMTA traces of *p*-MAATBTB with BA
60% BA Composition

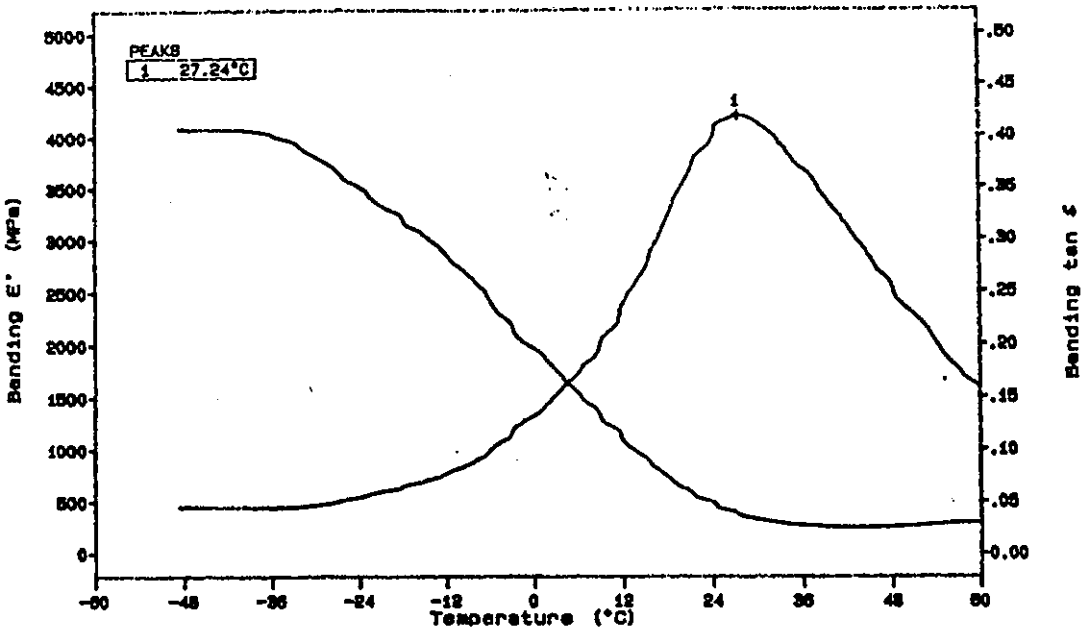

Fig. 4.42c DMTA traces of *p*-MAATBTB with BA
90% BA Composition

Table 4.29 : Values of T_g for butyl acrylate / acryalmido organotin copolymers.

	AATBTB		MAATBTB	
WC(%)	*meta*	*para*	*meta*	*para*
0	121	168	144	183*
40	58	88	73*	119
60	56	63*	54	98
90	5	15*	17*	27
100	-30	-30	-30	-30

WC: Butyl acrylate percentage weight composition.
AATBTB: Acrylamidotri-n-butyltin benzoate.
MAATBTB: Methacrylamidotri-n-butyltin benzoate.
* Poorly defined tan δ peak.

Fig. 4.43 Values of Tg for acrylamido organotin copolymers with butyl acrylate (BA)

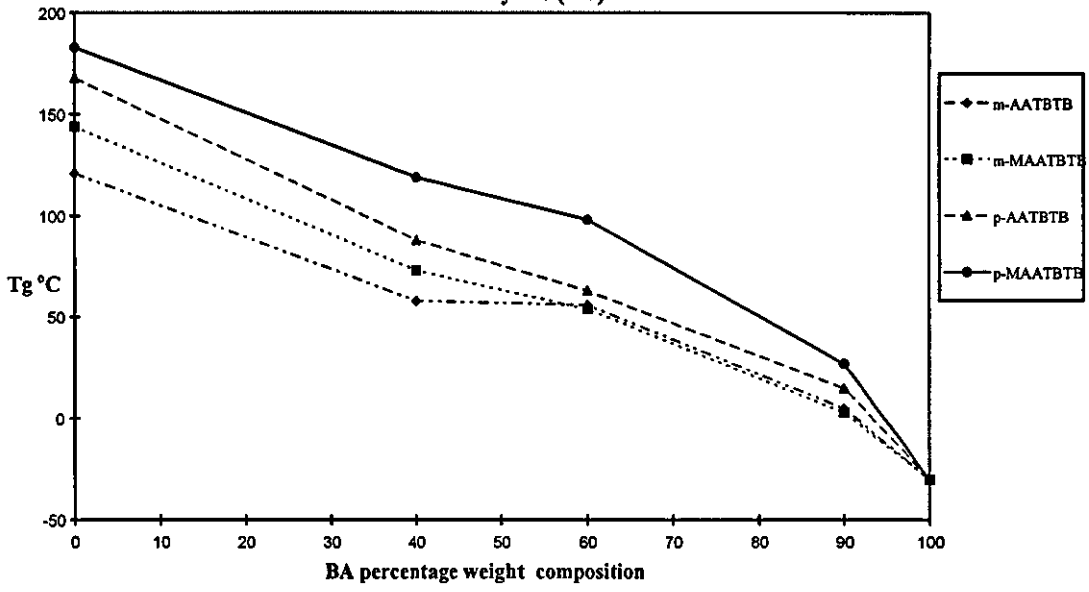

DMTA Results for Organotin Acrylamide Derivatives with MMA

DMTA traces of the copolymer system *m*-AATBTB-MMA figures (4.44a and 4.44b) show values of T_g as 113°C, and 123°C for MMA percentage weight compositions 60% and 90% respectively. This copolymer highlights one of the limitations of the technique. Poly(*m*-AATBTB) has a T_g of 121°C and poly (MMA) has a T_g of 133°C, so it is inevitable that there will be considerable overlap of the transitions of these polymers, so any dependence of T_g on copolymer composition may not be easily established. Similar trends appear for *p*-AATBTB and *m*-MAATBTB copolymers figures (4.45a, b, c and 4.46a, b, c). On the other hand the T_g values of *p*-MAATBTB copolymers decrease as MMA increases in the copolymer, see figures (4.47a, b, c and table 4.30). The overall effect of increasing MMA composition on the values of T_g of organotin acrylamide copolymers is illustrated in figure (4.48).

The effects of increasing percentage weight composition of the acrylic monomers on copolymers of individual methylated and non-methylated acrylamide monomers are depicted in figures (4.49-4.52). For purposes of comparison the theoretically determined values of Tg computed with the Fox relation, see equation (1.38), are illustrated as lines, while the experimental data are shown as points in these figures. Given that a number of results of T_g could not regarded as reliable as labelled by an asterisk in the tables, it is difficult to provide conclusions on the data in figures (4.49-4.52). However, it is interesting to observe that there is a good correlation for the MMA copolymers in figure (4.52), with the experimental T_g results for other acrylamide-MMA copolymers lying below the Fox curve in figures (4.49-4.51). For all BA copolymers the experimental T_g results are always placed above the Fox curves.

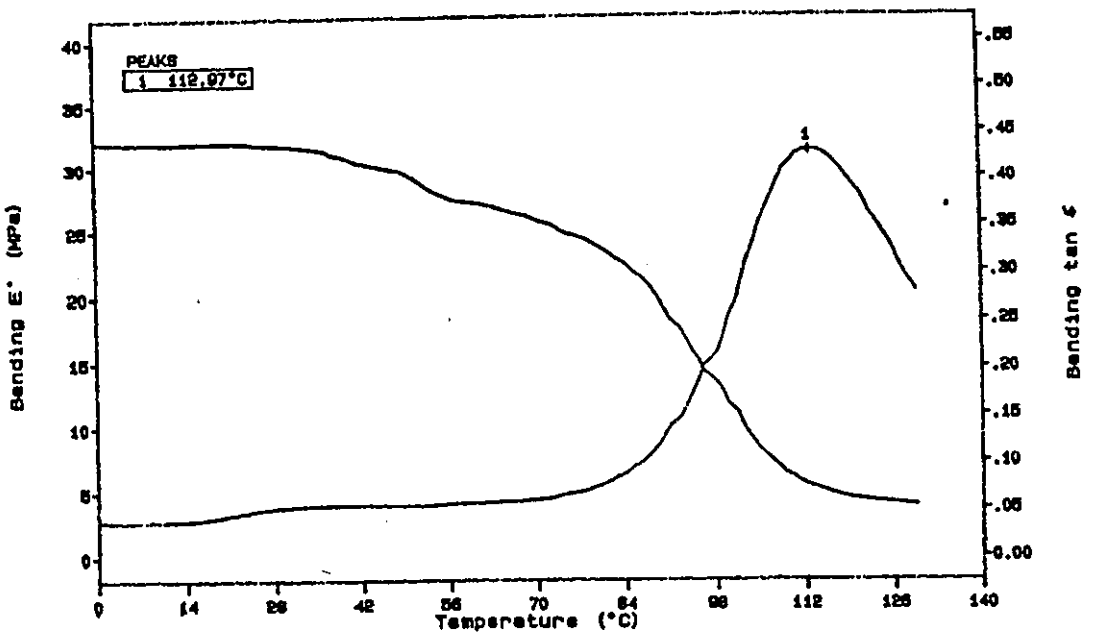

Fig. 4.44a DMTA traces of *m*-AATBTB with MMA
60% MMA Composition

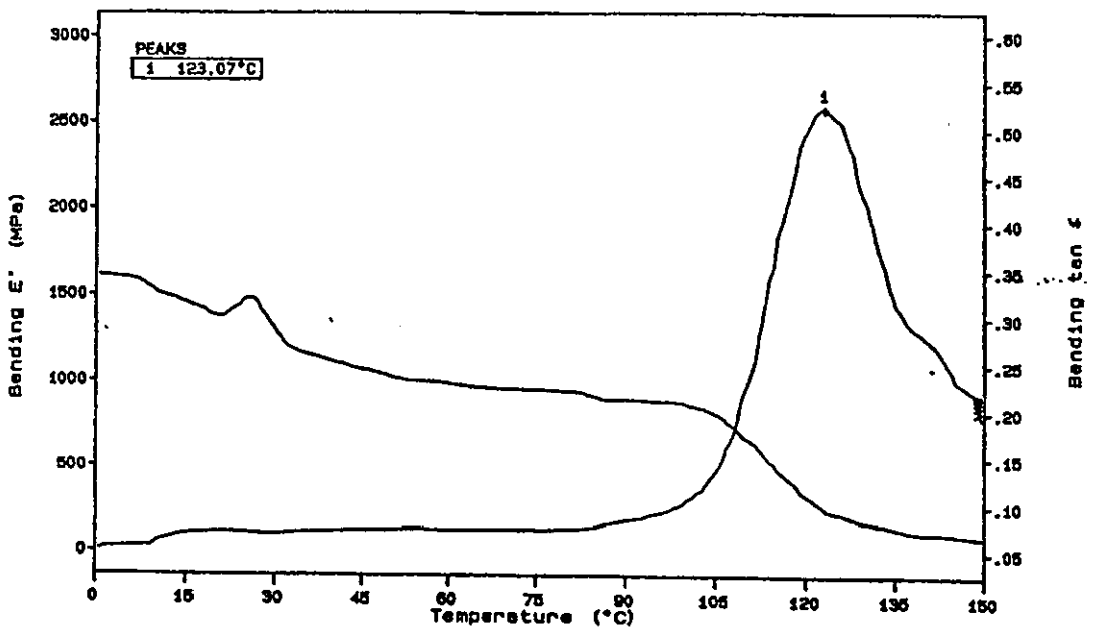

Fig. 4.44b DMTA traces of *m*-AATBTB with MMA
90% MMA Composition

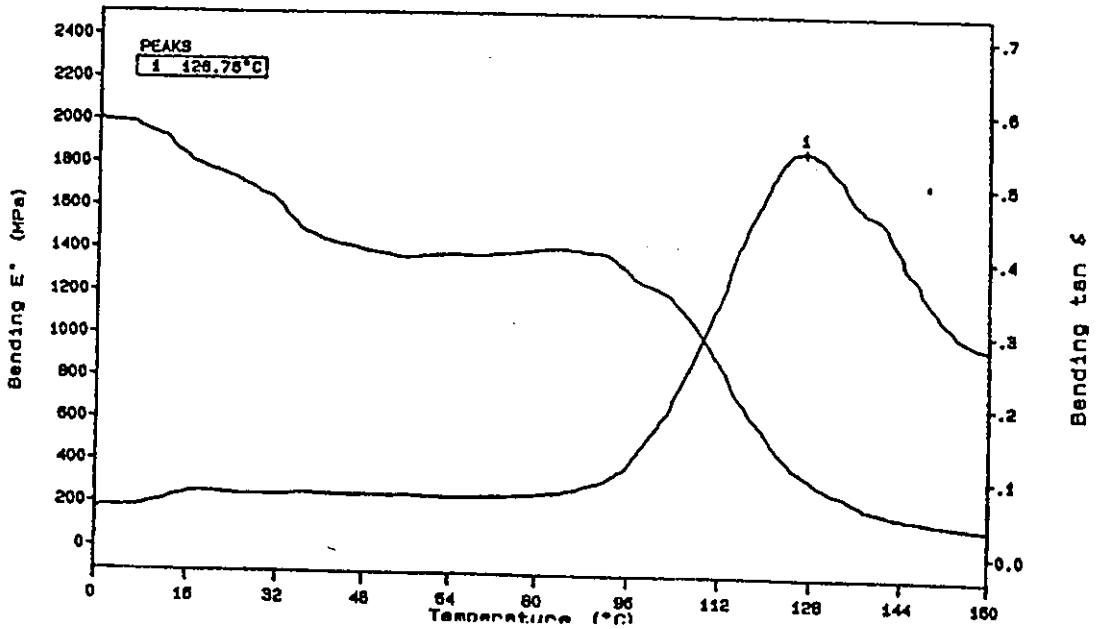

Fig. 4.45a DMTA traces of *p*-AATBTB with MMA
40% MMA Composition

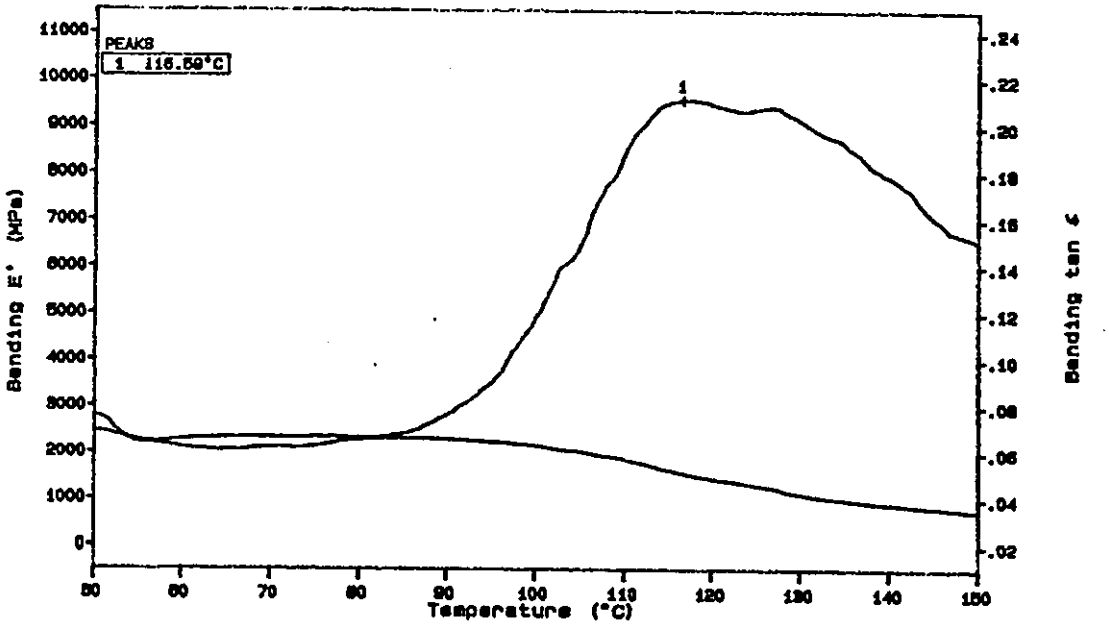

Fig. 4.45b DMTA traces of *p*-AATBTB with MMA
60% MMA Composition

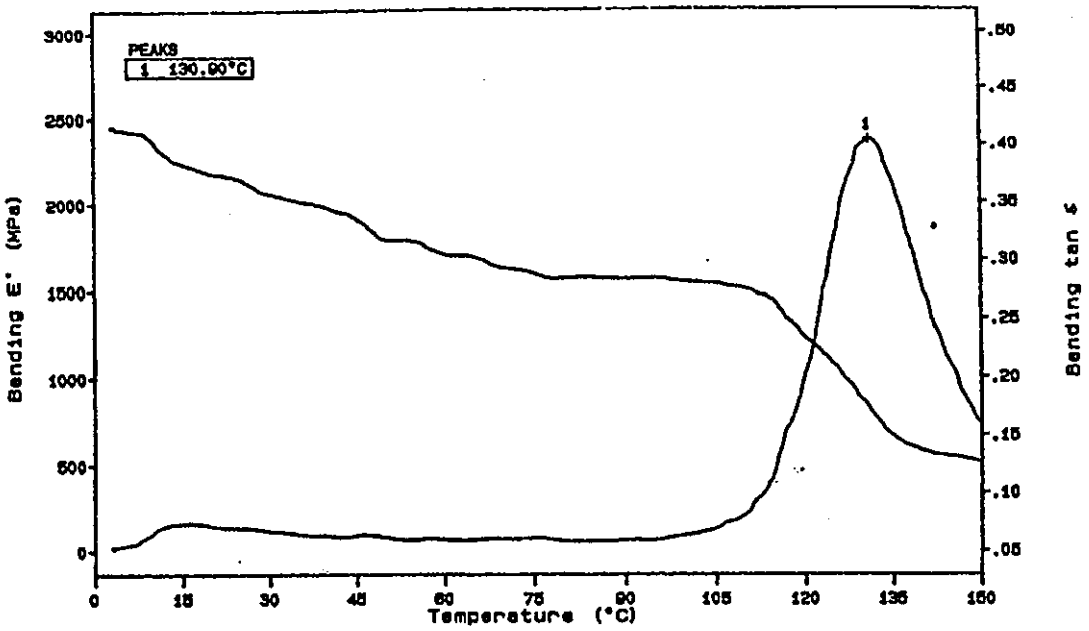

Fig. 4.45c DMTA traces of *p*-AATBTB with MMA
90% MMA Composition

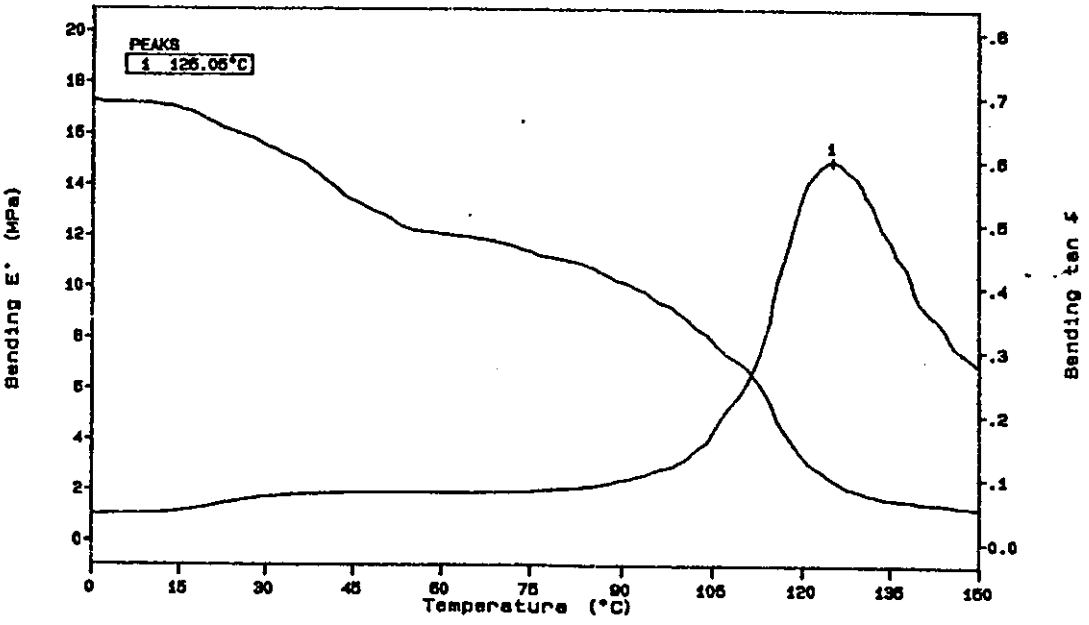

Fig. 4.46a DMTA traces of *m*-MAATBTB with MMA
40% MMA Composition

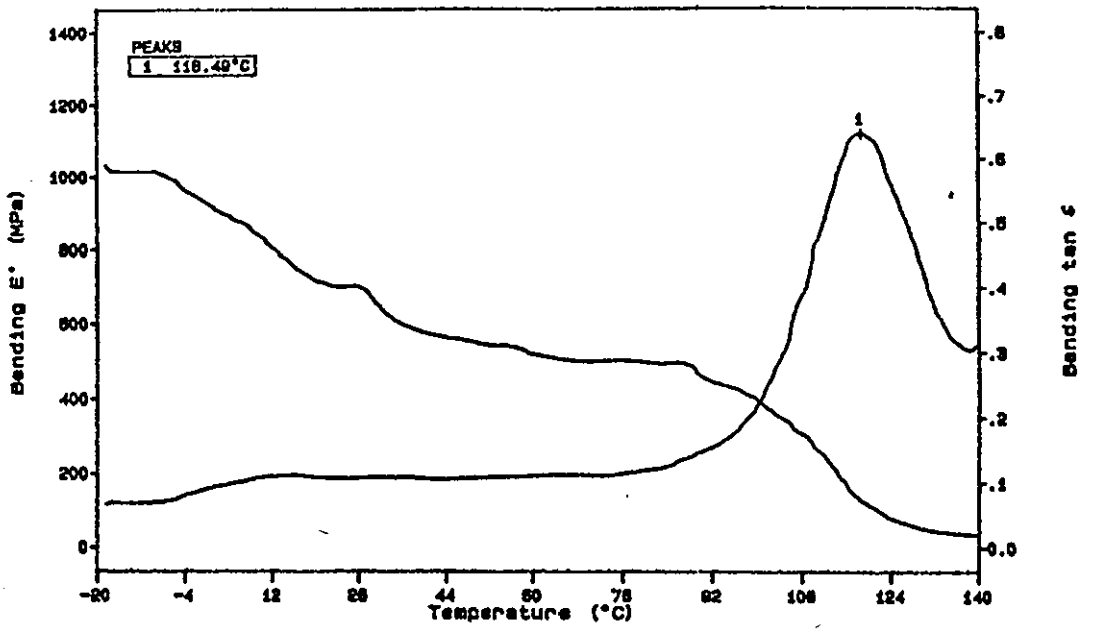

Fig. 4.46b DMTA traces of *m*-MAATBTB with MMA
60% MMA Composition

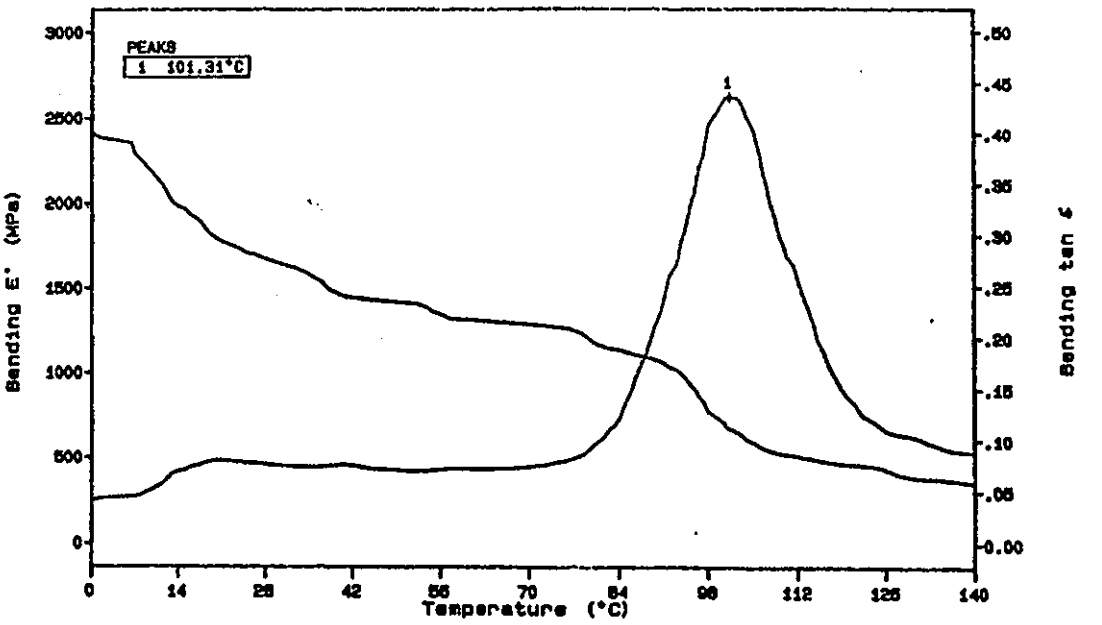

Fig. 4.46c DMTA traces of *m*-MAATBTB with MMA
90% MMA Composition

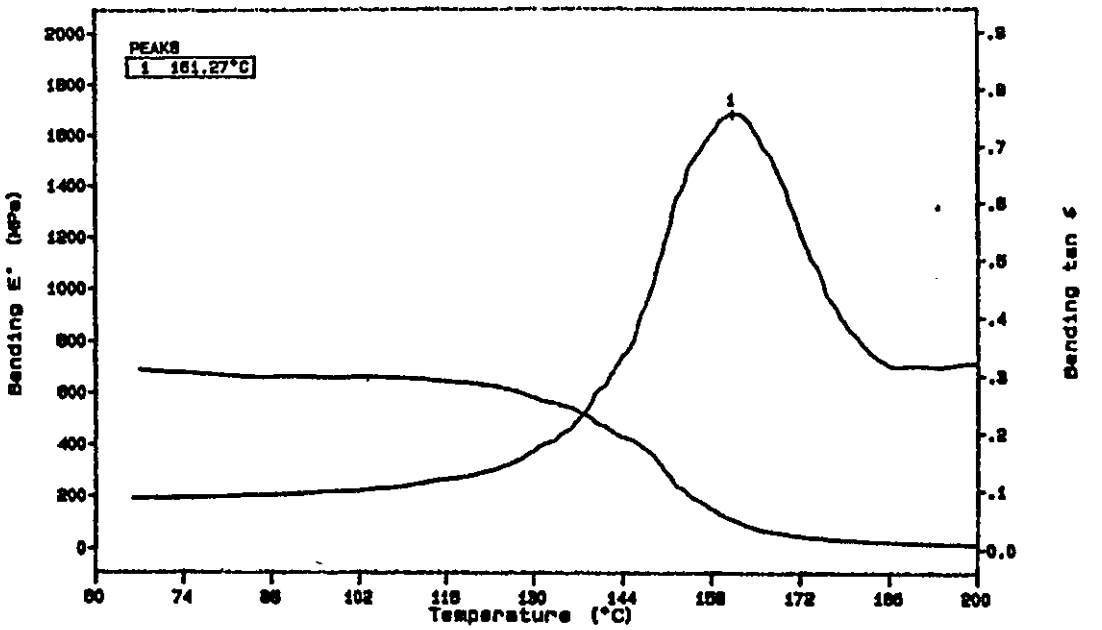

Fig. 4.47a DMTA traces of *p*-MAATBTB with MMA
40% MMA Composition

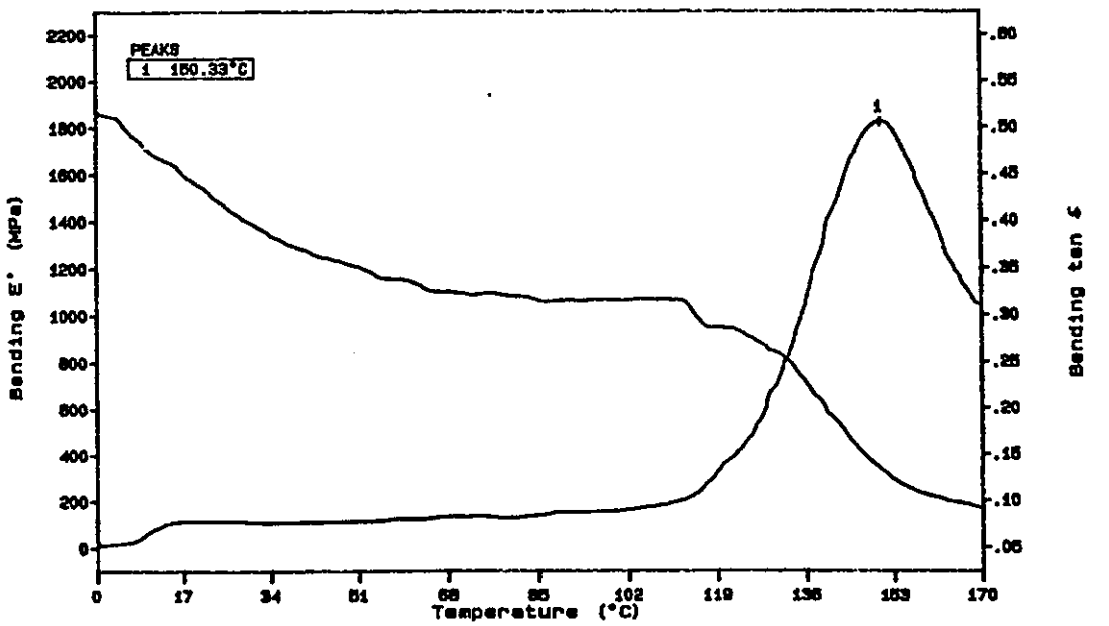

Fig. 4.47b DMTA traces of *p*-MAATBTB with MMA
60% MMA Composition

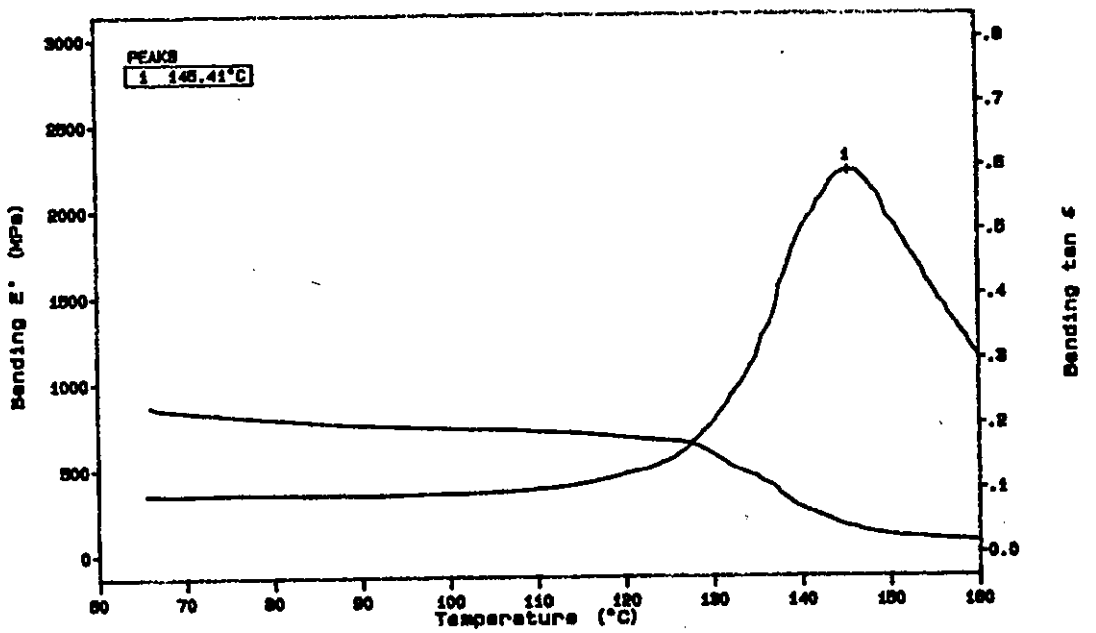

Fig. 4.47c DMTA traces of *p*-MAATBTB with MMA
90% MMA Composition

Table 4.30: Values of T_g for methyl methacrylate / acryalmido organotin copolymers.

	AATBTB		MAATBTB	
WC(%)	*meta*	*para*	*meta*	*para*
0	121	168	144	183*
40	N/A	127*	125	161
60	113	117*	118	150*
90	123	131	101	145
100	133	133	133	133

WC: Methyl methacrylate percentage weight composition.
AATBTB: Acrylamidotri-n-butyltin benzoate.
MAATBTB: Methacrylamidotri-n-butyltin benzoate.
* Poorly defined tan δ peak.

Fig. 4.48 Values of Tg for acrylamido organotin copolymers with methyl methacrylate (MMA)

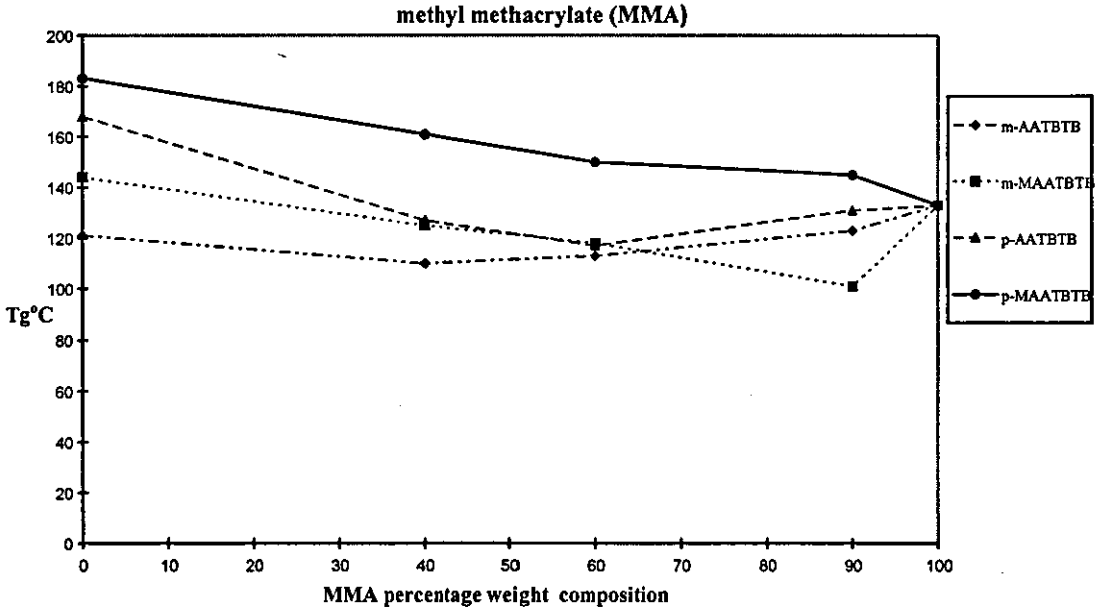

Fig. 4.49 Values of T_g for m-AATBTB with MA, BA and MMA versus copolymer percentage weight composition of acrylic monomer

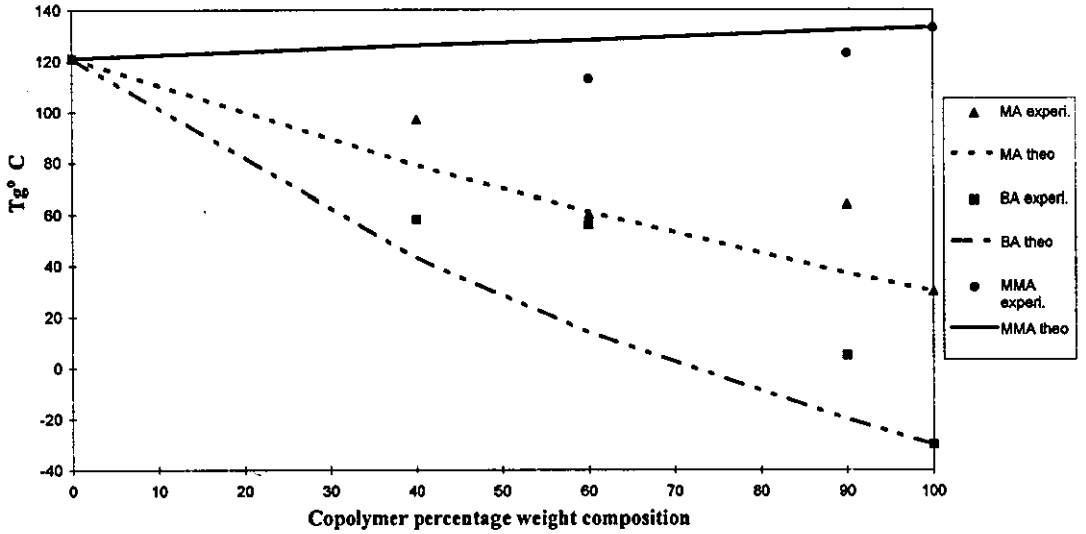

Fig. 4.50 Values of T_g for *p*-AATBTB with MA, BA and MMA versus copolymer percentage weight composition of acrylic monomer

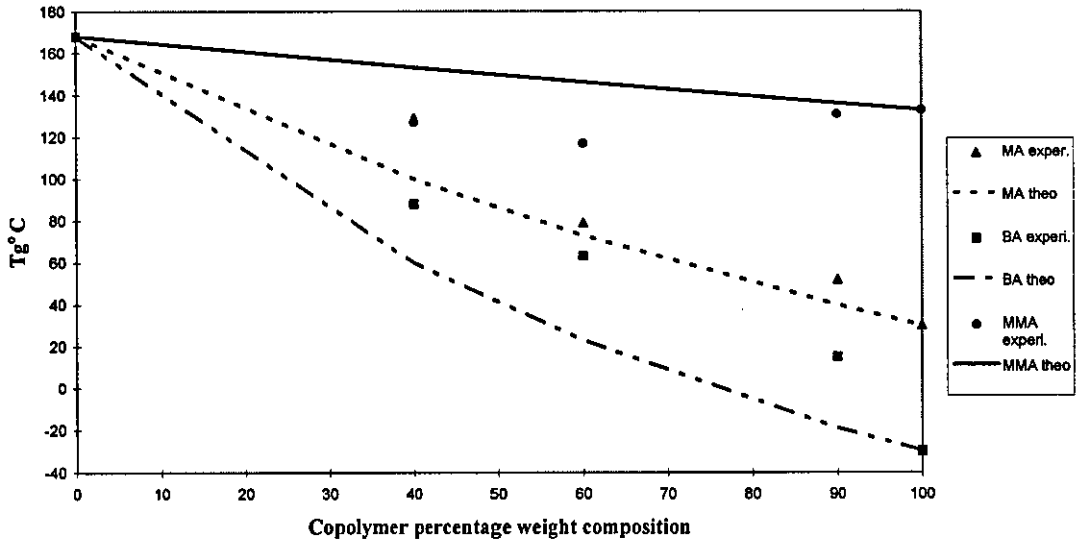

Fig. 4.51 Values of T_g for *m*-MAATBTB with MA, BA and MMA versus copolymer percentage weight composition of acrylic monomer

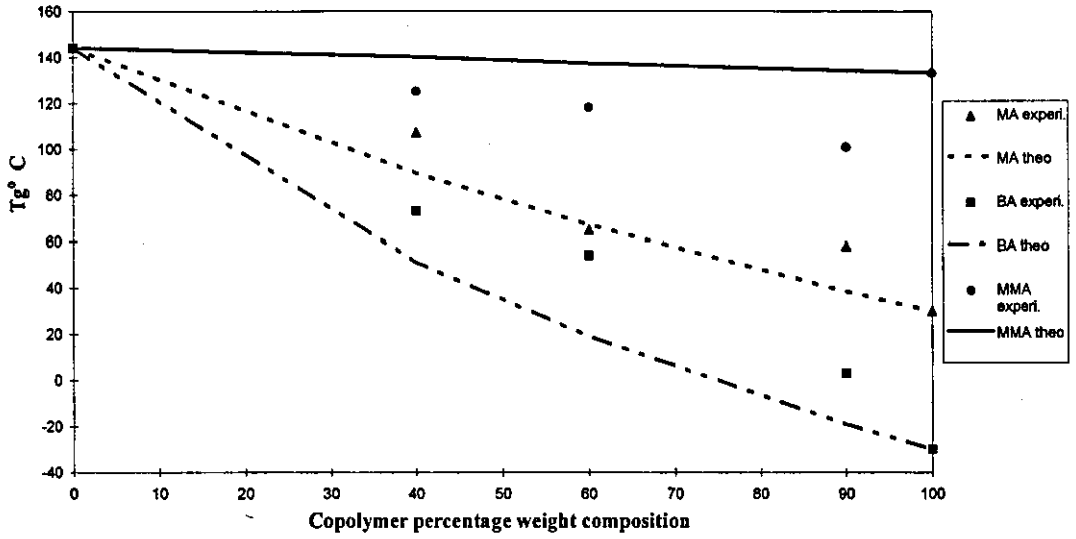

Fig. 4.52 Values of T_g for *p*-MAATBTB with MA, BA and MMA versus copolymer percentage weight composition of acrylic monomer

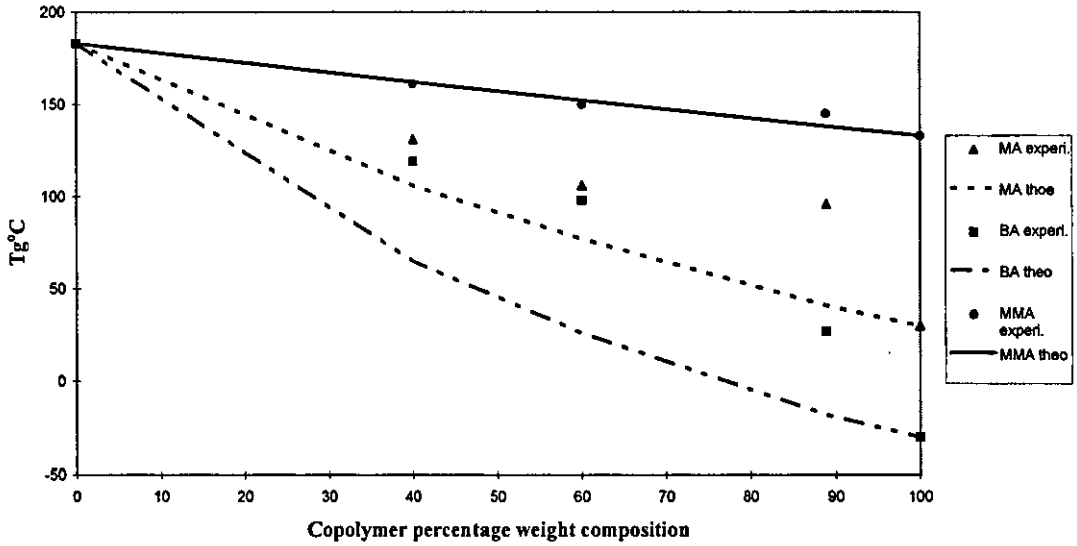

4.9.3.2 DMTA Results for Acryloyloxy Derivatives

Three samples were selected for each copolymer system (40%, 60%, and 90% percentage weight composition of MA, BA and MMA) to illustrate the effect of monomeric percentage on the values of T_g for copolymers.

DMTA Results for Organotin Acryloyloxy Derivatives with MA

DMTA traces of the copolymer system *o*-MAOTBTB-MA figures in (4.53a, b and c) show values of T_g as 36°C, 44°C and 38°C for MA percentage weight composition 40%, 60% and 90% respectively.

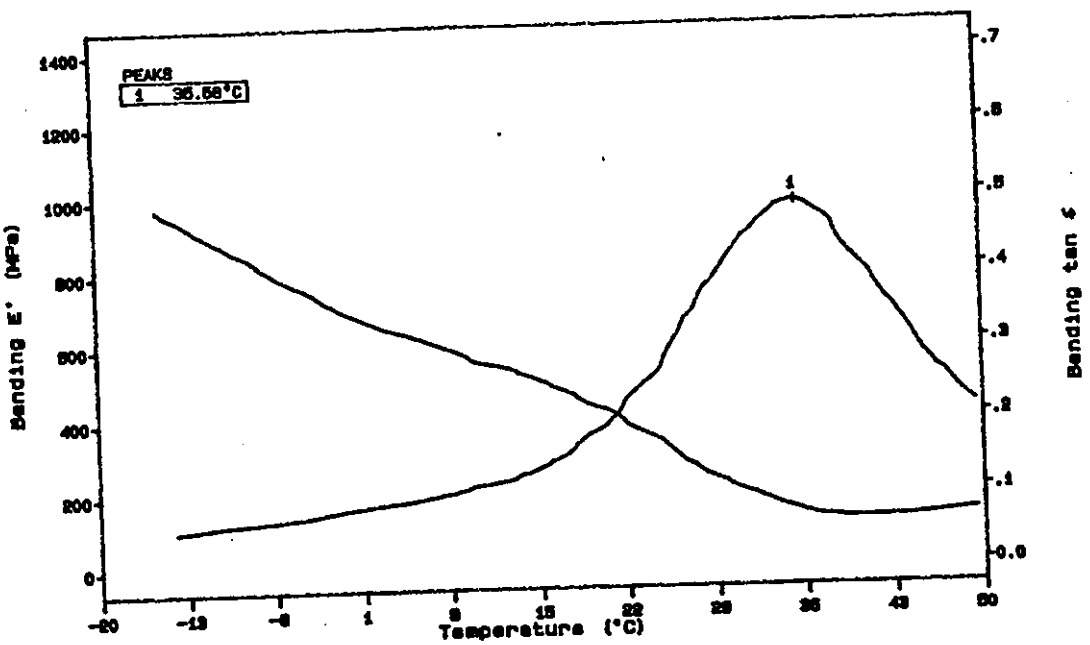

Fig. 4.53a DMTA tracesof *o*-MAOTBTB with MA
·40% MA Composition

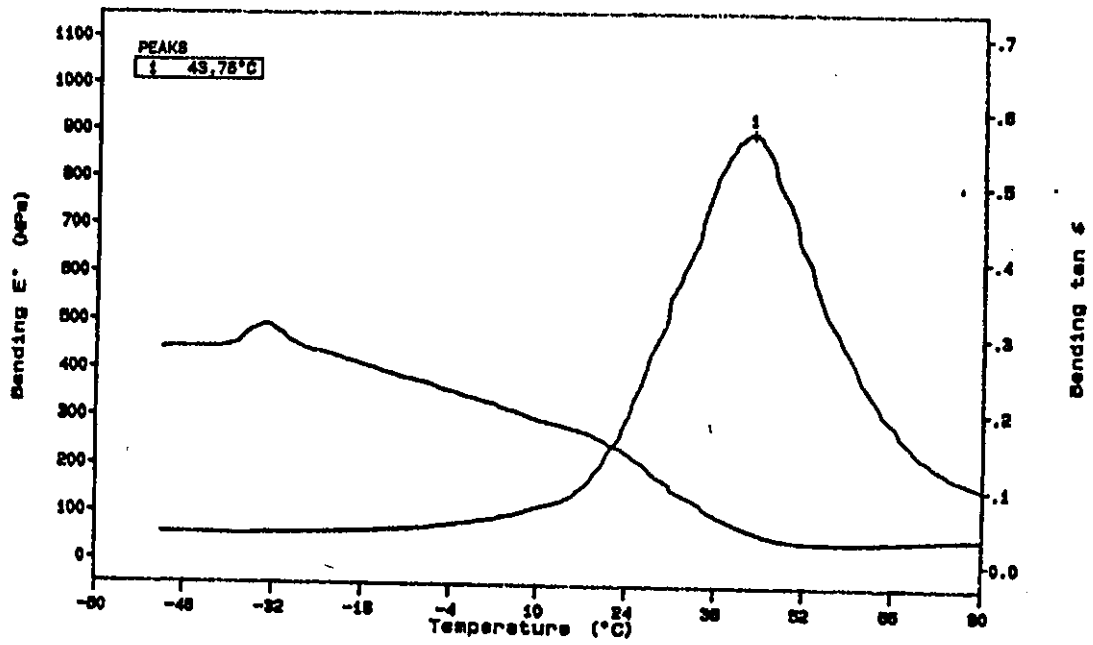

Fig. 4.53b DMTA tracesof *o*-MAOTBTB with MA

60% MA Composition

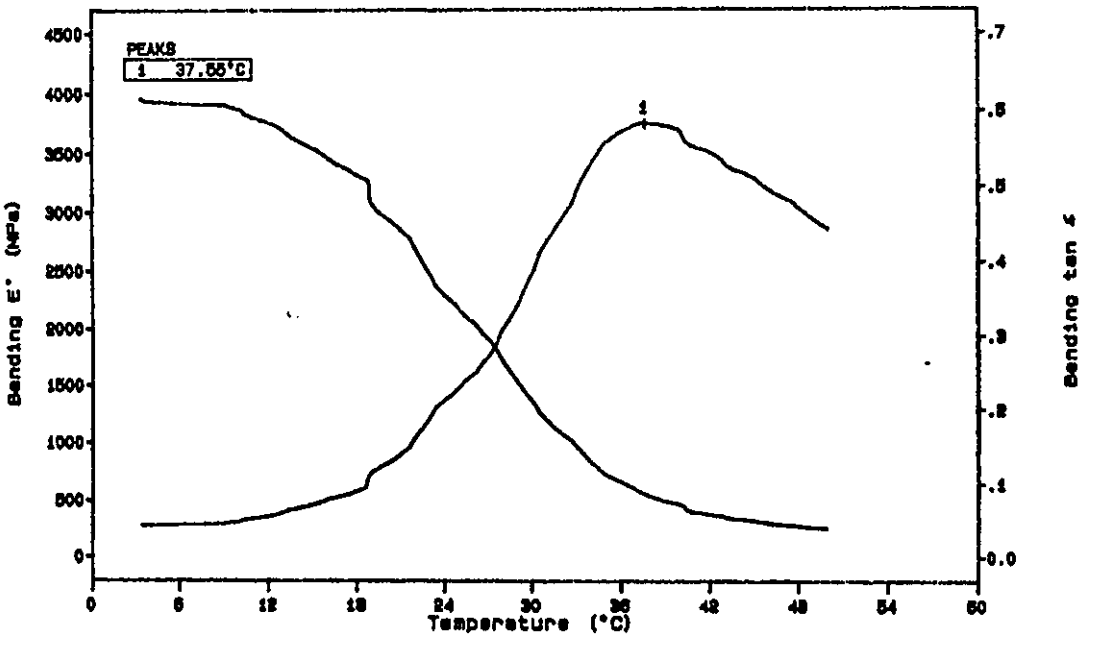

Fig. 4.53c DMTA tracesof *o*-MAOTBTB with MA

90% MA Composition

DMTA Results for Organotin Acryloyloxy Derivatives with BA

DMTA traces of the copolymer system *o*-MAOTBTB-BA in figures (4.54a, b and c) show values of T_g as 22°C, 36°C and -10°C for BA percentage weight composition 40%, 60%, and 90% respectively. Thus as the BA composition increases the values of T_g for the copolymers decrease. Such behaviour has been observed and explained for BA-acrylamide copoylmers (see section 4.9.3.1)

Table 4.31 Values of T_g for methyl acrylate or butyl acrylate / methacryloyloxy organotin copolymer

WC (%)	*o*-MOTBTB/MA	*o*-MAOTBTB/BA
0	73	73
40	36	22*
60	44	36
90	38*	-10
100	30	-30

WC: Methyl acrylate or Butyl acrylate percentage weight composition.
MAOTBTB: Methacryloyloxy tri-n-butyltin benzoate.
* Poorly defined tan δ peak.

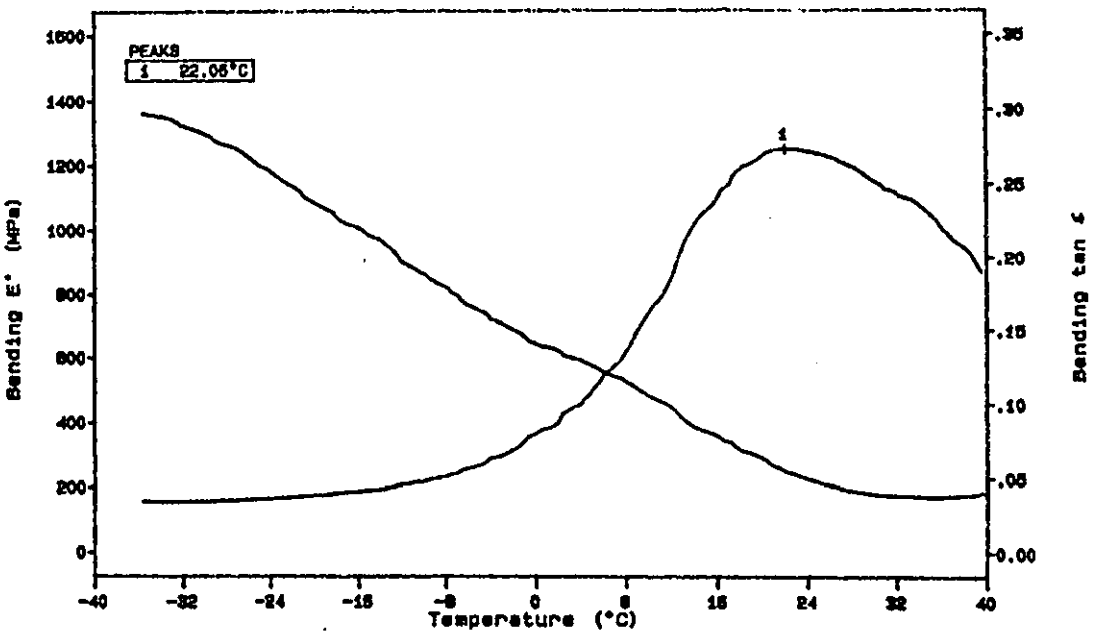

Fig. 4.54a DMTA traces of *o*-MAOTBTB with BA
40% BA Composition

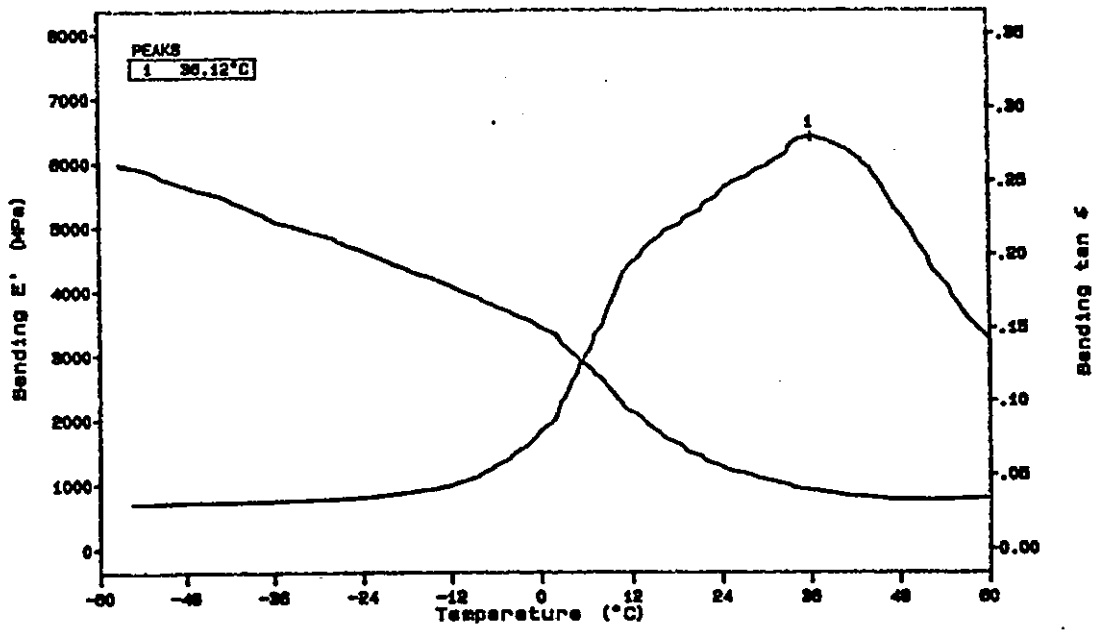

Fig. 4.54b DMTA traces of *o*-MAOTBTB with BA
60% BA Composition

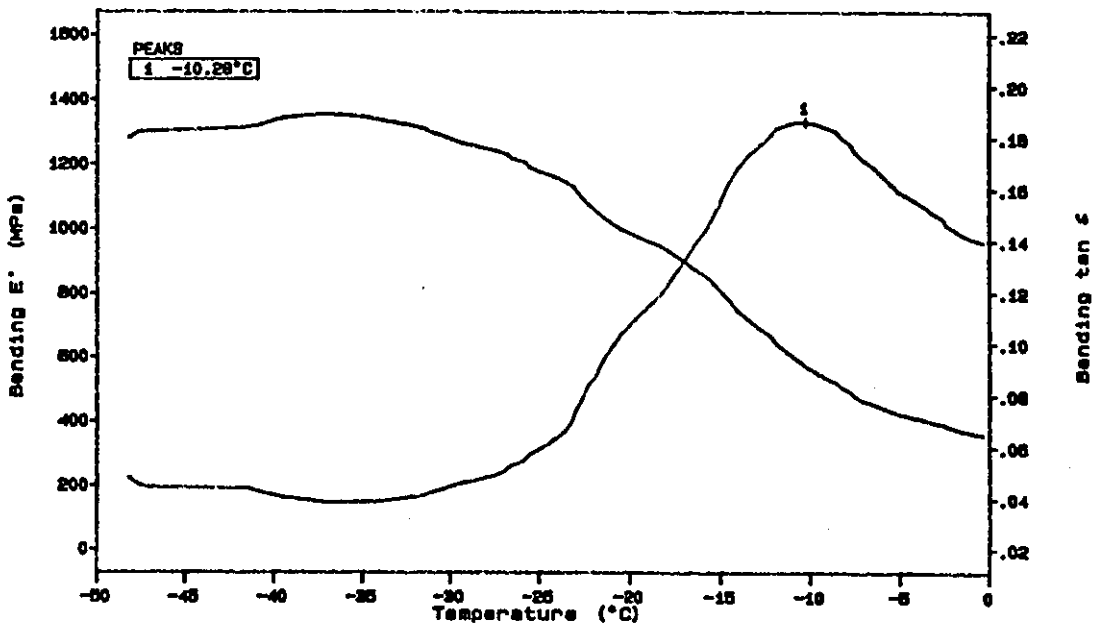

Fig. 4.54c DMTA traces of *o*-MAOTBTB with BA
90% BA Composition

DMTA Results for Organotin Acryloyloxy Derivatives with MMA

DMTA traces of the copolymer system *o*-AOTBTB-MMA in figures (4.55a, b and c) show values of T_g as 44°C, 49°C and 107°C for MMA percent weight compositions 40%, 60% and 90% respectively. The methyl group in the acrylic monomer tends to hinder rotation about the main chain leading to a stiffer material and higher values of T_g. Similar trends appear in *o*-MAOTBTB in figures (4.56a, b and c).

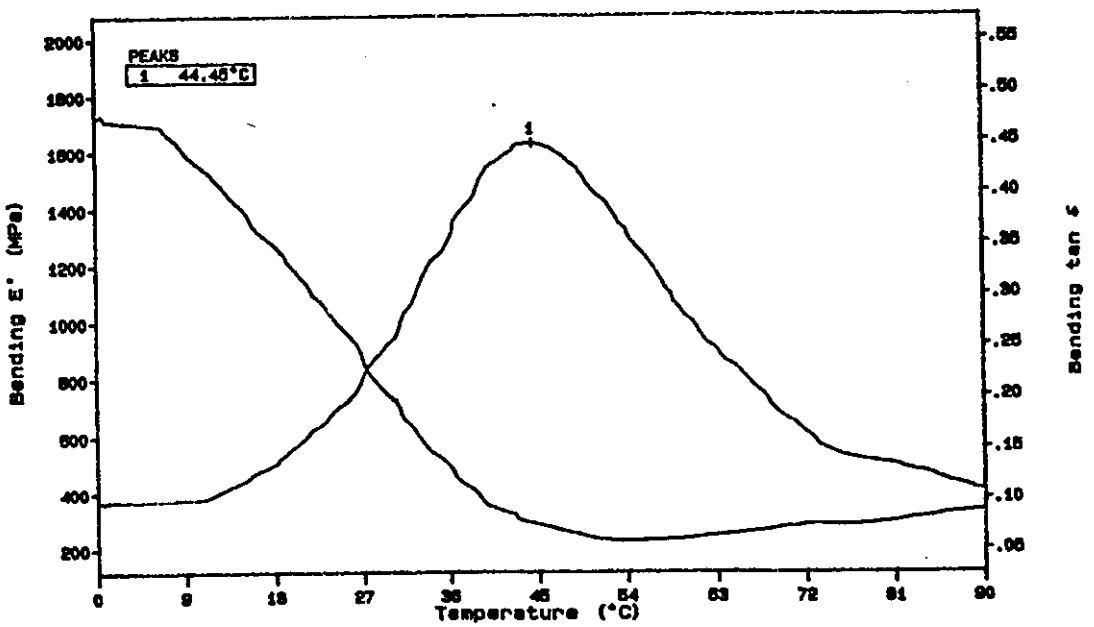

Fig. 4.55a DMTA traces of *o*-AOTBTB with MMA

40% MMA Composition

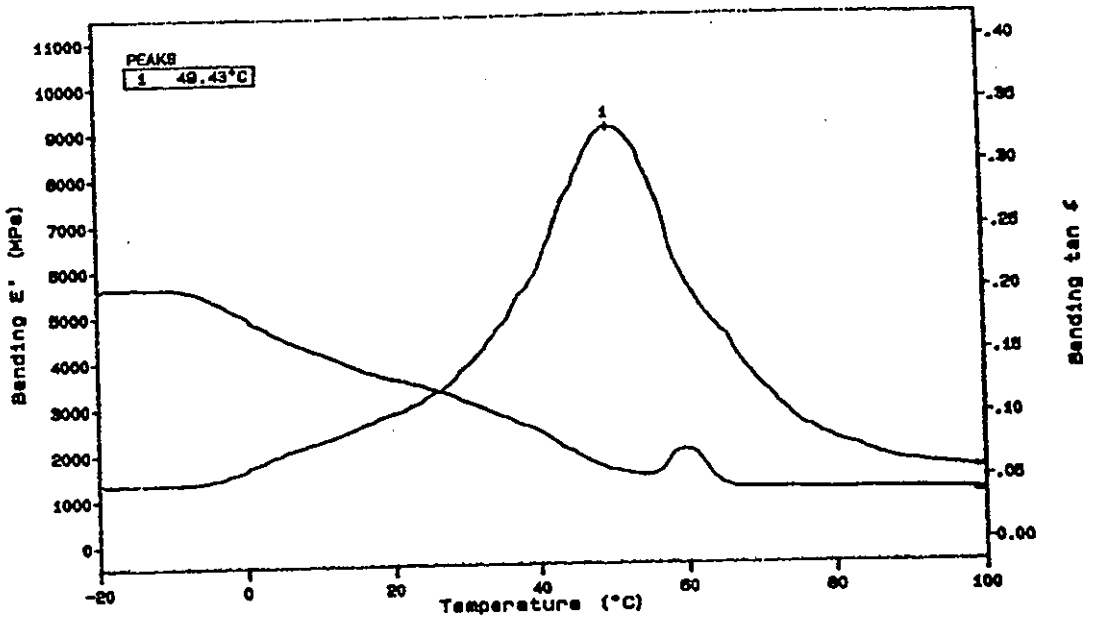

Fig. 4.55b DMTA traces of *o*-MAOTBTB with MMA
60% MMA Composition

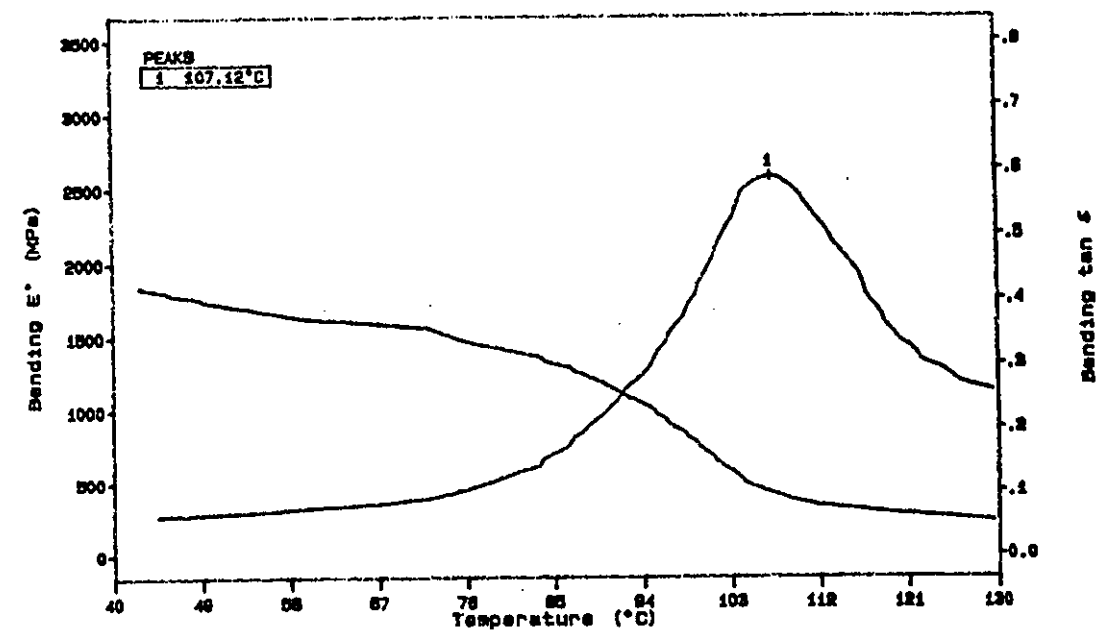

Fig. 4.55c DMTA traces of *o*-MAOTBTB with MMA
90% MMA Composition

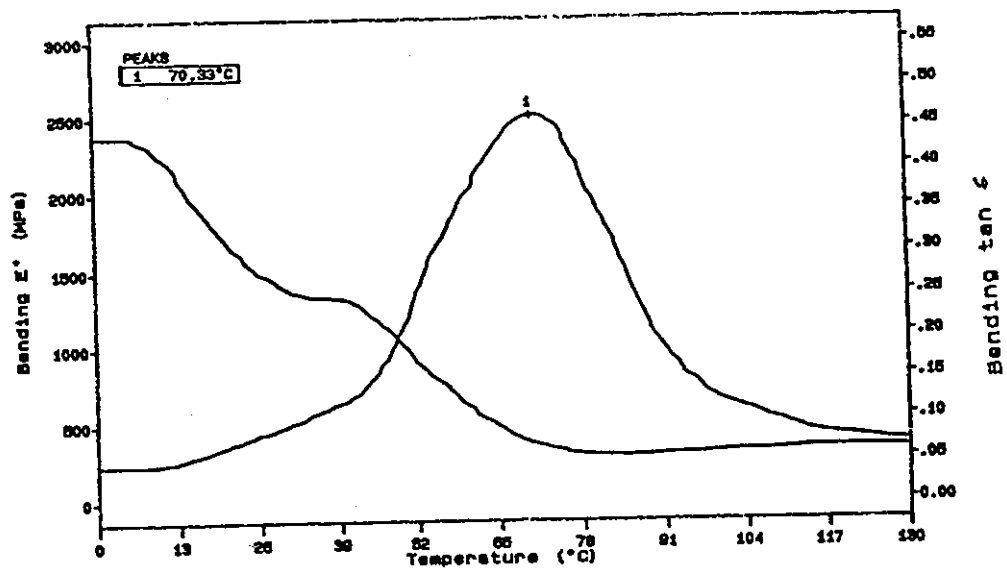

Fig. 4.56a DMTA traces of *o*-MAOTBTB with MMA

40% MA composition

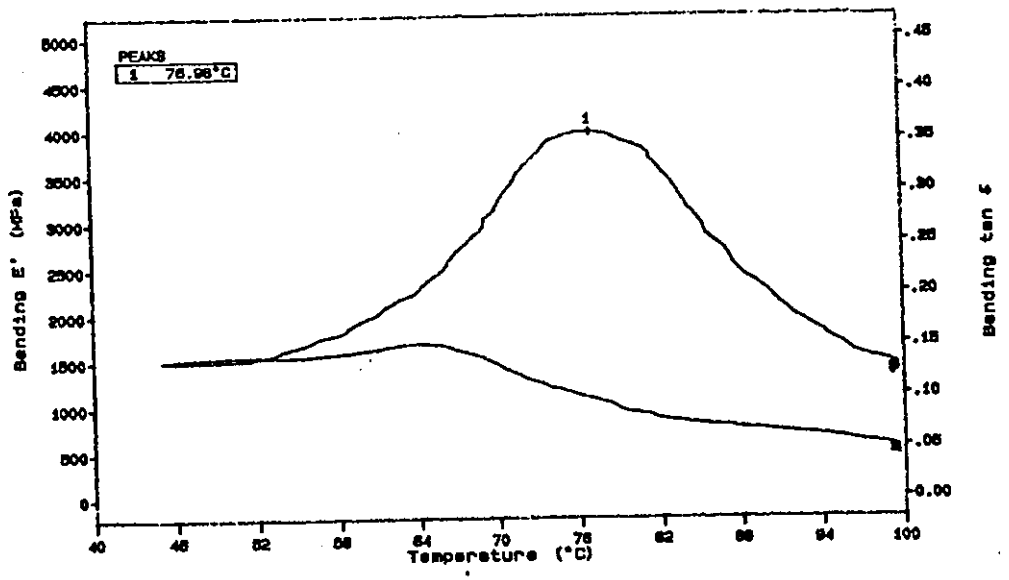

Fig. 4.56b DMTA traces of *o*-MAOTBTB with MMA

60% MMA composition

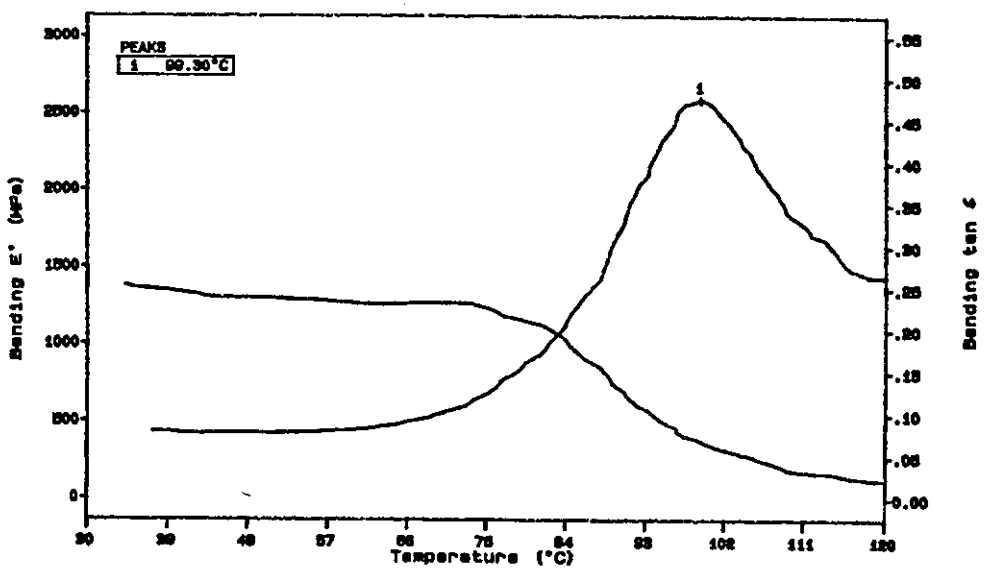

Fig. 4.56c DMTA traces of *o*-MAOTBTB with MMA

90% Composition

Table 4.32: Values of T_g for methyl methacrylate / acryloyloxy organotin copolymer.

WC (%)	*o*-AOTBTB	*o*-MAOTBTB
0	58	73
40	44	70
60	49	77*
90	107	99
100	133	133

WC: Methyl methacrylate percentage weight composition
AOTBTB: Acryloyloxy tri-n-butyltin benzoate.
MAOTBTB: Methacryloyloxy tri-n-butyltin benzoate.
* Poorly defined tan δ peak.

The effects of increasing percentage weight composition of the acrylic monomers on the values of T_g for copolymers of individual methylated and non-methylated acryloyloxy monomers are depicted in figures (4.57-4.58). For purposes of comparison the theoretically determined values of T_g computed with the Fox relation, see equation (1.38), are illustrated as lines, while the experimental data are shown as points in these figures. Further work on more copolymer samples is required in order to establish the nature of the deviations of the experimental results from the predicted Fox curves in figures (4.57) and 4.58) for acryloyloxy organotin copolymers.

Fig. 4.57 Values of T_g for *o*-AOTBTB with MMA versus copolymer percentage weight composition of acrylic monomer

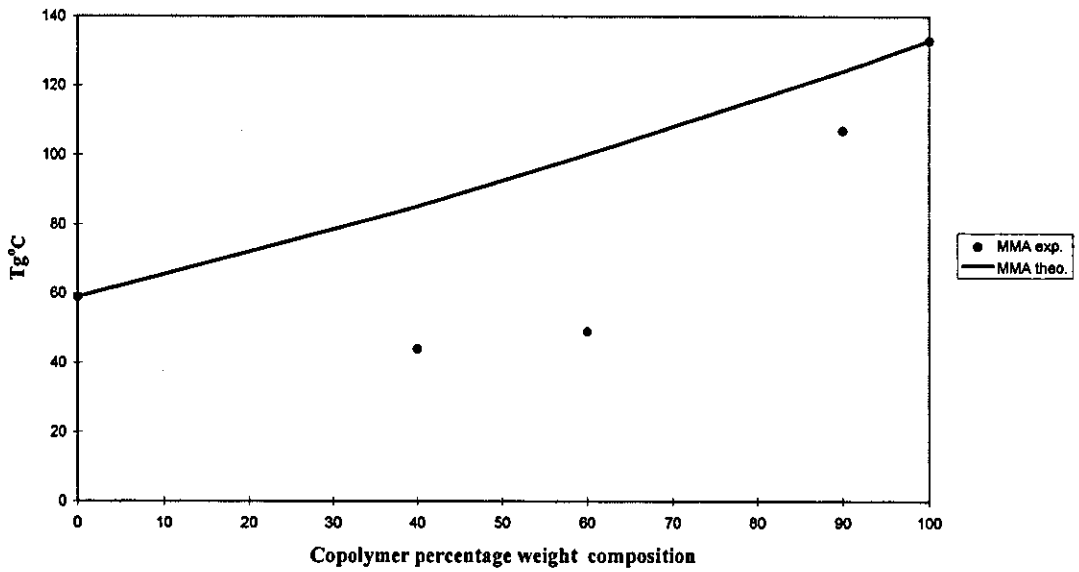

Fig. 4.58 Values of T_g for *o*-MAOTBTB with MA, BA and MMA versus copolymer percentage weight composition of acrylic monomer

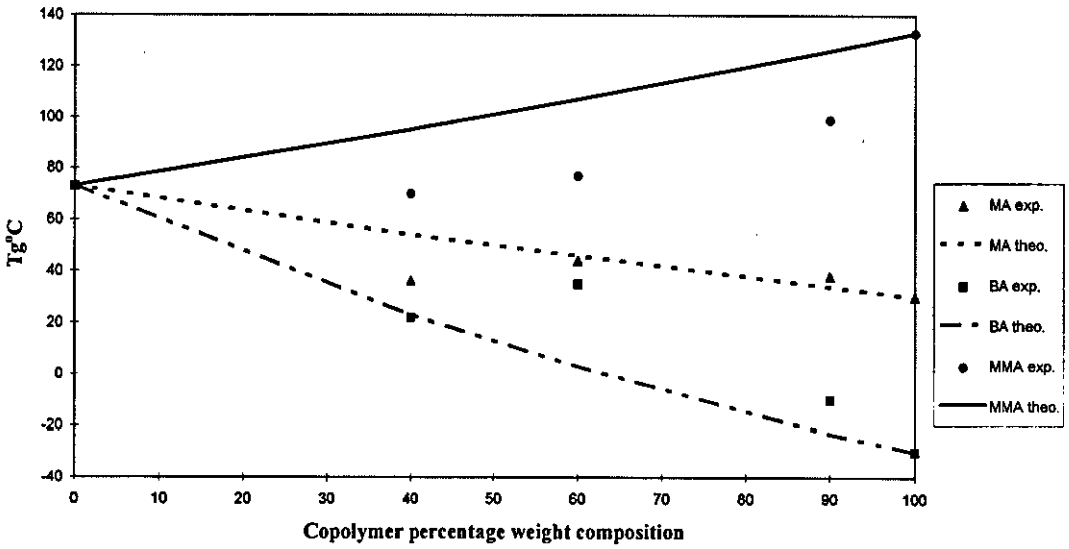

Chapter 5

Conclusions and Recommendations for further work

5.1 Conclusions

1- Organotin monomers described in this work have been produced from the reaction of TBTO with the corresponding acrylic monomers. Moderate yields were obtained.

2- Organotin monomers were polymerised in DMF solution using AIBN as the free radical initiator.

3- The prepared organotin polymers and copolymers were colourless, and soluble in most organic solvents.

4- The values of r_1r_2 obtained indicated that most of the studied copolymer systems should have statistical distributions of the monomer units in the copolymer chain.

5- The values of the parameters r_1 and r_2 for some copolymerisation systems exhibit azeotropic behaviour. These values are expected to be useful in selecting a suitable copolymer with a regular distribution of monomer units for obtaining optimum physical properties and to increase biocidal efficiency.

6- FTIR spectroscopy indicates significant hydrogen bonding in the (poly acrylamide) series, which was enhanced in the corresponding copolymers, leading to stiffer polymers. Such bonding was absent in the acryloyloxy series.

7- Gel permeation chromatography indicated larger polymer molecular weights in the methylated acrylamide series, while in the acryloyloxy derivatives short polymer chains were generated due to steric hindrance caused by the proximity of the bulky tri-n-butyltin group to the polymerisable double bond.

8- The organotin acrylamide homopolymers and copolymers show good thermal stability as indicated by high values of T_g compared to organotin acryloyloxy derivatives.

5.2 Recommendations for further work

1- Copolymerisation of generated organotin monomers with other acrylic and methacrylic monomers.

2- Prepare terpolymers involving organotin monomer to illustrate the variation of both instantaneous and average terpolymer compositions with conversion on the basis of determined reactivity ratios.

3- Detailed study on the effect of the tri-n-butyltin group on the physical and chemical characteristics of the previous polymers, by formulating copolymers containing the same monomers with and without tri-n-butyltin.

4- Testing the biocidal activity of polymers generated in this research.

Chapter 6

References

6.1 References

1 G. Odian, 'Principles of Polymerisation', 3rd Edition, John Wiley and Sons, New York (1991).

2 R. J. Young and P. A. Lovell, 'Introduction to Polymers', 2nd Edition, Champman & Hall, London (1991).

3 J. March, 'Advanced Organic Chemistry',4th Edition, John Wiley and Sons, New York (1992).

4 R. Lenz, 'Organic Chemistry of Synthetic High Polymers', John Wiley and Sons, New York (1967).

5 J. Cowie, 'Polymers : Chemistry & Physics of Modern Materials', 2nd Edition, Blackie A & P, Glasgow (1991).

6 H. Staudinger, Chem. Ber., 53, 1073 (1920).

7 H. Allcock and F. Lampe, 'Contemporary Polymer Chemistry', 1st Edition, Prentice-Hall, New Jersey (1981).

8 F.W. Billmeyer, 'Textbook of Polymer Science', 3rd Edition, Wiley-Interscience, New York (1984).

9 F. R. Mayo and F. M. Lewis, J. Am. Chem. Soc., 66,1594 (1944).

10 M. Fineman and S. D. Ross, J. Polymer Sci., 5, 259 (1950).

11 P.A.Tidwell and G.A. Mortimer, J. Macromol. Sci. Rev. Macromol. Chem. C4, 281 (1970).

12 P. W. Tidwell and G. A. Mortimer, J. Polymer Sci., part A 3, 369 (1965).

13 T. Kelen and F. Tudos, J. Macromol. Sci. Chem., 9, 1 (1975).

14 T. Kelen, F. Tudos and B. Turcsanyi, Polym. Bull. 2, 71 (1980)

15 J. P. Kennedy, T. Kelen and F. Tudos, J. Polymer Sci., part A 13, 2277 (1975)

16 T. Alfrey, and C. Price, J. Polymer Sci., 2, 101 (1947)

17 C. Walling, 'Free Radicals in Solution' John Wiley and Sons, New York, Chapter 4 (1957).

18 J. M. G. Cowie (editor), 'Alternating Copolymers', Plenum Press, New York, (1985).

19 J. Furukawa, J. Polym. Sci., Symp., 51, 105 (1975).

20 H. Hirai, J. Polym. Sci., Macromol. Rev., 11, 47 (1976).

21 K. Plochoka, J. Macromol. Sci., Rev. Macromol. Chem., C20, 67 (1981).

22 H. J. Harwood, Macromol. Chem., Macromol. Symp., 10/11, 331 (1987).

23 J.V. Dawkins, and G. Yeadon, 'Development in Polymer Characterisation-1", J.V. Dawkins Ed., Applied Science (1978).

24 E. G. Malawer, 'Handbook of Size Exclusion Chromatography', edited by Chi-San Wu, (1995).

25 T. G. Fox, and P.J. Flory, J. Appl. Phys., 21, 581 (1950).

26 K. Ueberreiter, and G. J. Kanig, J. Colloid Sci., 7, 569 (1952).

27 J. Brandrup, E. H. Immergut, 'Polymer Handbook', 3rd Edition, Wiley, New York (1989).

28 J. P. Kennedy, E. G. M. Torquist, eds., chapter 1 in 'High Polymers volume XXIII, Polymer Chemistry of Synthetic Elastomers, part 1', Interscience (1968).

29 J. F. Rabek, 'Experimental Methods in Polymer Chemistry', John Wiley and Sons, New York (1980).

30 T. G. Fox, Bull. Am. Phys. Soc., 1, 123 (1956).

31 M. Gordon, J. S. Taylor, J. Appl. Chem., 2, 493 (1952).

32 L. Maldelkern, G. M. Martin, and F. A. Quinn, J. of Res. Nat. Bur. Stand. 58, part 3 (1957).

33 L. E. Nielsen, 'Mechanical Properties of Polymers', Reinhold, New York, (1962).

34 R. Yocum, E. Nyquist, 'Functional Monomers', 1 Marcel Dekker, Inc. (1973).

35 K. Yokota, and J. Oda, Chemical Abstr., 72, 122003k (1970).

36 T. A. Sokolova and G. M. Chetyrkina, Chemical Abstr., 55, 27957h (1961).

37 J. W. Vanderhoff, and R. M. Wiley, Chemical Abstr., 66, 29348t (1967).

38 J. F. Bork, D. P. Wyman, and L. E. Coleman, J. Appl. Polymer. Sci., 7, 451 (1963).

39 F. Iwakura, F. Toda, and H. Suzuki, J. Poly Sci., part A 5,1599 (1967).

40 G. A. Petrova, G. A. Shtralkman, and A A. Vansheidt, Chemical Abstr., 54, 86131 (1960).

41 F. C. Lin, 'Handbook of Size Exclusion Chromatography', edited by Chi-San Wu, (1995).

42 J. E. Sheats, Macromol. Sci. Chem., A15, (6), 1173 (1981).

43 A. W. Sheldon, J. Paint Technol., 47, 54 (1975).

44 C. J. Evans and P. J. Smith, J. Oil Col. Chem. Assoc., 58, 160 (1975).

45 P. J. Smith and L. Smith, Chemistry in Britain, 11, 6 (1975).

46 J. A. Montemarano and E. J. Dyckman, J. Paint Technol., 47, 59 (1975).

47 T. M. Andrews, F. A. Bower, B. R. Laliberte and J. C. Montermoso, J. Amer. Chem. Soc., 80, 4102 (1958).

48 E. F. Jason, and E. K. Fields, U. S. Patent 3,262,915 (1966).

49 J. Leebrick, French Patent 1,400,617 (1965).

50 T. Tahara, K. Seto, and S. Takahashi, Polymer Journal, 19, (3) 301 (1987).

51 S. Takahashi, E. Murata, K. Sonogashira, and N. Hagihara, J. Polym. Sci. part A, 18, 661 (1980).

52 J. C. Montermoso, T. M. Andrews and L. P. Marinelli, J. Polymer Sci., 32, 523 (1958).

53 J. Leebrick, U. S. Patent, 3,167,532 (1965).

54 D. Atherton, J. Verborgt, and M. A. M. Winkeler, J. Coating Technol., 51, 88 (1979).

55 M. M. Koton, T. M. Kiseleva, and F. S. Florinskii, J. Polymer Sci., 52, 237 (1961).

56 S. R. Sandler, J. Dannin, and K. C. Tsou, J. Polymer Sci., A3, 3199 (1965).

57 R. V. Subramanian, B. K. Garg and Jaime Corredor Amer. Chem. Soc., Division of Organic Coatings and Plastics Chemistry, 173 rd Meeting 37 (1), 77 (1977).

58 B. K. Garg, J. Corredor, and R. V. Subramanian, J. Macromol. Sci. Chem. A11, (9) 1567 (1977).

59 N. A. Ghanem, N. N. Messiha, N. E. Ikaldious, and A. F. Shaaban, Eur. Polym. J., 15, 823 (1979).

60 N. A. Ghanem, N. N. Messiha, N. E. Ikaldious, and A. F. Shaaban, Eur. Polym. J., 16, 339 (1980).

61 N. A. Ghanem, N.N. Messiha, N. E. Ikaldious, and A. F. Shaaban, J. Appl.

Polymer Sci., 26, 97 (1981)

62 N. N. Messiha, Polymer, 22, 807 (1981).

63 J. R. Dharia, C. P. Pathak, G. N. Babu, and S. K. Gupta, J. Polymer Sci., part A, 26, 595 (1988).

64 S. S. Al-Diab, H. Kyusuh, J. E. Mark and H. Zimmer, J. Polymer Sci., part A, 28, 299, (1990).

65 G. E. Ham and E. J. Ringwald, J. Polymer Sci., part A, 8, 91 (1952).

66 G. Smets and A. Hertoghe, Macromol. Chem., 17, 189 (1965).

67 G. H. Burnett and W. W. Wright, Trans Farady Soc., 49 ,1108 (1953).

68 A. L. Dalton and T. T. Tidwell, J. Polymer Sci., part A, 12 , 2957 (1974).

69 B. S. Ready, R. Arshady and M.H. George, Eur. Polym. J., 21, 511 (1985).

70 J. S. Roman, E. L. Madruga, and Pargada, J. Polymer Sci., 25, 203 (1987).

71 T. Endo, H. Kawamoto, T. Takata, J. Macromol. Chem., 190, 1827 (1989).

72 O. Moriya, S. Arai, and T, Endo, J. Polymer Sci., part A, 26 , 2579 (1988).

73 A. B. Samui, M. Patri, P. Deb, J. Appl. Polymer Sci., 46 , 2216 (1992).

74 A. F. Shaaban, M. M. Azab and N. N. Messiha, J. Angewandte Makromolek.Chem., 169, 59 (1989).

75 M. M. Azab, J. Appl. Polymer Sci., 51, 1937 (1994).

76 R. R. Joshi, and S. K. Gupta, Eur. Polym. J., 26, 8, 911 (1990).

77 S.Y.Tawfik, N. N. Messiha, S. H. El-Hamouly, J. Polymer Sci., part A, 31 , 427 (1993).

78 S. H. El-Hamouly, S. A. Elkafrawy and N. N. Messiha, Eur. Polym. J., 28, 11, 1405 (1992).

79 A. A. Mahmoud, M. M. Azab and N. N. Messiha, Eur. Polym. J., 29 , 8, 1125 (1993).

80 D. K. Dandge, C. Taylor, and J.P. Heller, J. Polymer Sci., Part A 27, 1053 (1989).

81 D. K. Dandge, C. Taylor, J.P. Heller, K.V. Wilson and N. Brumley, J. Macromol. Sci. Chem. A26, (10) 1451 (1989).

82 P. Dunn and D. Oldfield, J. Macromol. Sci. Chem., A4, 1157 (1970).

83 Shotten-Baumann synthesis Vogel, 'Practical Organic Chemistry', 4th

Edition Longman Inc., New York (1978).

84 K. Patel, T. Desai, B. Suthar, Makromol. Chem. 186, 1151 (1985).

85 D. Manesh, B. Desai, S. Boreddy, R. Reddy, R. Arshady and M. H. George, Polymer, 27, 96 (1986).

86 B. Bortnowska, B. Barela, A. Polowinska, S. Polowiski, V. Vaskova, J. Barton, Acta Polym. 38 ,12, 652 (1987).

87 H. Gilman, D. Rosenberg, J. Am. Chem. Soc. 75, 3592 (1953).

88 R. A. Cummins and P. Dunn, Aust. J. Chem., 17, 185 (1964).

89 R. R. Joshi and S. K. Gupta, J. Polym. Mater. Sci. Eng., 62, 654 (1990).

90 A. J. Kirby, 'Stereoelectronic Effects', Oxford Scientific Publications (1996).

91 H. W. Siesler, K. Holland-Mortiz 'Infrared and Raman Spectroscopy of Polymers', Marcel Dekker, INC. (1980).

92 D. H. Williams, I. Fleming, 'Spectroscopic Methods in Organic Chemistry', 4th Edition, McGraw-Hill book Company (1989).

93 N. Grassie, B. J. D. Torrence, J. D. Fortune, and J. D. Gemmel, Polymer, 6, 653 (1965).

94 R. Z. Greenley, 'Polymer Handbook' (Eds, J.Brandrup and E. H. Immergut), 3rd Edition, pp. II / 267 John Wiley and Sons New York, (1989).

95 J. V. Dawkins, Pure and Appl. Chem., 51, 1473 (1979).

96 E. Meehan, Personal Communication, Polymer Laboratories Ltd., Church Stretton, Shropshire, United Kingdom.

97 R. Biran, PhD thesis, Loughborough University (1978).

98 W. W. Yau, J. J. Kirkland, and D. D. Bly 'Modern Size Exclusion Liquid Chromatography', John Wiley and Sons (1979).

99 B. J. Hunt, S. R. Holding, 'Size Exclusion Chromatography', Blackie and Son Ltd (1989).

100 E. A. Hoff, D.W. Robinson, and A. H. Willbourn, J. Polymer. Sci., 18, 161, (1955).